Diamino Diacid Assisted Macrocyclization of Apelin and Neopetrosiamide

by

Cameron Pascoe

A thesis submitted in partial fulfillment of the requirements for the degree of

Doctor of Philosophy

Department of Chemistry
University of Alberta

Abstract

Peptides can elicit a whole host of beneficial physiological effects. The market for peptide-based therapeutics is rapidly expanding due to their extreme specificity and low toxicity. Conversely, they often possess poor bioavailability, stability, pharmacokinetics and cell permeability, limiting their therapeutic potential. Macrocyclization of peptides has been used to increased peptide stability and cell permeability. Described herein is the expansion of chemistry to increase the accessibility of orthogonally protected diamino diacids and the efforts towards their incorporation to create carbon-based macrocycles of two biologically active peptides. An investigation into their activity through the use of biological assays is also presented.

Chapter 2 discusses efforts toward the synthesis of differentially protected diamino diacids. These molecules can be used to efficiently incorporate macrocycles into peptides and mimic natural linkages that are susceptible to degradation and strengthen them. The attempted use of a solid support to assist the synthesis of diaminosuberic acid analogues is described along with the use of a 1,2-benzenedimethanol scaffold to expand the orthogonally protected diamino diacids available using this methodology from one to four. Each of the synthesized diamino diacids analogues produced is immediately SPPS amenable.

Chapter 3 discusses the synthesis of methylene analogues of neopetrosiamide as potential antimetastatic agents. Neopetrosiamide is a 28-residue peptide isolated from a marine sponge that contains three disulfide bonds. It has been shown to inhibit mammalian tumour invasion *in* vitro but requires precise connectivity of the disulfide bonds for activity. Single disulfide bond replacement by methylene bridges through pre-

stapling of the peptide using orthogonally protected diaminosuberic acid results in three new active analogues comparable in activity to the native peptide and enhances correct folding of the remaining disulfide bonds. Formation of the remaining disulfide bonds is simplified to a single step, followed by HPLC purification.

Chapter 4 discusses the synthesis of apelin analogues. Apelin is a peptide that evokes significant cardio-protective effects such as increased myocardial contractility, increased heart rate and blood pressure lowering. However, apelin's therapeutic use is drastically hindered due to rapid degradation in plasma due to multiple degradation sites. Attempts for more stable analogues by isostere substitution of the KLKB1 degradation sites resulted in stable analogues able to evoke a biological response, however, at concentrations too high to be effective. Additional analogues incorporating macrocycles of the *C*-terminus with orthogonally protected diamino diacids to increase plasma stability and cell permeability were synthesized but proved to be inactive.

Preface

Parts of Chapter 2 (all of section 2.5) and all of Chapter 3 of this thesis have been published as Pascoe, C. A.; Engelhardt, D. B.; Rosana, A. R. R.; van Belkum, M. J.; Vederas, J. C. Methylene Analogues of Neopetrosiamide as Potential Antimetastatic Agents: Solid-Supported Syntheses Using Diamino Diacids for Pre-Stapling of Peptides with Multiple Disulfides. *Org. Lett.*, **2021**, *23*, 9216–9220. I was responsible for synthesizing all orthogonally protected diamino diacids except orthogonally protected *meso*-diaminopimelic acid, which Dr. Engelhardt synthesized. I was responsible for the initial manual synthesis and purification of neopetrosiamide analogues A1 and A2; Dr. Engelhardt re-synthesized these two analogues for manuscript revisions and also synthesized neopetrosiamide analogue A3 and native neopetrosiamide. I was responsible for the development of the one-step disulfide bond procedure. Dr. Engelhardt determined the yields for each disulfide bond formation and cyclization steps for the analogues. Dr. van Belkum cloned and expressed NeoA, I oxidized and purified the peptide. Dr. Rosana and myself performed growing of the cancer cells and I performed the biological testing with the help of Dr. Rosana. I performed approximately 60% of the work and wrote the manuscript.

Parts of Chapter 4 (sections 4.2.2, 4.2.3, 4.2.5, 4.2.6 and 4.2.7) have been published as Fischer, C.; Lamer, T.; Fernandez, K.; Gheblawi, M.; Wang, W.; Pascoe, C.; Lambkin, G.; Iturrioz, X.; Llorens-Cortes, C.; Oudit, G. Y.; Vederas, J. C. Optimizing PEG-Extended Apelin Analogues as Cardioprotective Drug Leads: Importance of the KFRR Motif and Aromatic Head Group for Improved Physiological Activity. *J. Med. Chem.* **2020**, *63*, 12073–12082. I was responsible for the synthesis and purification of αMeArg14 and NMeArg14 peptides. The others performed the rest of the work and wrote the majority of the manuscript. For this manuscript, I conducted approximately 10% of the work and assisted in writing the relevant sections for the peptides. The rest of Chapter 4 has not been published. I synthesized and purified all the peptides and performed approximately 90% of the work, our collaborators were responsible for the biological testing and radioligand displacement assays.

Acknowledgements

Perhaps the most difficult part of writing this thesis is summarizing five years of continued support in a few pages. Firstly, I would like to thank Dr. John Vederas for granting me the opportunity to work as a graduate student in his lab. Under his tutelage and mentorship, my skills as a researcher and scientist have improved in ways I could have never imagined.

To the support staff in the Department of Chemistry, I would like to thank you. Without your continued help and enthusiasm, I never would have been able to learn the things I did, nor uncover the answers to the questions with which I frequently came to you. Thank you in particular to Jing Zheng, Bela Reiz, Dr. Angie Morales and Dr. Randy Whittal for your excellent mass spec help, Dr. Wayne Moffat and Jennifer Jones for your analytical support, Mark Miskolzie and Dr. Ryan McKay for your immense NMR help and Gareth Lambkin for your biological help. Thank you to the Natural Sciences and Engineering Research Council and the University of Alberta for the funding support to allow me to conduct my research. A special thank you to Mike Barteski, for all the coffee bets wagered, all the endless sports banter and the many laughs shared, you made it easy to take a step back from the chemistry to admire everything else.

Thank you to the Vederas group, members of the past and the present, for always creating an environment where laughing and coffee seemed just as important as the work done. COVID made things difficult but I felt like our lab always made the difficult times a little easier. A heartfelt thank you to Dr. Jon Beadle for showing me how to balance work and play and at the same time, teaching me an inordinate amount about working smarter, not necessarily harder. Thank you to Dan Engelhardt and Wayne Vuong for putting up with living with me for many years, I won't forget the late nights spent playing games and hanging out. A big thank you again to Dan for always being easy to talk to and never taking life too seriously when things went wrong, you taught me how to cope with the ebb and flow of lab life. Thank you to Kleinberg Fernandez for our "tea time" together and for constantly being willing to come take Steele and Scout off my hands. Thank you to Dr. Bethan Donnelly and Tess Lamer for reading and editing my thesis and providing good laughs during the morning coffee sessions

An enormous thank you to my rock and confidant, Alexis Ochoa. Your continued support and help kept me going when times were tough. This journey would not have been possible without you or our growing family. You have given me the greatest gift of all, our son Steele. You have shown me an incredible amount of patience while I pursue my dreams and now it is time for me to return the favour.

To my best friends James Donohue and Matt Bickner, thank you for helping me blow off steam when you guys came out to visit. You two always provided an escape from the school life and always knew how to give me a good laugh. To my brother Chris and my sister Steph, you two were always just a phone call away when I needed support, advice or just a conversation.

To my mother and step-father, Paula and Peter Kast, none of this is possible without you two and all that you've done for me. From moving me and all my things to Edmonton, to the visits to help me not starve and keep me sane, to helping me with my newborn son, you two were always supportive in ways that I will never be able to fully repay. I thank you two from the bottom of my heart for the love and support.

I would not have been able to do this without everyone's help, advice and support. Thank you to all my family and my friends.

Table of Contents

List of Tables

List of Figures

List of Schemes

List of Abbreviations, Nomenclature and Symbols

Abbreviation	Definition
$[\alpha]_D^{26}$	Specific rotation at 26 °C
ACE-2	Angiotensin-converting enzyme 2
Ac	Acetyl
Ach	Acetocholine
Ac_2O	Acetic anhydride
AcOH	Acetic acid
ACP	Anticancer peptide
AC	Adenylyl cyclase
Aib	2-Aminoisobutyric acid
Akt	Protein kinase B
Ala, A	Alanine
Alloc	Allyloxycarbonyl
APJ	Apelin receptor
Arg, R	Arginine
Asn, N	Asparagine
Asp, D	Aspartic acid
ATP	Adenosine triphosphate
Bn	Benzyl
Boc	*tert*-Butyloxycarbonyl
Boc_2O	*tert*-Butyloxycarbonyl anhydride
***p*-BrPhe**	*para*-Bromophenylalanine
^{t}Bu	*tert*-Butyl
c	Concentration
cAMP	Cyclic adenosinemonophosphate
Cbz	Carboxybenzyl
CHO	Chinese hamster ovary

CVD	Cardiovascular disease
Cys, C	Cysteine
δ	Chemical shift
DADA	Diamino diacid
DAP	Diaminopimelic acid
DAS	Diaminosuberic acid
DBP	Diastolic blood pressure
DCC	*N*,*N*'-Dicyclohexylcarbodiimide
DCE	1,2-Dichloroethane
DEA	*N*,*N*'-Diethylamine
DIBAL-H	Diisobutlyaluminum hydride
DIC	*N,N*'-Diisopropylcarbodiimide
DIPEA	*N,N*'-Diisopropylamine
DMAP	4-Dimethylaminopyridine
DMF	Dimethylformamide
DMSO	Dimethylsulfoxide
DTT	1,4-Dithiothreitol
$p\mathbf{EC}_{50}$	Negative log of half maximal effective concentration
ECM	Extracellular matrix
EDCI	1-Ethyl-3-(3-dimethylaminopropyl)carbodiimide
eNOS	Endothelial nitric oxide synthase
ERK	Extracellular signal-regulated kinase
ESI	Electrospray ionization
EtOAc	Ethyl acetate
Fmoc	9-Fluorenylmethoxycarbonyl
Gln, Q	Glutamine
Glu, E	Glutamic acid
Gly, G	Glycine
GPCR	G protein-coupled receptor
GTP	Guanosine triphosphate

HATU	1-[bis(Dimethylamino)methylene]-1H-1,2,3-triazolo[4,5-b]pyridinium 3-oxide hexafluorophosphate
HFIP	Hexafluoroisopropanol
His, H	Histidine
HOBt	1-Hydroxybenzotriazole
HR	Heart rate
HRMS	High resolution mass spectrometry
***p*IC$_{50}$**	Negative log of half maximal inhibitory concentration
Ile, I	Isoleucine
IR	Infrared
J	Coupling constant
kDa	Kilodalton
KLKB1	Plasma kallikrein
KO^{t}Bu	Potassium *tert*-butoxide
LCMS	Liquid chromatography mass spectrometry
Leu, L	Leucine
Lys, K	Lysine
LiHMDS	Lithium bis(trimethylsilyl)amide
MABP	Mean arterial blood pressure
MALDI	Matrix-assisted laser desorption/ionization
Me	Methyl
MeCN	Acetonitrile
MeOH	Methanol
Met, M	Methionine
MHz	Megahertz
MI	Myocardial infarction
MIC	Minimum inhibitory concentration
MIRI	Myocardial ischemia-reperfusion injury
mmHg	Millimeters of mercury
mol	Mole
MS/MS	Tandem mass spectrometry

mTOR	Mammalian target of rapamycin
MW	Molecular weight
mw	Microwave
Mtr	4-Methoxy-2,3,6-trimethylbenzenesulphonyl
***p*NB**	*para*-Nitrobenzyl
NCL	Native chemical ligation
NEP	Neprilysin
Ni-NTA	Nickel affinity
Nle	Norleucine
NMR	Nuclear magnetic resonance
NO	Nitric oxide
NOE	Nuclear Overhauser effect
***p*NZ**	*para*-Nitrobenzyloxycarbonyl
OR	Optical rotation
Orn	Ornithine
Pbf	2,2,4,6,7-Pentamethyldihydrobenzofuran-5-sulfonyl
PEG	Polyethylene glycol
pGlu	Pyroglutamic acid
Ph	Phenyl
Phe, F	Phenylalanine
PI3K	Phosphoinositol 3 kinase
PLCβ	Phospholipase C β
ppm	2,2,5,7,8-Pentamethylchroman-6-sulfonyl
Pmc	Parts per million
Pro, P	Proline
PyAOP	(7-Azabenzotriazol-1-yloxy)tripyrrolidinophosphonium hexafluorophosphate
RCM	Ring closing metathesis
R_f	Retention factor
ROS	Reactive oxygen species
RP-HPLC	Reverse phase high performance liquid chromatography

SBP	Systolic blood pressure
Ser, S	Serine
SET	Single electron transfer
S_N1	Unimolecular nucleophilic substitution
sp.	Species
SPPS	Solid phase peptide synthesis
SUMO	Small ubiquitin-like modifier
TBAF	Tetrabutylammonium flluoride
Teoc	2-(Trimethylsilyl)ethoxycarbonyl
Teoc-OSu	1-(2-(Trimethylsilyl)ethoxycarbonyloxy)pyrrolidin-2,5-dione
Tf	Trifluoromethanesulfonyl
TFA	Trifluoroacetic acid
THF	Tetrahydrofuran
Thr, T	Threonine
TIPS	Triisopropylsilane
TLC	Thin-layer chromatography
TM	Transmembrane
TMS	Trimethylsilyl
TMSCl	Trimethylsilyl chloride
TMSE	2-(Trimethylsilyl)ethyl
TOCSY	Total correlation spectroscopy
TOF	Time of flight
t_r	Retention time
Trp, W	Tryptophan
Trt	Trityl
***p*TsOH**	*para*-Toluenesulfonic acid
UPLC-MS	Ultra performance liquid chromatography-tandem mass spectrometry
UV	Ultraviolet
Val, V	Valine

Chapter 1: Introduction

1.1 Pharmaceutical Importance

With the emergence of Western medicine over the last 100 years, the average life expectancy has dramatically increased. In the United States, the duration of the average life has inflated from 49 years in 1900, to 79 years of age in 2019.[1] This dramatic increase is primarily attributed to the development of better health care and improved medical care. However, overall healthier lifestyles, better hygiene, reduced child mortality and widespread access to vaccines have all played a role in human longevity.[2,3] Despite the above advances, there are still numerous diseases that culminate in premature death.

1.2 Peptides

1.2.1 Peptide-Based Therapeutics

Peptide-type drugs have been used clinically ever since the discovery of insulin to treat patients with diabetes (*Table 1-1*).[4,5] Many of these peptides were initially isolated from natural sources, but with sequencing and peptide synthesis, drugs such as oxytocin and vasopressin are synthetically made.[5] Now peptides and peptide derivatives are garnering immense support in pharmaceutical research and development. Peptide-based therapeutics have become one of the fastest growing classes of new drugs in clinical trials.[6] In 2017, there were 68 peptide based drugs approved for therapeutic use, with 155 more active in clinical development, of which half were in phase 2.[5,7] Looking ahead just 2 years, in late 2019 there were over 1000 ongoing peptide-based clinical trials.[8] Given that peptides often have complex and well-defined three-dimensional structures, except for linear peptides in water, they have incredible specificity for their respective targets, making them attractive drug candidates.[7,9] Unlike many small molecule drugs on the market, peptides are tailor-made for specific receptors, channels or pathways. The unique specificity leads to much less off-target binding and therefore they can have less off-target toxicity, mitigating many undesirable side-effects that are linked to small molecule drugs.[5] Furthermore, most peptide drugs have less drug-drug interaction potential, allowing them to be administered in conjunction with other treatments.[6] Although there are seemingly an

Peptide	Source (Synthetic or Natural)	Introduction to Clinic
Insulin	Natural	1920s
Adrenocorticotropic hormone	Natural	1950s
Calcitonin	Natural	1971
Oxytocin	Synthetic	1962
Vasopressin	Synthetic	1962
Leuprorelin	Synthetic	1984
Octreotide	Synthetic	1988

Table 1-1: Early peptide drugs approved for clinical use

abundance of advantages to peptide drugs, they also possess certain caveats not seen with small molecule therapeutics. The downside to peptide-based therapeutics can often be attributed to their pharmacokinetic profile and low bioavailability.[6] Considering that many peptides are natural products and found ubiquitously in the human body for an extensive array of purposes, the body has many ways to break them down to clear them from the bloodstream. Peptides generally have poor plasma half-lives as they are rapidly degraded via proteolytic cleavage by endogenous peptidases.[6,7] There are appropriate structural modifications that can be applied to further stabilize peptides, which will be discussed in Chapter 2. Another drawback is the low bioavailability of peptides. Their relatively large size when compared to small molecules, combined with somewhat complex solubility profiles and low metabolic stability contribute to poor oral bioavailability.[6] To circumnavigate this, peptides can be administered intravenously, subcutaneously and intramuscularly, allowing the drugs to avoid hepatic and gastrointestinal enzymes.[6,7] The alternate route of administration and various modifications that can be done to stabilize peptides help make peptide based therapeutics a promising avenue for various treatments. There are many new current advances on peptide drug development to help bring these therapies to market.[10]

1.2.2 Brief History of Peptide Chemical Synthesis

Given that peptides and proteins are made up of amino acid building blocks, the process to synthesize them, biologically or chemically, is simply an iterative process. Although these peptide bonds are made relatively easily in the lab, large peptides are not always simple to synthesize chemically. Amino acids possess multiple functionalities, and amide bonds are not so straightforward to form. Extensive work in this area has transpired over the last century to simplify peptide synthesis. The term peptide was first reported by Emil Fischer and Ernest Fourneau in 1901, who completed the first peptide synthesis.[11] In 1932, Max Bergmann and Leonidas Zervas invented the first reversible N^{α} protecting group amenable to peptide synthesis, the carbobenzoxy (Cbz) group.[12] The first synthesis of a peptide hormone, oxytocin, was conducted in 1953 by Vincent du Vigneaud. This work, along with his synthesis of vasopressin, won du Vigneaud the Nobel prize in 1955.[13] While solution-phase peptide synthesis still has niche applications,[14] the field of peptide synthesis flourished following the advent of solid-phase peptide techniques by Robert Bruce Merrifield.[15]

1.2.3 Solid-Phase Peptide Synthesis

Solid-phase peptide synthesis (SPPS) was pioneered by Dr. Merrifield, for which he won the Nobel Prize in 1984. The concept uses the same chemistry as previous solution-phase methodology with one major difference: the nascent peptide is covalently linked by its terminal carboxylic acid to an insoluble support, commonly of polystyrene. The peptide grows from *C* to *N* terminus, the opposite of the way nature builds peptides. Anchoring the peptide to a solid support allows for filtration of the vast excess of reagents that are used to drive the reactions to completion. Repeating addition cycles with desired amino acids can extend the peptide. The mature peptide can then be released following completion. Initially, SPPS made use of N^{α}-Boc protecting groups, with Cbz side chains, to allow for iterative acid deprotection and coupling with *N,N'*-dicyclohexylcarbodiimide (DCC).[15] Release of the peptide from the solid support was achieved using HF, meaning this first rendition of SPPS relied on "relative acidolysis", where the Boc groups were labile in a moderate acid, such as trifluoroacetic acid (TFA), and the resin-linkage was labile under strong acid (HF).[14]

In 1970, a crucial new *N*-terminal protecting group was introduced by Louis Carpino.[16] The 9-fluorenylmethoxycarbonyl (Fmoc) group requires moderate base for removal, allowing for selective deprotection of Fmoc in the presence of acid labile and hydrogenation sensitive protecting groups. Application of the Fmoc group revolutionized SPPS as amino acids could be N^{α}-Fmoc protected (*Scheme 1-1*) and side chains protected with acid labile groups, allowing for exquisite control over peptide synthesis.[17]

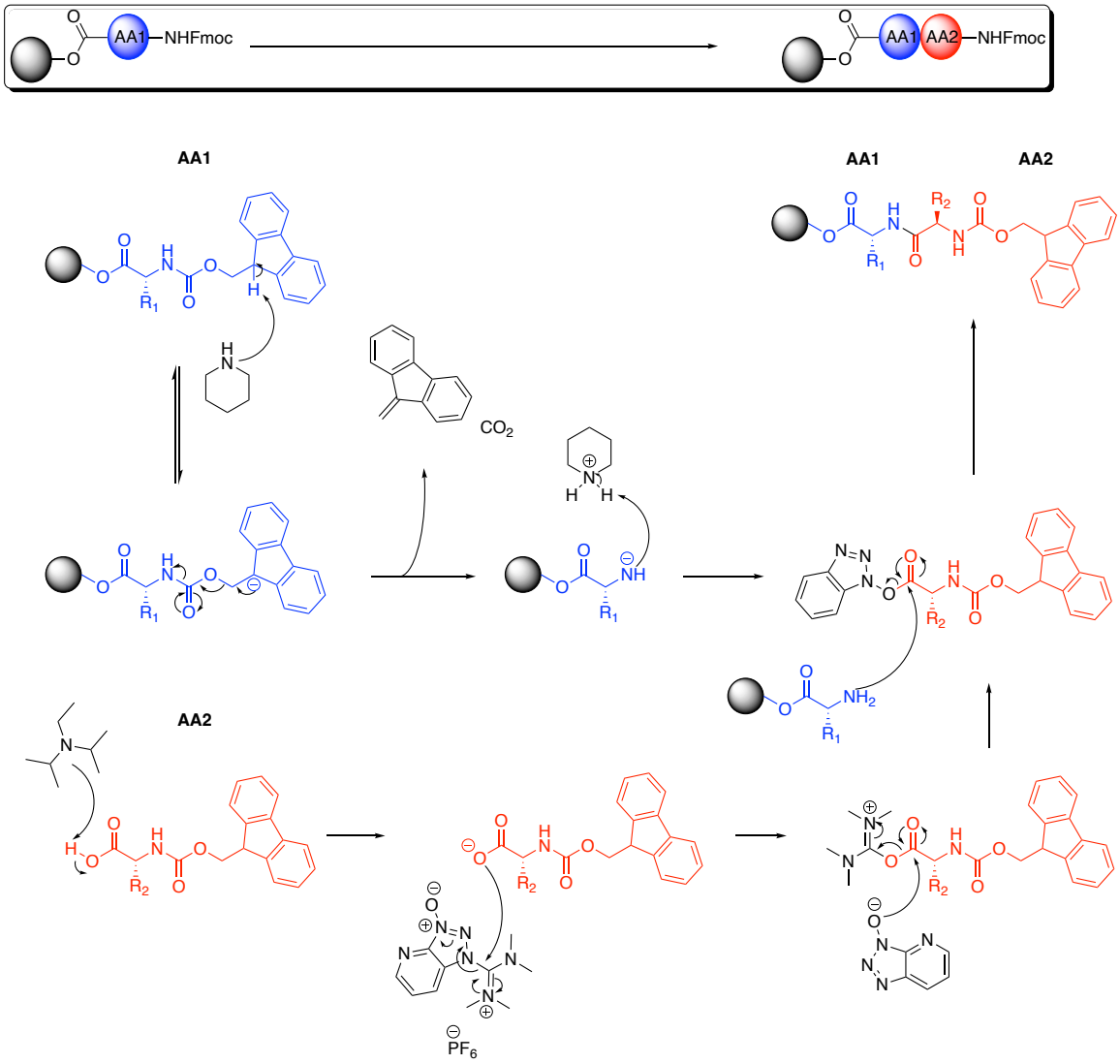

Scheme 1-1: A general strategy for Fmoc based SPPS

With the rapid development of SPPS and concomitant protecting groups, the need for more effective coupling reagents arose. Many earlier peptide coupling reagents had a tendency to epimerize the alpha carbon of the activated residue (*Scheme 1-2*). This is often detrimental to the peptide's activity as the stereochemistry of the natural substrate is

usually critical; therefore, racemization of any residue could render the peptide inactive. N^{α}-Carbamate protecting groups slow the process of epimerization. However, they do not eliminate it entirely, so new, more active coupling agents were developed.[18,19] These coupling reagents activate the amino acid such that it reacts very quickly to the incoming amine nucleophile, and many have strategically placed atoms capable of participating in the neighbouring group effect to direct the incoming amine.[18,19] The development of new coupling reagents has resulted in much lower instances of racemization during peptide synthesis. Additionally, many new resins have been invented, each with their own chemical susceptibility for cleavage, allowing a variety of resins and protecting group combinations to be used in SPPS.

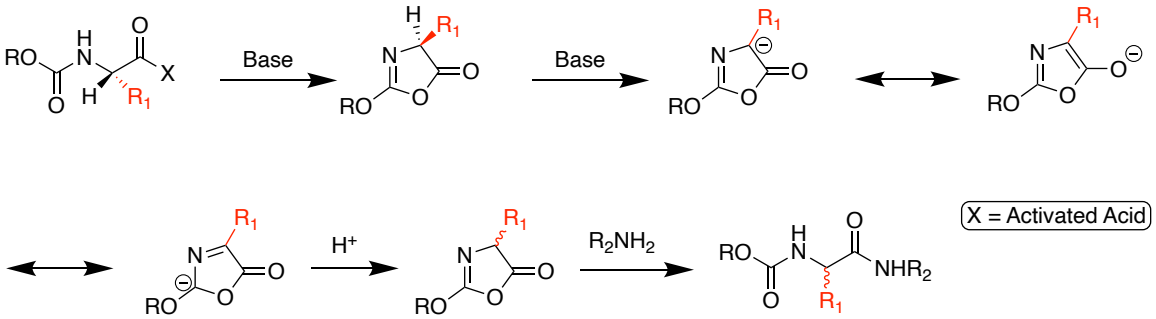

Scheme 1-2: The racemization mechanism of activated amino acids

Although most amino acid couplings go to completion due to the superstoichiometric amount of reagent used, some bulkier or non-canonical amino acids may not couple to completion with the growing peptide chain. The result is a free primary amine on the growing peptide chain, rather than an Fmoc-protected amine. The free amino group can react undesirably with other peptide chains on resin, or it can couple with the subsequent incoming residues, resulting in peptides that will continue to grow as peptide synthesis is done, but will be missing one or more, residues. This dramatically complicates purification of the desired product. A Kaiser test using ninhydrin can be done to test for the presence of free amino groups on the resin.[20] Should an amine remain unreacted, the coupling can simply be repeated with fresh reagents, or the peptide chain can be terminated by "end-capping" with acetic anhydride. "End-capping" results in truncated peptides, overall reducing the yield; however, these fragments are typically easier to separate from the product during purification.

1.2.4 Advances in Peptide Synthesis

With the development of SPPS, synthetic peptide hormones and peptide therapeutics have become much more readily accessible. Much larger peptides have also been synthesized using novel discoveries such as native chemical ligation (NCL) (*Scheme 1-3*).[21] This incredible methodology allows two peptide fragments to be joined together by an amide bond. The process is initiated using an *N*-terminal cysteine residue on fragment 2 that undergoes trans-thioesterification with a *C*-terminal thioester on fragment 1 to join the fragments together. The trans-thioesterification sets the stage for a thermodynamically favourable *S* to *N* acyl transfer. This ligates the two fragments together with an amide bond, regenerating the cysteine residue.[21]

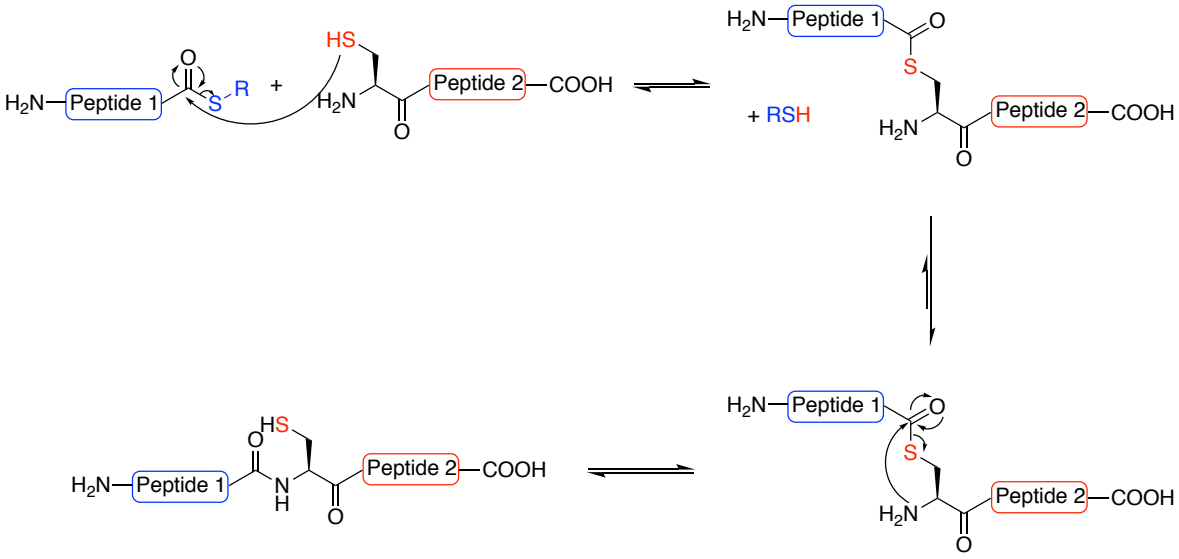

Scheme 1-3: The general mechanism of native chemical ligation

Automated peptide synthesizers have made the field of peptide synthesis much more efficient. Combining automated synthesis with flow chemistry, exceedingly long peptides (164 amino acids) that demonstrate enzymatic properties comparable to the naturally expressed peptide are now synthetically accessible.[22] Peptide synthesis continues to evolve with new advancements continually achieved. It is now not inconceivable to produce whole proteins using these new methodologies.[23] Residue substitutions to study active sites or structure-activity relationships are becoming much more convenient. Peptide synthesis has evolved tremendously since the first synthesis of insulin as seen in this review,[24] making it a very exciting and encouraging area of research.

1.2.5 Peptide Stability

As mentioned previously, peptides have extraordinary potential for use as a therapeutic for numerous diseases; however, they have many limitations as well. On top of solubility and administration difficulties, many drugs in blood plasma become oxidized to help the body clear them from the bloodstream. This also transpires with certain amino acid residues, altering the structure of the peptide and therefore its activity. But, perhaps the most glaring impediment for peptides is their susceptibility to degradation by proteases. These enzymes recognize certain amino acid sequences and cleave the amide bond at the recognition site, eviscerating the therapeutic activity.

Considerable efforts have been undertaken to mitigate the limitations of peptides by augmenting their stability *in vivo*. This is typically done through chemical modification of the peptides. Since proteases often recognize amino acid sequences or even a single residue, like trypsin which recognizes lysine or arginine,[25] replacing or altering these residues by isostere substitution can slow or stop premature degradation.[26] These peptide backbone modifications can be fairly subtle, such as D-amino substitution,[27] which can effectively deter proteolysis. Other commonly used methods are methylation of the amide nitrogen (or α-carbon),[27,28] incorporation of β-amino acids,[29] and aza-amino acids,[30,31] among others.[24]

Moreover, there are much larger changes that can be done to increase stability and effectiveness. Peptides frequently form a secondary structure that contributes to their function, held together by intramolecular forces, such as hydrogen bonds, van der Waals forces and hydrophobic interactions. While these forces are adequate for endogenous hormones to activate their receptor without disruption, they are often not suitable for therapeutics to maintain secondary structure conformation in solution.[32] By enforcing this 3D structure in a more rigid manner, proteases may not be able to bind as effectively to degrade the amide backbone.[24] Modifications to the peptide that allow for stabilization of secondary structure are usually by means of covalent linkages. α-Helices are a familiar secondary structure motif, making up anywhere from 30 – 40% of all protein structures.[33] These helices are formed by intramolecular hydrogen bonds between residues on the same side of the helix at positions i, $i + 4$, $i + 7$ etc. (*Figure 1-1 A*).[34] By attaching the residues located at these positions together through their side-chains, the α-helix can be mimicked

with a much more rigid linkage. Some examples of such linkers are lactone (Ser residue to Glu or Asp), lactam (Lys residue to Glu or Asp), disulfide (two Cys residues), or alkene/alkane via cross-metathesis (two allyl glycine residues).[24] Another routinely encountered secondary structure motif is a β-sheet. These motifs possess parallel or antiparallel strands of linear peptide, in which the N-H bonds of one strand initiate hydrogen bonding with the carbonyl of the other stand (*Figure 1-1 B*). While covalent

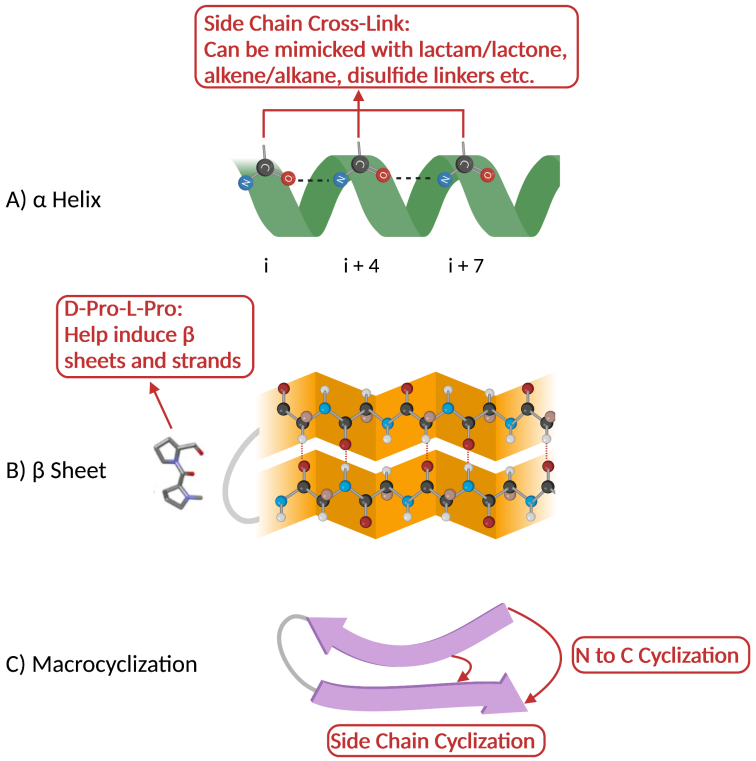

Figure 1-1: Graphical representation of common secondary structures seen in peptides with chemical modifications for stability shown in red. 1) α-Helix showing interactions between i, i +4 and i +7 residues; 2) β-sheet showing peptide backbone interactions; 3) linear peptide showing potential sites for macrocyclization. Image made with Biorender.com and modified from Wang et al.[24]

linkages of β-sheets are difficult due to the multitude of hydrogen bonds holding it together, the overall structure can be enforced through incorporation of a D-Pro-L-Pro, thereby stabilizing the antiparallel stands.[35] Lastly, macrocyclization of peptides is becoming an increasingly popular modification. There are many macrocyclization variations, such as head-to-tail, side chain-to-side chain, side chain-to-tail and head-to-side chain (*Figure 1-1 C*).[24,36] Peptide cyclization, termed peptide stapling, is garnering

interest due to the benefits associated with it. Not only can it increase proteolytic stability,[37] but stapled peptides are also correlated with increased cell-permeability.[38] Due to the nature of macrocyclization, it often facilitates the formation of α-helices, and to a lesser extent β-sheets, by pre-assembling the intramolecular interactions necessary.[24,39] Many methods used to pre-form α-helices are used to form macrocycles.[24,36] Consequently, macrocycle incorporation encompasses most larger peptide stabilization methods, demonstrating its immense importance to peptide stabilization and function.

1.3 Cancer

1.3.1 Premature Cause of Death

Currently, cancer is the second leading cause of death worldwide.[40] In 2018, there were an estimated 9.6 million deaths due to cancer, with another 18.1 million diagnosed cases.[40] In the United States alone, there were 600,000 deaths in 2019, accounting for 21% of total deaths.[41]

1.3.2 What is Cancer?

Defined as a plethora of diseases affecting virtually any part of the body, the title of cancer is generic.[42] There is no singular cause of cancer, as it is often the result of genetic predisposition, environmental factors, or diet among many others. [43–46] The term cancer describes the uncontrolled growth of cells that cannot effectively be regulated, eventually possessing the potential to become malignant through acquisition of atypical characteristics, thereby allowing spread to the rest of the body.[42,47] Although there is extensive knowledge on cancer and its hallmarks,[43,44] cancerous cells are able to develop through countless mechanisms making targeted therapies difficult.[48]

1.3.3 Common Treatment Options

Presently, there exist three main therapeutic strategies to broadly or non-specifically treat cancer. Surgery is an viable option for obvious tumours, but it can leave patients with trauma, pain, bleeding and isn't suitable for advanced or inaccessible tumours.[49] Radiation therapy is an effective substitute for surgery but can entail a long list of complications, on top of being expensive.[50] Chemotherapy acts upon rapidly dividing

cancer cells, but is nonspecific and will kill normal rapidly dividing cells such as the lining of the gut.[51] As a result, many scientists are researching newer, more effective means of treatment.

1.3.4 Anti-Cancer Peptides

From the emergence of molecular biology and sequencing, there have been a large number of short peptides that have been discovered from a wide variety of organisms.[52] Among the recent discoveries have been low molecular weight, cationic peptides that possess anti-tumour activity.[48] Termed anti-cancer peptides (ACPs), these short, positively charged peptides were initially assessed for anti-microbial activity due to their cationic properties (*Figure 1-2*).[53] The reasoning stems from the fact that bacteria cells and mammalian cancer cells both contain a higher proportion of negative charge on the surface of their membranes.[54] ACPs are quite selective and usually toxic to cancer cells.[55] Given that they have high selectivity, excellent penetration and are easy to modify,[56–58] ACPs are a flourishing and encouraging method for cancer treatment.

Anti-cancer peptides are generally classified by 4 structural features: α-helical, β-pleated sheets, random coil and cyclic.[48,59] Mastoparan I (**1**) is an α-helical peptide that acts upon the cell surface negative charge of prostate and liver cancer cells.[60] Alloferon 2 (**2**) is a glycine rich, random coil ACP which been shown to have anti-tumour activity by upregulating natural killer cells.[61] Plitidepsin (**3**) is a cyclic ACP currently in Phase II clinical trials. It has been shown to be active against advanced kidney, thyroid and skin cancers and potent against small cell lung cancer.[62] Finally, SVS-1 is a β-pleated sheet ACP containing almost exclusively lysine and valine residues, giving it a formal charge of +9.[63] This interesting KVKV motif is effective at membrane disruption in lung, epidermal and breast cancer cells.[63,64] These peptides demonstrate the wide assortment of conformations and 3D conformations with which ACPs are able to effectively target tumour cells for destruction.

Between 2017 and late 2019, there was an eruption of peptide-based clinical trials, with over 500 new peptides entering testing in a 2 year span.[5,8] Despite around only 20 of these being anti-cancer peptides approved for clinical use, they are exceedingly effective and have encountered minimal drug resistance due to their unique modes of actions.[8] With

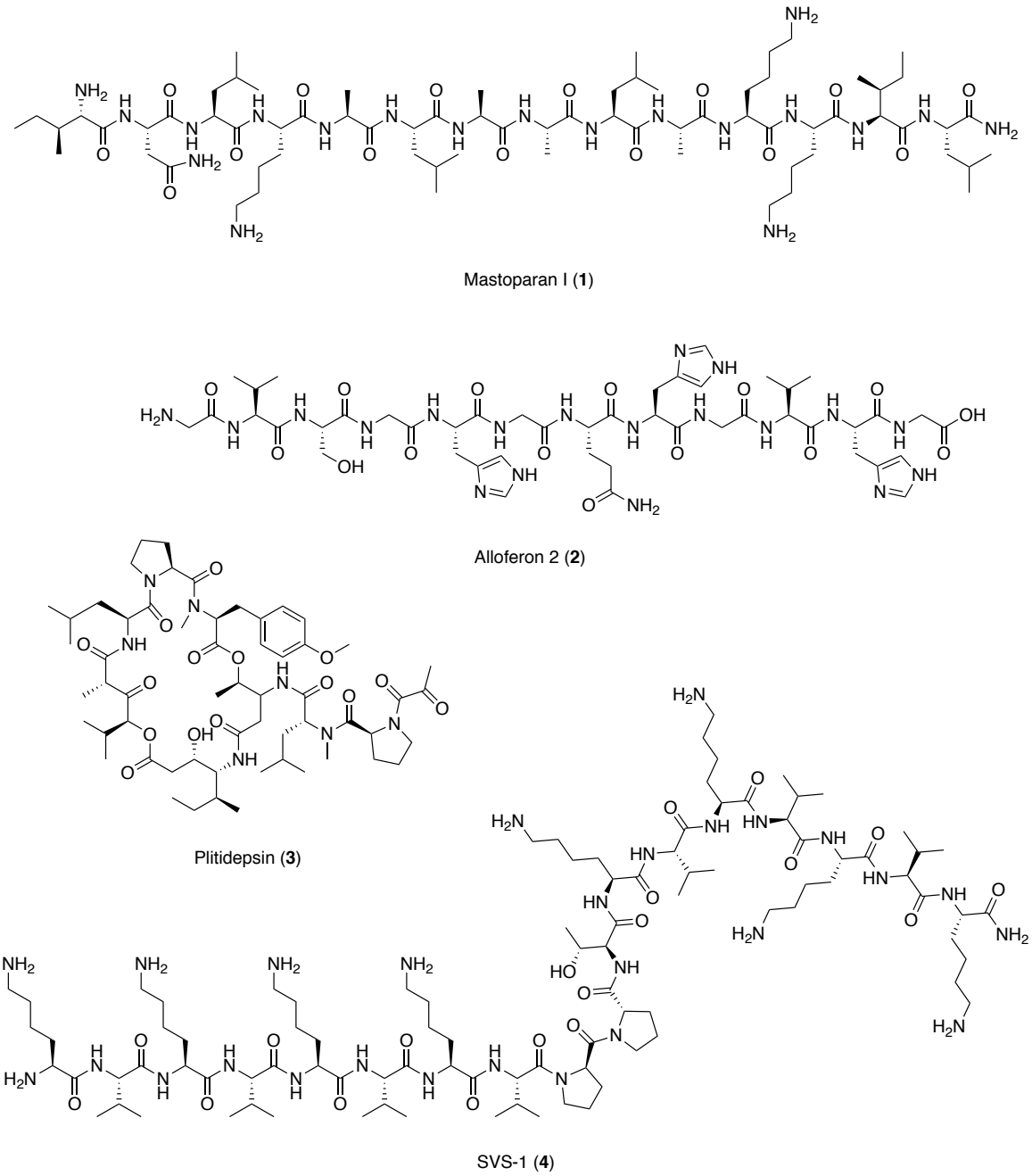

Figure 1-2: Examples of anti-cancer peptides in each of the 4 structural classifications

such an enormous amount of new peptides being tested almost yearly, there will likely be many more ACPs approved for clinical use. Anti-cancer peptides and peptide-based therapeutics are rapidly becoming some of the most important areas in drug discovery.[8,10,48,59]

1.4 Neopetrosiamide

1.4.1 Introduction

Neopetrosiamides A and B, from the *Neopetrosia* sp., are naturally occurring peptides originally isolated from a sea sponge collected in Papua, New Guinea.[65] They are interesting from an anti-cancer peptide aspect as they are active against cancerous cells, but appear to leave healthy cells unscathed.[66] The peptides do not exhibit lethal anti-cancer properties such as membrane permeation, ultimately resulting in cell death, but rather they inhibit the growth and spread of the targeted cancer cells.[66] This activity occurs at low micromolar concentration and potentiates neopetrosiamides' use as an antimetastatic agent.[65]

1.4.2 Natural Structure

Neopetrosiamide (A and B isomers) is a 28-residue peptide, containing all L-amino acids. The peptide was first isolated as a mixture of two sulfoxide diastereomers, neopetrosiamides A and B, which are the result of aerobic oxidation of the methionine residue at position 24, although this sulfoxide is not required for activity (*Figure 1-3*).[65]

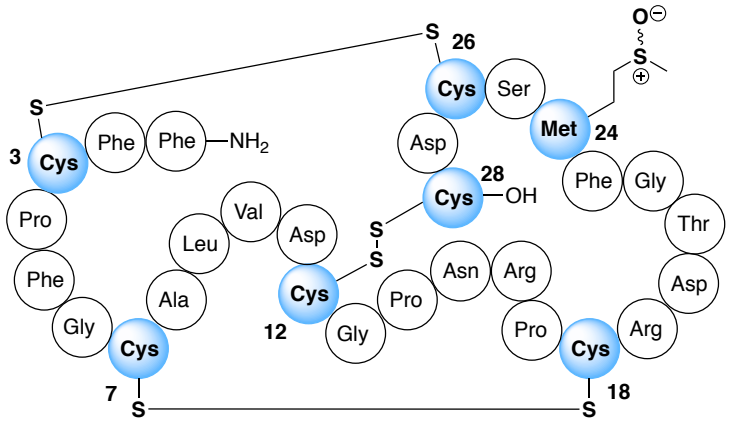

Neopetrosiamdes A and B (**5**)

*Figure 1-3: Cartoon representation of neopetrosiamides A and B **5** with disulfide bridges and oxidized methionine at position 24*

There are three disulfide bonds in the natural peptide and their correct connectivity is crucial for activity. Incorrectly linked isomers are biologically inactive, despite one of them possessing a nearly identical backbone conformation and 3D-structure as the active conformation.[67] Our group ascertained the correct connectivity of the disulfide bonds, as the initial report of the structure proposed had incorrect disulfide connectivity.[65,67]

Through partial disulfide reduction, alkylation of resulting thiols and MS/MS sequencing, the correct disulfide linkages were deduced (*Figure 1-4*).[67]

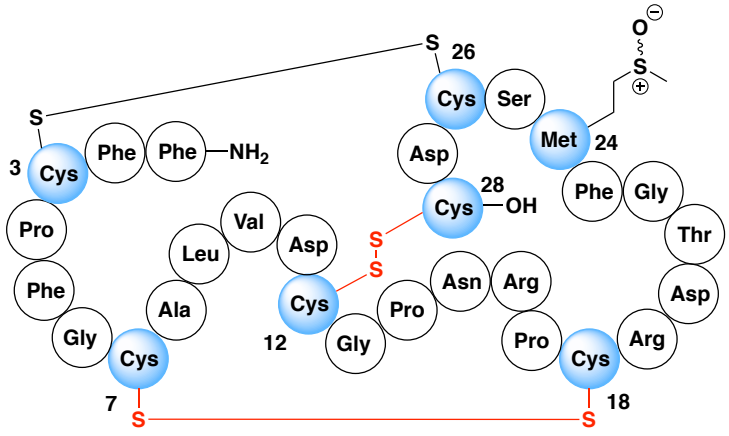

Neopetrosiamdes A and B (**5**)

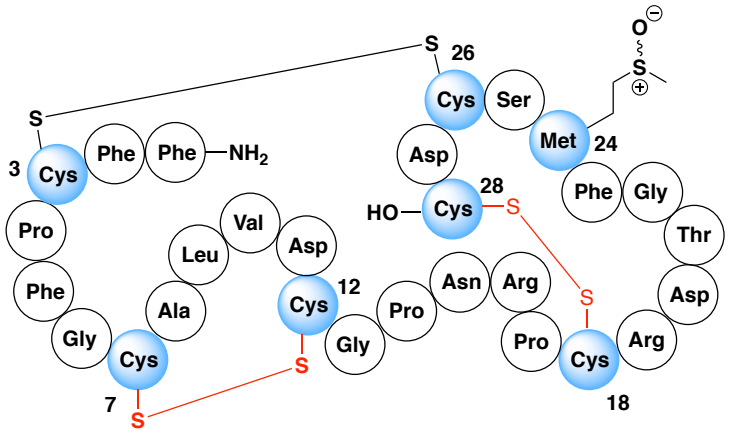

Originally Proposed Neopetrosiamide Structure (**6**)

Figure 1-4: Cartoon representation of the revised neopetrosiamide disulfide bond linkages ***5*** *and the originally proposed disulfide bond linkages* ***6***

1.4.3 Chemical Synthesis

The chemical synthesis of neopetrosiamide poses a synthetic challenge due to the presence of the multiple disulfide bonds. Furthermore, natural neopetrosiamide is undesirable therapeutically as the peptide is isolated as a mixture of diastereomers. Our group has demonstrated that the methionine residue can be replaced with norleucine, resulting in marginally reduced activity, but completely eliminating the presence of sulfoxide diastereomers.[67] Unfortunately, standard disulfide bond formation of the linear peptide under redox equilibration conditions generates up to eight isomers, with the active

isomer **5** being very minor.[67] To effectively synthesize neopetrosiamide, selective oxidation of the cysteine residues to form each of the three disulfide bonds sequentially is essential. Orthogonal protection/deprotection strategies have been used to control the disulfide bond formation between the cysteine residues in neopetrosiamide, forming the desired isomer in greater proportions than the incorrect isomers.[67,68] When combined, these two methods have vastly improved the accessibility of neopetrosiamide via synthetic means.

1.4.4 Mode of Action

The exact mechanism through which neopetrosiamide acts upon cancer cells is still largely unknown; but there are some insights into how it affects the migration and growth of cancer cells. Amoeboid migration is characterized by the expansion and contractions of protrusions from the tumour cell, much like amoeba, to invade into surrounding tissues or extracellular membrane (ECM).[69,70] Mesenchymal type migration is characterized by polarization of the tumour cell, creating a leading edge, sometimes with many pseudopods.[69] The cancer cell adheres to the ECM and begins to proteolytically degrade it, carving a path for the cancer cell's migration.[69,71] Many cancerous cells are able to switch between the two types of movement depending on micro-environmental conditions, making it difficult to target only one migration pathway. Neopetrosiamide is able to hinder tumour cell growth and invasion by both mesenchymal and amoeboid pathways.[65,66] Inhibiting the adhesion of cancer cells to the ECM causes the cells to detach from the underlying ECM and become round in shape, rather than the elongated form they adopt when attached to the ECM.[66] This retraction from the ECM is characteristic of cancer cells with lower expression of cell surface β1 integrins and the dissolution of focal adhesions.[66] Neopetrosiamide likely acts in a similar manner by inhibiting cancer cell adhesion as cancer-cells treated with neopetrosiamide round-up and detach from the ECM.[66] This type of mechanism has been exploited in the development of anti-cancer peptides by use of an Arg-Gly-Asp (RGD) tripeptide motif.[72] The RGD motif binds to integrins, preventing them from binding to the ECM.[72,73] This motif can be utilized to create anti-cancer peptides that target both modes of cancer cell migration. Interestingly, neopetrosiamide does not contain this motif, nor any other known integrin binding domains, meaning its mechanism of action is still unclear. Cells treated with

neopetrosiamide rapidly developed membrane protrusions on the cell surface, within 5 mins of exposure.[66] Neopetrosiamide also triggered the release of membrane-bound vesicles that were found to contain high concentrations of important cell adhesion molecules, such as integrin subunits, growth factor receptors and other proteins associated with cellular adhesion.[66] The effects of neopetrosiamide are rapid, but do not result in cellular death, as the effects are reversible upon removal of the peptide.[66] More importantly, these peptides do not seem to affect non-cancerous cells. The effects of neopetrosiamide are well documented, but there is still much to be done to discover how it evokes a biological response.

1.5 Cardiovascular Disease

1.5.1 Premature Cause of Death

While cancer is the second leading cause of premature death worldwide, it pales in comparison to cardiovascular disease (CVDs). With an estimated 523 million cases and 18.6 million deaths worldwide in 2019, CVD is the leading cause of death in the world.[74] In the United States, CVDs accounted for 23.1% of all deaths, amounting to 660,000 total deaths in 2019.[41]

1.5.2 What is Cardiovascular Disease?

Much like cancer, the term cardiovascular disease encompasses a variety of diseases. These diseases under the broad term CVD include ischemic heart disease, cerebrovascular disease, hypertension, congenital heart disease and many more.[75] Factors that promote CVD are primarily attributed to poor diet (tobacco use, alcohol, fatty diet) and physical health (inactivity, obesity), although there is genetic predisposition to the diseases as well.[75] Atherosclerosis describes the process in which cholesterol and fatty material are deposited in the walls of arteries, forming a plaque. This plaque has the capacity to rupture and travel around the bloodstream, resulting in heart attacks or strokes.[75] After a myocardial infarction (heart attack), reperfusion of the affected area with oxygenated blood has devastating consequences. This phenomenon is known as myocardial ischemia-reperfusion injury (MIRI). [75–77] Upon reperfusion of the ischemic tissue, reactive oxygen species (ROS) are generated that wreak havoc on the surrounding cells. The ROS contribute to an inflammatory response by causing oxidative injury to

cells, eliciting recruitment of cytokine and chemokines, resulting in cellular apoptosis.[76,77] Heart attacks stop the blood flow to the affected tissue, but it is the sudden reintroduction of oxygen that causes extensive damage.

1.5.3 Common Treatment Options

One of the most common treatment options for CVDs begins with prevention of the disease. Diet,[78] medication,[79] and physical activity[80] have all been linked to lower instances of CVD; however, there are many cases where prevention does not work or is not possible, namely those with genetic history.[81] In such cases, medications, such as statins and aspirin, are viable treatment options to prevent, or slow the progression of CVDs.[82,83] Unfortunately, these medications are not curative, nor will they treat MIRI, but rather they serve to lower the chances of a myocardial infarction. Long-term use of these medications carry their own risks as they are associated with a wide array of side-effects.[84] Myocardial infarctions can be treated using percutaneous coronary intervention (PCI).[85] This surgery is done to open clogged, or narrowed arteries and involves inflating a balloon to open affected arteries, and placing a stent to keep it widened.[86] While this is relatively minimal invasive, it still requires surgery, may need to be repeated and can still lead to MIRI upon opening of the vessels.[85,86] The lack of treatment options exacerbate the need for new, more effective techniques.

1.5.4 Peptide Therapeutics for Cardiovascular Disease

Stemming from the lack of medications approved for treatment or intervention of CVD, research into cardio-protective peptides has become increasingly popular.[84,87] Expression of cardio-protective peptides is naturally augmented in those presenting acute ischemia; however, studies have shown that exogenously administering therapeutic cardio-protective peptides serve to further protect against MIRI.[84,88] Naturally expressed peptide hormones have exceedingly short half-lives in plasma due to enzymatic degradation.[7,84] The idea of being able to supplement the body's natural protection against oxidative damage from an MI with longer-lasting therapeutic peptides derived from the same hormones is intriguing to researchers and medical experts.[87]

As shown in *Table 1-1*, octreotide (**7**) is a peptide-based therapeutic that was approved for clinical use in 1988 (*Figure 1-5*).[5] It mimics the structure of the natural

hormone somatostatin (**8**), although it is more potent.[5] Octreotide can be used to treat gastrointestinal and oesophageal bleeds;[89] more recently it has been approved by the FDA for long-term treatment of acromegaly (excessive growth hormone production).[90,91] The potential uses of octreotide continue to be explored. There are many reports suggesting it is protective against MIRI for an assortment of different tissues.[92–96] Cortistatin-14 (**9**) is a recently discovered endocrine peptide with a remarkable structural resemblance to somatostatin, sharing many biological properties.[97] However, it can evoke unique responses as well, such as reducing locomotive activity,[98] inducing sleep,[99] among others.[100] Due to its similarity to somatostatin, cortistatin-14 was thought to be a possible cardio-protective peptide, an idea that is supported by its expression in the cardiovascular system.[101] Indeed, recent research has shown that cortistatin-14 exerts myocardial protection after an MI,[102,103] bolstering the notion that peptide therapeutics could be a viable avenue to protect against MIRI. Annexin-A1 is a large 37 kDa endogenous protein found to possess cardio protective-properties,[104] and while its large size complicates its exogenous therapeutic potential, annexin-A1 mimetics are displaying promise in this regard.[84,105] CGEN-855A (**10**), a 21-amino acid mimic of annexin-A1, demonstrates effective treatment for inflammation of cardiac tissues from neutrophils, but more importantly, CGEN-855A is able to protect myocardial infarction-reperfusion injury.[105]

With the aforementioned outpouring of peptides being discovered and entering clinical trials, many more cardio-protective peptides will undoubtedly be identified. Ideally, the use of therapeutic peptides, in combination with the body's natural defence against MIRI, will become an effective treatment option for cardiovascular disease.

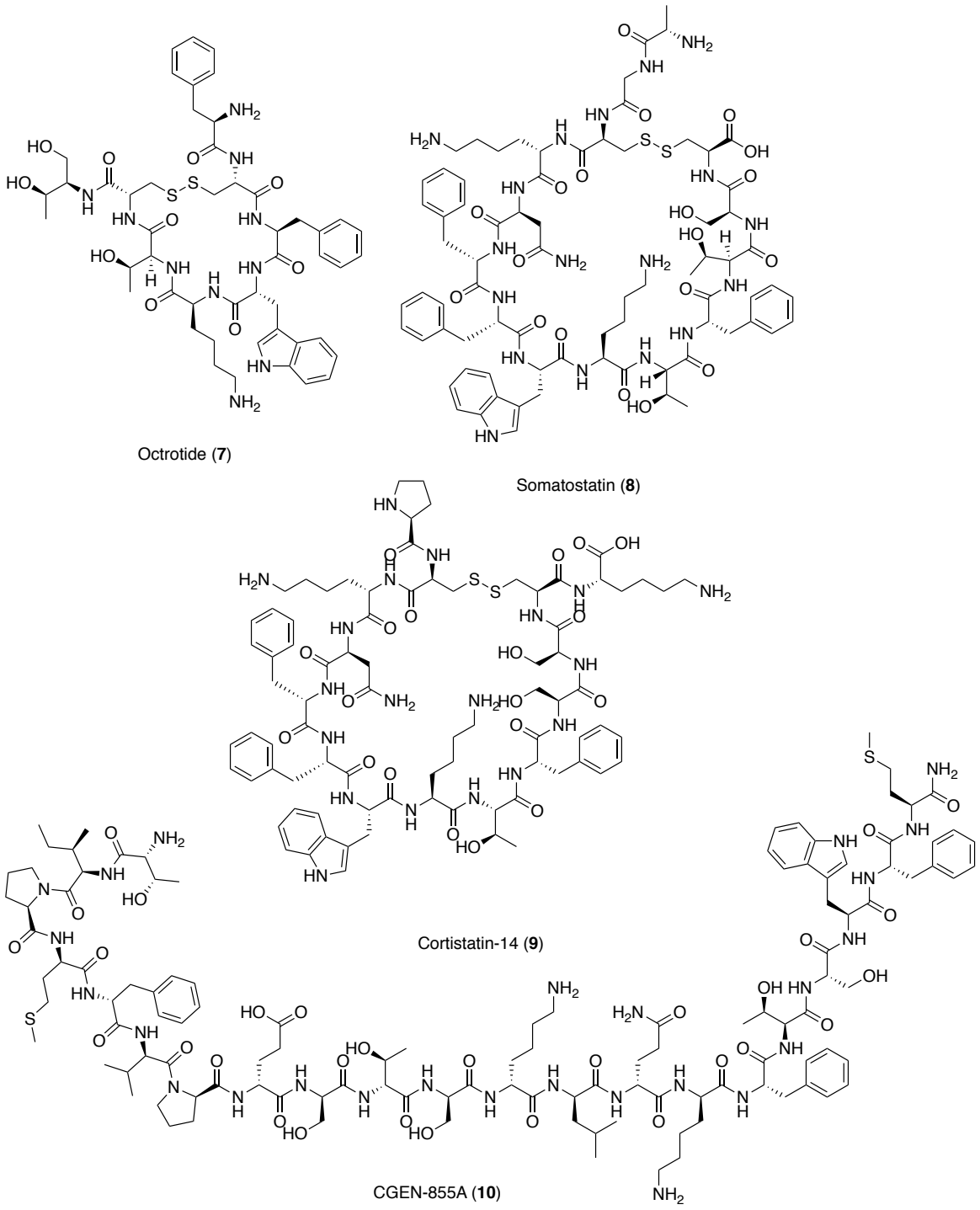

Figure 1-5: Examples of natural and synthetic cardio-protective peptides

1.6 Apelin

1.6.1 Introduction

Apelins are a class of endogenous mammalian peptide hormones, discovered in 1998,[106] that are expressed in endocardial and vascular epithelial cells.[107] They bind to the human G protein-coupled receptor (GPCR) apelin receptor (APJ),[106] and have been found to induce a wide variety of physiological responses, including effects in the adipoinsular axis, cardiovascular regulation and body fluid homeostasis.[108,109] Upon binding to the APJ receptor, studies have shown that a host of cardio-protective physiological effects are triggered such as increased myocardial contractility and heart rate, and vasodilation.[107,108] Interestingly, the loss of apelin in animal models correlates with an impairment towards recovery from MIRI.[110] These results are encouraging for apelin's use as a potential therapeutic for CVD and MIRI.

1.6.2 Natural Structure

Endogenous apelin begins as a 77-amino acid prepropeptide, containing all L-amino acids, which gets processed into three major isoforms, two of which our group has particular interest in: [pyr]^{1}-apelin-13 (**11**), apelin-17 (**12**) (*Figure 1-6*).[107] These are denoted by length of the isoforms and have 12 conserved *C*-terminal residues, while the 13th residue in apelin-13 cyclizes to a pyroglutamic acid residue. These isoforms circulate in the bloodstream and activate the APJ receptor, with [pyr]^{1}-apelin-13 being the dominant isoform in the cardiovascular system, although the peptides have varying distributions in different organs and systems.[111] A crystal structure of an inactive modified

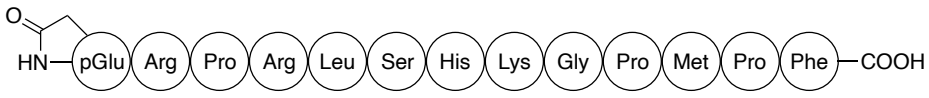

[pyr]^{1}-apelin-13 (**11**)

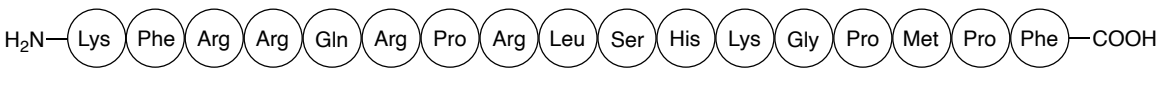

apelin-17 (**12**)

Figure 1-6: Select isoforms of the 77-amino acid prepropeptide of apelin

APJ receptor bound with an inactive peptide derivative provides evidence of two binding sites with the receptor.[112] Unfortunately, these peptides have a half-life of less than 5 mins in plasma due to various proteases that cleave the peptides at these receptor binding sites (*Figure 1-7*).[113] This vastly hinders the peptide's ability to be used as a therapeutic. Angiotensin-converting enzyme 2 (ACE-2) cleaves at receptor binding site 1, specifically at the *C*-terminal phenylalanine residue, partially inactivating the peptide.[114] Neprilysin (NEP) cleaves at two locations in the critical "RPRL" receptor binding site, fully inactivating the peptide,[115,116] while apelin-17 is further cleaved by plasma kallikrein (KLKB1).[117]

1.6.3 Chemical Synthesis

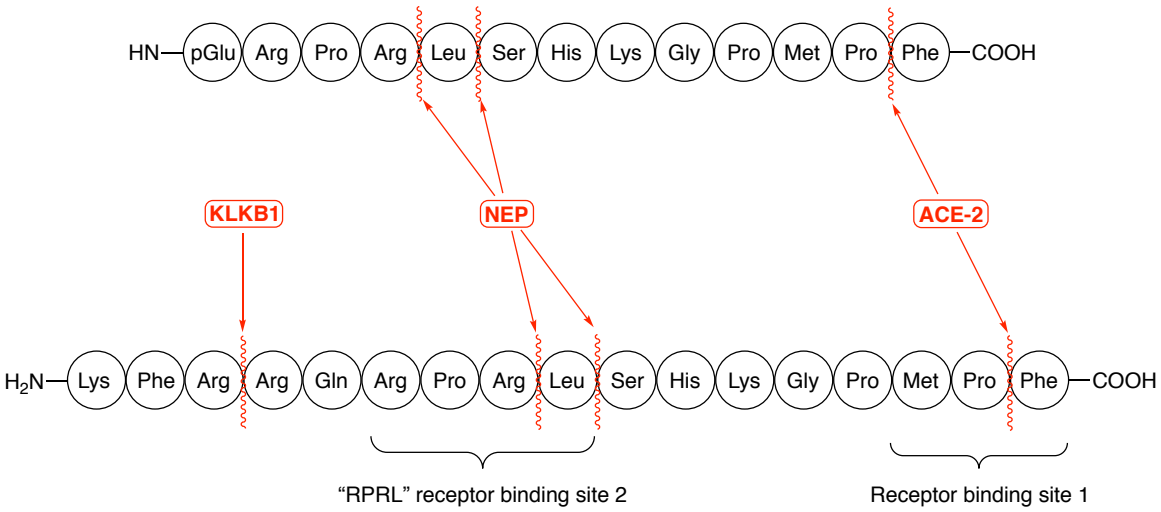

Figure 1-7: Native [pyr]^{1}-apelin-13 and apelin 17 protease cleavage sites

The low half-life of native apelin isoforms in plasma drastically reduces its consideration as a potential therapeutic agent. Our group, and others, have done extensive work to mitigate degradation by ACE-2 on analogues of [pyr]^{1}-apelin-13 and apelin-17, termed "A2" analogues.[110,118] Substitution of the three *C*-terminal amino acids with Nle11, Aib12 and *p*-BrPhe13 (residue numbers based on apelin-13) results in apelin analogues with complete ACE-2 stability, improved pharmacokinetics by virtue of increased plasma stability, but most importantly they retained all advantageous cardiovascular activity.[114] In order to prevent cleavage of the apelin peptides by NEP, Shaun McKinnie tested a myriad of isostere substitutions of Arg4 and Leu5 in the

"RPRL" region. These substitutions included D-amino acid incorporation, *N*-methylation, α-carbon methylation, and aza-linkages. Ultimately, *N*-methylation (termed "NMe" analogues) of the Leu5 residue provided improved proteolytic stability towards NEP and a higher half-life in plasma, coupled with conservation of beneficial cardiovascular effects and receptor recognition.[115] More recently, relatively conservative substitutions of Arg4 with homoarginine and NMeLeu5 with NMe-cyclohexylalanine have contributed to enhanced metabolic stability and physiological effects, indicating some structural promiscuity of the RPRL motif with respect to APF receptor binding.[119] Lastly, the apelin-17 isoform contains an additional KLKB1 cleavage site, but our group discovered that extension of the *N*-terminus with polyethylene glycol (PEG) units, equipped with a terminal head-group resists degradation by KLKB1, and incidentally NEP, but maintains

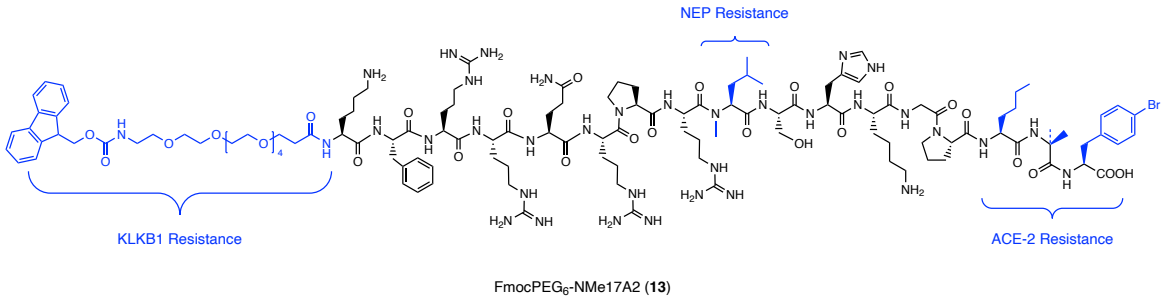

*Figure 1-8: Structure of FmocPEG$_6$-NMe17A2 (**13**), an apelin 17 analogue with improved function and half-life*

excellent activity.[117] Various head-groups, linker types (PEG or palmitoyl) and PEG lengths were tested by our group, resulting in an optimized PEG$_6$ chain bearing an Fmoc head-group. Combining the above modifications results in an apelin-17 analogue **13** with a half-life of over 27 h, as opposed to 5 mins with the native isoforms (*Figure 1-8*).[117,120] Furthermore, the physiological effects were found to be improved upon when compared to the native apelin peptides.[117]

1.6.4 Mode of Action

Apelin was discovered a few years after the initial discovery of the APJ receptor in 1993.[106,121] The GPCR was identified because it bears a high gene sequence homology to the angiotensin II receptor type I; however, it did not seem to interact with angiotensin II, as there was no physiological response when in the presence of this peptide.[121] Therefore, the natural ligand for the APJ receptor was unknown until 1998, when the receptor was

deorphanized due to the discovery of the apelin-36 ligand, found from bovine colostrum extracts.[106]

The APJ receptor contains the characteristic seven hydrophobic transmembrane (TM) regions of GPCRs, with sites for phosphorylation by cyclic adenosinemonophosphate (cAMP), palmitoylation and glycosylation.[121] The receptor is activated by a classic GPCR mechanism: an extracellular ligand, such as apelin, activates the receptor resulting in a structural change in the seven TM helices. This conformational change leads to downstream effects inside the cell. These changes are mediated via a heterotrimeric ($\alpha\beta\gamma$) G protein complex that is bound to the GPCR.[122] This conformational change is conferred to the bound Gα subunit. There are four classes of α subunits, each regulating a different physiological effect.[122] The APJ most closely associates with the $G\alpha_{i/o}$ subunit;[123] however, some reports indicate GPCR signalling of the APJ receptor in some cell lines proceed through the $G\alpha_{q/11}$ subunit.[124] Activation of the primary APJ subunit $G\alpha_{i/o}$ by apelin results in multiple downstream effects (*Figure 1-9 A*). Phosphorylation of ERK (extracellular signal-regulated kinase) and Akt (protein kinase B) are brought on by the conformational change of the GPCR, with adenylyl cyclase (AC) also being inhibited.[123] Akt can then activate eNOS (endothelial nitric oxide synthase), that synthesizes nitric oxide (NO), a critical biological vertebrate messenger, from L-arginine.[125,126] NO promotes vasodilation, increasing blood flow.[125] Akt also leads to activation of mTOR (mammalian target of rapamycin), which promotes angiogenesis.[127] The result is the promotion of two key cardiovascular processes, angiogenesis and vasodilation. The activation of $G\alpha_{q/11}$ subunit has very similar effects via different regulatory enzymes. Beginning with phosphorylation of PLCβ, intracellular levels of Ca^{2+} are elevated, leading to increased calmodulin activity, activating the eNOS pathway, resulting in vasodilation (*Figure 1-9 B*).[128] The aforementioned phosphorylation of ERK results in regulation of cell proliferation, such as upregulating cytoskeletal components for entry into the cell cycle.[129] This pathway can also be activated via β-arrestin recruitment (*Figure 1-9 C*). The result is internalization of the APJ receptor, leading to the eventual activation of ERK.[130] There are still many pathways that require elucidation, such as the exact mechanism through which apelin protects against MIRI. Loss of apelin is associated with increased myocardial cell death following a heart attack,

via increased expression of inflammatory cytokines, metalloproteases and greater neutrophil and macrophage infiltration, although the precise pathway for MIRI protection is still unknown.[110] With a multitude of cardiovascular effects brought on through apelin binding to the APJ receptor, the potential of apelin as a cardio-protective therapeutic is compelling.

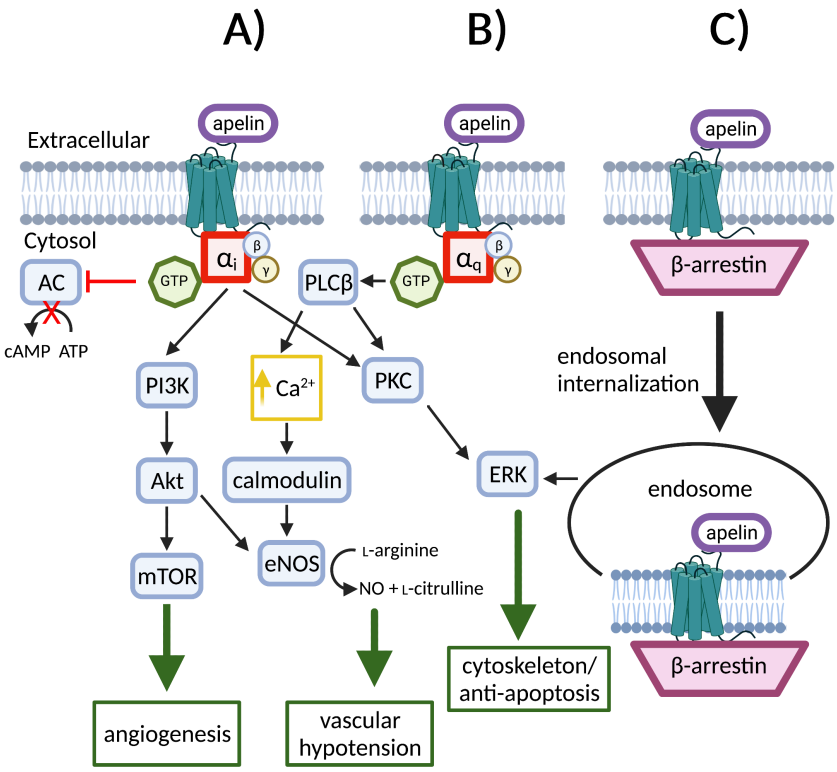

Figure 1-9: Important cardiovascular signalling pathways for apelin-APJ receptor. A) $G\alpha_{i/o}$ subunit activation leads to inhibiting of AC, and downstream activation of eNOS and mTOR pathways; B) $G\alpha_{q/11}$ subunit activation of ERK pathway, and also results in increased intracellular calcium ions, activating eNOS pathway; C) Endosomal internalization of the apelin receptor mediated by β-arrestin, leading to activation of the ERK pathway. AC = adenylyl cyclase, cAMP = cyclic adenosinemonophosphate, ATP = adenosine triphosphate, GTP = guanosine triphosphate, PLCβ = phospholipase C β, PKC = protein kinase C, ERK = extracellular signal-regulated kinase, PI3K = phosphoinositol 3 kinase, Akt = protein kinase B, eNOS = endothelial nitric oxide synthase, NO = nitric oxide, mTOR = mammalian target of rapamycin. Figure made with BioRender.com; Figure adapted from Chapman et al.[128], Kalea et al.[127] and Dr. Shaun McKinnie's thesis.

2 Chapter 2: Development and Synthesis of Orthogonally Protected Diamino Diacids

2.1 Introduction to Diamino Diacids

2.1.1 Pre-Stapling of Peptides

Peptidic macrocycles have become a thrilling area of research for peptide-based therapeutics. As previously discussed, incorporation of macrocycles confers an abundance of positive effects for peptides. Many methods for their incorporation rely on cyclization using heteroatoms, such as lactones, lactams and disulfides.[24] These linkages themselves possess certain drawbacks, as they can be broken down due to their chemical susceptibilities.[131–133] An alternative is ring closing metathesis (RCM) of olefinic residues in the peptide sequence to form the cyclic linkages with much more robust C-C bonds.[134] A double bond is produced, and unless measures are taken to control the double bond geometry,[135] the result is often a mixture of *E*- and *Z*-isomers, which can be difficult to separate from one another.[134,136] Reduction of the double bond by catalytic hydrogenation alleviates the stereochemical issue;[136] however, this is difficult to do in some cases, such as for inaccessible double bonds in bulky peptides, or hydrogen sensitive groups. Unfortunately, RCM is not possible with certain peptides, due to self-aggregation or conformation of the peptide.[137] A similar result can be achieved through incorporation of orthogonally protected chiral diamino diacids (DADA).[138,139] Unlike RCM, where the cyclization step is conducted after the peptide has been completed, DADAs are incorporated during SPPS and the macrocycle is formed as the peptide is built out from the resin (*Figure 2-1*). This pre-stapling of the peptides induces a 3-dimensional structure to the peptide as it is growing, which may help further cyclizations occur more readily. A tremendous advantage of the DADA strategy is its ease of use. Both ends of the macrocycle are incorporated through amide bond formation, a reaction that has been exceedingly optimized for SPPS; therefore, these amino acid building blocks are readily amenable to peptide synthesis.[140] Additionally, there is a wide variety of DADAs that can be used to fine-tune the ring size for peptides.

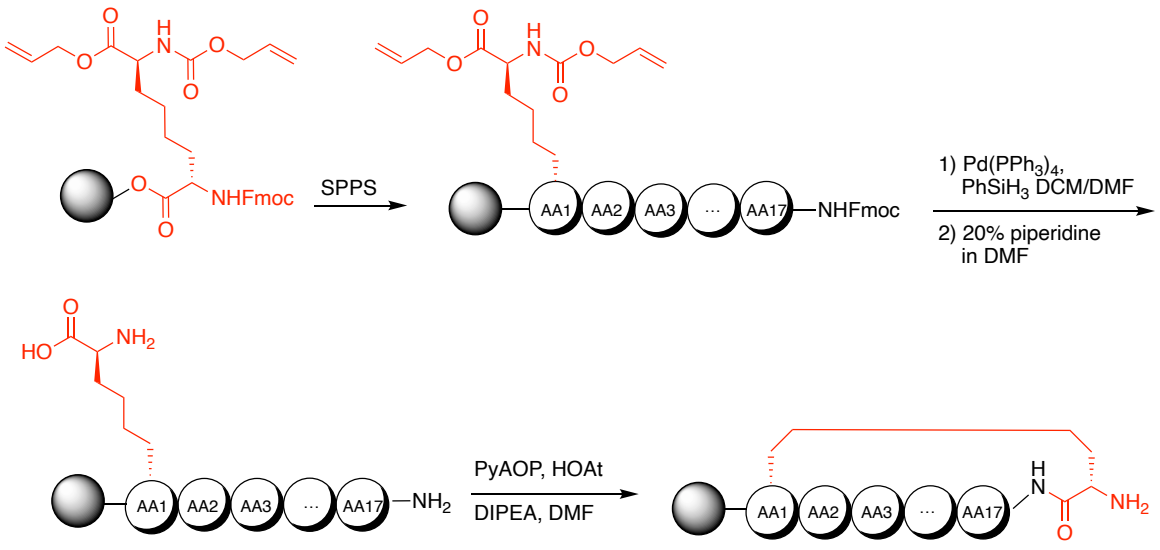

Figure 2-1: General strategy for incorporation and cyclization of orthogonally protected diamino diacids

2.1.2 Diamino Diacids as Surrogates for Sulfur

Though the use of orthogonally protected diamino diacids is attractive for generating peptide macrocycles, there is also a growing application for their use as isosteres. Replacement of sulfur in peptide linkages by methylene or methine to generate more stable peptide analogues is of great interest to our group, and others.[139–142] The reasoning behind replacing sulfur is based on metabolic stability. Sulfur-based linkages are rapidly reduced *in vivo* by endogenous glutathione, abolishing peptide activity and leading to faster clearance from the body as they are detoxified by glutathione.[131,143] Selectively protected diamino diacids are an excellent candidate to mimic these native linkages, while producing more metabolically stable peptides. Diaminoadipic acid (**14**) could potentially be used to mimic base sensitive sulphur to alpha carbon linkages seen in sactibiotics,[144] diaminosuberic acid (**15**) (DAS) is excellent at replacing disulfide bridges,[140] while naturally occurring diaminopimelic acid (**16**) (DAP), found in the cell wall of Gram-negative bacteria,[145] is an effective lanthionine mimic (*Figure 2-2*).[146] Certain peptides with naturally occurring disulfide linkages have had one, or both of the sulfurs replaced with carbon and retained activity comparable to the parent peptide, while showing increased metabolic stability.[147–149] Unfortunately, sulfur to carbon replacements

are accompanied by a change in bond length. The average bond length of a S-S bond is 2.0 Å, due to the larger size of the atoms, while the average C-S bond is shorter, around 1.8 Å, and the average C-C bond is 1.5 Å.[150] This decrease in bond length when replacing sulfur with carbon may alter or abolish the activity of the peptide. However, studies have shown that such replacements can lead to active compounds, in part due to the preference of sulfur to possess a dihedral angle close to 90º, making up for disparity in bond length.[149] Overlaid energy-minimized structures of oxytocin and a dicarba analogue revealed very little difference in the overall 3D structure and the activity of the analogue was not perturbed.[149] Certainly, the use of orthogonally protected DADA as a surrogate for sulfur is of great interest and possesses many advantages over RCM methods to introduce macrocycles.

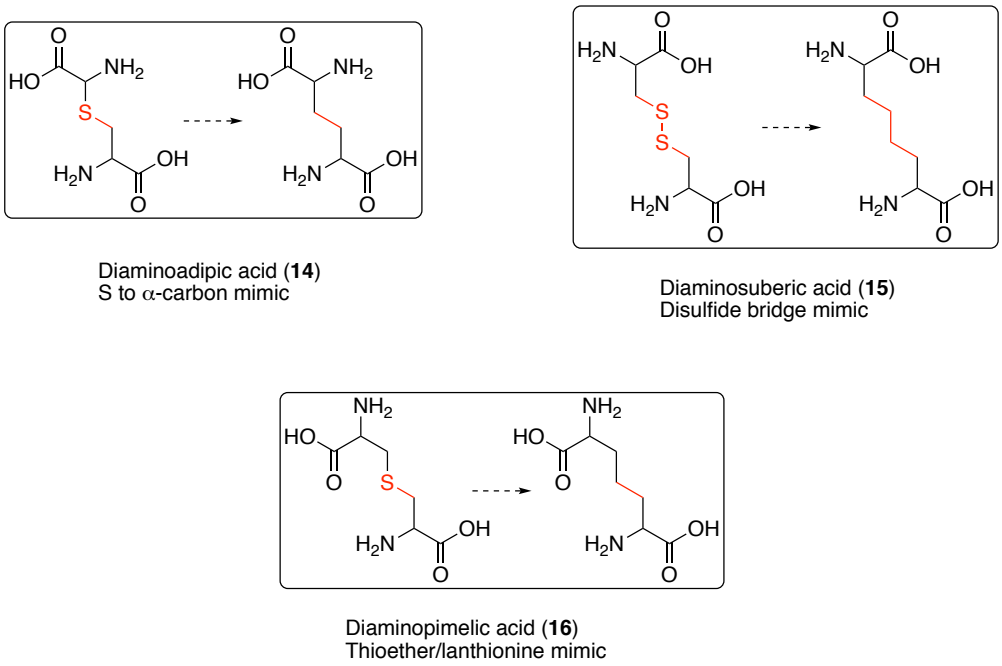

Figure 2-2: Natural sulphur linkages and their diamino diacid counterparts.

2.1.3 Accessing Diamino Diacids

Despite the many advantages that the diamino diacids afford, synthesis of these building blocks is often long and tedious. It involves bringing together two orthogonally protected amino acids and forming a C-C bond between the two halves, without scrambling the stereochemistry of the amino acids. There exist multiple ways to synthesize the diamino diacids, each with their own pros and cons. Arguably the most

direct route to obtain the necessary building blocks is via cross-metathesis.[151] This method takes two olefinic halves (**17** and **18**), each protected with specific protecting group, and joining them together by using a catalyst, such as Grubbs catalyst, followed by hydrogenation, to generate the orthogonally protected diamino diacid **19** (*Scheme 2-1 A*). This method is quite straightforward and scalable, but it utilizes solution phase cross coupling. The downside to this method is often there is a statistical 1:2:1 mixture of products, resulting in yields less or equal than 50% for this key step. Furthermore, the undesired homocoupling side products are usually difficult to separate via column chromatography depending on the protecting groups used due to their similar polarity. This can be circumnavigated using the protecting group scheme illustrated. Our group has a particular interest in DADAs due to our work with sulfur containing peptides; thus we have helped develop alternate routes to complement the above method. Dan Spantulescu pioneered the application of diacyl peroxides towards making diamino diacids.[152] This method involves the synthesis of a diacyl peroxide functional group inserted between either end of the diamino diacid **20** (*Scheme 2-1 B*). Upon exposing this molecule to UV light, radical decarboxylation occurs to produce a primary radical on either end, which recombine, without scrambling at low temperatures, to yield an orthogonally protected DADA **21**. While innovative, it is difficult to scale up, must be run for a number of days to observe transformation, and is low yielding if not attentive to the temperature. Recently, Yu-Ting Hsiao of our group modified the work of Phil Baran[153] to efficiently synthesize stereocontrolled diamino diacids.[154] This method employs an enantiopure methylideneoxazolidinone **22** functioning as a radical dehydroalanine radical acceptor, and a redox-active *N*-hydroxyphthalimide ester, glutamic acid derivative **23** (*Scheme 2-1 C*). Upon reaction of the *N*-hydroxyphthalimide with the redox additives listed, a radical decarboxylation occurs following cleavage of the N-O bond, generating a primary radical. The radical can add in a stereochemically controlled, conjugate fashion to generate the diamino diacid **24**. This method provided modest yields for the key C-C bond formation step and has excellent stereochemical control. However, it has not yet been scaled up and certain redox-active esters have proven to be unstable and can decompose. It should be noted that the diamino acids depicted in *Scheme 2-1* are protected versions of *meso*-DAP as an example. These methods are also applicable to the synthesis of selectively protected

DAS, and the method developed by Yu-Ting Hsiao is also amenable to the synthesis of orthogonally protected diaminoadipic acid. These schemes also depict protecting groups that are not orthogonal to SPPS, but are used in the synthesis for ease of purification or further manipulation. After acquiring the DADAs described, a protecting group shuffle is required to prepare them for incorporation into SPPS. There are still new synthetic routes being developed to improve the accessibility of DADAs[155] for their application in multiple different areas of research.

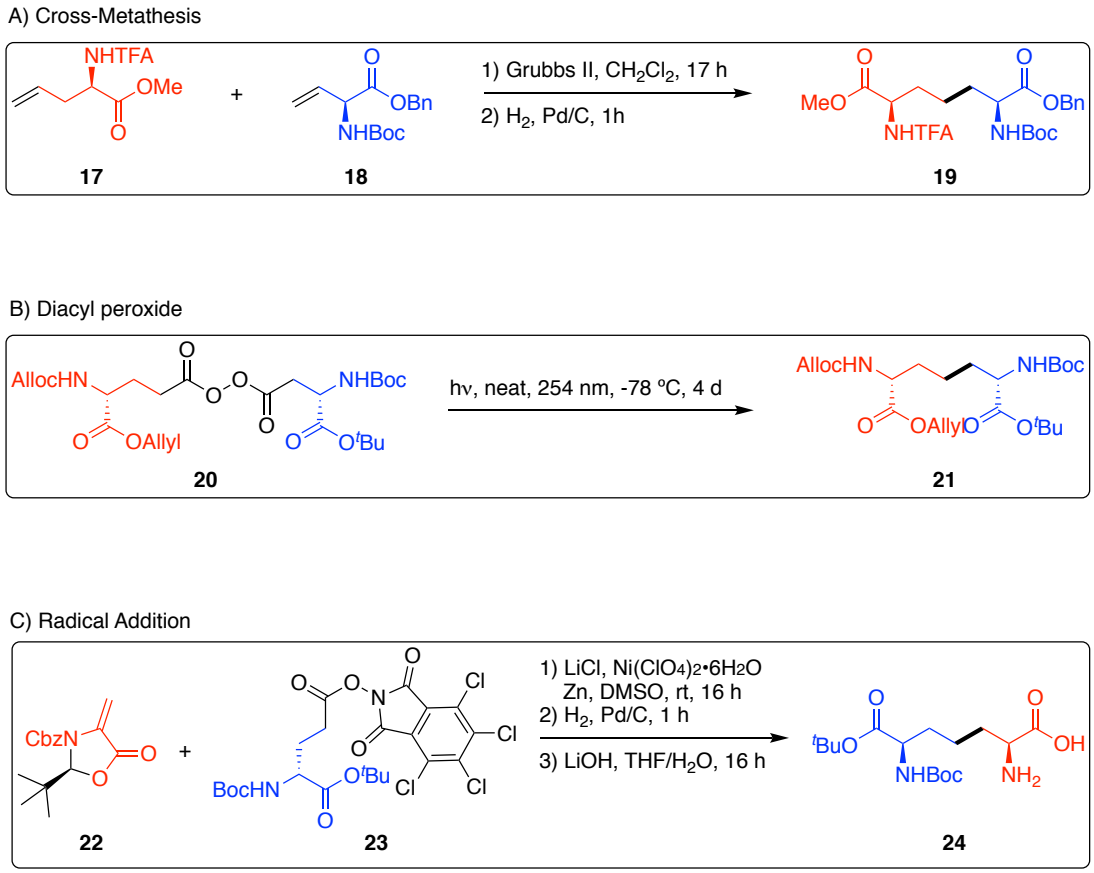

Scheme 2-1: Select methods to generate selectively protected meso-diaminopimelic acid as an example. New C-C bond is bolded. A) Cross-metathesis of olefins; B) UV irradiation of diacyl peroxides; C) conjugate radical addition to chiral dehydroalanine

2.2 Resin-Assisted Diamino Diacid Synthesis

As will be discussed in the chapters to come, there was a growing interest to develop a new method for the rapid synthesis of orthogonally protected diacids, preferentially ones that would be applicable for SPPS without much protecting group tailoring. In particular, there was a need for orthogonally protected diaminosuberic acid.

Using a solid support to complement the synthesis was identified as being beneficial, with the overall goal being an SPPS-ready DADA containing an *N*-terminal Fmoc and free *C*-terminus. Any chemistry conducted on solid support to generate a building block would have to be orthogonal to the cleavage conditions for the resin; thereby also making the building block compliant to rigours of SPPS. Using cross-metathesis to join the two olefins together, one olefin could be affixed to resin, while the other was added in solution in vast excess, along with a catalyst to join the two fragments together, followed by hydrogenation to reduce the double bond (*Scheme 2-2*). Low resin loading (~0.1 mmol/g) would afford a high effective dilution on resin, mitigating the interactions between the amino acids on the solid support. Moreover, any undesired homocoupling product between the moieties in solution could be washed out, leaving only the desired cross-metathesis product affixed to the resin. Ideally, the orthogonally protected diamino diacid could then be cleaved off resin and purified, if needed, by column chromatography.[156–158]

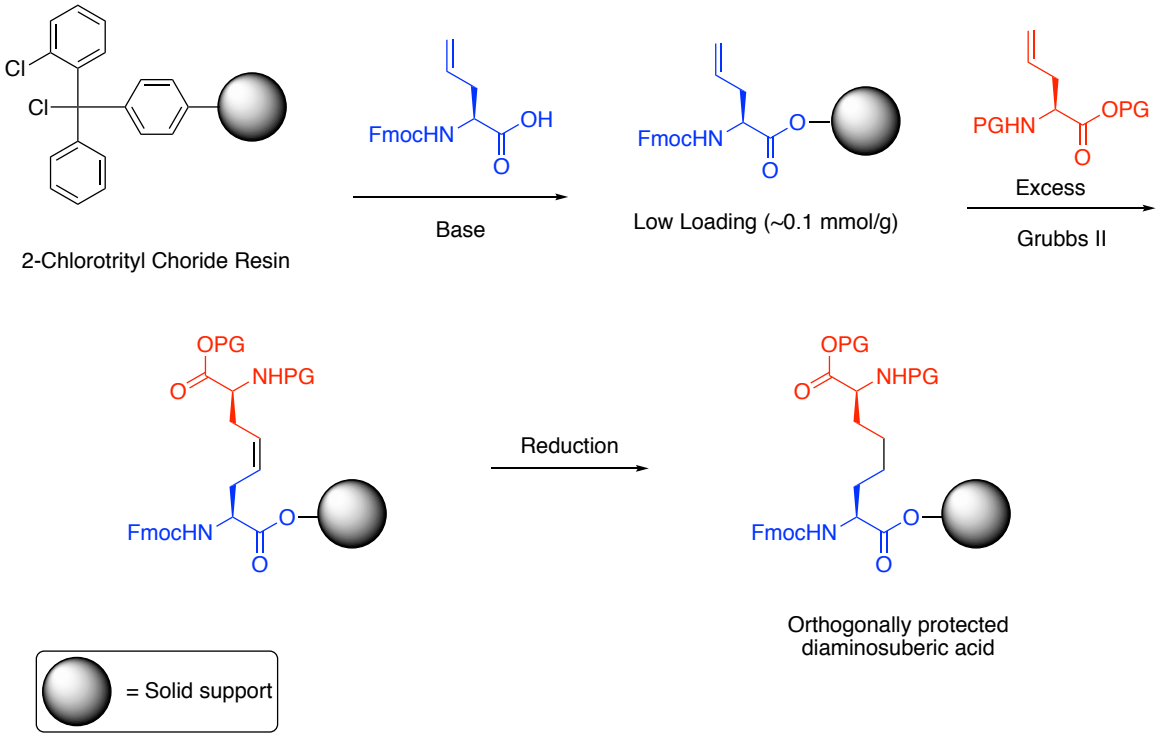

Scheme 2-2: General proposed scheme for resin assisted synthesis of diaminosuberic acid.

2.3 Results of Resin-Assisted Synthesis

2.3.1 Synthesis of Protected Amino Acids

The first step was to determine a set of protecting groups that would work with the chemistry proposed. Ultimately, allyl/alloc protecting groups, although routinely used in SPPS for their orthogonality, would not be compatible with double bond reduction or alkene metathesis. There were two main protecting group schemes proposed that would be orthogonal to SPPS and the resin cleavage conditions, depending on the choice of resin. The first proposed set of protecting groups were 2-(trimethylsilyl)ethyl (TMSE)[159] and 2-(trimethylsilyl)ethoxycarbonyl (Teoc),[160] which could be cleaved using a fluoride source such as tetrabutylammonium fluoride (TBAF), or by anhydrous TFA (*Scheme 2-3 A*). The second proposed scheme made use of *p*-nitrobenzyl (*p*NB)[161] and *p*-nitrobenzyloxycarbonyl (*p*NZ)[162] which can be removed with 6 M $SnCl_2$ in DMF (*Scheme*

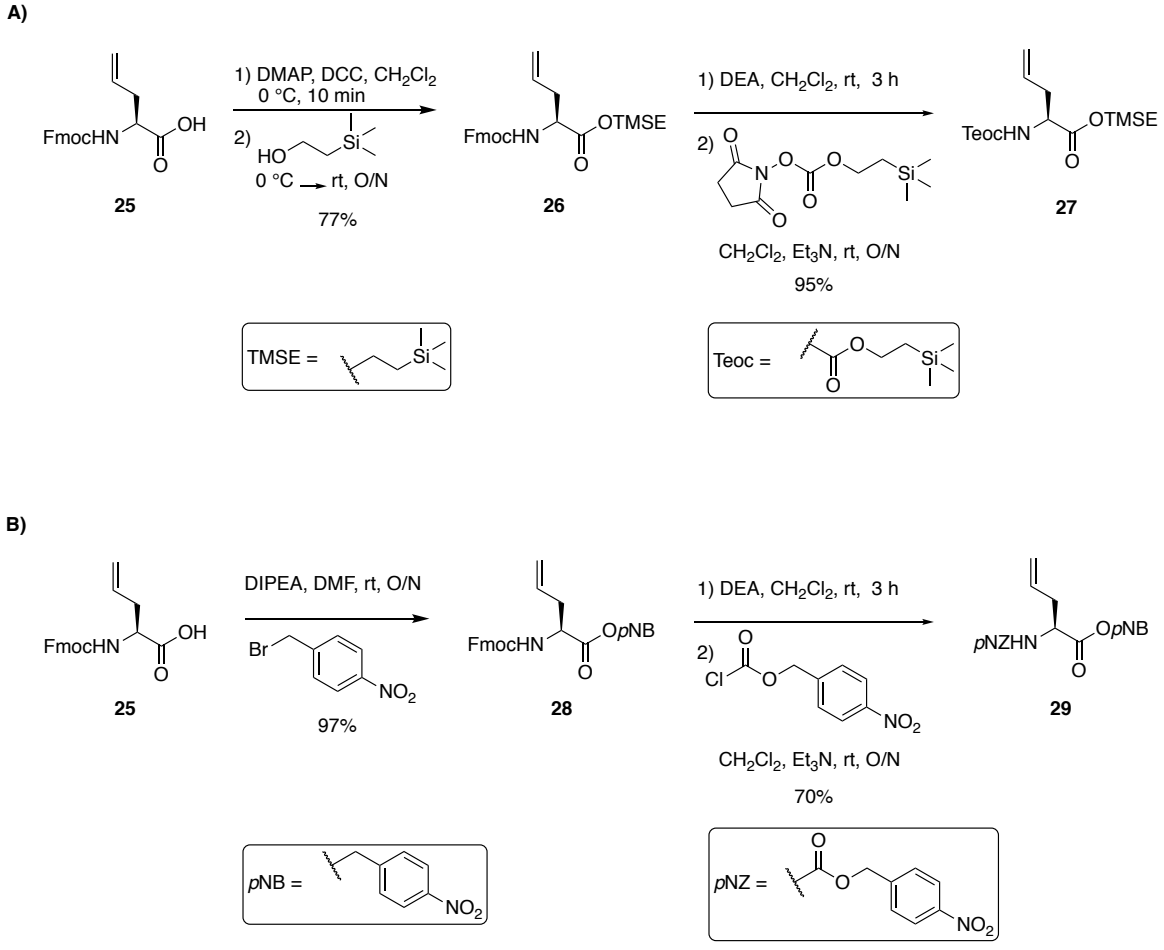

*Scheme 2-3: Synthesis of protected allyl glycines A) **27** and B) **29***

2-3 B). Starting from commercially available Fmoc-allylglycine-OH (**25**), the carboxylic acid was protected as TMSE ester **26**, by dicyclohexylcarbodiimide (DCC) activation in the presence of dimethylaminopyridine (DMAP) in 77% yield. The Fmoc group was removed with diethylamine (DEA) and the crude mixture was stirred with 1-(2-(trimethylsilyl)ethoxycarbonyloxy)pyrrolidin-2,5-dione (Teoc-OSu) and triethylamine (Et_3N) as a base to give the fully protected allyl glycine **27** in 95% over two steps. Synthesis of the *p*NB/*p*NZ protected amino acid was done in a very similar fashion. Starting from **25**, a nucleophilic displacement by the carboxylate onto *p*-nitrobenzyl bromide produced **28** with near quantitative yields. Subsequent Fmoc deprotection with DEA and reaction of the crude amine with *p*-nitrobenzyloxycarbonyl chloride with Et_3N furnished **29** in 70% over two steps. With fully protected allyl glycines **27** and **29** in hand, attempts to cross-couple them with a resin bound allyl glycine began.

2.3.2 Cross-Metathesis on 2-Chlorotrityl Chloride Resin

There are many different types of resins with different chemical susceptibilities; however, polystyrene based 2-chlorotrityl chloride and Wang resin were the ones chosen to try the cross metathesis. Beginning with 2-chlorotrityl chloride resin, allylglycine **25** was loaded onto the solid support with *N*,*N*-diisopropylethylamine (DIPEA) with a loading of 0.1 mmol/g (*Scheme 2-4*). Remaining sites on the resin were then capped using methanol and DIPEA to give the loaded resin **30**. To conduct the cross-metathesis a procedure was adapted according to the literature.[158] Initially, the loaded resin **30** was suspended in degassed 1,2-dichloroethane (DCE), followed by Grubbs second generation catalyst and heated to 70 °C. This was stirred for 5 mins to let the reaction equilibrate under argon. To this, a large excess of dissolved amino acid **27** was added and stirred for 4 h with a slow, constant stream of argon bubbling through the system. The resin was filtered and the entire reaction was repeated once more with fresh reagents/solvents to ensure cross-metathesis occurred. Following the second round of reactions, the resin was cleaved with hexafluoroisopropanol (HFIP) and the solid support was filtered. Analysis of the filtrate by LCMS showed no desired product **31**, but had a fair amount of the homodimer **32**, indicating that despite low resin loading, there was still interaction between the resin bound amino acids. The major component of the mixture was unreacted

Fmoc-allylglycine. Attempted purification of the homodimer **32** by silica for future reference was unsuccessful.

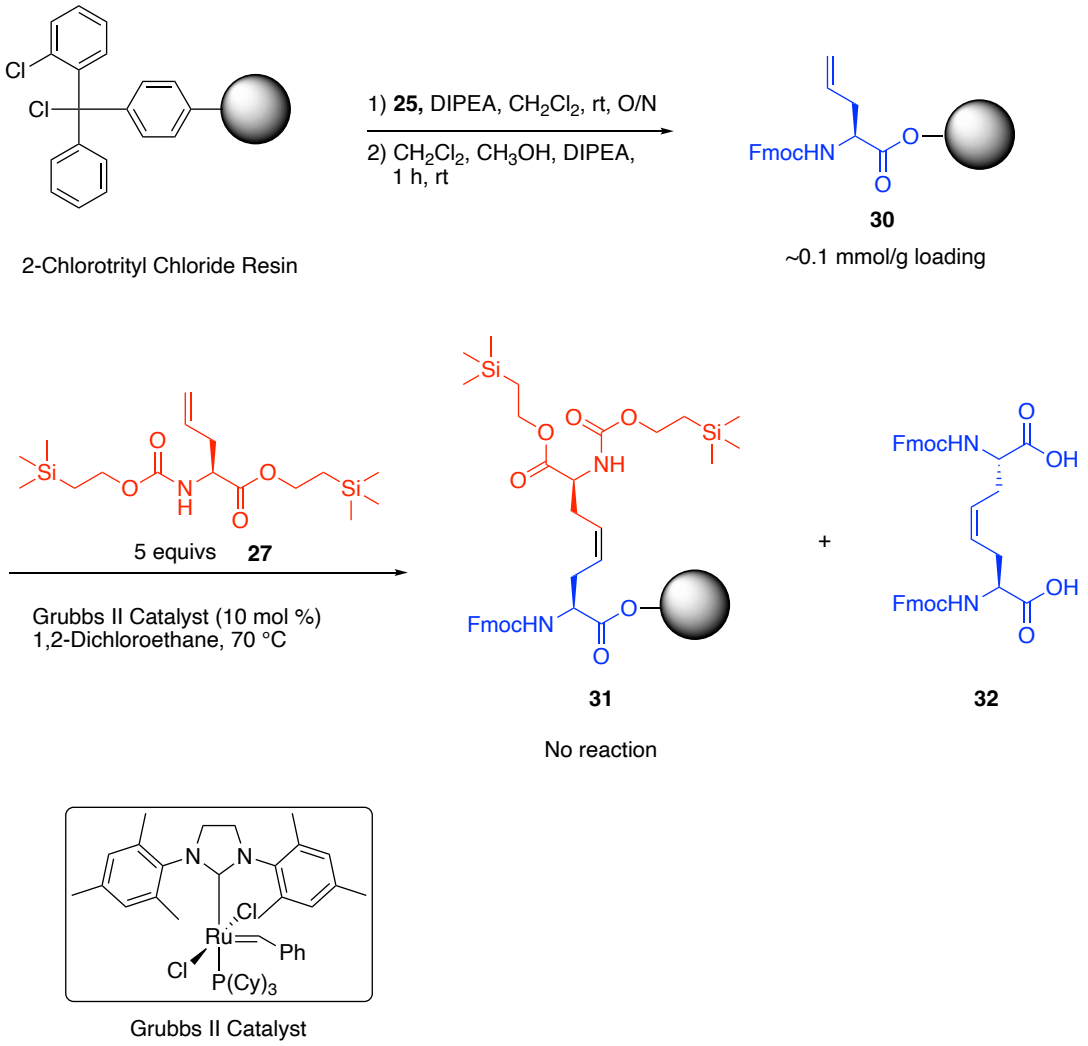

*Scheme 2-4: Loading of 2-chlorortrityl chloride resin and subsequent cross-metathesis with **27***

It was thought that pre-incubation of the catalyst with **30** may have promoted conversion to the homodimer, so the reaction was repeated as above but the fully protected amino acid **27** was added to **30** prior to addition of the catalyst. This was stirred for a few minutes, and then followed by the addition of Grubbs II catalyst. The reaction was repeated twice more with fresh reagents. Cleavage of the resin and filtrate analysis by LCMS showed a lower amount of homodimer **32** but there was still no trace of the

Entry	Rounds of Metathesis (n)	Amount of **27** (equiv)	Catalyst Amount (mol %)	Addition of catalyst prior to **27**?	Product (**31**) Present?	Homodimer (**32**) Present?
1	2	5	10	Yes	No	Yes
2	2	3	10	No	No	Yes
3	3	10	10	No	Trace	Yes
4	3	10	10	No	Trace	Yes
5	2	10	15	No	Trace	Yes
6	2	20	10	No	Trace	Yes

*Table 2-1: Optimization conditions for reaction between **27** and **30***

product. A look into the literature showed that repeated rounds on the cross-metathesis and higher equivalents of the amino acid added in solution worked for other applications.[156,163]

Attempts to optimize the reaction can be seen in *Table 2-1*. The time for each round of metathesis was 4 h if only two rounds were done, any third rounds were conducted overnight. As is evident, there was only ever trace amount of product being formed according to LCMS and was not detectable on TLC, thus was not easily purified. Despite a large excess of **27** being added as the literature suggested, the product was not forming, with the majority of the mixture being unreacted Fmoc-allylglycine. It was theorized that due to the steric bulk of the resin, the catalyst and the protecting groups on **27**, there was too much steric hindrance to easily facilitate cross coupling between the two olefin moieties. The reaction was therefore attempted again with the smaller Wang resin to try and reduce the steric bulk around the reacting substrates.

2.3.3 Cross-Metathesis on Wang Resin

Using Wang resin could alleviate some steric bulk, but unfortunately, the Teoc/TMES protecting groups would likely be removed under TFA conditions required to cleave the product from the resin, so the amino acid was switched to **29**. With a less bulky resin, the rate of homodimerization would likely also increase in accordance with the results seen from 2-chlorotrityl chloride resin. The general approach was similar to previous, except when loading the resin with Fmoc-allylglycine **25**. The olefin **25** was mixed with Boc-Ala-OH (1:5) and the mixture was coupled onto the resin using *N,N′*-

diisopropylcarbodiimide (DIC), DMAP and 1-hydroxybenzotriazole (HOBt) (*Scheme 2-5*) to give low loading (0.1 mmol/g) of **25** on resin. The remaining sites were occupied by Boc-Ala-OH. Boc-Ala-OH to try to fill the vacant space between the olefinic amino acids loaded onto the resin. This would hopefully reduce any allylglycine homocoupling by filling the interstitial space between loading sites on the resin. This step was then repeated again but without any Fmoc-allylglycine, to ensure coupling of any remaining open sites, and finally capped with pyridine and acetic anhydride (Ac_2O) to provide the loaded resin **33**.

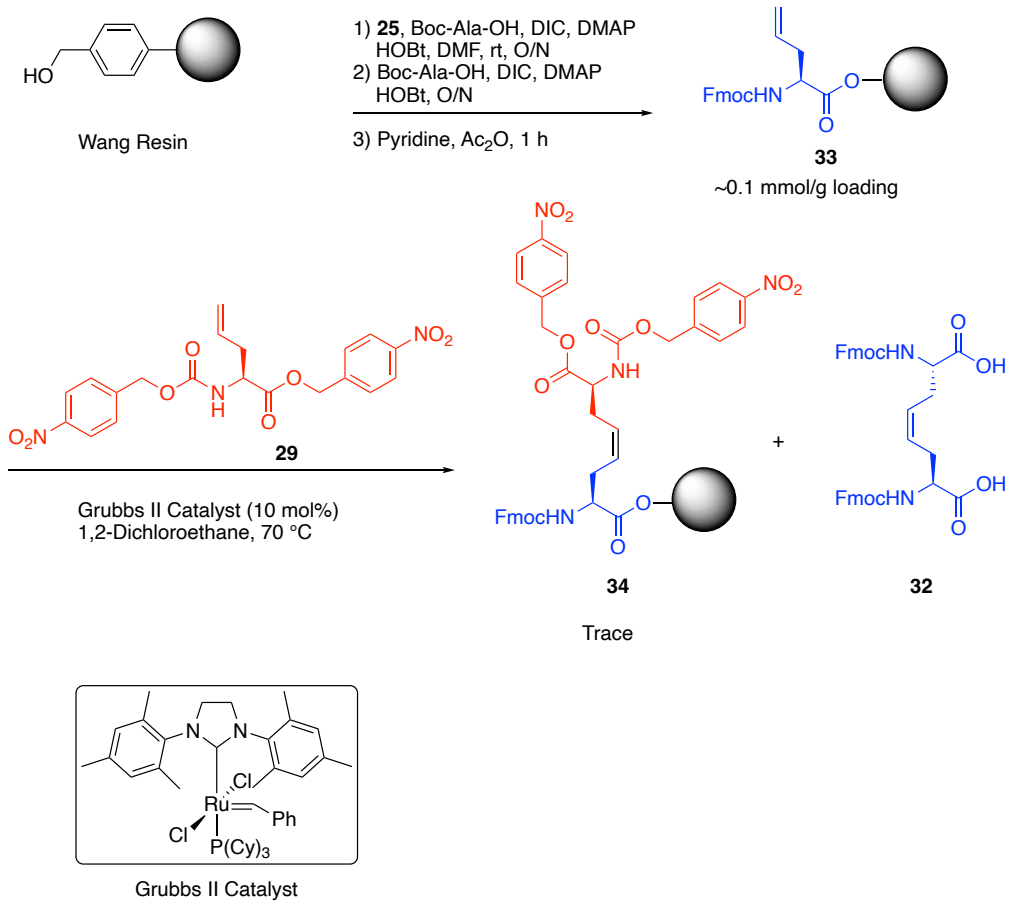

*Scheme 2-5: Loading of Wang resin and subsequent cross-metathesis with **29***

The first attempt at cross metathesizing the protected allylglycine **29** with the freshly loaded resin **33** was done almost the same way, except Grubbs II catalyst was always added after amino acid **29** was added. Unfortunately, there was still only a trace amount of product, substantial homodimer **32** and primarily starting material observed by

LCMS analysis. Further attempts at optimization were conducted, including varying the amino acid loaded on the resin in place of Boc-Ala-OH (*Table 2-2*).

Despite repeated attempts at optimization of the conditions, changing the resin and the protecting groups, there was only ever trace amount of product. While it seems like the amount of homodimer **32** decreased with the addition of a bulkier amino acid based on entries 4 and 5 in *Table 2-2*, this did not correlate with noticeable increase in product. Attempts to purify the little amount of product or side product were unsuccessful. Homodimerization is a seemingly unavoidable problem to combat when trying to use this methodology even on resin.[157]

Entry	Rounds of Metathesis (n)	Time per Round	Amount of **29** (equiv)	Catalyst Amount (mol %)	A.A Loaded with **25**	Product (**34**) Present?	Homodimer (**32**) Present?
1	2	4	5	10	Ala	Trace	Yes
2	2	8	5	10	Ala	Trace	Yes
3	3	4	10	10	Ala	Trace	Yes
4	3	4	10	10	Val	Trace	Trace
5	2	8	10	15	Val	Trace	Trace
6	2	4	5	10	None	Trace	Yes
7	2	4	10	10	None	Trace	Yes

*Table 2-2: Optimization conditions for reaction between **29** and **33***

2.3.4 Future Considerations

A great many conditions were altered and tested in a substantial effort to try to get an orthogonally protected diamino diacid on resin. Although the reaction did not proceed as desired, there are still avenues that could be tested. A variable that was left constant through the process is the catalyst and there are reports of using Hoveyda-Grubbs catalyst rather than Grubbs II.[156,163] Perhaps the temperature needs to remain low to decrease the flexibility of the chains on resin, but this may reduce overall metathesis. Because a cross-metathesized product was not obtained, the reduction of the double bond was not attempted. The simplest way to reduce the double bond would likely be hydrogenation; however, this would not be compatible with the *p*NB/*p*NZ protecting group scheme.

Instead, a diimide based approach to reduce the olefin could be an effective substitute.[164] The reaction in principle seems promising, but it appears to lack the ease of scaling up. If the reaction were optimized to give higher yields, many grams of resin would still be needed and an exorbitant amount of the protected amino acid in solution would be required. This methodology would likely be ideal for the immediate synthesis of a peptide from the amino acid produced on resin.

2.4 Development of Robert Williams Methodology

2.4.1 Robert Williams Scaffold

Given that a large amount of orthogonally protected diamino acids were sought for Chapters 3 and 4, an alternative method was explored. To acquire the large amounts needed, the method used by Robert Williams to synthesize differentially protected diaminosuberic acid was employed (*Scheme 2-6*). [165] This ingenious method uses a 1,2-benzenedimethanol scaffold to facilitate an intramolecular cross-metathesis to out-

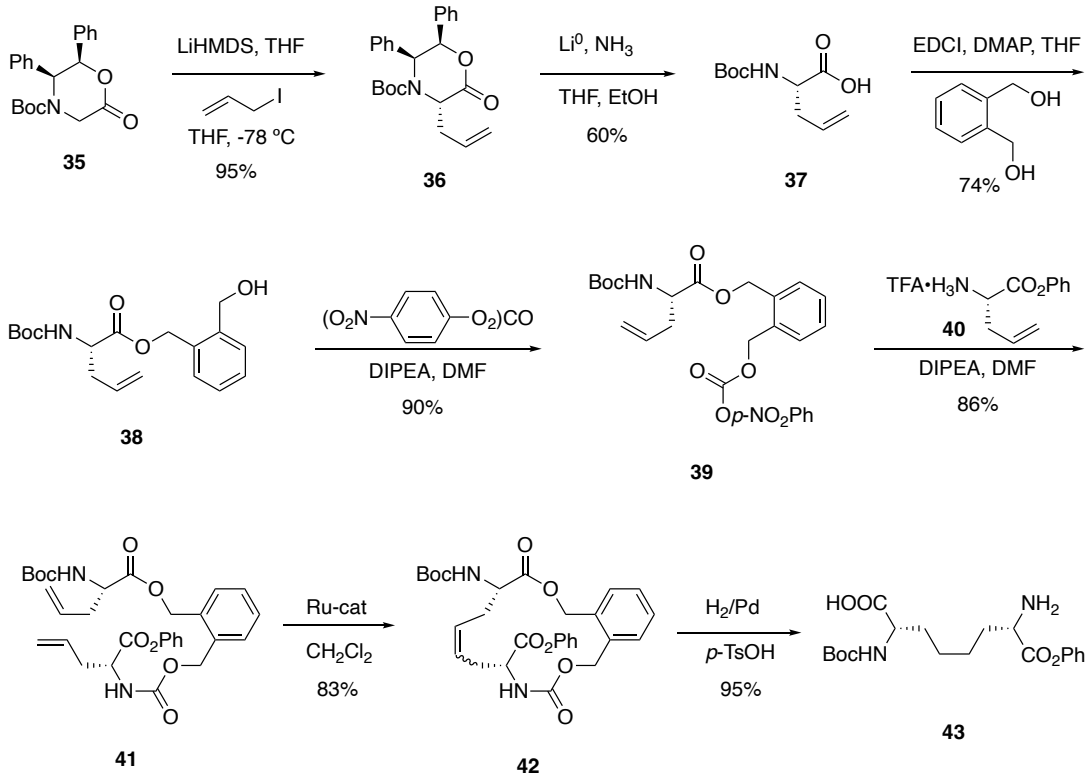

Scheme 2-6: The original scheme developed by Dr. Williams and coworkers to synthesize differentially protected diaminosuberic acid ***43***

compete intermolecular interactions. The scaffold can then be removed using simple hydrogenolysis. Instead of purchasing allylglycine, Dr. Williams and coworkers used their previously developed diphenyloxazinone **35**[166] to alkylate a glycine moiety with allyl iodide, to generate **36** as a single diastereomer. A dissolving metal reduction provides the required allyl glycine **37**. Condensation onto the 1,2-benzenedimethanol scaffold produces **38** as the monosubstituted product. Using a vast excess of the scaffold in the reaction mixture drastically reduces formation of the disubstituted scaffold side product. The unreacted scaffold can easily be recovered during purification of the reaction mixture on silica. The monosubstituted product **38** is subjected to phosgene type chemistry using bis(*p*-nitrophenyl) carbonate to give **39**.[167] Reaction of this with amino acid **40**, made in 2 steps from **37** gives the di-alkene **41**. Cross-metathesis using a Grubbs ruthenium catalyst forms the key C-C bond between the two ends to give **42** with no homodimerization observed, provided the reaction is conducted in dilute conditions (0.005 M). Subsequent hydrogenation reduces the double bond and removes the scaffold to provide differentially protected diaminosuberic acid **43**. The advantage to the above route is that it eliminates the caveat of traditional cross-couplings of a 1:2:1 statistical mixture of products, greatly increasing the overall theoretical yield for this critical bond formation. The product **43** could then be altered for use on SPPS.

2.4.2 Expanding on the Applicability of the 1,2-Benzenedimethanol Scaffold

The ease with which an orthogonally protected DAS building block could be made with this method prompted questions about whether it could be used to create DADAs of varying lengths. There exists a need for DADAs for many reasons, such as creating macrocycles of differing sizes, isostere substitution and even for synthesizing lipid II to study the cell wall of Gram-negative bacteria.[145] As a result, an expansion on Robert Williams chemistry was done to make it pertinent to production of different diamino diacids that are immediately amenable to SPPS (*Figure 2-3*). DAS analogue **44** was the first to be synthesized, following by DAP analogues **45** and **46**. *meso*-DAP analogue **46**, synthesized by Daniel Engelhardt, is a lanthionine isostere for lantibiotics,[168] as well as a crucial building block for bacterial cell wall precursors, while LL-DAP **45** is a stereoisomer that is beneficial for introducing macrocycles into peptides. The longer DADA analogues, diaminoazelaic acid **47** and diaminosebacic acid **48** are not direct

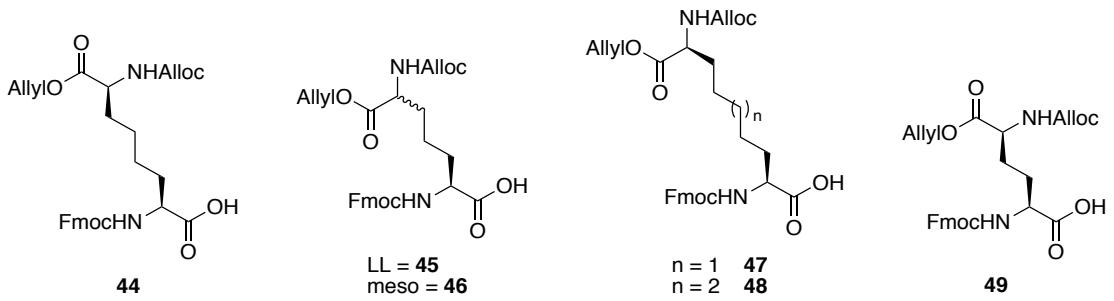

Figure 2-3: Various SPPS ready, orthogonally protected diamino diacids that were attempted to be synthesized using Dr. Williams 1,2-benzenedimethanol chemistry.

isosteres for any known linkages in peptides, but they can incorporate larger macrocycles into peptides and can possibly be used to study the effect of ring expansion of natural disulfides, while replacing the sulfurs with carbon. The last DADA **49** was unable to be made using the chemistry described, but significant progression was made towards its synthesis. However, our group has made considerable progress towards the accessibility of orthogonally protected diaminoadipic acid.[154]

2.5 Results of 1,2-Benzenedimethanol Chemistry Development

2.5.1 Synthesis of Orthogonally Protected LL-Diaminosuberic Acid

Commercially purchased Boc-L-allylglycine **37** was first subjected to *C*-terminal protection by reacting it with *tert*-butyl 2,2,2-trichloroacetimidate (*Scheme 2-7*). The long reaction time is necessitated by the nature of the reaction, as it proceeds slowly via an S_N1 mechanism to generate a *tert*-butyl cation, which is trapped by the carboxylate of **37**. The trichloroacetamide by-product was removed by filtration and the crude mixture was carried forward without purification. Boc deprotection with TFA and subsequent purification provided the TFA salt **50** in 78% yield over two steps.

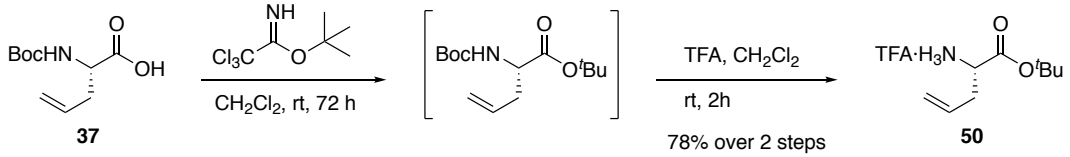

*Scheme 2-7: Synthesis of C-terminal protected L-allylglycine **50***

Using the same initial methodology as *Scheme 2-6*, commercially purchased Boc-L-allylglycine **37** was coupled to 1,2-benzenedimethanol to give **38** in 82% yield, followed by reaction with bis(*p*-nitrophenyl) carbonate to furnish **39** with 95% yield

(*Scheme 2-8*). During the synthesis of **38**, upwards of 8 equivalents of 1,2-benzedimethanol was added, yet there were still small amounts of the disubstituted product detected by LCMS. Extensive washing (~1 L per mmol) of the reaction mixture with saturated aqueous Na_2CO_3 solution was required to remove the *p*-nitrophenol by-product. Immediately performing column chromatography on the crude mixture led to substantial co-elution of *p*-nitrophenol with **39**. Investigation into the need for excessive washing led to the discovery that sodium carbonate consumed any residual bis(*p*-nitrophenyl) carbonate, generating additional *p*-nitrophenol. This could be fixed by triturating the crude reaction with diethyl ether at -78 ºC and filtering the suspended unreacted bis(*p*-nitrophenyl) carbonate. The workup was greatly shortened via this method. Amino acid **50** was then added to **39** to provide the desired di-alkene for cross

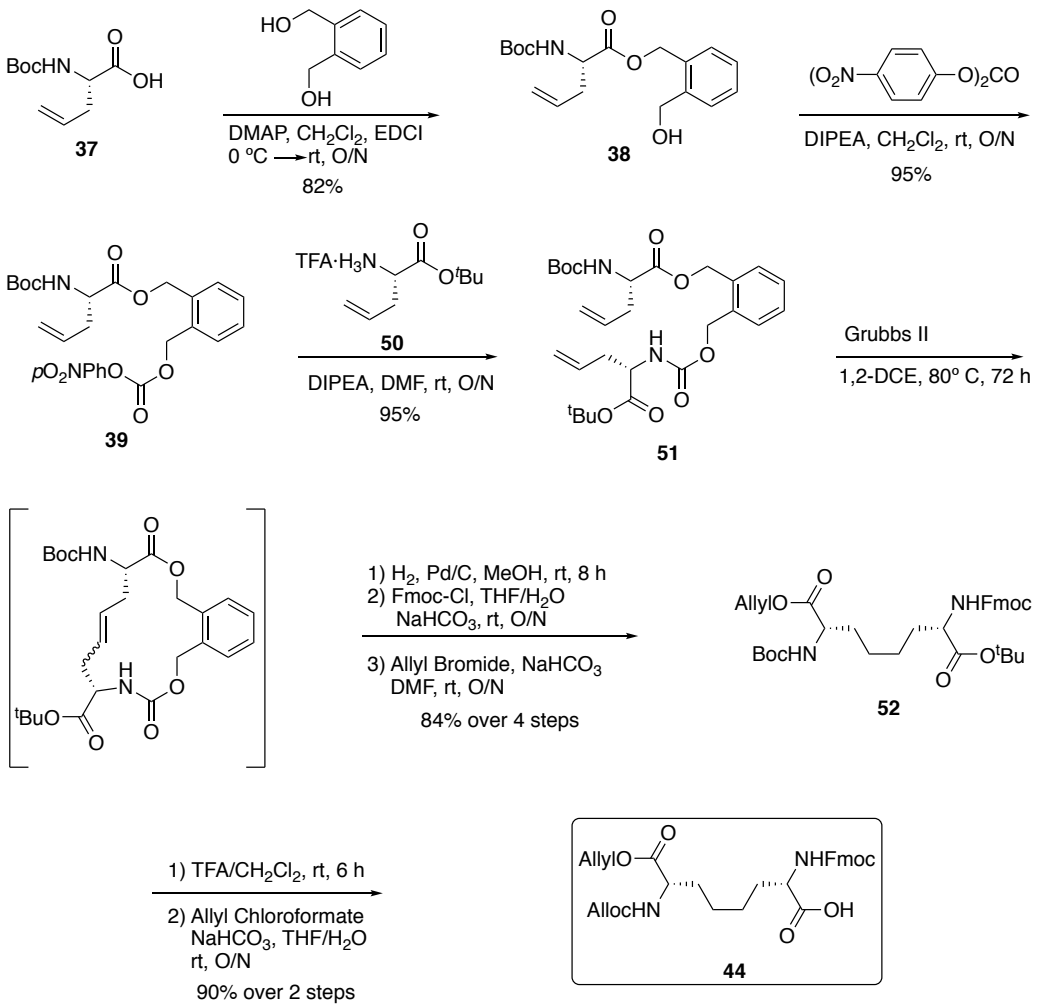

*Scheme 2-8: The synthesis of orthogonally protected diaminosuberic acid **44***

coupling in 95% yield.

The intramolecular cross-metathesis step was then done under extremely dilute conditions using Grubbs second-generation catalyst. The reaction was tracked by TLC and seen to be complete after 72 h. The length is presumably due to the high dilution (0.005 M) required for the reaction to proceed without side-products and the relatively small amount of catalyst (10 mol%) for such a dilution. The crude material is then carried forward to hydrogenation, eliminating the double bond isomers and freeing the DADA from the scaffold. The crude DADA was then *N*-terminally protected with Fmoc in the presence of sodium bicarbonate ($NaHCO_3$), and then the *C*-terminus was protected with allyl bromide in the presence of $NaHCO_3$ to provide the fully protected diamino diacid **52** in an astonishing 84% over four steps. Lastly, to make **52** SPPS amenable, the Boc and ^{t}Bu groups were removed with TFA and the free *N*-terminus was protected with allyl chloroformate and a weak base to furnish orthogonally protected diaminosuberic acid **42** in 90% yield over two steps. Although there are many synthetic steps to produce **44**, the yields are high in virtually every step and many steps can be done contiguously without first purifying, proving it to be a viable method to make DADAs on an appreciable scale.

2.5.2 Synthesis of Orthogonally Protected LL-Diaminopimelic Acid

It was postulated that diaminopimelic acid analogues could be made much the same way. Unlike the synthesis of differentially protected diaminosuberic acid, only one of the alkene moieties will be an allylglycine. The second alkene moiety linked to the scaffold needs to be a vinylglycine in order to synthesize DAP analogues. Vinylglycine is rarely commercially available, as it isomerizes to an α,β-unsaturated system over time. Therefore, it had to be synthesized. Beginning with the same steps as LL-diaminosuberic acid to generate **39**, H-L-Glu-^{t}Bu (**53**) was added to the asymmetric carbonate with DIPEA to produce **54** (*Scheme 2-9*). However, the yields for the reaction were quite low (50–70%) when compared to the yields for the same step in the DAS synthesis. The basic work-up led to deprotonation of the product, causing it to become washed into the aqueous layer with *p*-nitrophenol. By sopping the reaction by addition of 1 M HCl, **54** remained protonated and due to the disparity in polarities between **54** and *p*-nitrophenol, purification by silica column was facile, with no need for a basic work-up.

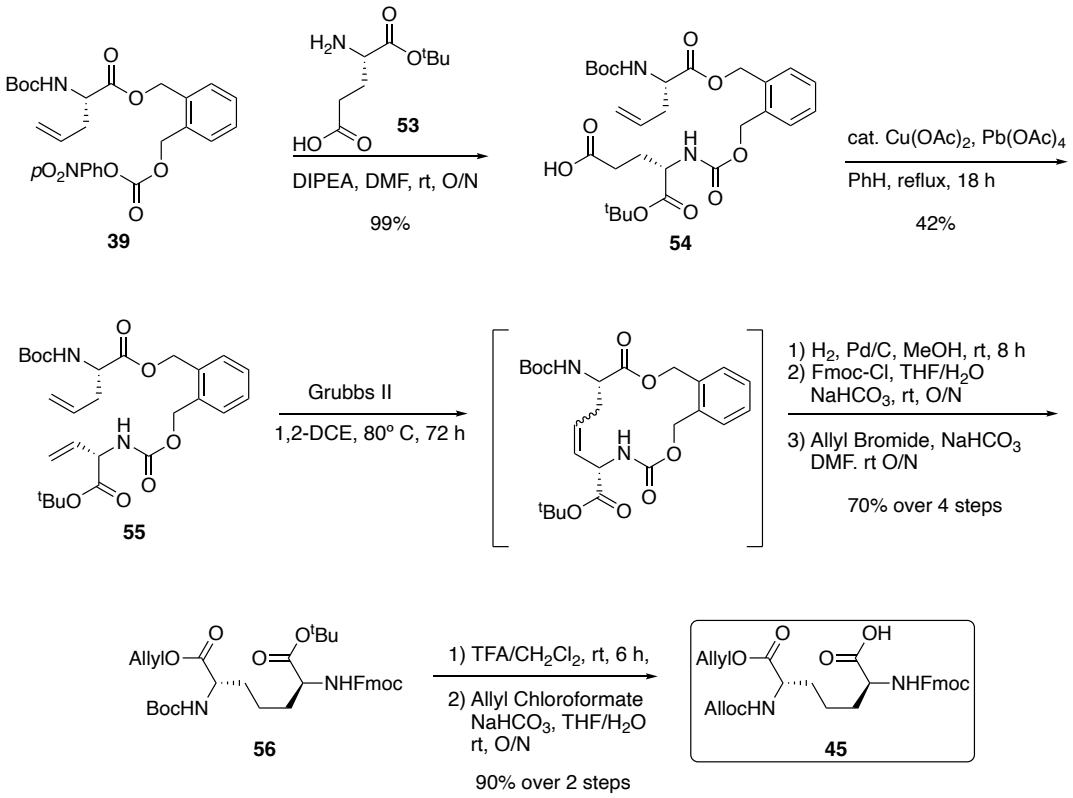

*Scheme 2-9: The synthesis of orthogonally protected diaminopimelic acid **45***

To generate the required vinylglycine functionality, an oxidative decarboxylation procedure using lead(IV) tetraacetate ($Pb(OAc)_4$) and copper(II) acetate ($Cu(OAc)_2$) was employed.[169] Upon refluxing **54** with $Pb(OAc)_4$ and $Cu(OAc)_2$ in benzene, a radical decarboxylation occurs to give the di-alkene species **55**. The exact mechanism through which the alkene is generated is not known. However it is widely considered to proceed through a free radical-chain mechanism (*Scheme 2-10*).[170] Beginning with a ligand exchange, the free carboxylic acid coordinates to the Pb^{IV} atom, displacing a molecule of acetic acid. Upon heating (or exposure to UV), the radical initiation commences. The bond between Pb^{IV} and the carboxylate homolytically cleaves, leading to a radical decarboxylation, generating a free alkyl radical and a Pb^{III} species. During the propagation steps, a single electron transfer (SET) presumably occurs between the radical and the Cu^{II} species to reduce copper to Cu^{I} and give a transient carbocation, which undergoes rapid elimination to the alkene and generating another molecule of acetic acid. The Cu^{I} species can then act as a reductant to reduce another Pb^{IV} species bound to the carboxylic acid to regenerate the reactive Pb^{III} species, resulting in the oxidation of copper back to Cu^{II}. The

newly generated Pb^{III} species can then undergo thermal homolytic cleavage again to produce a new alkyl radical to propagate the chain. Termination of the reaction is presumed occurs upon quenching of the reaction or reaction of two radical species.[170]

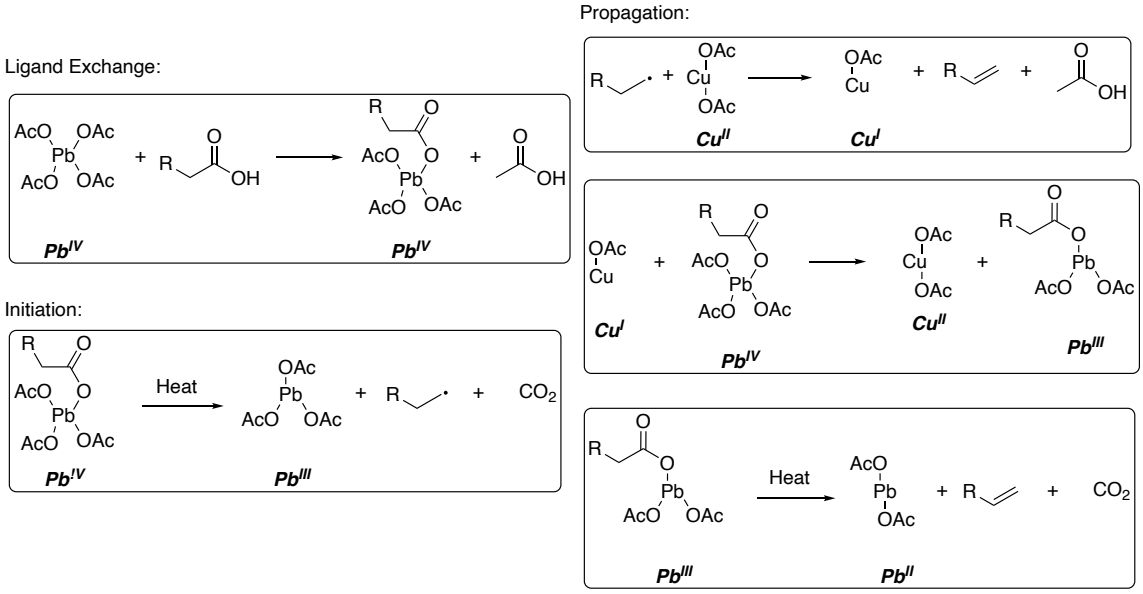

Scheme 2-10: Proposed mechanism for the conversion of a carboxylic acid to an alkene by $Pb(OAc)_4$ and $Cu(OAc)_2$

The logic behind generating the L-vinylglycine functionality from reaction of **54**, as opposed to straight from the H-L-Glu-O^{t}Bu amino acid was to avoid isomerization. Appending an amino acid to the asymmetric carbonate **39** requires basic conditions and prolonged exposure of vinylglycines to acid or base would promote isomerization to the unreactive dehydrobutyrine. Thus transformation on the scaffold would serve to mitigate unwanted transformations. Although the yield for the transformation was low at 42%, it was found that quenching with 1 M HCl, rather than H_2O as the literature suggested,[169] and extraction allowed for recovery of unreacted starting material **54** in as much as 30%.

With **55** in hand, the cross-metathesis was done over 72 h, as tracked by TLC and proceeded smoothly to give the cyclized intermediate. Akin to the DAS analogue, the hydrogenation, followed by *N*-terminal Fmoc protection, and lastly *C*-terminal allyl protection furnished the fully protected DAP **56** in 70% over 4 steps. The final protecting group shuffle by exposure to TFA and subsequent *N*-terminal protection with allyl chloroformate gave the orthogonally protected LL-DAP **45** in 90% over 2 steps.

Synthesizing both *meso*-DAP (done by Dr. Engelhardt) and LL-DAP via the 1,2-benzenedimethanol scaffold significantly increases the accessibility to these crucial

diamino diacids. The yields of vinylglycine transformation were low, but the yield of the cross-metathesis step was greatly improved over the analogous route described earlier, which used the same method for generating vinylglycine with poorer C-C bond formation.[151]

2.5.3 Synthesis of Orthogonally Protected LL-Diaminoazelaic Acid

With the Williams scaffold functioning to make shorter chain diamino diacids, investigation was done to see if longer chains would be applicable. To do so, a homoallylglyine building block would need to be synthesized. After searching the literature, a high yielding and scalable route was found to extend a cheap glutamic acid by a methylene unit.[171] Commencing with commercially available Boc-L-Glu-O^{t}Bu **57**, the side chain is protected as a methyl ester (*Scheme 2-11*). Methanol is generated *in situ* using methyl chloroformate in the presence of Et_3N and catalytic DMAP. Methyl chloroformate is activated by DMAP, which then facilitates attack by the carboxylate of the amino acid to produce a mixed anhydride (*Scheme 2-12*). The newly regenerated DMAP breaks down the mixed anhydride to a molecule of CO_2 and methoxide. Nucleophilic attack on the activated carbonyl by the methoxide then furnishes the final methyl ester protected amino acid. The excellent procedure yields the fully protected glutamic acid **58** in 92% yield with a very short reaction time of only 30 mins. Next, a second Boc group is added to the *N*-terminus using Boc anhydride (Boc_2O) and DMAP to produce the di-Boc protected glutamic acid **59** quantitatively. This second Boc group is essential to deter intramolecular cyclizations of nitrogen onto the aldehyde formed in the next step of the reaction in *Scheme 2-11*. The aldehyde **60** is produced by careful reduction of the methyl ester with diisobutylaluminum hydride (DIBAL-H) at -78 °C. The addition of DIBAL-H must be done slowly to avoid heating, which promotes over reduction to the corresponding alcohol rather than the aldehyde.[172] The reaction is completed very quickly, in 5 mins at 74% yield. However, when done on large scale, the work-up of the reaction is done overnight to simplify removal of large amounts of aluminum from the reaction. Conversion to homoallylglycine **61** is done using Wittig chemistry. The aldehyde is reacted with methyltriphenylphosphonium iodide and potassium *tert*-butoxide (KO^{t}Bu) to give the extended allylglycine **61** needed for longer DADAs in 92% yield. This was then tailored for the scaffold by fully removing all the

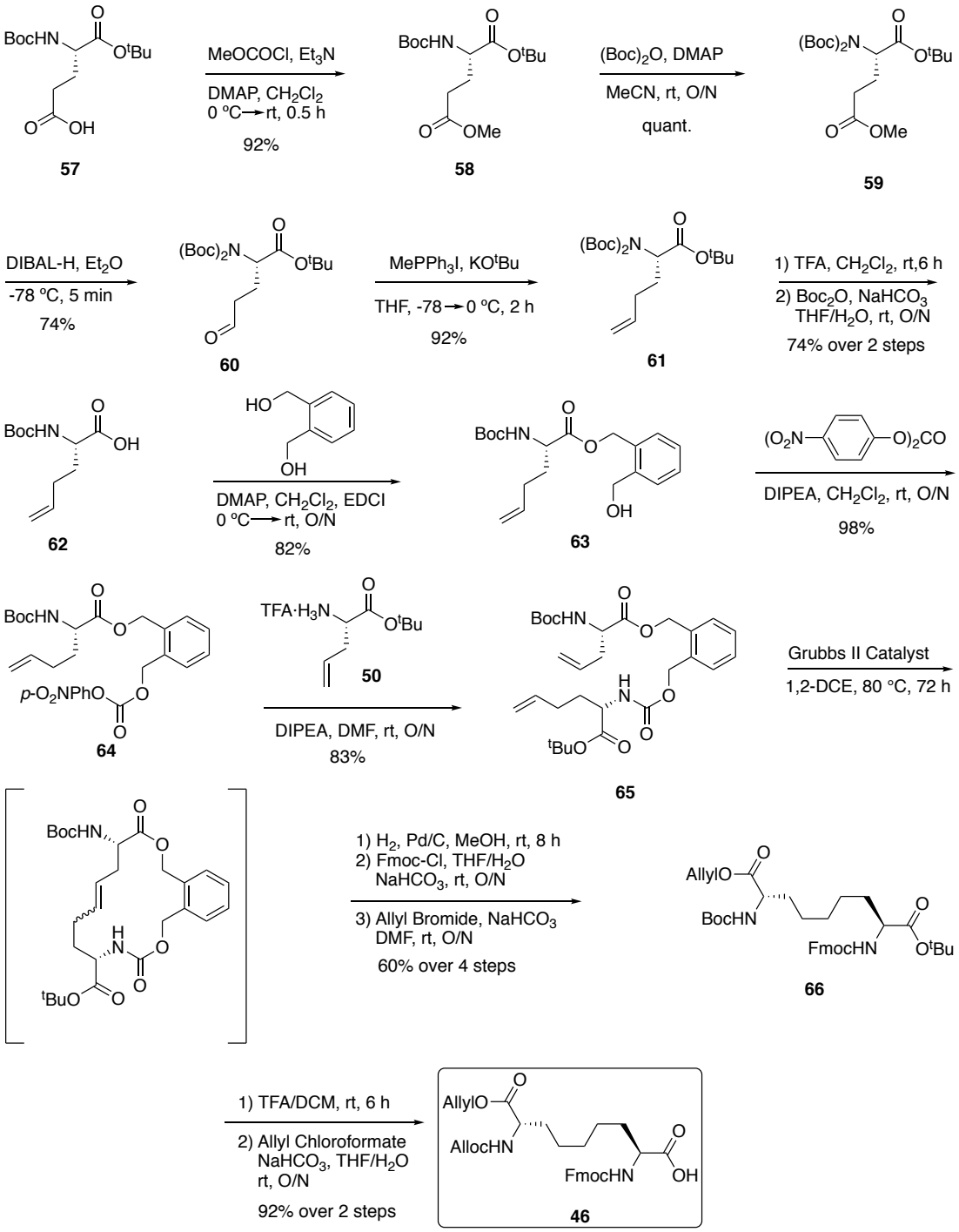

Scheme 2-11: The synthesis of orthogonally protected diaminoazelaic acid ***46***

protecting groups with TFA, and then the crude material was *N*-terminally mono-Boc protected with Boc_2O, giving the free carboxylic acid **62**. Coupling to 1,2-benzenedimethanol (**63**, 82%), reaction with bis(*p*-nitrophenyl) carbonate (**64**, 98%) and addition of amino acid **50** (**65**, 83%) all proceeded smoothly with the longer amino acid.

The cross-metathesis, followed by hydrogenation, and Fmoc and allyl protection was not as high-yielding as with DAP or DAS; however, fully protected diamino diacid **66** was still produced in 60% over 4 steps (avg. 88% yield per step). The final TFA deprotection and subsequent reprotection of the *N*-terminus with ally chloroformate gave differentially protected diaminoazelaic acid **46** in 92% yield over the final 2 steps.

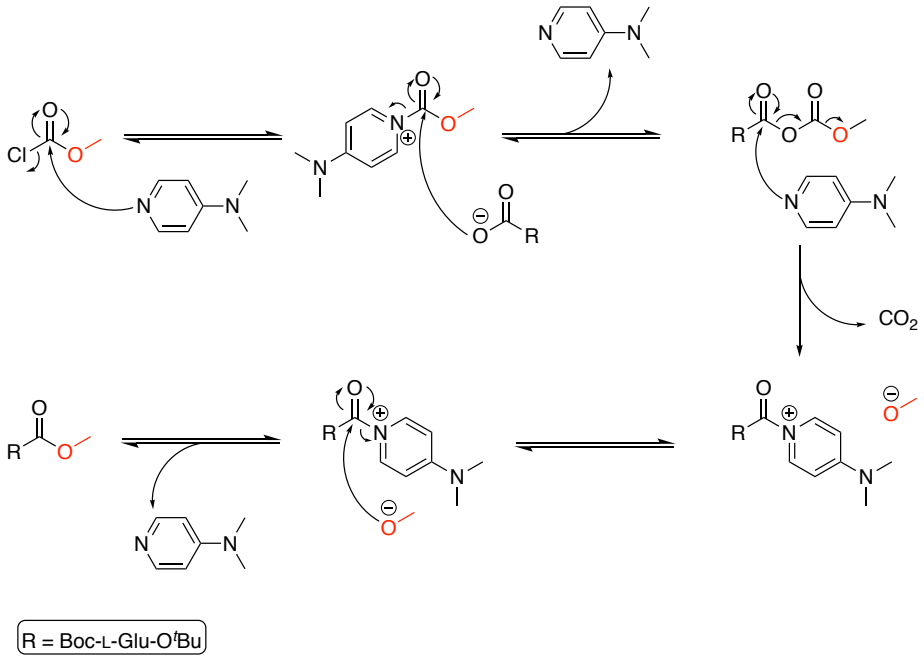

*Scheme 2-12: The proposed mechanism for the methyl ester protection of **57** with methylchloroformate and DMAP.*

2.5.4 Synthesis of Orthogonally Protected LL-Diaminosebacic Acid

Because the synthesis of diaminoazelaic acid analogue **46** worked well, it would stand to reason that the cross-metathesis of two homoallylglycine moieties to generate diaminosebacic acid would also work. The chemistry to make homoallylglycine is straightforward and has been established above. Beginning with the amino acid **62**, the coupling to 1,2-benzenedimethanol reaction with bis(*p*-nitrophenyl) carbonate remained unchanged, but the reaction of the next amino acid required a change. The fully protected homoallylglycine **61** was split with the majority of it being converted to **62**, but some of it was reacted only briefly (15 mins) with TFA to keep the *C*-terminal protecting group intact, but revealing the free amine to obtain **67** (*Scheme 2-13*). To avoid over-reaction of **61** to the free amine and carboxylic acid, the reaction was monitored by gas evolution arising from Boc deprotection. Upon addition of TFA, there was excessive bubbling as the

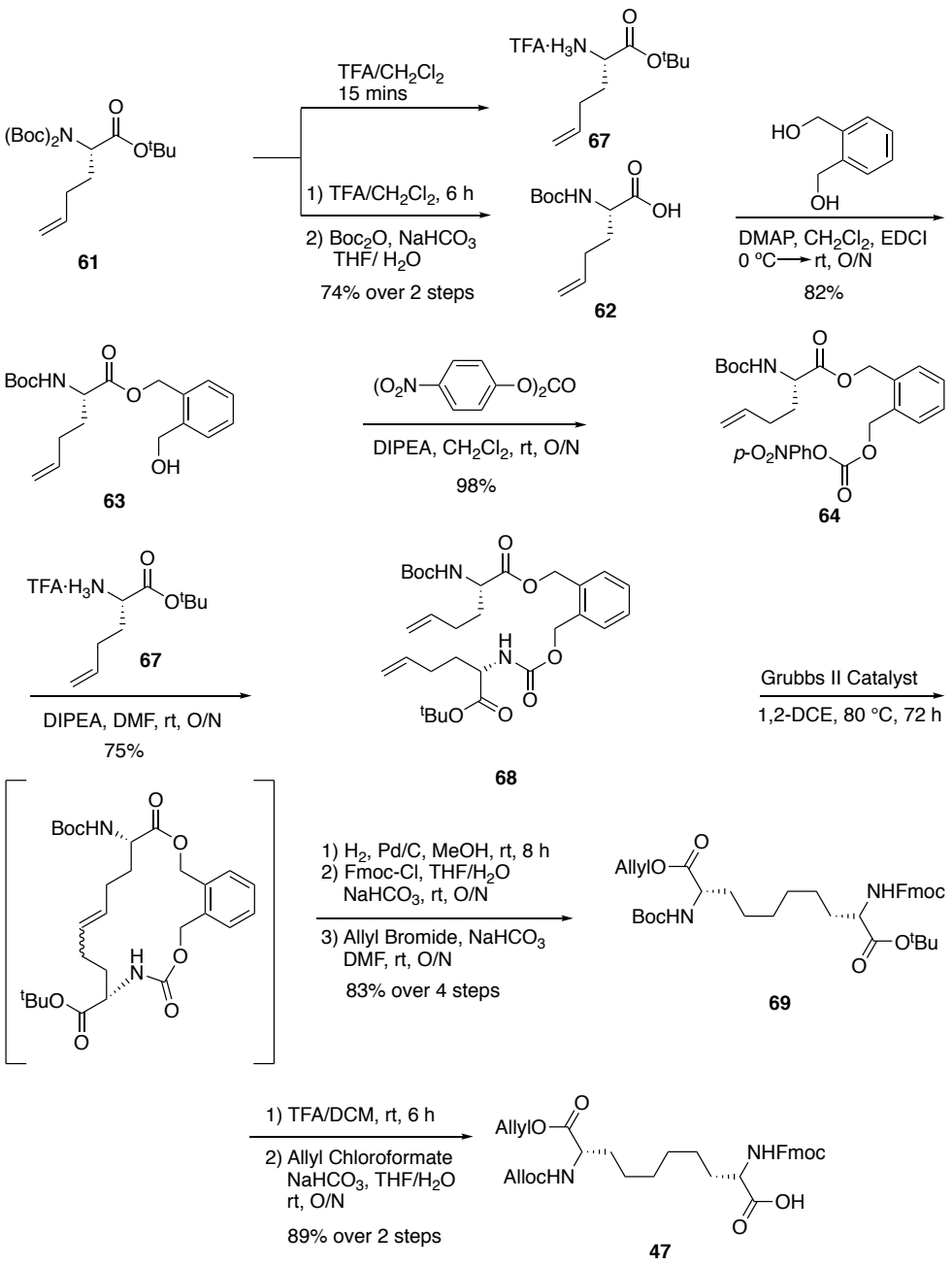

*Scheme 2-13: The synthesis of orthogonally protected diaminosebacic acid **47***

di-Boc groups were removed. Effervescence persisted for approximately 10 mins. The reaction was left for an additional 5 mins before stopping the reaction with $NaHCO_3$ until the pH was around 9. The reaction mixture was analyzed by TLC and LCMS and all the starting material had been entirely consumed Therefore, the basified reaction mixture was extracted to remove the trace amounts of the fully deprotected amino acid. The crude product **67** was carried forward and reacted with **64**, yielding the di-alkene **68** in 75%

over 2 steps. Incubation with Grubbs II, followed by hydrogenation, Fmoc protection and allyl protection provided the longer chained DADA **69** in 83% yield over 4 steps. The final 2 steps provided selectively protected diaminosebacic acid **47** in 89% over 2 steps.

Indeed, using 1,2-benzenedimethanol for the synthesis of SPPS amenable, longer diamino diacids is effective with both diaminoazelaic acid **46** and diaminosebacic acid **47** being made with good yields for every step in the synthesis. These two analogues do not have a known direct homologue in naturally-occurring peptides; nevertheless, they can effectively be used for incorporation of larger macrocycles via the pre-stapling method.

2.5.5 Synthesis of Orthogonally Protected LL-Diaminoadipic Acid

Given that the Williams method worked for the synthesis of diaminopimelic analogues, there was optimism that use of lead tetraacetate would produce two vinylglycine moieties on the scaffold, leading to the eventual synthesis of a diaminoadipic acid analogue. To begin, commercially available Boc-L-Glu(OAllyl)-OH (**70**) was appended to the scaffold using EDCI coupling conditions to give **71** in relatively low yield (54%) when compared to the previous syntheses (*Scheme 2-14*). Adding bis(*p*-nitrophenyl) carbonate to make **72** worked quantitatively. Amino acid **53** that was used in the DAP synthesis was added to the scaffold providing **73**, but only in 56% yield. The allyl ester was removed with tetrakis(triphenylphosphine)palladium(0) ($Pd(PPh_3)_4$) in the presence of morpholine as a scavenger to yield the free diacid **74** in 60% yield. The purification of **74** proved quite difficult, as increasing polarities of eluent to help elute the product caused frequent co-elution with polar side-products. With some of the diacid in hand, a double oxidative decarboxylation using $Pb(OAc)_4$ and $Cu(OAc)_2$ was attempted. The di-vinylglycine containing product **75** was obtained, albeit in only 16% yield. The majority of the reaction mixture was recovered as unreacted starting material. The product **75** was carried forward to attempt a cross-metathesis. Despite reacting for 72 h at elevated temperatures, the reaction would not proceed with only isolation of the starting material. Surprisingly, neither of the double bonds of **75** isomerized after the failed reaction, based on NMR.

It was at this point that this route was abandoned due to the fact that many of the yields were lower for this synthesis, many purifications were difficult and the di-

vinylglycine product may be too sterically encumbered to effectively undergo cross-metathesis with the large ruthenium catalyst.

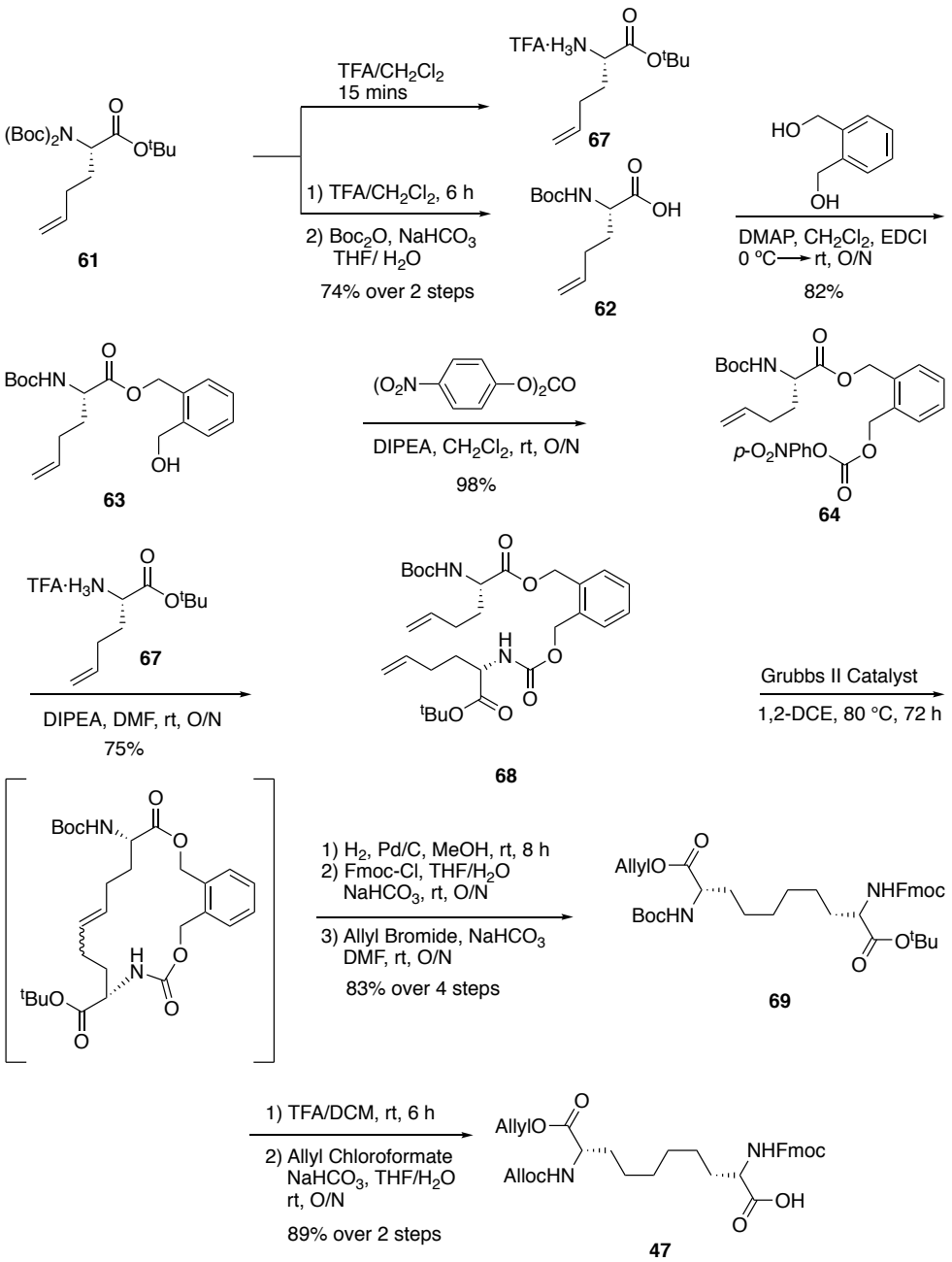

*Scheme 2-13: The synthesis of orthogonally protected diaminosebacic acid **47***

2.6 Conclusions and Future Directions

A variety of orthogonally protected diamino diacids were synthesized by expanding the use of a 1,2-benzenedimethanol scaffold. Orthogonally protected diaminosuberic acid **44**, a critical component for Chapters 3 and 4, was synthesized by

adapting a literature procedure[165] to give the building block in 56% overall yield in 9 linear steps. By expanding the chemistry amenable to the 1,2-benzenedimethanol scaffold, orthogonally protected diaminopimelic acid **45**, diaminoazelaic acid **46**, and diaminosebacic acid **47** were all successfully synthesized. Compound **45** was produced in 26% overall yield with a longest linear sequence of 11 steps, while compounds **46** and **47** were synthesized in 17% and 21% overall yields respectively, both with a longest linear sequence of 15 steps. Unfortunately, the method described did not work for generating differentially protected diaminoadipic acid **48**.

Pre-stapling of peptides with diamino diacids has been proven to be an effective method for the introduction of macrocycles into a growing peptide chain.[138,139] Unlike traditional RCM stapling methods, which usually require macrocycles between two olefinic residues to be installed after the peptide has been fully extended. Pre-stapling peptides enforces a rigid 3D structure to the nascent peptide. While this strategy may ultimately prove inconsequential to peptides containing only 1 ring, those with multiple rings, such as peptides with multiple disulfides, often benefit from the imposed structural constraints provided by pre-stapling.[140,173] Furthermore, incorporation of DADA's for cyclization is relatively easy to use. After deprotection, completion of macrocyclization is achieved simply by amide formation, a step that can be automated on most SPPS instruments nowadays.

Despite being unable to synthesize orthogonally protected diaminoadipic acid **48** as attempted in *Scheme 2-14*, there exist different, more effective and expensive catalysts to conduct cross-metathesis.[174,175] Perhaps a more powerful catalyst would be sufficient to facilitate formation of the key C-C bond between the vinylglycine moieties. Alternatively, a McMurry type coupling on a molecule such as **76** could be attempted with a much smaller titanium species to produce the cyclized material **77** (*Scheme 2-15*).[176] From there on, the chemistry would be similar to the previously synthesized DADAs to generate **48**. The active titanium species is originally generated using $TiCl_3$ and $LiAlH_4$; however, these strongly reducing conditions could lead to epimerization of the amino acid stereocenters, or reduction of the various carbonyl functional groups. Related active species have been generated using various other reducing agents such as zinc, magnesium and potassium.[177] Synthetic routes for the production of orthogonally protected

diaminoadipic acid is less represented in the literature when compared to DAP, DAS and various lanthionine based DADAs. Therefore, expanding the synthetic toolbox for these types of molecules would be beneficial to the fields of peptidomimetics and peptides.

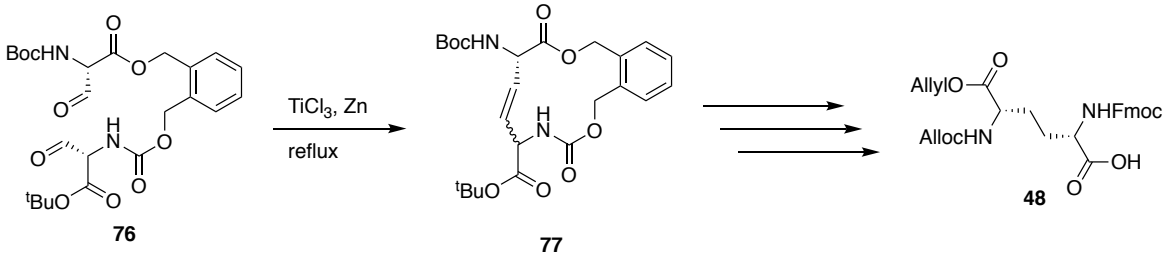

*Scheme 2-15: Proposed scheme for the synthesis for orthogonally protected diaminoadipic acid **48** by McMurry coupling.*

Strategic installation of macrocycles in place of specific residues can enforce the α-helical nature of the peptide in that region. Interestingly, this effect is further exaggerated in α,α-disubstituted amino acids.[178,179] Amino acids bearing an extra α-methyl group confer extra restriction of rotational conformations of side chains, resulting in restricted conformational freedom of their peptides.[178] When combined with DADAs, the effect can be an overall enhancement in the α-helical conformation formation.[179,180] In future applications, the chemistry using 1,2-benzenedimethanol could be applied to the synthesis of such diamino diacids (*Scheme 2-16*). Beginning with alanine, a stereoselective alkylation could be done with allylic electrophile,[181] generating α,α-disubstituted amino acids that could be appended to the scaffold (**78**). The electrophile could be alternated to pave the way for longer chains such as diaminoazaleic acid (n=1 for one chain and n=0 for the other) or diaminosebacic (n=1 for both chains). Subsequent steps could be done as before to generate a new set of orthogonally protected, α,α-disubstituted diamino diacids **79** that could be investigated for their ability to mimic α-helices, or other linkages with a more rigid conformation.

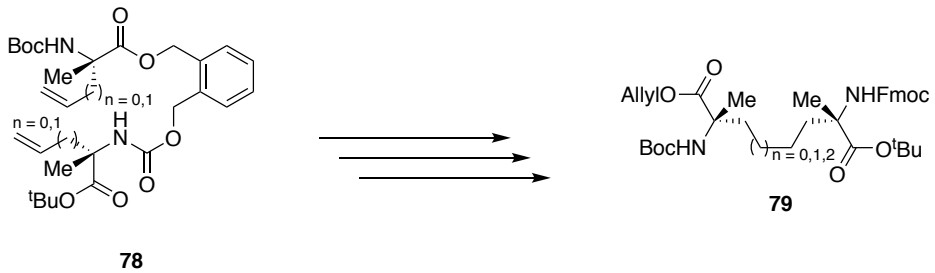

Scheme 2-16: Proposed synthesis for the application of 1,2-benzenedimethanol to generate α,α-disubstituted diamino diacids.

3 Chapter 3: Synthesis of Neopetrosiamide Analogues

3.1 Introduction to Neopetrosiamide

3.1.1 Overview of Neopetrosiamide Discovery and Function

Tropical marine sponges and the symbiotic bacteria and microorganisms that live inside them are host to a wide variety of secondary metabolites,[182–184] many of which have intriguing bioactivity or unknown function.[185–187] The acquisition of natural products through synthetic means is highly sought after in laboratories for further studies of their functions and applicability. The synthetic complexity that natural products provide often drives the discovery of new methodologies for chemical synthesis. Consequently, gathering of many exotic sponges or organisms proves difficult due to various government regulations or ecological reasons, resulting in a supply of the metabolite being entirely dependent on chemical means or heterologous expression.[188] As outlined briefly in Chapter 1, neopetrosiamide (**5**) is a 28-residue natural peptide containing all L-amino acids (*Figure 3-1*). It was initially discovered by Raymond Andersen when analyzing methanolic extracts of a marine sea sponge salvaged off the coast of New Guinea.[65] The peptide consists of a mixture of A and B isomers, differing only at the chiral sulfoxide on the methionine at position 24. The sulfoxide is not required for activity and the peptide maintains full activity with a methionine.[65] The peptide is a potent inhibitor of cancer cell migration through both mesenchymal and amoeboid invasion pathways. However, neopetrosiamide does not display activity against healthy, non-cancerous cells, making it an intriguing target as a potential anti-cancer peptide therapeutic. The peptide contains three disulfide bonds whose correct connectivity is absolutely essential for any activity to be exhibited. Unfortunately, the exact species of sponge responsible for the biosynthesis of neopetrosiamide cannot be found anymore, meaning there needs to be a different way to access it for future studies or applications.

3.1.2 Previous Work on Neopetrosiamide by the Vederas Group

There is a long-standing interest in sulfur-containing bioactive peptides in the Vederas group,[189,190] but more recently, it has evolved with the inclusion of a methine or a methylene in place of sulfur, to produce more stable analogues.[141,191] Neopetrosiamide

was a perfect candidate for investigative studies on sulfur replacement. Previously, Patrick Liu revised the disulfide bond connectivity from the initial assignment and reported that

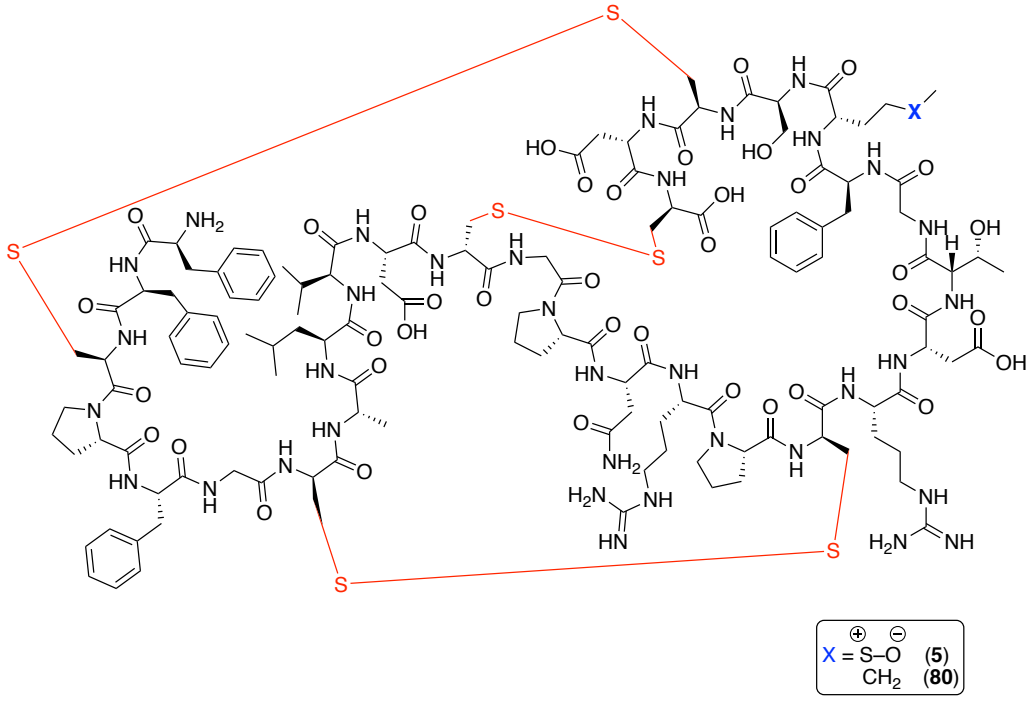

*Figure 3-1: Chemical structure of native neopetrosiamide with the amino acid position 24 being the natural methionine sulfoxide (**5**) or the norleucine analogue (**80**).*

methionine replacement with norleucine results in an active analogue (**80**) possessing activity on par with the natural substrate.[67] The initial disulfide assignment was found to be incorrect when a synthetic version of neopetrosiamide, made by SPPS, followed by selective deprotection/oxidation to form the disulfide bonds, had a different retention time on HPLC than the natural product standard. Correct assignment was made using a combination partial reduction of the disulfide bonds, followed by alkylation, and enzymatic digestion, followed by MS/MS sequencing.[67] Interestingly, the initial connectivity that was proposed using nuclear Overhauser effect (NOE) data from NMR fit the NMR data just as well as the revised assignment, suggesting the two disulfide bond isomers were very similar. Indeed, a 3D-model made for our group by Scott Walker at UBC displayed almost indistinguishable backbone differences and very minimal 3D-structural changes between the initial connectivity and revised connectivity. This indicates that their NMR data would be nearly identical and making it impossible to determine the correct linkage solely by NMR.

Further work on neopetrosiamide was done by Kaitlyn Towle. On top of scanning which other residues could be used to replace the methionine at position 24, she investigated whether or not a covalent linkage between cysteine residues was required for neopetrosiamide activity, or if hydrophobic interactions could replace these linkages.[68] By replacing one of the three disulfide bonds with a hydrophobic pair, the remaining two disulfide bonds could in theory allow for the beginnings of folding to occur, such that the hydrophobic pair are brought in close proximity to one another to complete the proper folding. This method has proven successful in our group before with the antimicrobial

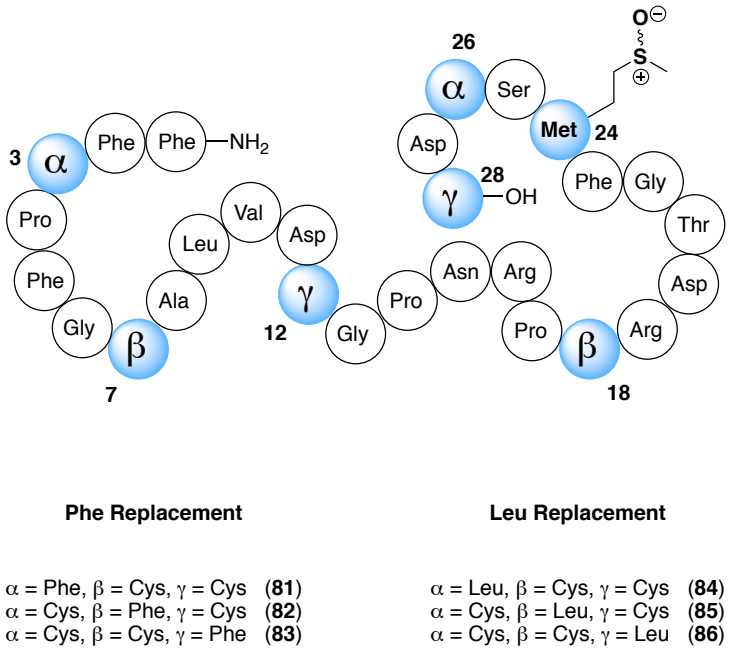

*Figure 3-2: Various neopetrosiamide analogues with disulfide bonds replaced with hydrophobic interactions. Cys 3-26 disulfide bond replaced with 2 Phe (**81**) or 2 Leu (**84**), Cys 7-18 disulfide bond replaced with 2 Phe (**82**) or Leu 2(**85**), and Cys 12-28 disulfide bond replaced with 2 Phe (**83**) or 2 Leu (**86**).*

peptide leucocin A, where replacement of the disulfide bond with two leucine residues resulted in an active peptide.[192] Dr. Towle synthesized six new neopetrosiamide analogues (**81-86**) using phenylalanine or leucine residues in place of a cysteine pair (*Figure 3-2*). In each analogue, one of the three disulfide pairs was replaced with Phe or Leu during SPPS. Systematic disulfide bond formation after the linear peptide was complete afforded analogues with two disulfide bonds, with the third being mimicked with hydrophobic interactions. Sadly, none of the analogues proved active in biological testing, indicating

that a covalent bond between the residues appears to be necessary for any activity. Conversely, substitutions at the methionine residue seemed to be much more tolerated. These substitutions were of interest as methionine is not stable to oxidation, which readily occurs in neopetrosiamide to generate a diastereomeric mixture, nor can norleucine be easily genetically encoded for methionine replacement in heterologous expression. Dr. Towle discovered that substitutions with glutamic acid, phenylalanine and alanine were tolerated. Glutamic acid appeared to possess the highest activity of the three active substitutions, almost on par with the natural peptide and norleucine analogue. Glutamic acid is much more readily incorporated into the genetic sequence and could be formed via site-directed mutagenesis to generate a peptide that can be heterologously expressed with increased oxidative stability.[68]

With the work done previously by our group to determine correct disulfide bond connectivity and that a covalent bond between cysteine pairs appears to be necessary, investigation into replacing a single disulfide bond with methylenes seemed like a logical progression to further probe the structure-activity relationship of neopetrosiamide.

3.2 Results and Discussion of Methylene Analogues of Neopetrosiamide

3.2.1 Synthesis of Methylene Analogous of Neopetrosiamide

With orthogonally protected diaminosuberic diacid **44** from Chapter 2 in hand, the synthesis of three novel analogues of neopetrosiamide (**87-89**) was embarked upon wherein a single disulfide bond in each analogue was replaced with carbons (*Figure 3-3*). The analogues are referred to by the order in which the cysteines participating in disulfide bonds were encountered during SPPS (i.e. for the *C*-terminus). Neopetrosiamide analogue A1 (**87**) has the first *C*-terminal cysteine replaced (Cys 12-28 bridge), neopetrosiamide analogue A2 (**88**) has the second *C*-terminal cysteine replaced (Cys 3-26 bridge), and neopetrosiamide analogue A3 (**89**) has the third *C*-terminal cysteine replaced (Cys 7-18 bridge).

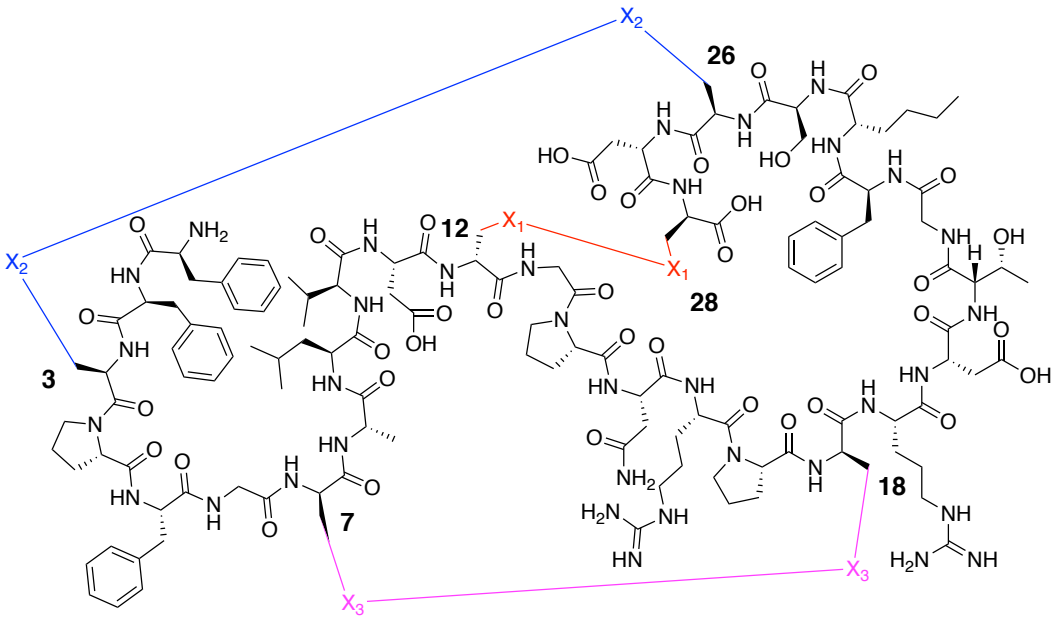

Neopetrosiamide Analaogue A1 (**87**): $X_1 = CH_2$, $X_2 = S$, $X_3 = S$
Neopetrosiamide Analaogue A2 (**88**): $X_1 = S$, $X_2 = CH_2$, $X_3 = S$
Neopetrosiamide Analaogue A3 (**89**): $X_1 = S$, $X_2 = S$, $X_3 = CH_2$

*Figure 3-3: Structure of each of the neopetrosiamide analogues synthesized. Cys 12-28 disulfide bond replaced with CH_2's (**87**), Cys 3-26 disulfide bond replaced with CH_2's (**88**) and Cys 7-18 disulfide bond replaced with CH_2's (**89**)*

The neopetrosiamide analogues **87-89** were initially manually synthesized on resin, moving to an automated synthesizer when additional rounds of testing and synthesis needed to be done. All three of the desired targets were set to have L-norleucine in place of methionine to avoid aerobic oxidation, which would result in a mixture of diastereomers for each analogue. Using Fmoc-based SPPS, the starting amino acids were loaded onto 2-chlorotrityl chloride resin at a reduced loading (~0.1 mmol/g) to achieve a high effective dilution. This is critical so as to deter intermolecular interactions when the cyclizations on resin are conducted, enforcing primarily intramolecular reactions. Couplings were done using (1-[bis(dimethylamino)methylene]-1H-1,2,3-triazolo[4,5-b]pyridinium 3-oxide hexafluorophosphate (HATU) to minimize side-reactions and epimerization.[193] The diaminosuberic acid derivative **44** was incorporated as if it was a canonical amino acid, but with fewer equivalents so as to not waste the precious material that remains uncoupled.

After incorporation of the orthogonally protected diaminosuberic acid, the peptides were extended until the other end of the disulfide bond being replaced was encountered. At this point, the allyl/alloc groups were selectively deprotected using $Pd(PPh_3)_4$ and phenylsilane as a scavenger to unveil the amino acid functionality. Importantly, prior to deprotection of the Fmoc group, there was extensive washing of the resin to remove palladium. The conditions required to remove the protecting groups turned the resin a dark brown/black colour due to residual palladium in the polystyrene beads. This could interfere with subsequent couplings, thus the resin was washed with DMF, CH_2Cl_2 to remove any surface impurities, then to remove palladium, the resin was washed with 0.5% diethyldithiocarbamate in DMF,[138] and then again with DMF and CH_2Cl_2. The extra washing steps greatly improved the purity of the peptides during analysis of the next couplings. The cyclization was done using (7-azabenzotriazol-1-yloxy)tripyrrolidinophosphonium hexafluorophosphate (PyAOP) and HOBt (*Scheme 3-1*). Dr. Engelhardt was able to determine the yields of the cyclization steps. By cleaving a small portion of the resin after deprotection (**90-92**) and after cyclization (**93-95**) and purifying both truncated peptides by HPLC, the yields can be determined relative to the resin loading. As seen in *Scheme 3-1*, with analogue A1 shown as an example, the yields of the cyclization step were relatively modest and did not vary greatly.

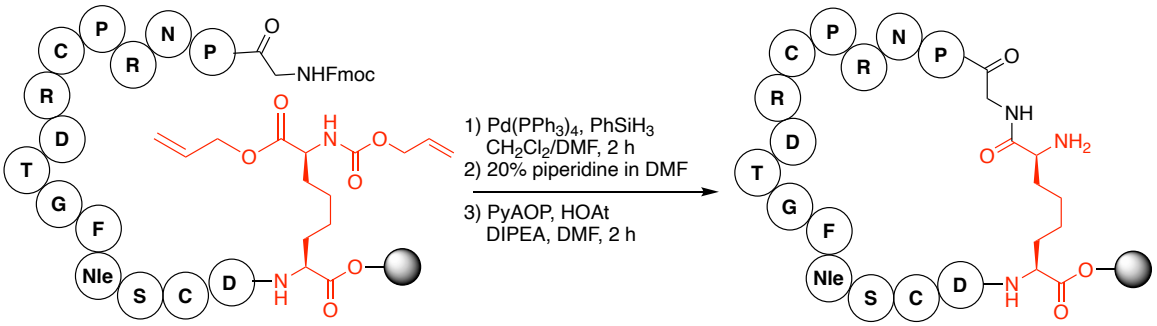

Analogue A1 **90**
Analogue A2 **91**
Analogue A3 **92**

Analogue A1 **93**: 84%
Analogue A2 **94**: 79%
Analogue A3 **95**: 65%

Scheme 3-1: The cyclization step of neopetrosiamide analogues as done on resin. Neopetrosiamide analogue A1 depicted as a representative peptide.

After the cyclizations were complete, the rest of the peptides were extended using SPPS to give the monocyclic peptides **96-98** without any disulfide bonds in 29%, 30%, and 40% yields respectively, determined by Dr. Engelhardt based on resin loading (*Figure 3-4*).

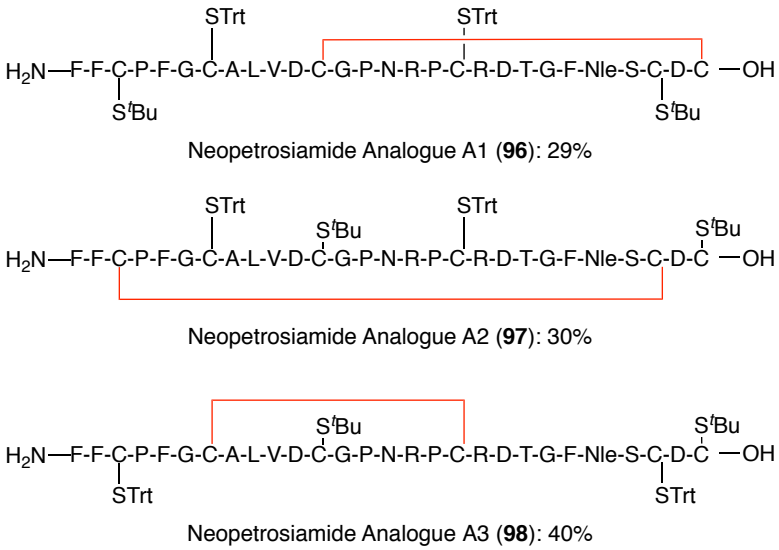

Figure 3-4: Linear sequences of monocyclic neopetrosiamide analogues ***96-98***

3.2.2 Sequential Deprotection/Oxidation for the Formation of Disulfide Bonds for Methylene Neopetrosiamide Analogues

Once the monocyclic peptides **96-98** were obtained, the formation of the disulfide bonds was required to furnish the completed peptides. To begin, the method utilized by Dr. Towle was followed. As seen in *Figure 3-4*, the remaining two pairs of cysteines were differentially protected with trityl (Trt) and *tert*-butyl (^{t}Bu). This allowed for selective deprotection and oxidation to form the correct linkages. To begin, the peptide was cleaved from the resin and acid-labile side-chain protecting groups were removed using a mixture of TFA/thioanisole/1,4-dithiothreitol(DTT)/anisole (90:5:3:2), which also facilitated the removal of the S-Trt protecting groups on the pair of cysteines (*Scheme 3-2*).

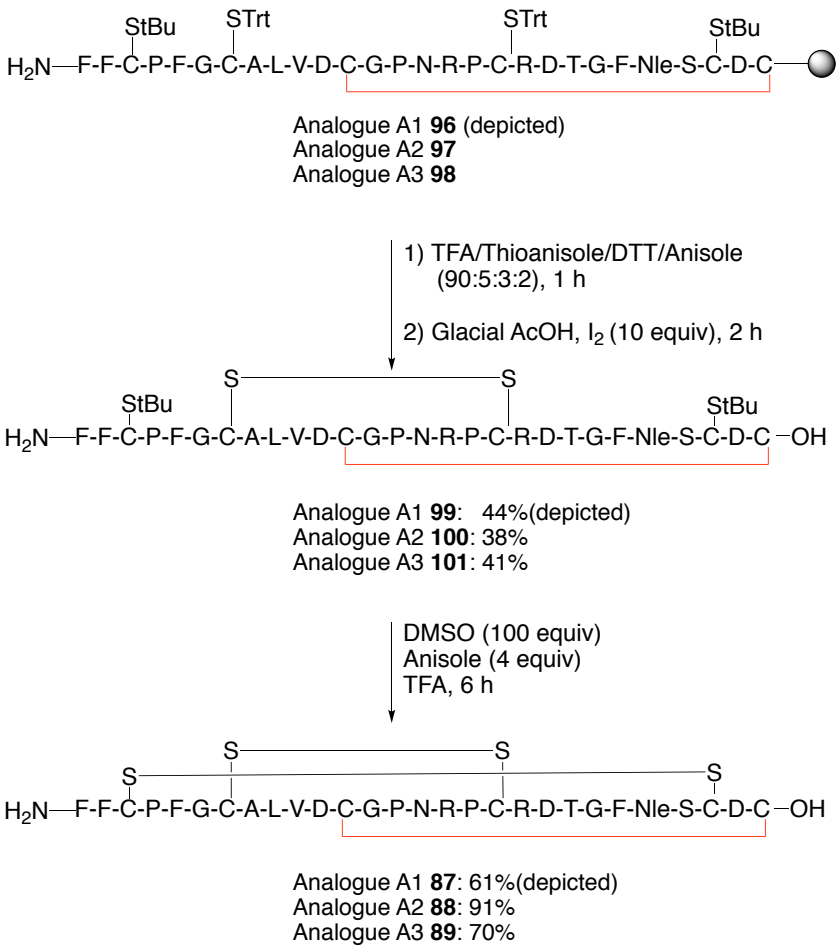

*Scheme 3-2: Synthetic route to form the disulfide bonds of methylene neopetrosiamide analogues **87-89**.*

Upon concentration *in vacuo* to remove the cleavage cocktail, the linear crude peptide was redissolved in glacial acetic acid to give a concentration of 0.5 mg/mL. The concentration was kept low to avoid disulfide bond formation between different peptides. Iodine dissolved in minimal methanol was then added slowly to the reaction to form the first disulfide bonds between the cysteines that were previously protected with S-Trt (**99-101**). After the oxidation was complete, as monitored using matrix-assisted laser desorption/ionization (MALDI) spectroscopy, the reaction was concentrated to remove acetic acid. At this point, the residual iodine had to be removed to prevent overloading the HPLC instrument during the initial attempts to purify the final peptides. The crude peptide mixture was desalted using a Strata C18-E column, before redissolving in TFA, DMSO and anisole (0.1 mg/mL) to remove the S-^{t}Bu protecting groups and form the second disulfide bond, with DMSO acting as the oxidant, to give the crude products **87-89**

(*Scheme 3-2*). Dr. Engelhardt determined the yields of each of the disulfide bond formation steps.

At this stage, it was quickly observed that the S-^{t}Bu groups were quite robust with respect to the deprotection conditions of the S-Trt. While monitoring the oxidation to form the first disulfide bond by MALDI, the mass for the peptide with the S-^{t}Bu groups removed was not seen, even when incubated with pure TFA. A very small portion of one of the analogues was stirred in pure TFA to test the robustness of the S-^{t}Bu groups. After monitoring by MALDI for over 8 h, the mass corresponding to a small amount of peptide with one S-^{t}Bu cysteine removed was observed. LCMS analysis determined the quantity of peptide bearing both S-^{t}Bu protecting groups was much greater than that with only one S-^{t}Bu and there was virtually no peptide that had been fully deprotected. Only upon addition of DMSO did deprotection begin to occur.[194] As a result, disulfide bond formation of the neopetrosiamide analogues **87-89** could be drastically shortened and simplified with no desalting step or iodine usage (*Scheme 3-3*). By taking the resins bearing the monocyclic peptides **96-98**, the peptides were cleaved from resin, and the protecting groups, including the S-Trt groups, were removed using TFA/thioanisole/DTT/anisole cleavage conditions as done previously. However, the resulting crude peptide was redissolved in TFA, DMSO and anisole (0.1 mg/mL) to begin oxidation to the disulfides. The difference in stability between the S-^{t}Bu and the S-Trt groups allow the first disulfide bond to be formed much more quickly, with the second disulfide bond being formed after removal of the S-^{t}Bu protecting groups. The result is a more simple and faster method to form both disulfide bonds, producing the correct isomer in excess of 70% over the other disulfide bond isomers.

Total isolated yields (for 28 amino acids coupled and 3 cyclizations) of the novel analogues from the two-step oxidation method were 2% (**87**), 3% (**88**) and 6% (**89**), while the yields from the improved, one-step oxidation method increased slightly to were 3% (**87**), 3.5% (**88**) while analogues **89** remained roughly the same.

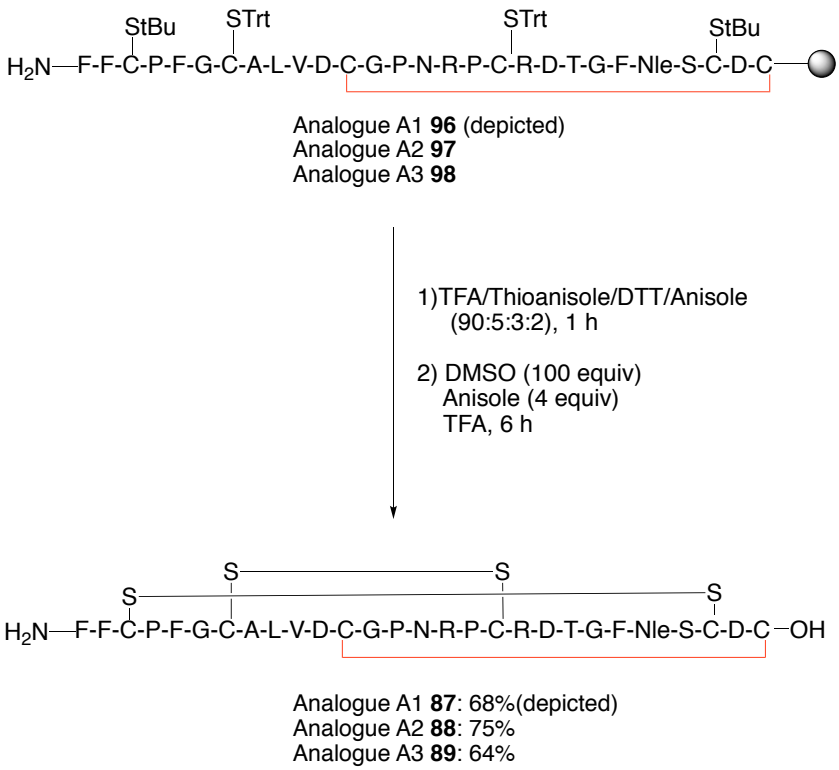

*Scheme 3-3: Synthetic route for improved method for disulfide bond formation for neopetrosiamide analogues **87-89**.*

3.2.3 Purification of Methylene Neopetrosiamide Analogues

Having completed the peptide synthesis on resin and oxidizing the monocyclic peptides **96-98** to form the various disulfide bonds of the neopetrosiamide analogues **87-89**, the peptides needed to be purified by HPLC for testing and characterization. Initial disulfide bond formation using the two-step method described and subsequent purification provided preliminary retention times for the novel analogues. The oxidation of cysteine using both the one-step and two-step method described to form the necessary disulfide bonds also resulted in the formation of small amounts of the other disulfide bond isomers, making purification a more difficult task as they possessed similar retention times to the desired isomer and occasionally co-eluted.

After developing an HPLC method to purify the peptides and their disulfide bond isomers, each of the completed peptides were injected and purified by reverse-phase HPLC. The fractions were analyzed by MALDI and as expected, the mass of the desired product was found in multiple HPLC peaks, corresponding to the different disulfide bond isomers. Despite the different conditions used for oxidation of the cysteines, the results

only varied slightly, indicating that the initial two-step oxidation method and the improved one-step oxidation method were comparable in efficacy for all three analogues with respect to the formation of disulfide bonds (*Figure 3-5*). In each method, the largest peak by HPLC containing the product mass was assumed to be the desired isomer. The desired isomer was produced in greater than 70% yield by isolated weight when compared to the minor isomers. The production of the minor isomers is thought to be the result of too short reaction times, leading to incomplete oxidations, or the result of disulfide bond scrambling between formed disulfide bonds and the transient free thiols prior to oxidation.[143] Each disulfide bond isomer of analogues **87**-**89** was collected separately to be tested against cancer cells.

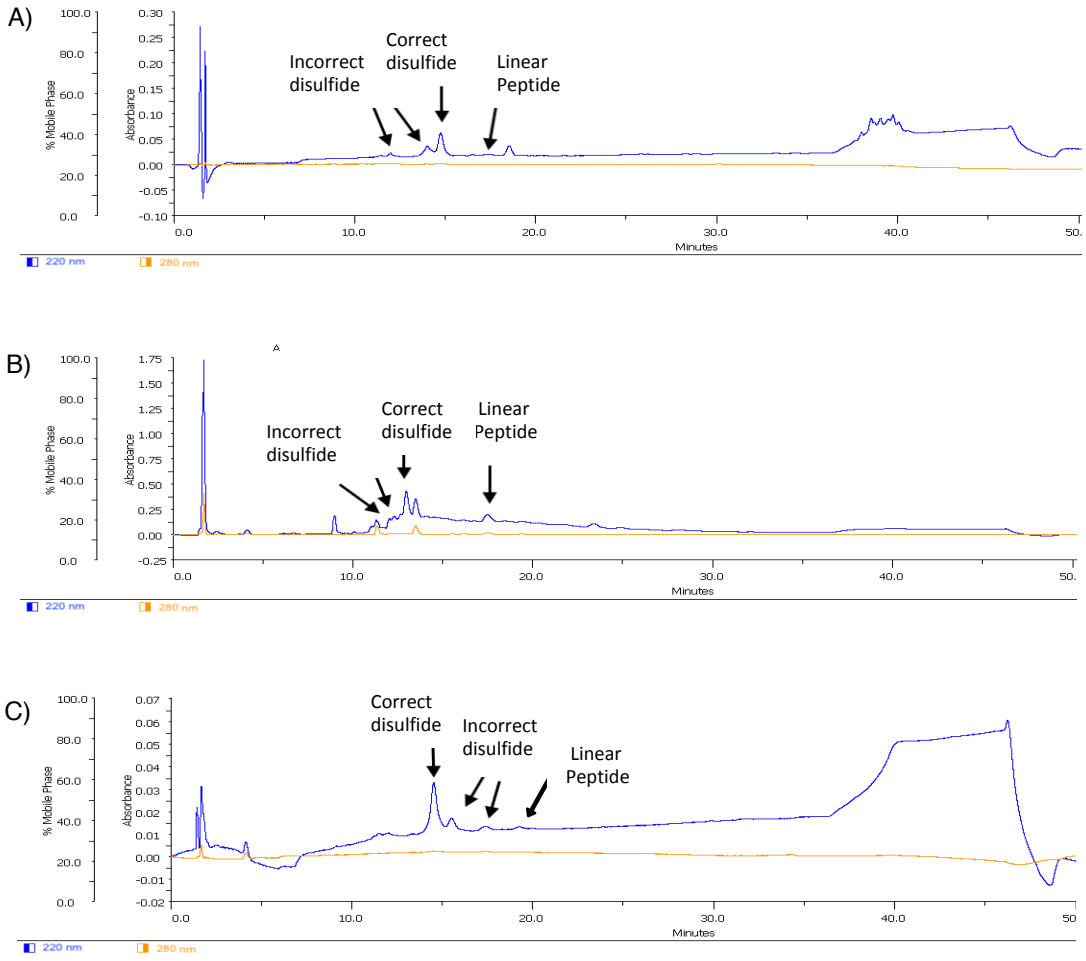

Figure 3-5: HPLC traces of different disulfide bond isomers for A) neopetrosiamide analogue A1 ***87****; B) neopetrosiamide analogue A2* ***88****; and C) neopetrosiamide analogue A3* ***89****; B)*

3.2.4 Global Oxidation for the Formation of Disulfide Bonds for Methylene Neopetrosiamide Analogues

To determine whether or not pre-forming one of the disulfide bridges via carbon-based macrocyclization helps to facilitate the correct formation of the remaining disulfide bonds, resin containing the monocyclic peptide was cleaved from the resin. The cleavage was done using a different method than the previous described conditions. The resin was cleaved with TFA and DMSO to remove S-^{t}Bu groups and oxidize, with anisole as a scavenger, and shaken to give a mixture of fully deprotected and oxidized peptides (*Scheme 3-4*). After removing TFA, the crude peptide was precipitated and collected but

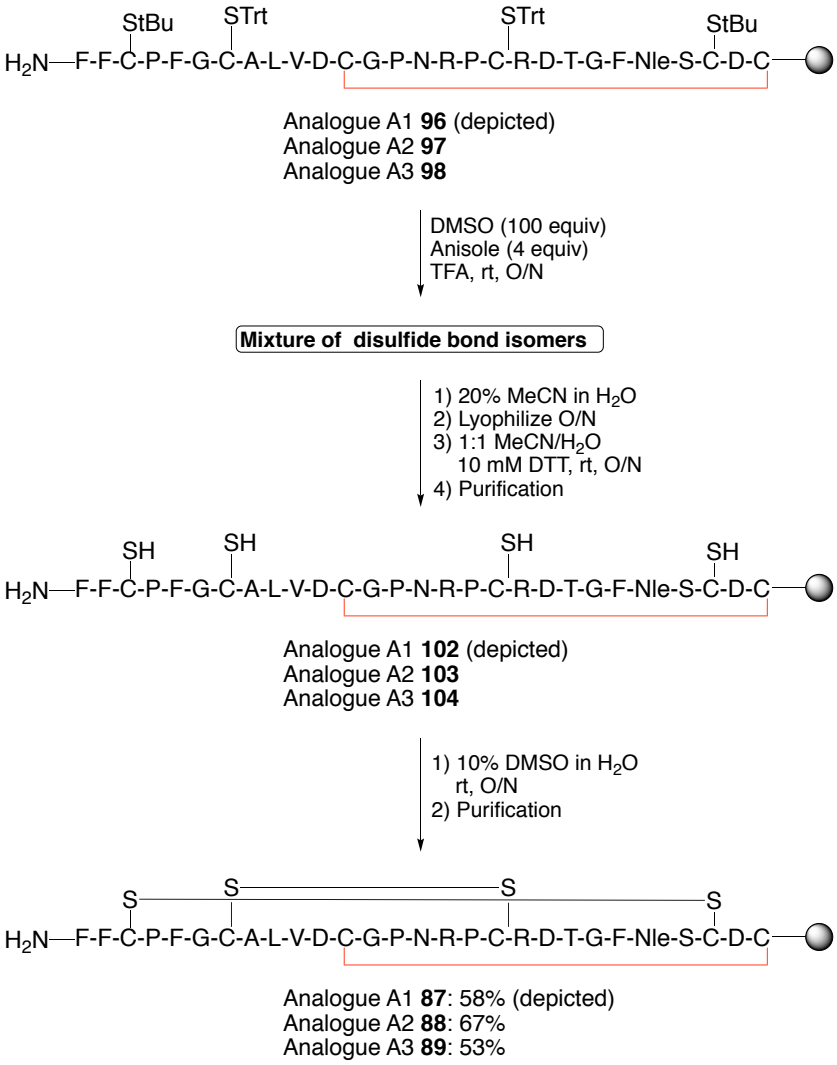

*Scheme 3-4 - Synthetic route for global oxidation of **102-104** to give neopetrosiamide analogues **87-89***

still contained substantial DMSO; therefore, it was redissolved in 20% MeCN in H_2O to be lyophilized to ensure the majority of DMSO was removed. Then, the crude peptide was dissolved in 1:1 MeCN:H_2O and the pH was adjusted with 0.1 M NaOH until it was around pH 8. A basic pH is required for DTT to fully reduce the peptide back to free thiols, because when attempted directly on the TFA deprotected material, a mixture of oxidized and reduced peptide was seen by MALDI. Enough DTT was added to make a 10 mM solution, fully reducing the peptides to give **102-104**.

The resulting reduced peptides were purified by HPLC; however, some oxidized peptide could be seen in the HPLC trace while running subsequent purifications. The oxidized peptide was separated from the reduced peptide by HPLC and re-subjected to the reduction conditions. The pure, reduced peptides **102-104** were then globally oxidized in a non-specific manner using 10% DMSO in H_2O. The new mixture of disulfide isomers was purified once more by HPLC to furnish the desired neopetrosiamide analogues **87-89** in 58%, 67% and 53% yields when compared to the other disulfide bond isomers combined.

Based on the isolated yields from the non-specific, global oxidation, the pre-formed ring seems to impart some conformation bias on the peptide prior to the formation of the disulfide bonds. The yields of the desired isomer for all three analogues were greater than the statistical mixture would presumably be, neglecting any intrinsic bias towards specific disulfide bonds based on the linear sequence. The results indicate that pre-stapling one of the rings helps to pre-form the 3D structure of the peptide. This method could be used to enhance proper formation of remaining disulfides in peptides containing multiple disulfide bonds.

3.2.5 Biological Testing of Methylene Neopetrosiamide Analogues Against Human Cancer Cells

To assess the activity of the novel neopetrosiamide analogues **87-89**, the peptides were tested against human breast cancer cells (MDA-MB-231). A modified morphological assay was conducted according to protocol from previous group members. MDA-MB-231 cells are a line of highly metastatic breast cancer cells and have the ability to invade surrounding tissue in a mesenchymal manner.[137] The freshly trypsinized cells were aliquoted onto a 96-well plate. Initial morphology of the cells showed they were spherical and suspended in the growth media. Neopetrosiamide **80**, which was synthesized

by Dr. Engelhardt, and native neopetrosiamide **5**, which was cloned and expressed, were used to act as positive controls. The cloning and expression was done by Marco van Belkum. Cloning was done by fusing the gene for neopetrosiamide to a small ubiquitin-like modifier (SUMO) protein, carrying an *N*-terminal His_6 tag for purification. The new gene was overexpressed in *E. coli* BL21(DE3). A Ni-NTA column was used to purify the fusion protein and the SUMO tag was cleaved with SUMO protease to furnish the crude linear peptide. The linear peptide was then purified by HPLC, and disulfide bonds were fully oxidized using 10% DMSO in H_2O, followed by 30% H_2O_2 in H_2O to oxidize methionine to the sulfoxide, affording the native neopetrosiamides A and B (**5**) as a mixture.[67]

Each of the disulfide bond isomers (major isomer and minor isomers) for each neopetrosiamide analogue (**87**-**89**) was then tested against the MDA-MB-231 cells in triplicate, at 20 μg/mL and 50 μg/mL, dissolved in 30% acetonitrile in water. The major and minor analogue isomers, native neopetrosiamides A and B (**5**) and neopetrosiamide **80** were added to each of the wells and incubated at 37 ºC under an atmosphere of 5% CO_2. The cell morphology was checked at two different time points: 2.5 h and 24 h. Active peptides/analogues will inhibit the cancer cells from spreading into the plated media, meaning the cells will remain spherical like the initial morphology, while inactive analogues will not inhibit cancer cell migration, causing them to appear elongated as they invade into the media.[137] Each well was inspected at the time points listed for cell adhesion, invasion and morphological changes at 20× magnification. The morphology of the cancer cells was compared to both positive controls (**5** and **80**) and the negative controls (30% acetonitrile in water).

After 2.5 h of incubation, the major disulfide bond isomer of each neopetrosiamide analogues **87-89** that was isolated all appeared to be active at both concentrations tested, when compared against the positive and negative controls, suggesting these isomers were correctly folded. The wells with the active analogues only contained cells that were round in shape and virtually none that seemed to be invading (*Figure 3-6A*), while the wells with the minor isomers displayed many cells that had begun to invade the media (*Figure 3-6B*), similar to the negative control. The preliminary results suggest that the novel neopetrosiamide analogues **87-89**, bearing a carbon-based macrocycle in place of a

disulfide bridge, did not lose their activity and are capable of inhibing the mesenchymal migration of MDA-MB-231 cells after 2.5 h. The assay was left to incubate for longer before the cell morphology was checked once more.

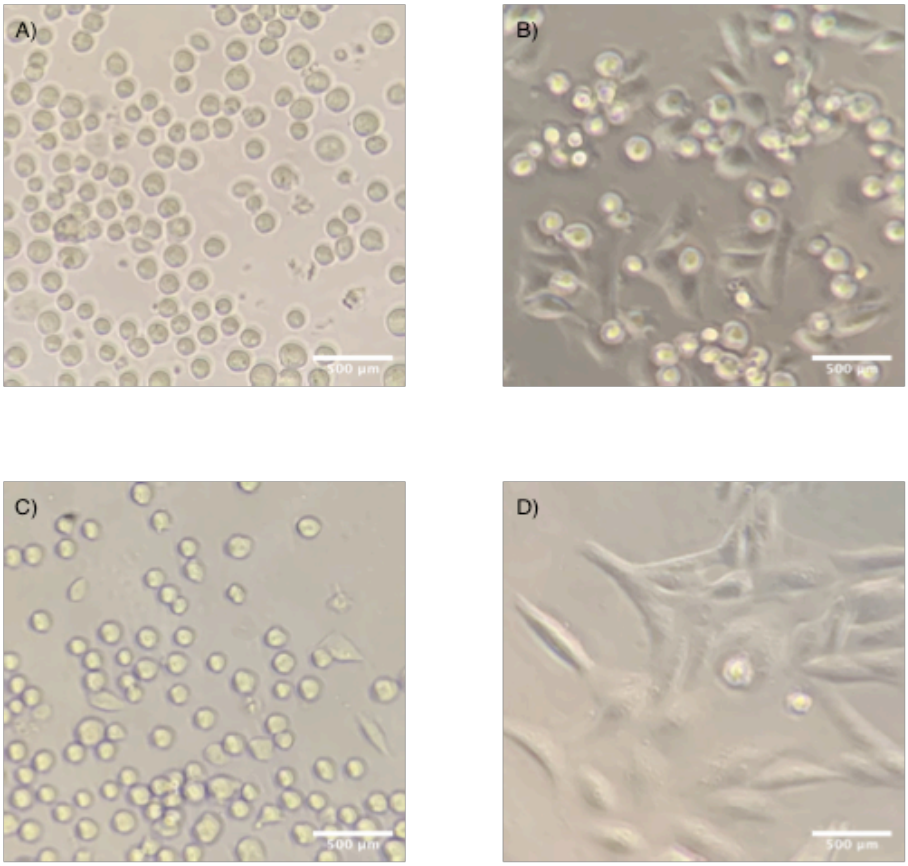

*Figure 3-6: Representative microscope images at 20× magnification of MDA-MB-231 breast cancer cells post treatment with neopetrosiamide analogues **87-89**. Concentrations of analogues in each image are 20 μg/mL. Analogues were dissolved in 30% acetonitrile in water. Image scale bars set to 500 μm. A) Representative image of rounded cells from analogue **89** after 2.5 h ; B) Representative image of cells beginning to invade from inactive isomer of analogue **89** after 2.5 h; C) Representative image of rounded cells from analogue **89** after 24 h; D) Representative image of invading cells from inactive isomer of analogue **89** after 24h.*

After 24 h of incubation, wells containing the major disulfide bond isomer of **87-89** once again contained primarily cells that were spherical in shape, with very few beginning to invade the media (*Figure 3-6C*); however, wells with the inactive analogue isomer displayed virtually all cells invading into the media, appearing very elongated (*Figure 3-6D*). Microscopic analysis after 24 h corroborate the results seen after 2.5 h, that the methylene bridge replacement of one of the disulfide bonds does not abolish the activity of analogues **87-89**.

To better understand the level of activity of the carbon analogues, the assay was done once more to determine minimum inhibitory concentrations (MICs) of each of the analogues. Beginning with 128 μg/mL, the MICs were determined using the standard two-fold dilution technique, once again testing in triplicate with native peptide **5** and norleucine analogue **80** as the positive controls and solvent (30% acetonitrile in water) as the negative control. The cells were left to incubate at 37 ºC for 24 h before being analyzed. MICs were determined by comparing to the negative control. The analogues were deemed no longer active when the quantity of rounded cells in the microscope field of view were within 10% of the quantity of rounded cells in the negative control. It was found that analogue A3 (**89**) possessed an MIC of 8 μg/mL, on par with the reported MIC for **5** and **80** (*Table 3-1*).[67] Conversely, analogues A1 (**87**) and A2 (**88**) possessed slightly higher MICs of 16 μg/mL.

Compound	Native (**5**)	**80**	**87**	**88**	**89**
MIC (μg/mL)	8	8	16	16	8

*Table 3-1: Minimum inhibitory concentrations of native neopetrosiamide **5**, norleucine analogue **80** and dicarba analogues **87-89** against MDA-MB-231 cells*

Biological testing of the three newly synthesized neopetrosiamide analogues **87-89** confirms that they retain the ability to inhibit mesenchymal cancer cell invasion as demonstrated on MDA-MB-231 cells. These results indicate that the sulfur to carbon substitution maintains the crucial 3D structure of the peptides required for activity, while also possessing MICs equivalent or on par with the natural product and that the major isomer peak on HPLC was the desired isomer.

3.2.6 NMR Assignment of Methylene Neopetrosiamide Analogues

Although high-resolution MALDI spectra and HPLC traces were obtained for each of the pure methylene analogues (**87-89**), attempts to assign the residues of each analogue using NMR was undertaken to further characterize the peptides. Dr. Andersen was able to successfully assign the residues of native neopetrosiamide **5** using a NMR solvent system of 4:1 MeCN-d_3/H_2O.[65] Unlike most NMR solvents that use purely deuterated material, H_2O was required to be used to ensure there was no exchange of the amide protons, as

these are crucial for assigning peptide NMRs. Total correlation spectroscopy (TOCSY) is often used for peptide NMR assignments as each of the amino acid residues are separate spin systems. By ensuring the amide protons are not exchanged with deuterium of the solvent system, the spin system can be seen using the relayed spin information from the amide hydrogen along the side chain. The same information can be gathered using any other signals from the amino acid residue; however, the region of the spectra containing the amide protons frequently contains fewer signals, thereby containing less signal overlap. Consequently, using H_2O as an NMR solvent means the signal from the water molecules must be suppressed in order to see any signal from the desired peptide. A repercussion of H_2O suppression is that any signals underneath the solvent signal or immediately adjacent may distorted or suppressed. This bolsters the importance of analyzing the amide region as the information that may be lost from solvent suppression can be inferred from the amide correlations.

By using the same solvent system as the Anderson lab, their assignments of neopetrosiamide can be used as a guide to assign the residues of the methylene analogues. Due to the relatively subtle changes done to the peptides, the local microenvironments and secondary structure of analogues **87-89** should be similar to that of the native peptide, meaning the chemical shifts of the residues will likely be similar. Unfortunately, the analogues displayed very poor solubility in the 4:1 MeCN-d_3:H_2O solvent system. Altering the NMR solvent used could likely alleviate the solubility issue, but this would negate the ability to use NMR assignments from the original neopetrosiamide discovery. Therefore, the same solvent system was used, but due to the poor solubility of analogue A1 (**87**), an NMR spectrum could not be obtained; however, NMRs for analogues A2 (**88**) and A3 (**89**) were successfully obtained (*Figure 3-7*).

When analyzing the TOCSY spectra, there was lots of background noise resulting from the low concentration of the peptide in solution due to the solubility issues. Nevertheless, the information that could be extracted was astounding. Neopetrosiamide analogue A2 (**88**) possesses the longest carbon bridge, spanning from residues 3-26, yet the signals arising from the bridge connecting those 2 residues were able to be seen on TOCSY (*Figure 3-7A*). Beginning with the amide proton of residue 3 (Das^3), assigned to the signal at 7.88 ppm, the spin information from this signal could be 'walked along' the

carbon chain, up until H_γ (*Figure 3-8A*). When looking at the structure of the diaminosuberic acid bridge, H_γ from 3rd third residue correlates to H_δ when counting from the 26th residue (F*igure 3-8*). Because of the linkage, the same signals should be reciprocated when looking at residue 26 (Das^{26}). Indeed, many of the signals from the opposite end of the carbon bridge can be seen. The amide hydrogen of Das^{26}, assigned to the signal at 7.95 ppm, has correlations up until H_γ (*Figure 3-8B*). Therefore, when analyzing either end of the DAS linkage between residues 3 and 26 on the TOCSY spectrum, the same correlations can be seen up until H_γ. Furthermore, the chemical shift values between the two ends of the linkage agree with ones another. The minute differences in values likely stem from a combination of the large molecule having a slower tumbling time in solution. Lower tumbling times would lead to small changes in the transfer of the spin information from end to end during the NMR acquisition of data. Additionally, the low intensity of the spectra from the solubility problems likely contributes to the error when interpreting the absolute chemical shift values.

After analyzing the amide hydrogen peaks in the 7-9 chemical shift range and cross-referencing their chemical shifts with native neopetrosiamide **5**, 85% of the amino acid residues from analogue **88** were assigned (*Table 3-2*). The amide hydrogens of the first two *N*-terminal amino acid residues are often not visible by NMR. The *N*-terminus is usually protonated as $NH_3^{+\cdot}$ resulting in rapid exchange with water, nullifying its ability to be seen, the second residue also exchanges rapidly with water due to its proximity to the protonated *N*-terminus, and because it is commonly solvent exposed.[195] Consequently, the first two phenylalanine residues of **88** were exceedingly difficult to assign as alternate cross-peaks appeared with overlapping signals, and many aromatic signal were not prominent on the spectrum. Proline residues proved more difficult to assign, due to their lack of amide hydrogen; however, cross-peaks from Pro^{14} and Pro^{17} were able to be discerned and assigned, leaving only Pro^4 unassigned. Lastly, the residue signals from Phe^5 were unable to be definitively assigned with respect to neopetrosiamide **5**. In the end, 24 of 28 residues, including the DAS methylene bridge were confidently assigned to analogue **88**.

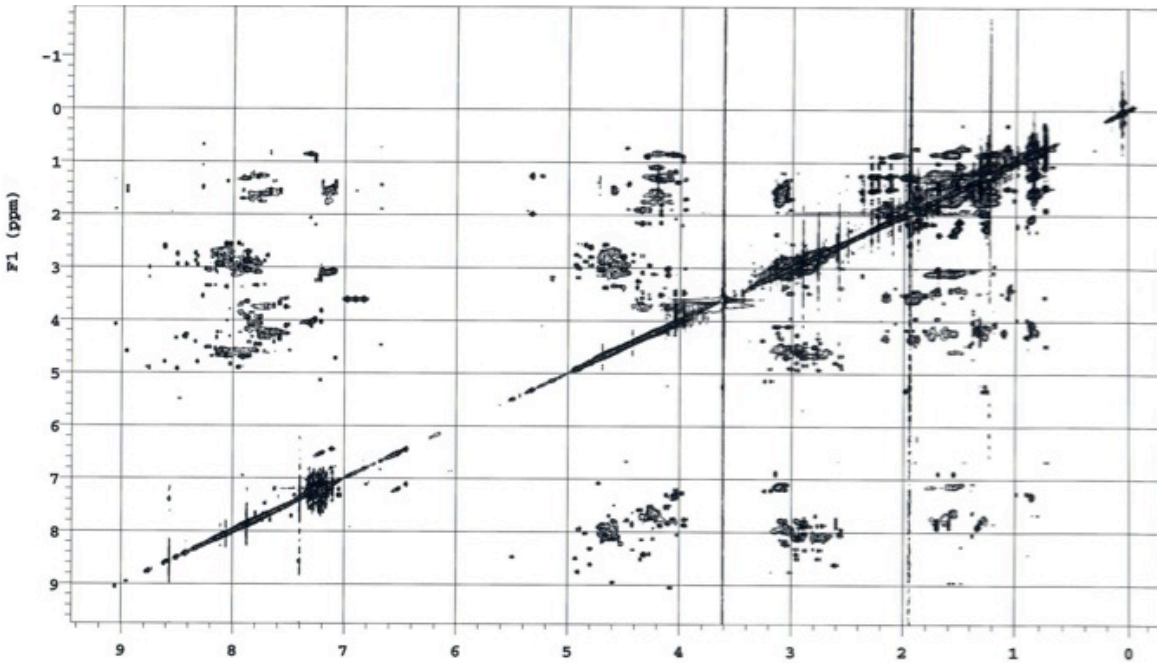

*Figure 3-7A: 2D TOCSY NMR spectrum of neopetrosiamide analogue A2 (**88**)*

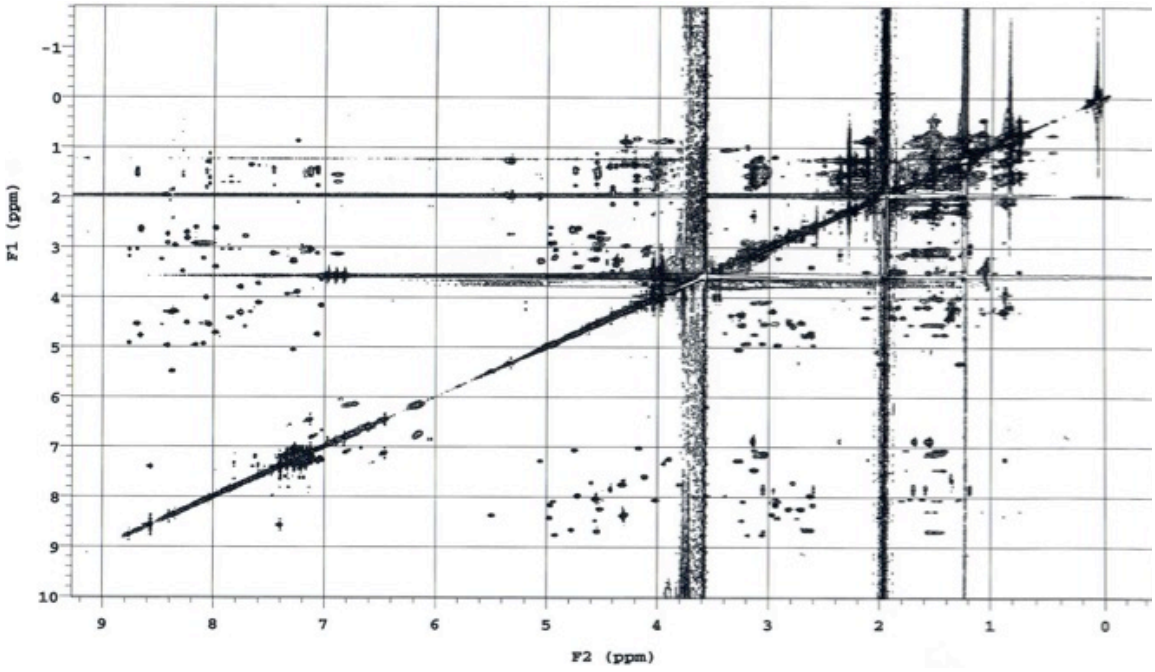

*Figure 3-7B: 2D TOCSY NMR spectrum of neopetrosiamide analogue A3 (**89**)*

Signal (ppm) / Residue	NH	Hα	Hβ	Hδ	Hγ	Others
Phe[1]	–	–	–	–	–	–
Phe[2]	–	–	–	–	–	–
Das[3]	7.88	4.69	3.35, 3.12	2.87	1.75, 1.58	
Pro[4]	N/A	–	–	–	–	–
Phe[5]	–	–	–	–	–	–
Gly[6]	7.21	4.09, 3.88				
Cys[7]	8.34	4.43	2.90, 2.70			
Ala[8]	8.11	4.05	1.45			
Leu[9]	7.34	3.96	1.93	1.69	1.19	
Val[10]	7.27	4.01	2.19	1.01, 0.92		
Asp[11]	7.96	4.97	3.02, 2.58			
Cys[12]	8.62	4.82	2.59			
Gly[13]	8.23	4.34, 3.40				
Pro[14]	N/A	4.01	1.01	2.23	3.73	
Asn[15]	8.43	4.33	2.90			
Arg[16]	8.01	4.69	1.39	1.80	3.37, 2.59	
Pro[17]	N/A	4.34	2.15	1.90	3.38, 3.28	
Cys[18]	8.51	4.93	2.99, 2.78			
Arg[19]	9.06	4.12	1.95, 1.81	1.35, 1.21	3.10	
Asp[20]	8.75	4.95	3.23, 3.01			
Thr[21]	8.47	4.32	4.20	1.01		
Gly[22]	7.53	4.08, 3.81				
Phe[23]	8.13	4.58	2.96, 2.69			7.90
Nle[24]	8.28	3.58	1.51	1.09	0.69	
Ser[25]	7.23	5.15	3.31, 3.25			
Das[26]	7.95	4.21	3.48	1.90, 1.81	2.69	
Asp[27]	8.96	4.62	1.62, 1.52			
Cys[28]	8.03	4.85	2.91, 2.58			

*Table 3-2: Amino acid residue assignments based on TOCSY for neopetrosiamide analogue A2 (**88**)*

Analysis of the TOCSY spectrum for neopetrosiamide analogue A3 (**89**) yielded similar results for residue assignments to those seen for **88** (*Table 3-3*). The DAS bridge linking residues 7-18 could be visualized much like neopetrosiamide analogue A2 (**88**), although it appears as though the microenvironment experienced by the methylene bridge

Signal (ppm) / Residue	NH	Hα	Hβ	Hδ	Hγ	Others
Phe[1]	–	–	–	–	–	–
Phe[2]	–	–	–	–	–	–
Cys[3]	8.16	4.97	2.93, 2.63			
Pro[4]	N/A	–	–	–	–	–
Phe[5]	7.98	4.76	3.41, 2.66			7.51
Gly[6]	–	–	–	–	–	–
Das[7]	8.05	4.58	1.79, 1.61	1.31	1.52	
Ala[8]	7.70	4.31	1.4			
Leu[9]	6.89	4.74	2.34	1.76, 1.52	1.22	
Val[10]	7.25	3.89	2.15	0.89		
Asp[11]	8.28	5.04	2.84, 2.34			
Cys[12]	–	–	–	–	–	–
Gly[13]	7.76	4.34, 3.80				
Pro[14]	N/A	4.20	1.71, 1.60	2.16, 1.92	3.57, 3.41	
Asn[15]	8.25	4.55	2.87, 2.72			
Arg[16]	7.05	4.76	1.54, 1.41	1.82	3.17	7.27
Pro[17]	N/A	4.38	2.76	1.32, 1.25	3.46	
Das[18]	8.07	4.01	1.82	1.49	1.31	
Arg[19]	8.70	4.53	1.55, 1.47	1.35	3.10	
Asp[20]	8.82	4.93	3.21, 3.06			
Thr[21]	8.36	4.33	4.23	0.93		
Gly[22]	7.61	4.13, 3.71				
Phe[23]	8.47	4.60	3.26, 2.94			7.30
Nle[24]	8.29	3.53	1.61, 1.52	1.13	0.72	0.51
Ser[25]	7.29	5.06	3.32			
Cys[26]	8.38	5.49	2.44, 1.87			
Asp[27]	8.67	4.77	2.69, 2.62			
Cys[28]	8.10	4.94	3.26, 2.93			

*Table 3-3: Amino acid residue assignments based on TOCSY for neopetrosiamide analogue 3 (**89**)*

of analogue **89** is vastly different from analogue **88**. The Hβ's appear at much lower chemical shift than seen in *Table 3-2* (~1.8 ppm vs. ~3.5 ppm), indicating these two bridges exists in different electronic environments. Once more, the first two phenylalanine residues of **89** could not definitively be assigned, nor could Pro[4] again. Gly[6] and Cys[12]

were also unable to be assigned; yet 24 of the 28 residues for neopetrosiamide analogue A3 (**89**) were assigned with confidence in consultation with the original assignments.

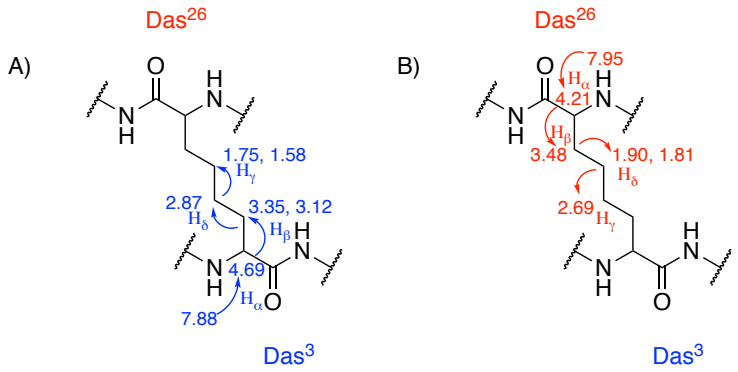

*Figure 3-8: TOCSY correlations of the diaminosuberic acid bridge in neopetrosiamide analogue A2 (**88**); A) TOCSY correlations beginning with the amide hydrogen of residue Das[3]; B) TOCSY correlations beginning with the amide hydrogen of residue Das[26].*

All in all, TOCSY NMR spectra for 2 of the 3 novel methylene analogues of neopetrosiamide were collected with 85% of the residues being assigned for each of them. The pre-installed methylene bridges using diaminosuberic were able to be visualized from either end through the NMR spectra. Residue assignments did not differ greatly from literature assignments of the native peptide, corroborating the assumption that the minute isostere changes did not drastically alter the unique microenvironments of the peptide.

3.3 Conclusions and Future Directions

Orthogonally protected diaminosuberic acid **44** was used to efficiently install methylene bridges as a replacement for disulfide bridges in the potential anti-metastatic therapeutic peptide neopetrosiamide, generating 3 novel analogues **87-89**, each with a single disulfide bond replaced. The formation of the remaining disulfide bonds was simplified to a single step, as opposed to two sequential deprotection/oxidations, eliminating the requirement for a desalting step in between. The new method produces similar yields to the two-step method, but with an increased convenience, generating the desired isomer in excess of 70% in a single oxidation step. Pre-stapling of the growing chains on resin leads to a conformation bias in the peptides, predisposing them to fold correctly in proportions of greater than 50% when oxidized non-specifically. The novel analogues demonstrate biological activity against human breast cancer cell line MDA-

MB-231 in levels equal to (8 μg/mL), or on par (16 μg/mL) with the native peptide **5**. 2D NMR experiments allow visualization of the pre-installed bridges by TOCSY correlations in 2 of the 3 analogues, along with 85% of the residues confidently assigned based on literature data. Furthermore, a more efficient synthesis of active neopetrosiamide analogues has been described by reducing overall disulfide bond isomers. Lastly, a method for cloning, expressing and purifying the native peptide has been developed. These methods serve to increase the accessibility to an otherwise difficult peptide to acquire, as the sea sponge from which it is gathered can no longer be readily located.

It is known that disulfide bonds scrambling regularly occurs in blood plasma and disulfide bond reduction occurs intracellularly to their corresponding thiols. In the case of neopetrosiamide, not only does this negate any activity, but recombination of the thiols to disulfides likely results in scrambling of the disulfide bonds and disulfide bond shuffling result in an inactive isomer. By replacing one of them with methylene, there is a probable increase to metabolic stability against glutathione in blood plasma. Furthermore, there are fewer possible isomers, leading to an increased chance that disulfide bond scrambling would lead back to the correct isomer. For neopetrosiamide to be considered for any therapeutic purposes, an assay would need to be done to determine the half-life and stability of neopetrosiamide and its analogues in blood plasma. Further, the potential toxicity of the peptide would need to be discerned. Although the whole peptide does not seem to interact with healthy cells, the potential toxicity of any fragments that are produced upon enzymatic degradation of the peptide needs to be assessed. There is much about neopetrosiamide that remains a mystery for it to be moved forward as an anti-cancer peptide. However, beginning with stability and toxicity assays would go a long way to garnering a better understanding of neopetrosiamides potential.

The allyl/alloc protecting group scheme used to incorporate orthogonally protected diaminosuberic acid **44** into the neopetrosiamide analogues is one such scheme that is compatible with SPPS. As mentioned in Chapter 2, TMSE/Teoc and *p*NB/*p*NZ are routinely used as orthogonal protecting groups, although experiences with their removal have coincided with lower yields compared to allyl/alloc. There exist numerous highly efficient photolabile groups compatible with SPPS,[196] any of which can be used in tandem with the aforementioned protecting groups schemes. Through variation of the protecting

groups used on **44**, (such as **105** and **106**), a neopetrosiamide analogue wherein all three disulfide bonds have been replaced with methylene (**107**) can be synthesized (*Figure 3-9*). This type of analogues would benefit from a complete lack of disulfide bonds; thereby rending intracellular glutathione a non-issue and eliminating any disulfide bond isomers by disulfide bond scrambling. This theoretical analogue would then need to be tested via the described MDA-MB-231 invasion assay.

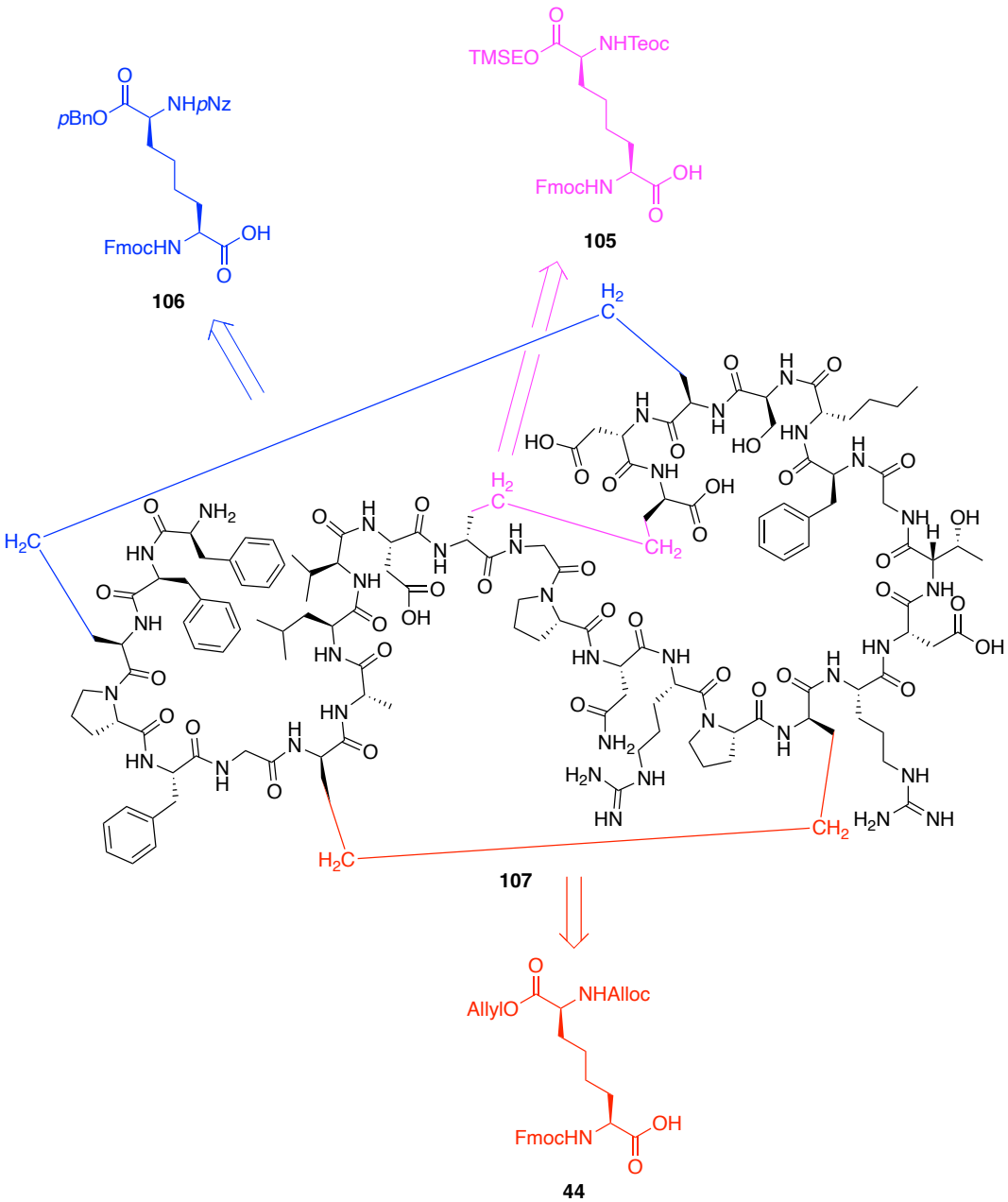

*Figure 3-9: Retrosynthetic analysis of the amino acid building blocks (**44, 105** and **106**) required to generate an entirely carbon neopetrosiamide analogue (**107**)*

4 Chapter 4: Synthesis of Apelin Analogues

4.1 Introduction to Apelin

4.1.1 Overview of Apelin

With cardiovascular disease (CVD) being the largest cause of death worldwide, the development of new treatment options is of the utmost importance. Apelin presents a unique opportunity to help combat CVD and myocardial infarction-reperfusion injury. It is a physiologically active peptide hormone that binds to the G protein-coupled (GPCR), apelin receptor (APJ).[106,121] Since its discovery, the interest in the apelin-APJ system has flourished as a result of the various physiological functions it affects. There is extensive literature on the apelin-APJ system, its mode of action and its many physiological effects.[197,198] Highlighted below are a few key discoveries made with respect to the questions probed by this chapter.

Binding of apelin to the receptor elicits numerous beneficial cardiovascular effects, namely the ability to protect against myocardial ischemia-reperfusion injury (MIRI).[107] The receptor itself displays a certain level of promiscuity. Elabela has been elucidated as another ligand for the APJ receptor,[199] indicating that the receptor may tolerate modifications to its endogenous ligands for therapeutic purposes. Unfortunately, apelin is limited in its potential to become a therapeutic peptide because it is promptly degraded *in vivo* by multiple proteases.[114,116,117] Two separate alanine scans have been conducted to gather a better understanding of the role of each amino acid in the apelin sequence.[200,201] Both scans deemed the RPRL region critical to binding and physiological activity of the [pyr]^{1}-apelin-13 isoform (**11**) (*Figure 4-1*). Altering the *C*-terminus of **11** resulted in the discovery that the terminal phenylalanine residue is essential for β-arrestin-mediated internalization of the APJ receptor.[118,202] In turn, this removes the ability to induce vasodilation via the NO-mediated pathway and to protect against MIRI.[111,202]

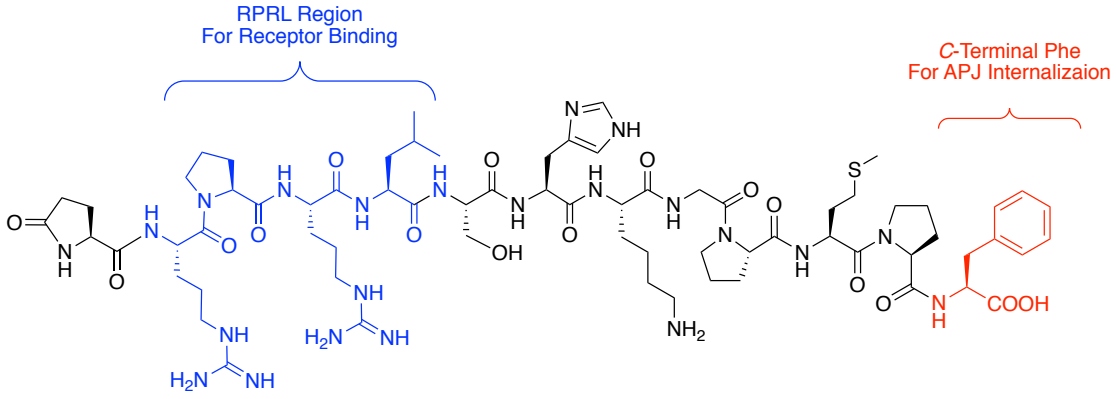

*Figure 4-1: The RPRL region of [pyr]^{1}-apelin-13 (**11**) critical for receptor binding and the C-terminal phenylalanine residue for APJ internalization.*

Apelin-17 (**12**) is another isoform that the apelin prepropeptide can be cleaved into when being processed. It can exert similar effects as [pyr]^{1}-apelin-13, albeit with a shorter half-life and an increased efficiency. The apelin-17 isoform possesses an additional protease site, resulting in the lower plasma half-life.[117] Both the [pyr]^{1}-apelin-13 and apelin-17 isoforms have extensively been studied by our group to produce more active and metabolically stable derivatives.

4.1.2 Previous Work on Apelin by the Vederas Group

Apelin has been of interest to the Vederas group for its potential for protection against MIRI. While it was known that ACE-2 cleaves the apelin peptide to inactive it,[114,127] the remaining proteases responsible for cleaving [pyr]^{1}-apelin-13 and apelin-17 were unknown for some time. Previous group members were able to determine that neprilysin deactivates [pyr]^{1}-apelin-13 and apelin-17,[116] while kallikrein KLKB1cleaves apelin-17.[117]

With the knowledge of the proteolytic cleavage sites and the important regions of the peptides from the alanine scans, there has been extensive work conducted by our group to produce stable and active analogues of both [pyr]^{1}-apelin-13 and apelin-17 **12** (*Figure 4-2*). Dr. McKinnie pioneered the A2 analogues of apelin. Modification of the *C*-terminus resulted in ACE-2 stability, while modification of the Leu5 residue provided NEP stability (**108**).[115] This analogue serves as the basis for other variations on the A2

analogues synthesized by our group. Tess Lamer and Conrad Fischer probed the effect of extending the apelin peptide with PEG chains equipped with an aromatic head group, such as Fmoc (**13**). In addition to analogue **13**, Tess Lamer tested different lengths of PEG linkers and tested palmitoyl linkers on both [pyr]^{1}-apelin-13 and apelin-17 as well as modifications of the head group to a Cbz, a phenylalanine residue and a *p*-benzoylphenylalanine residue.[120] These analogues provide increased stability to KLKB1 without directly modifying the KLKB1 cleavage site. Kleinberg Fernandez has recently further investigated the neprilysin cleavage site by incorporating homoarginine and *N*-methyl cyclohexylalanine in place of Arg4 and Leu5, to give an active and stable analogue **109**. Kleinberg Fernandez also synthesized various analogues containing combinations of these two modifications, and some without a methylated nitrogen.[119] These analogues maintained the NEP stability and displayed activity on par to native apelin and active analogues **13** and **108**.

Isostere substitution and modifications of [pyr]^{1}-apelin-13 and apelin-17 by our group have generated a vast array of metabolically stable synthetic apelin analogues, many of which possess equal or slightly greater activity to the native peptides. Each analogue has their own benefits and disadvantages, such as ease of synthesis and purification, solubility properties and cost of production. The more analogues that are produced, the greater the chance that one of them will fit the needs of an academic group, such as understanding mechanism of action or for a structure-activity relationship. More analogues also increase the possibility of one becoming the analogue possessing vastly enhanced properties to be taken forward to help protect against MIRI.

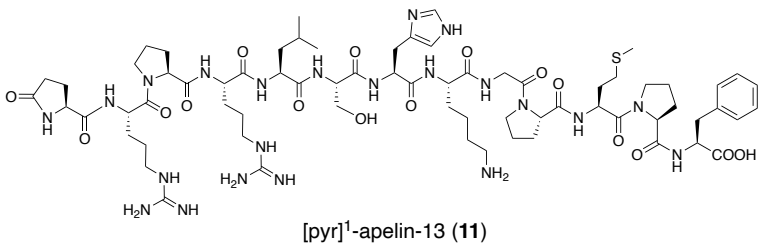

[pyr]^{1}-apelin-13 (**11**)

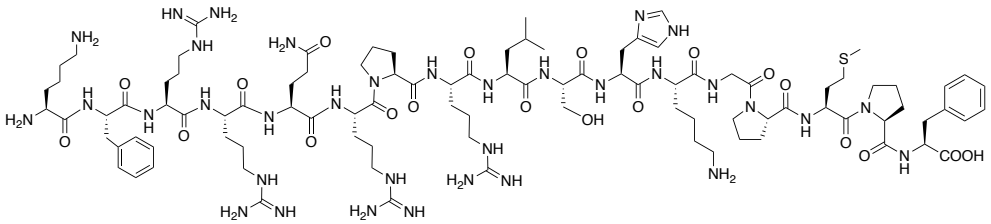

apelin -17 (**12**)

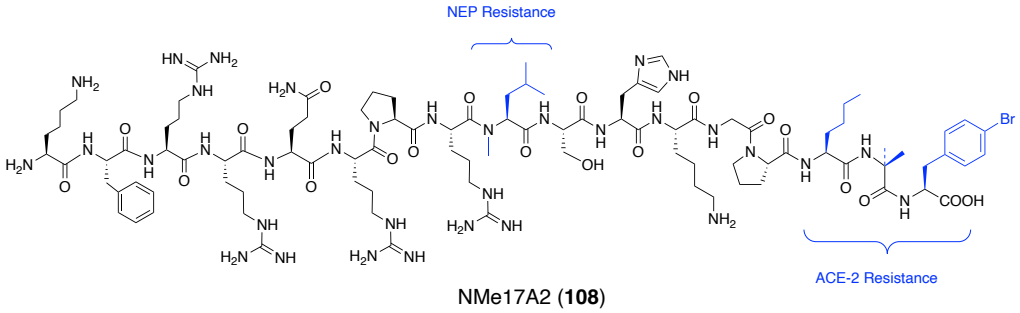

NMe17A2 (**108**)

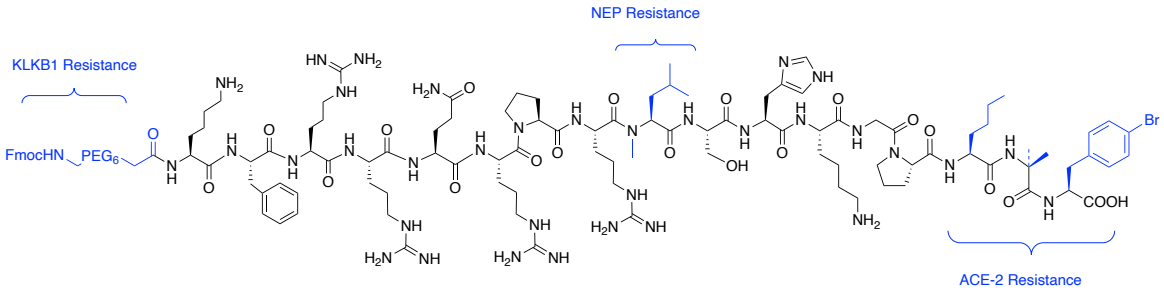

FmocPEG6-NMe17A2 (**13**)

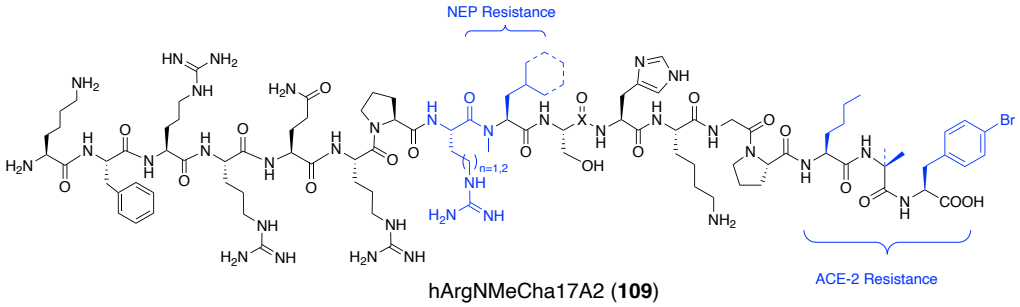

hArgNMeCha17A2 (**109**)

*Figure 4-2: Various apelin (**11** and **12**) and apelin derivatives (**13**, **108**, **109**) synthesized by our group.*

4.2 Results and Discussion of KLKB1 Resistant Apelin Analogues

4.2.1 Isostere Substitution of KLKB1 Cleavage Site

Prior to the discovery that the extension of apelin-17 with a PEG_6 chain furnishes a KLKB1 stable apelin analogue that maintains activity, resistance to cleavage by plasma kallikrein was sought through isostere substitution. KLKB1 is known to cleave between Arg14 and Arg15 (residues numbered from *C*-terminus of apelin-17). Akin to generation of NEP resistant analogue **108** through *N*-methylation, resistance to KLKB1 could likely be achieved in a similar fashion. There are many isostere substitutions that could be utilized to confer KLKB1 stability, such as *N*-methylation, α-methylation, aza-linkage and D-amino acid substitution (*Figure 4-3*). Substitutions with D-amino acids in apelin analogues have proven to be ineffective.[116,118] The other three substitutions have had moderate effectiveness for stabilization of the neprilysin degradation site and would attempt to be incorporated into the apelin analogues to achieve KLKB1 stability (*Figure 4-4*).

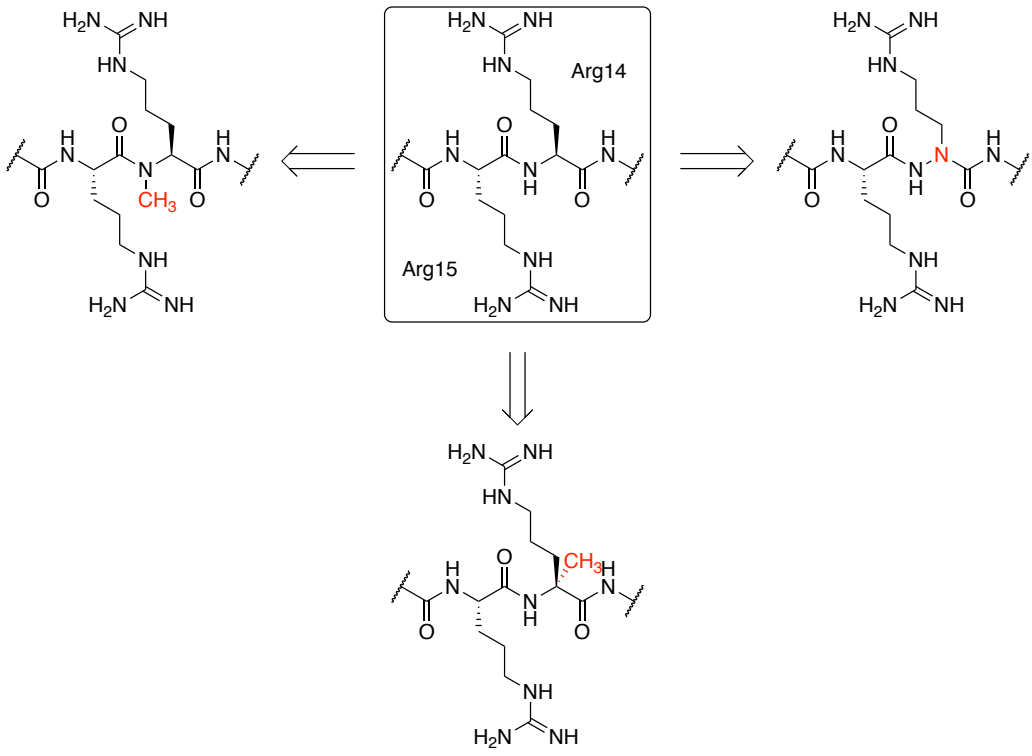

Figure 4-3: Proposed synthetic modification to Arg14 at the KLKB1 cleavage site.

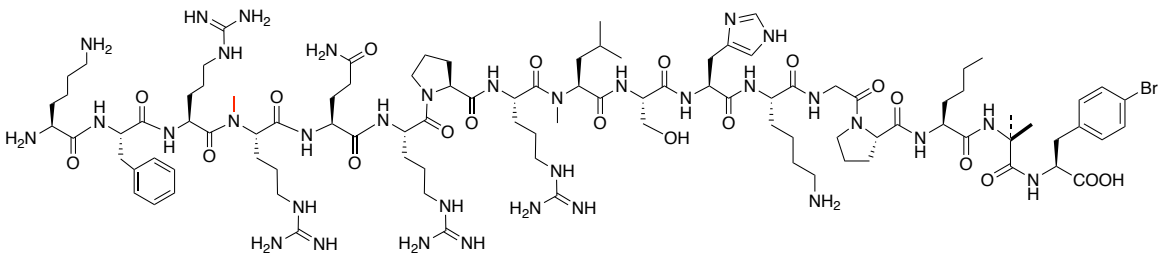

NMeArg14-NMe17A2 (**109**)

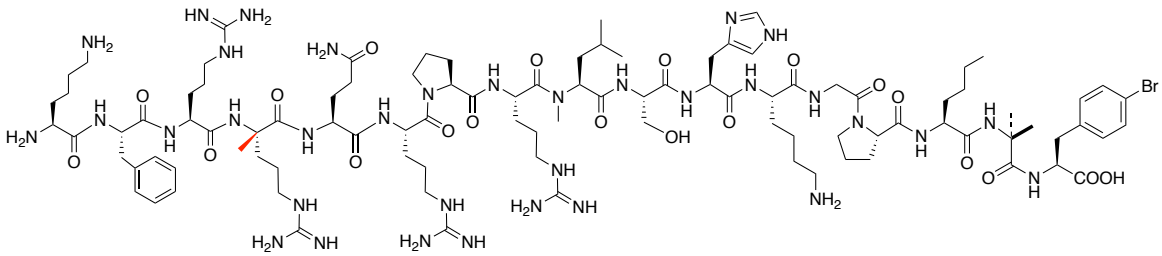

αMeArg14-NMe17A2 (**110**)

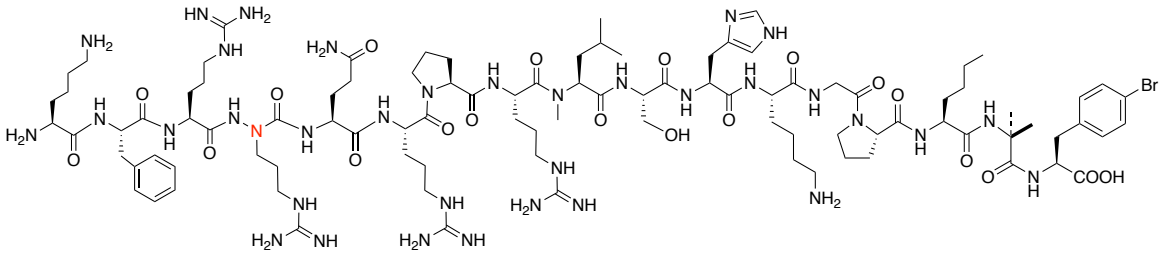

azaArg14-NMe17A2 (**111**)

Figure 4-4: Proposed apelin analogues with isostere substitution at Arg14 for KLKB1 stability

4.2.2 Synthesis of NMeArg14-NMe17A2 Apelin Analogue

The synthesis of effective A2 apelin analogue often requires the incorporation of the NMe leucine moiety (**113**) into the peptide chain. Dr. McKinnie previously discovered that this was best done by incorporating the amino acid as a dipeptide with Arg10 (*Scheme 4-1*). Direct coupling of the commercially available *N*-methyl-L-leucine benzyl ester *p*-toluenesulfonate salt **113** to a Pbf or Pmc protected arginine was not conducted, as these protecting groups are not orthogonal to benzyl ester removal. Furthermore, arginine amino acids have a propensity to react intramolecularly when they are *C*-terminally activated, an effect that is accentuated when coupling to a hindered amino acid such as

113.[203,204] These pitfalls are mitigated by coupling first to a protected ornithine **112** through the use of PyBOP and HOBt in the presence of base, giving the dipeptide **114** in 72% yield. Removal of the ornithine side chain Boc group using TFA and subsequent reaction with 1,3-di-Boc-2-(trifluoromethylsulfonyl)guanidine (**115**) affords an arginine moiety in the dipeptide (**116**) in 94% yield over 2 steps. The *C*-terminal benzyl ester was removed under hydrogenation conditions to furnish the SPPS amenable dipeptide **117**.

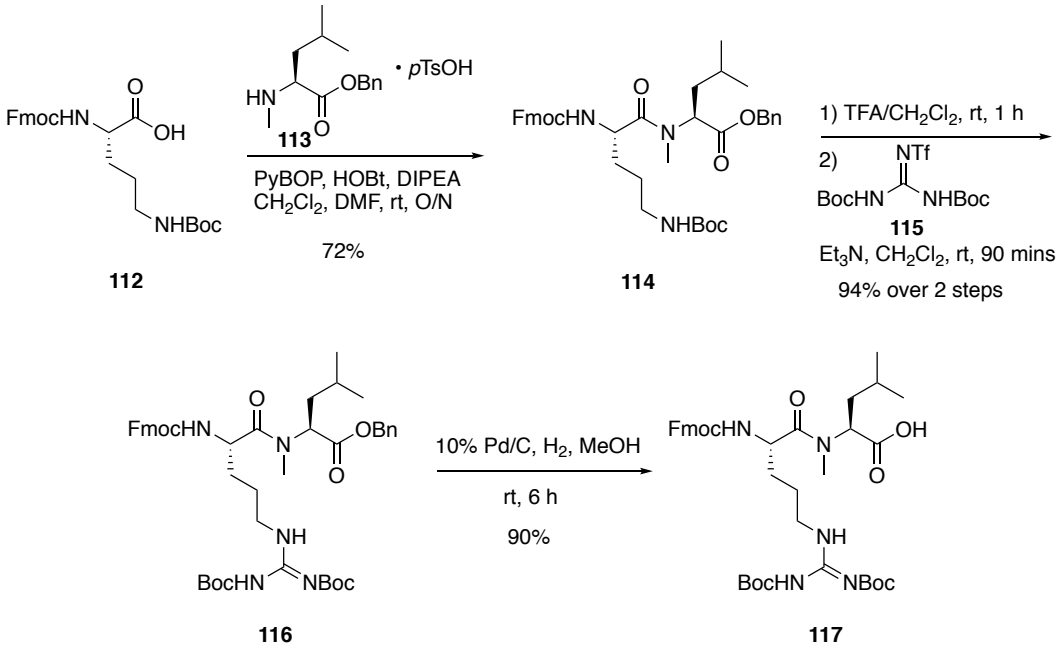

*Scheme 4-1: Synthesis of Fmoc-Arg-NMeLeu dipeptide **117***

Following the synthesis of **117**, the synthesis of NMeArg14-NMe17A2 (**109**) was commenced on resin. Following general Fmoc based SPPS using 2-chlorotrityl resin, Fmoc-*p*BrPhe was loaded onto resin at a loading of 0.8 mmol/g to give **118** (*Scheme 4-2*). The peptide was extended using the general SPPS method, up until the dipeptide **117** would need to be incorporated, at the octapeptide **119**. To couple the dipeptide, two rounds of couplings were done in succession with new materials each time. However, only 2 equivalents of the dipeptide were used, as opposed to the standard 5 equivalents for canonical amino acids. After coupling **117** to the growing chain to give **120**, ensuring coupling had been completed by analysis with MALDI, followed by a ninhydrin test, the peptide was further elongated out until the KLKB1 cleavage site at Arg14 (**121**).

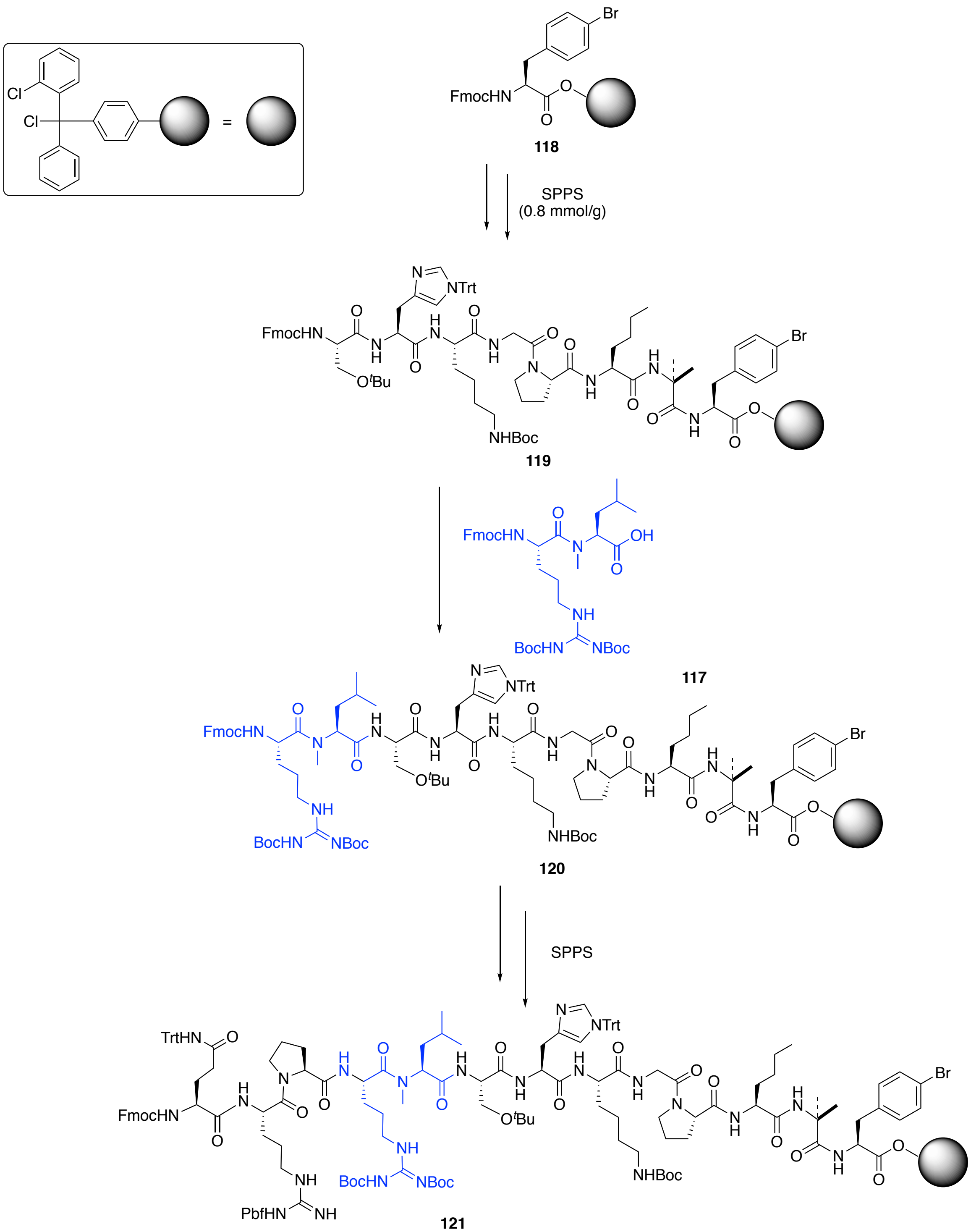

Scheme 4-2: General synthetic scheme for the SPPS synthesis of KLKB1 stable apelin analogues.

With the tridecapeptide **121** in hand, the next step was to incorporate the *N*-methyl arginine moiety. Commercially available Fmoc-NMe-Arg(Mtr)-OH (**122**) was then coupled to the peptide **121** using the same conditions as the dipeptide **117** to ensure that the coupling went to completion (*Scheme 4-2*). The resulting peptide **123** was then carried forward and coupled to the next arginine. This next coupling was difficult to achieve as a

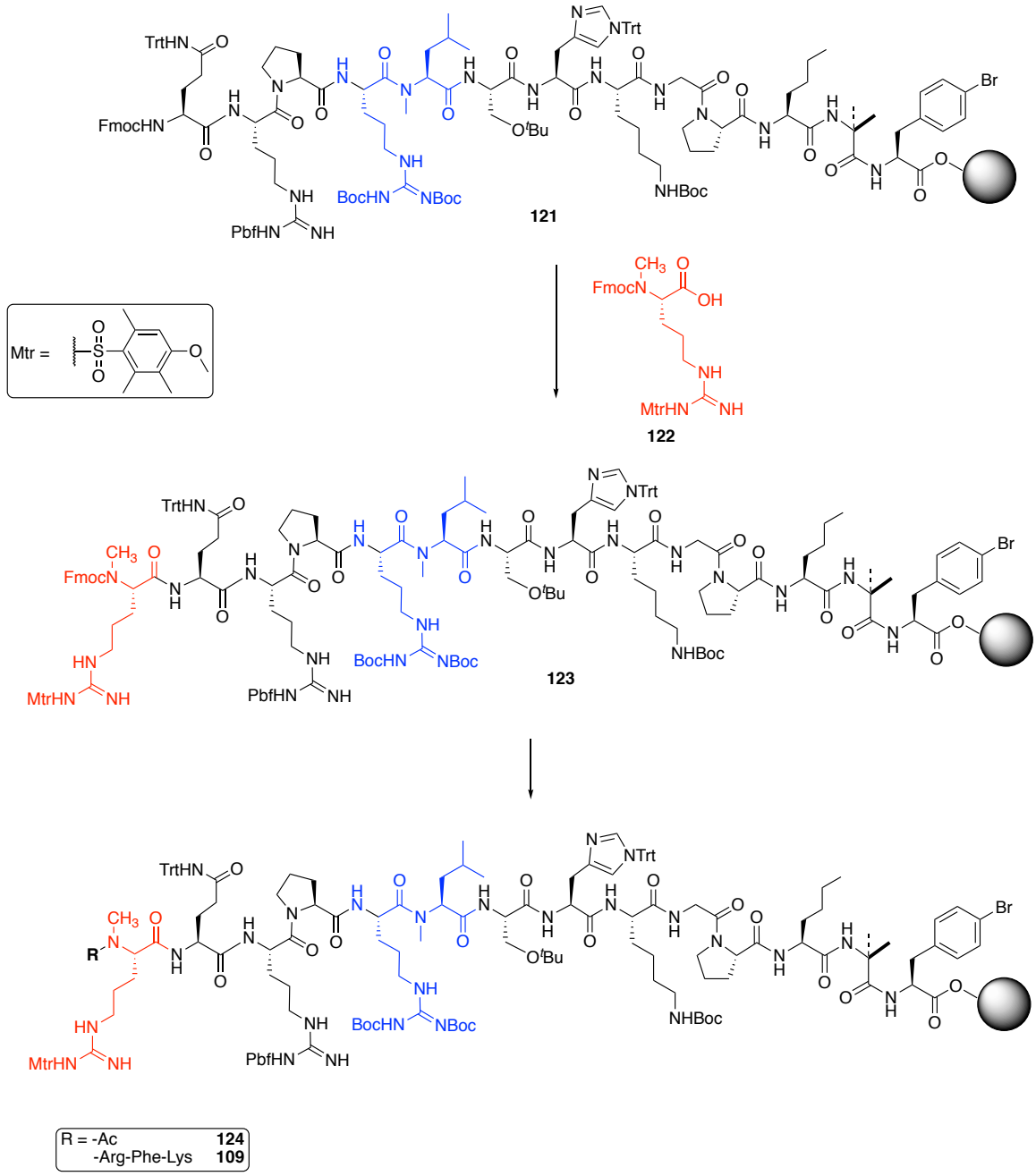

*Scheme 4-3: The synthetic scheme for the synthesis NMeArg14-NMe17A2 apelin analogue **109** and the side product **124**.*

result of the hindered secondary amine of the methylated arginine. Despite repeated attempts to couple Arg15, the reaction would not proceed fully to completion; yet no unwanted lactam side product was formed either. It was at this point that the peptide was end-capped to avoid undesired extension of the incomplete growing peptide to give **124** on resin as a truncated peptide. This Ac-NMeArg14-NMe17A2 (**124**) derivative proved to be interesting as it bore a close resemblance to the native [pyr]^{1}-apelin-13 isoform, yet it possessed the NEP stabilization and potential KLKB1 resistance, thus it could be an active analogue. Following the addition of the last few amino acids to furnish the completed apelin analogue **109** on resin, the peptide was cleaved from resin using 95:2.5:2.5 TFA:H_2O:TIPS, also removing all the side chain protecting groups. Peptides **109** and **124** were then purified using RP-HPLC and lyophilized for testing.

4.2.3 Synthesis of αMeArg14-NMe17A2 Apelin Analogue

Unlike the *N*-methyl arginine moiety that was commercially purchased, α,α-disubstituted amino acids needed to be synthesized. Moreover, this needed to be done in an asymmetric, stereoselective fashion to retain the desired stereochemistry of the amino acid. There exist many auxiliaries to do this type of chemistry to provide access to α,α-disubstituted amino.[181] One such method to alkylate glycine or alanine amino acids to generate unnatural or noncanonical amino acids from cheap starting materials is the use of the Belokon complex.[205] This chiral nickel(II) Shiff base complex provides stereoselective alkylation of alanine or glycine by effectively blocking one face of the amino acid, controlling the approach of the incoming electrophile to the desired face. This method works well for the synthesis of αMe amino acids (*Scheme 4-4*). Beginning with the alanine complex (**125**), the enolate can be formed under relatively mild conditions using KO^{t}Bu at low temperatures, and then trapped with an electrophile such as benzyl bromide

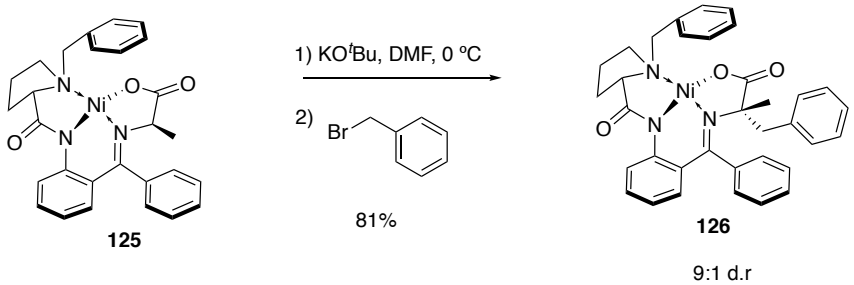

Scheme 4-4: Belokon complex for the formation of α-methyl amino acids

to provide efficient access to α-methylated amino acids (**126**).[205] This same method was applied to generate the α-methyl arginine building block required for the synthesis of the apelin analogue **110**. Dr. Fischer synthesized **127** by alkylating the corresponding alanine complex **125** (*Scheme 4-5*). A mixture of diastereomers was initially formed; however, the two isomers were separable on silica. The correct stereochemistry was confirmed by comparing to literature.[115] Decomplexation of **127** in the presence of acid, followed by purification using ion-exchange chromatography, providing the free α,α-disubstituted amino acid **128** in 84% yield. The extreme polarity of **128** caused solubility issues when attempting to react the material with the desired reagents in CH_2Cl_2. This was

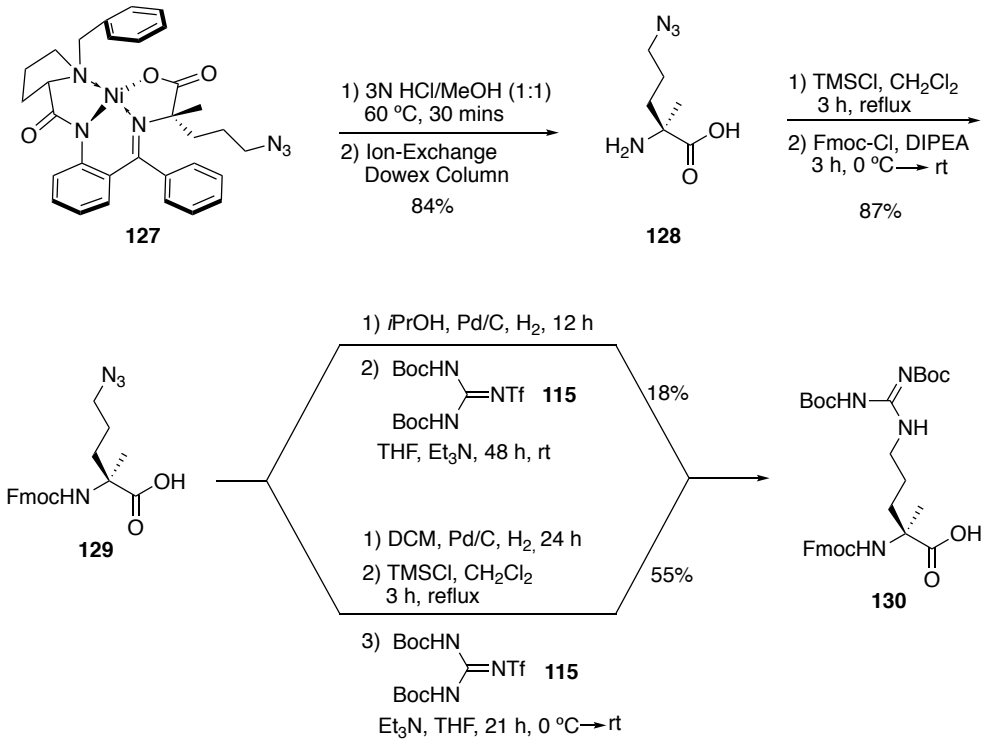

*Scheme 4-5: Synthetic scheme for the synthesis of αMe arginine building block **130***

circumnavigated by refluxing the amino acid in the presence of trimethylsilyl chloride (TMSCl). This fully solubilized the amino acid in CH_2Cl_2 by masking the free amine with a trimethylsilyl (TMS) group. Reaction of the resulting solution with Fmoc-Cl in the presence of base yielded the Fmoc protected amino acid **129** in 87% yield over 2 steps. The TMS group on the nitrogen was removed upon aqueous work up. The azido group of **129** was reduced using hydrogenolysis, forming a free amine. Upon work-up, the crude mixture was immediately reacted with 1,3-di-Boc-2-(trifluoromethylsulfonyl)guanidine

115. The reaction proceeded slowly, as there were solubility issues with the amino acid in THF, even with prolonged reaction times of 2 days. The product **130** was initially isolated in 18% yield over 2 steps. The reaction was attempted once more using TMSCl again. Following reduction of the azide, the crude mixture was reacted with TMSCl at elevated temperatures to help solubilize the reactants. Once everything had dissolved, the reaction mixture was cooled down to 0 ºC and **115** was added. Warming up to room temperature overnight provided **130** in a vastly improved 55% over three steps in a shorter period of time.

Beginning from the previously synthesized tridecapeptide **121**, the αMeArg building block **130** was added to the growing chain (*Scheme 4-6*). The amino acid coupling proceeded smoothly compared to the coupling of the NMeArg amino acid, and only one round of coupling was needed to achieve sufficient conversion to **131**. The resin was checked by MALDI mass spectroscopy to confirm the presence of the product, while a ninhydrin test indicated that the starting material was consumed. The peptide was then extended with the final three amino acids to afford the αMeArg14-NMe17A2 **110** on resin. The peptide was cleaved from resin using 95:2.5:2.5 TFA:H_2O:TIPS and purified using RP-HPLC and lyophilized to provide the pure peptide **110**.

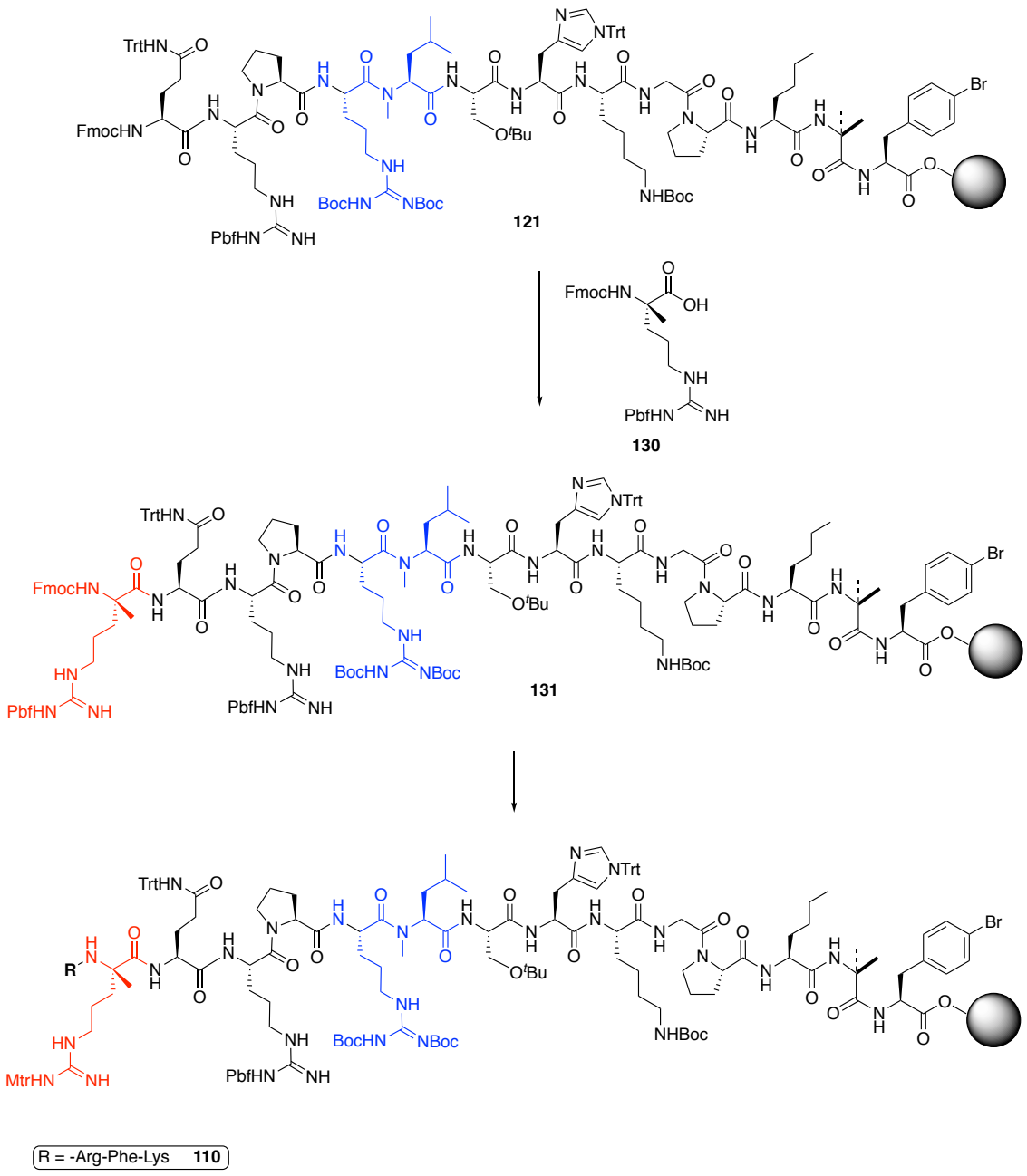

*Scheme 4-6: The synthetic scheme for the synthesis αMeArg14-NMe17A2 apelin analogue **110***

4.2.4 Synthesis of azaArg14-NMe17A2 Apelin Analogue

The synthesis of an azaArg building block was attempted by using a method derived from Dr. McKinnie. Instead of synthesizing a single amino acid building block, it has been proven to be easier to synthesize the aza-moiety as a tripeptide.[115] To construct the aza backbone of the peptide, benzophenone hydrazone (**132**) was reacted with

disuccinimidyl carbonate (**133**), followed by the addition of a solution of commercially available H-Gln(Trt)-O^{t}Bu (**134**) with DIPEA via a cannula at low temperatures (*Scheme 4-7*). Despite repeating the conditions and technique analogous to the literature procedure,

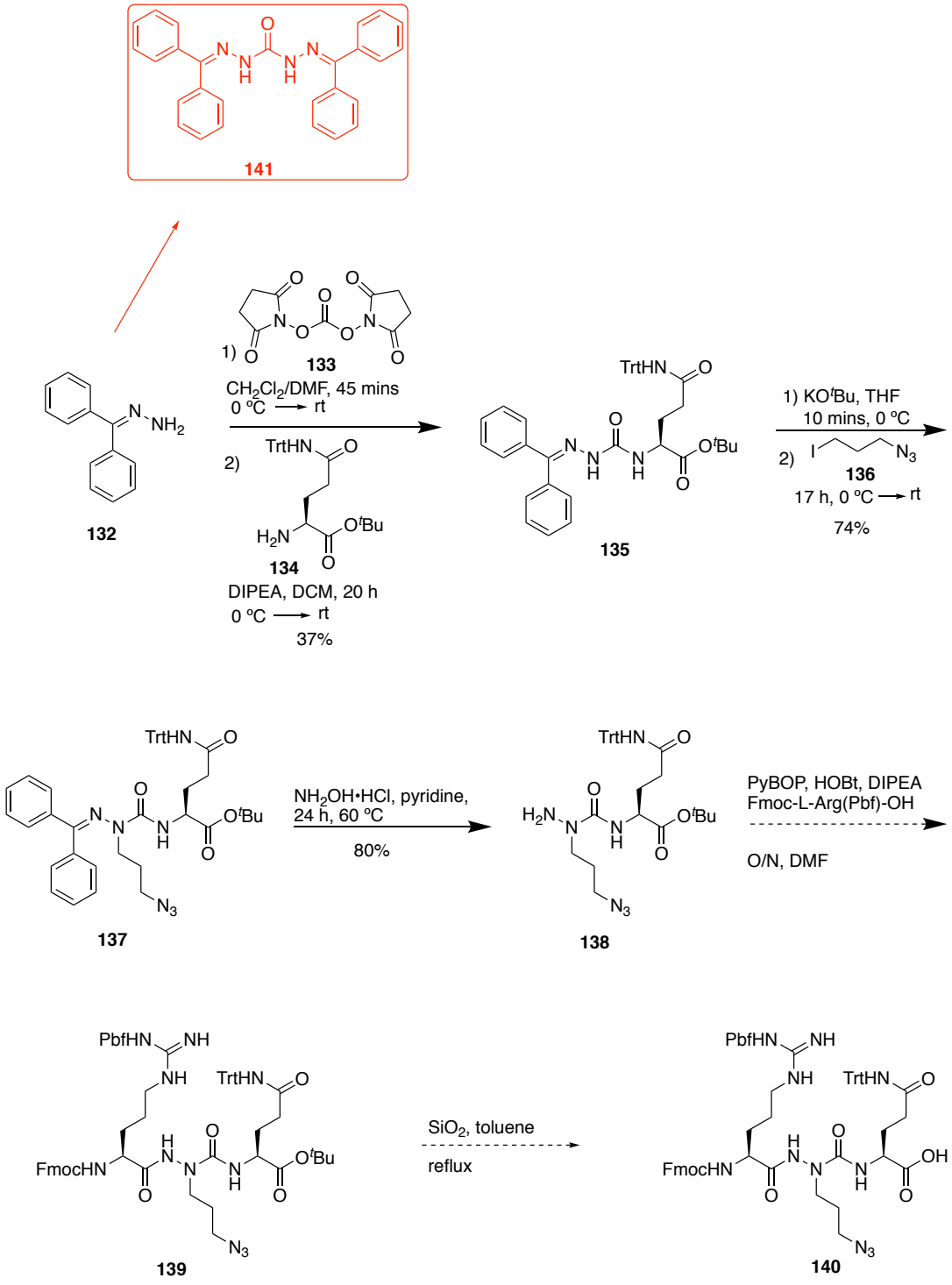

*Scheme 4-7: Proposed synthetic scheme for the synthesis of azaArg building block **140***

the yield for the semicarbazone **135** never rose above 37% over 2 steps.[31] In fact, a large amount of the side product urea **141** was isolated from the column. Attempts to mitigate the formation of this urea side product were unsuccessful, so the reaction was repeated several times to gather enough material to be carried forward. Deprotonation of the sermicarbazone with KO^{t}Bu and subsequent alkylation of **135** with 1-azido-3-iodopropane (**136**) provided **137**. A transimination with hydroxylamine hydrochloride at elevated temperatures in pyridine gave the semicarbazide **138**. At this point, the mixture was to be taken to tripeptide **139** by coupling with Fmoc-Arg(Pbf)-OH, followed by deprotection of the *C*-terminal ^{t}Bu group (**140**) with SiO_2 in toluene at reflux in order to keep the trityl protecting group intact.

Unfortunately, there was very little material left due to the poor yielding first step. An attempt was made to couple the arginine to **138** on less than 0.1 mmol (100 mg) of material; yet no product could be detected. At the same time, the previously synthesized apelin analogues **109** and **110** had been submitted for testing to collaborators (Gavin Oudit) and the results, to be discussed later in the chapter, were underwhelming.

The azaArg building block synthesis and azaArg14-NMe16A2 apelin analogue were abandoned at this stage in favour of the newly synthesized PEGylated apelin derivatives, which possessed excellent biological results.

4.2.5 Plasma Stability Assay of KLKB1 Resistant Analogues

To determine if the isostere substitutions at Arg14 were efficient at resisting cleavage by KLKB1, the analogues were incubated with human plasma. Analogues **109** and **110** (5 μL, 400 μM) were incubated in Eppendorf tubes with human plasma (20 μL) and the tubes were then incubated at 37 ºC for varying lengths of time. The solutions were quenched by adding 10% aqueous TFA, and then an internal standard peptide (Dansyl-YVG-OH) was added. The mixtures were centrifuged to remove any solid particulates and the supernatant was loaded onto a C_{18} spin column and successively washed with 0.1% aqueous TFA and varying concentrations of MeCN with 0.1% TFA, centrifuging between each wash. Finally, the peptides were eluted from the spin column using 40% MeCN with 0.1% TFA. The eluant was then purified by RP-HPLC. The amount of analogue remaining was determined as a percent. This was done by comparing the area under the peaks on the HPLC chromatogram between the apelin analogue and the internal standard.

The 0 minute timepoint of incubation of the internal standard/analogue area ratio (determined by RP-HPLC) was then used to compare to the ratio of remaining analogue/internal standard. These results were done in triplicate to ensure accurate measurements.

Interestingly, the isostere substitution at Arg14 by αMe or NMe drastically increased the half-life of the peptides in plasma. When compared to the half-life of native apelin-17 (**12**) (0.02 h ± 0.01 h), the peptides were about 300 times more stable (**109** = 5.2 h ± 0.2 h; **110** = 7.1 h ± 0.5 h). Furthermore, when compared to the half-life of ACE-2 and NEP stable NMeLeu17A2 analogue **108** (1.2 h ± 0.1 h), the newly synthesized peptides increased the half-life about 5 times. These results indicate that the isostere substitution at position 14 had a beneficial effect with regards to stability to cleavage by KLKB1. The Ac-NMeArg14-NMe17A2 analogue (**124**) was not tested as it did not possess the KLKB1 cleavage site.

4.2.6 Calcium Mobilization and Receptor Binding of KLKB1 Resistant Analogues

Binding to the receptor and subsequent activation can be measured through radioligand displacement and Ca^{2+} mobilization assay. The radioligand displacement assay was done by our collaborator Catherine Llorens-Cortes in Paris, while the Ca^{2+} mobilization assay was done in house by Dr. Fischer.

The receptor binding of apelin analogues is monitored through the displacement of radioactive ligand, bearing an iodine isotope ([^{125}I]-pyr-1-apelin-13). The ligand is bound to a wild-type rat apelin receptor expressed CHO cells. Incubation with analogues will displace the ligand and the radioactivity can be measured to determine the amount of ligand that has been displaced when compared to the control where no analogue was added to provide pIC$_{50}$ concentrations.

Calcium mobilization is monitored using the stable expression of the APJ receptor in suitable cells. The cells are plated on a 96-well plate and have a fluorescent dye added to them and incubated at 37 ºC. The apelin analogues are added to the cells according to a serial dilution and the change in fluorescence is monitored to determine the concentration required for Ca^{2+} mobilization, providing pEC$_{50}$ concentrations

The radioligand displacement assay was done by collaborators on apelin analogues **109** and **110**. Both analogues seemed to be able to displace the radioactive ligand,

indicating they were binding to the receptor. The NMeArg14 analogue **109** possessed a pIC_{50} of 8.82 nM ± 0.08 nM, while the αMeArg14 **110** possessed a pIC_{50} of 9.00 nm ± 0.10 nM. Both analogues are able to bind to the APJ receptor with low nanomolar affinities, comparable to the NMeLeu17A2 (**108**) and better than native apelin-17 (**12**) (*Table 4-1*). Due to the cost and logistics of shipping the apelin analogues to Paris for testing, Ac-NMeArg14-NMe17A2 analogue (**124**) was not sent for testing, as preliminary Ca^{2+} mobilization results were not promising.

The calcium mobilization assay was conducted on analogues **109**, **110** and **124** to determine the pEC_{50} of the compounds. Each of the analogues seemed to show downstream G-protein activation due to the triggering of calcium release. The NMeArg14 analogue **109** possessed pEC_{50} of 8.46 nM ± 0.18 nM, while the αMeArg14 **110** possessed a pEC_{50} of 8.62 nm ± 0.21 nM. Even the Ac-NMeArg14-NMe17A2 analogue (**124**) possessed a comparable pEC_{50} (9.15 ± 0.22 nM) to the native apelin-17 (**12**) and NMeLeu17A2 (**108**) (*Table 4-1*).

	apelin-17 (native) (12)	**NMeLeu 17A2 (108)**	**NMeArg14-NMe17A2 (109)**	**αMeArg14-NMe17A2 (110)**	**Ac-NMeArg14-NMe17A2 (124)**
***p*IC$_{50}$ (nM)**	10.30 nM ± 0.08	9.22 nM ± 0.07	8.82 nM ± 0.08	9.00 nM ± 0.10	N/A
***p*EC$_{50}$ (nM)**	8.72 nM ± 0.18	8.31 nM ± 0.08	8.46 nM ± 0.18	8.62 nM ± 0.21	9.15 ± 0.22

*Table 4-1: pIC_{50} values from radioligand displacement assays and pEC_{50} from calcium mobilization assays of native apelin-17 (**12**), NMeLeu17A2 analogue (**108**), NMeArg14-NMe17A2 (**109**) and αMeArg14 –NMe17A2 (**110**).*

These results suggest that the KLKB1 resistant apelin analogues **109** and **110**, and the side-product analogue **124** are capable of binding to the GPCR APJ and activating it by virtue of downstream calcium release. Binding and activation concentrations are comparable to native apelin-17.

4.2.7 Physiological Testing of KLKB1 Resistant Analogues

Physiological tests on apelin analogues **109** and **110** were conducted by the laboratory of Gavin Oudit at the Mazankowski Alberta Heart Institute. Each analogue was administered to male mice via cannula to the right carotid artery at a concentration of 1.4 μM/Kg. Saline was used as a negative control. Various values were measured including heart rate (HR), mean arterial blood pressure (MABP), systolic (SBP) and diastolic blood pressure (DBP).

Effective analogues display a quick and stable increase in the heart rate, coupled with a prolonged decrease in the MABP, which can also be visualized in a prolonged decrease in SBP and DBP.

When the newly synthesized apelin analogues **109** and **110** were administered to the mice, there was a noticeable increase in HR from the αMeArg14 analogue **110**, while the NMeArg14 analogue **109** did not show an increase in HR when compared to native apelin-17 (**12**) (*Figure 4-5*). The MABP for **110** initially dropped lower than native

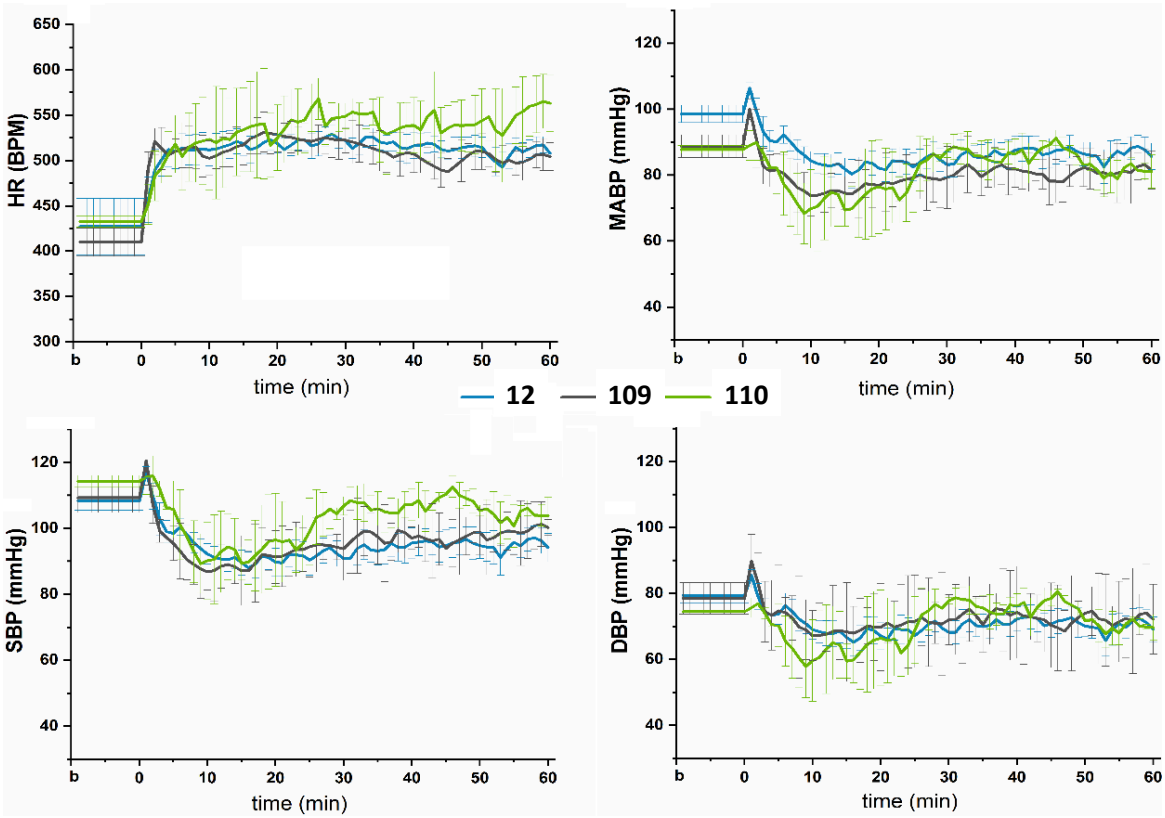

*Figure 4-5: Blood pressure and heart rate data for apelin analogues **109** and **110** compared to native apelin-17 **12**.*

apelin-17 **12**; however, the results were not sustained, and the blood pressure slowly began to rise up to the initial pressure. Analogue **109** proved capable of sustaining a lower MABP for a longer period of time, but the results were not as pronounced as desired for an active analogue. The effects of **109** and **110** on both SBP and DBP displayed very similar results to that of the control **12**.

Both analogues **109** and **110** possessed physiological capabilities on par or slightly better than the native apelin-17 isoform **12**. Consequently, the results were nowhere near the most active analogue NMeLeu17A2 **108** at the time of submission to the collaborators. At the same time the αMeArg14 and NMeArg14 analogues were being submitted, the PEGylated generation of analogues were also being tested, resulting in the PEGylated analogues **13** being carried forward for further testing.

4.2.8 Conclusions

The synthesis of two novel KLKB1 resistant apelin analogues (**109** and **110**) was completed, each incorporating backbone modification at arginine 14. Both analogues displayed much greater plasma stability compared to the native isoforms and possessed increased stability to the previous most stable analogue **108**. Additionally, another novel apelin analogue (**124**) was isolated as a side-product during the synthesis of the NMeArg14 analogue. Each of the three apelin derivatives were capable of activating the APJ receptor as seen through Ca^{2+} mobilization and the results were comparable to the native hormone. Radioligand displacement showed efficient binding of **109** and **110** to the APJ receptor; however, the physiological testing of the KLKB1 resistant analogues provided poor results. Neither **109** nor **110** were effective at lowering the MABP or increasing HR when administered to mice, ultimately leading to the abandonment of further analogues along this line, such as the azaArg14 synthesis that was halted. While the peptides seemed promising at first based on their activation of the APJ receptor, their physiological results paled in comparison to the newly synthesized PEGylated generation of apelin analogues **13**.

4.3 Macrocyclic Apelin Analogues

As the isostere substitution at Arg14 produced ineffectual apelin analogues, attention was turned towards the potential of cyclic apelin derivatives. As previously stated, interest in stapled peptides is becoming increasingly popular for peptide therapeutics.[36] They routinely display increased proteolytic stability,[37] increased cell-permeability, improved pharmacokinetics, increased bioavailability and possess a higher potential to be orally active.[36, 38] Strategic placement of the macrocycle, such as at *i* and *i* + 4 residues, will often enforce an α-helix secondary structure. For the above reasons, incorporation of a macrocycle into apelin may very well be beneficial.

Cyclic apelin analogues have been synthesized before, albeit many of them possess drastically reduced binding affinity and potency.[206,207] However, Éric Marsault was able to synthesize macrocyclic apelin-13 derivatives with respectable binding affinities when compared to native apelin-13.[208] This was achieved through incorporation of two allylglycine residues, followed by RCM to generate a macrocycle (*Scheme 4-8A*). Based on previous alanine scans, the olefinic residues replaced the amino acids at positions 3

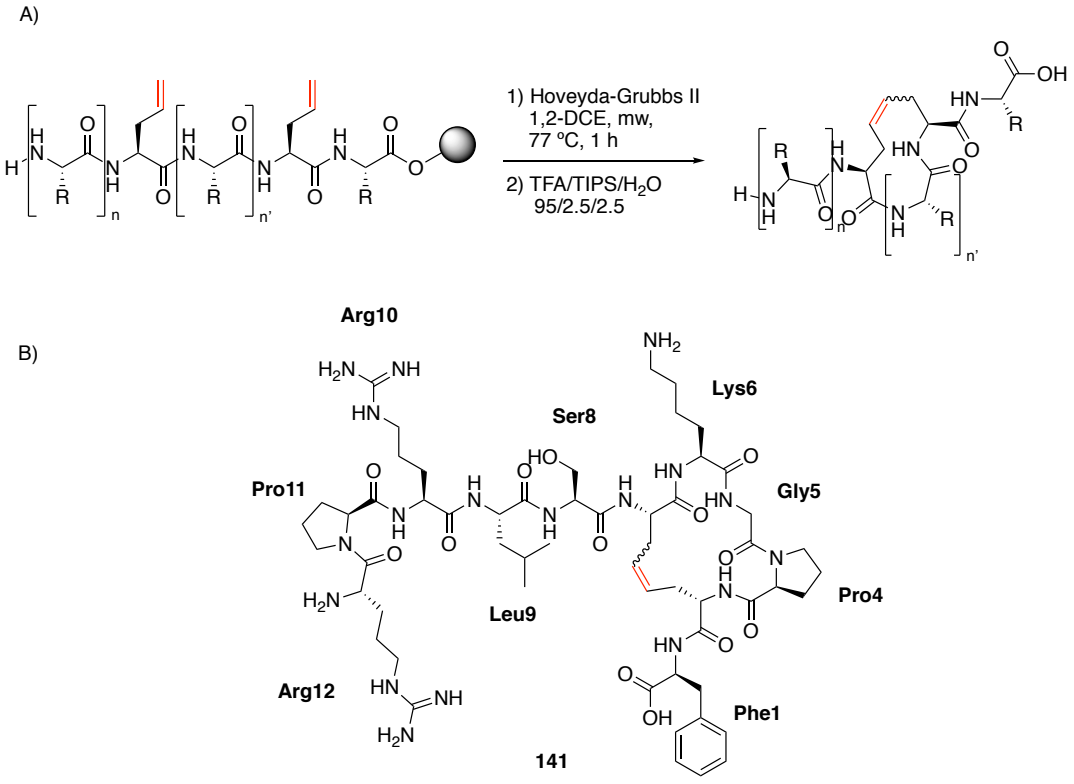

*Scheme 4-8: Incorporation of macrocycles into apelin-13; A) General scheme for RCM of apelin derivatives and B) macrocyclic derivative of apelin (**141**)*

(methionine) and position 7 (histidine), counting from the *C*-terminus. RCM of the residues generated analogue **141** (*Scheme 4-8B*), which also has the Pro2 residue removed, as well as pGlu13. This cyclic derivative possessed activity 20-fold lower than apelin-13 but provided Dr. Marsault with a starting point. Through modification, replacement and insertion of various residues, a variety of cyclic apelin analogues with nanomolar activity were produced.[208] Unfortunately, due to the cyclization method used, the cyclic derivatives were isolated as a mixture of double bond isomers. Attempt to purify the two by UPLC-MS or HPLC was futile, thus they were carried forward as a mixture, something that is undesirable for potential therapeutics.

Through the use of orthogonally protected diamino diacids, a macrocycle could be installed into the apelin backbone without the presence of a double bond, resulting in a single peptide isomer being produced. Knowing that Gly5 is not essential for binding or activity,[115,208] one end of the macrocycle could be attached there. In the structure-activity studies conducted by Dr. Marsault on analogues **141**, replacement of the *C*-terminal Phe residue by Ala (**142**) or Tyr(OBn) (**143**) or deletion of the residue altogether (**144**) resulted in active analogues, in stark contrast to the linear peptide where replacement of the *C*-terminal Phe to an Ala residue correlates to a >10 fold decrease in activity. (*Figure 4-6*).[200] The analogues **142-144** only resulted in a mild decreased in activity. These results strongly suggest that macrocycles in this position are able to interact with the APJ receptor, despite the loss or change of the *C*-terminal Phe residue. Given that Gly5 would be replaced with one end of the proposed macrocycle using the DADA strategy for macrocyclization, the Phe1 residue makes sense to anchor the other end based on the results seen in analogues **142-144**. Furthermore, substitution of Phe1 and Gly5 residues with a ring constitutes the *i*, *i* + 4 motif required for enhancement of an α-helix in stapled peptides. With these considerations in mind, the synthesis of novel cyclic apelin analogues was commenced.

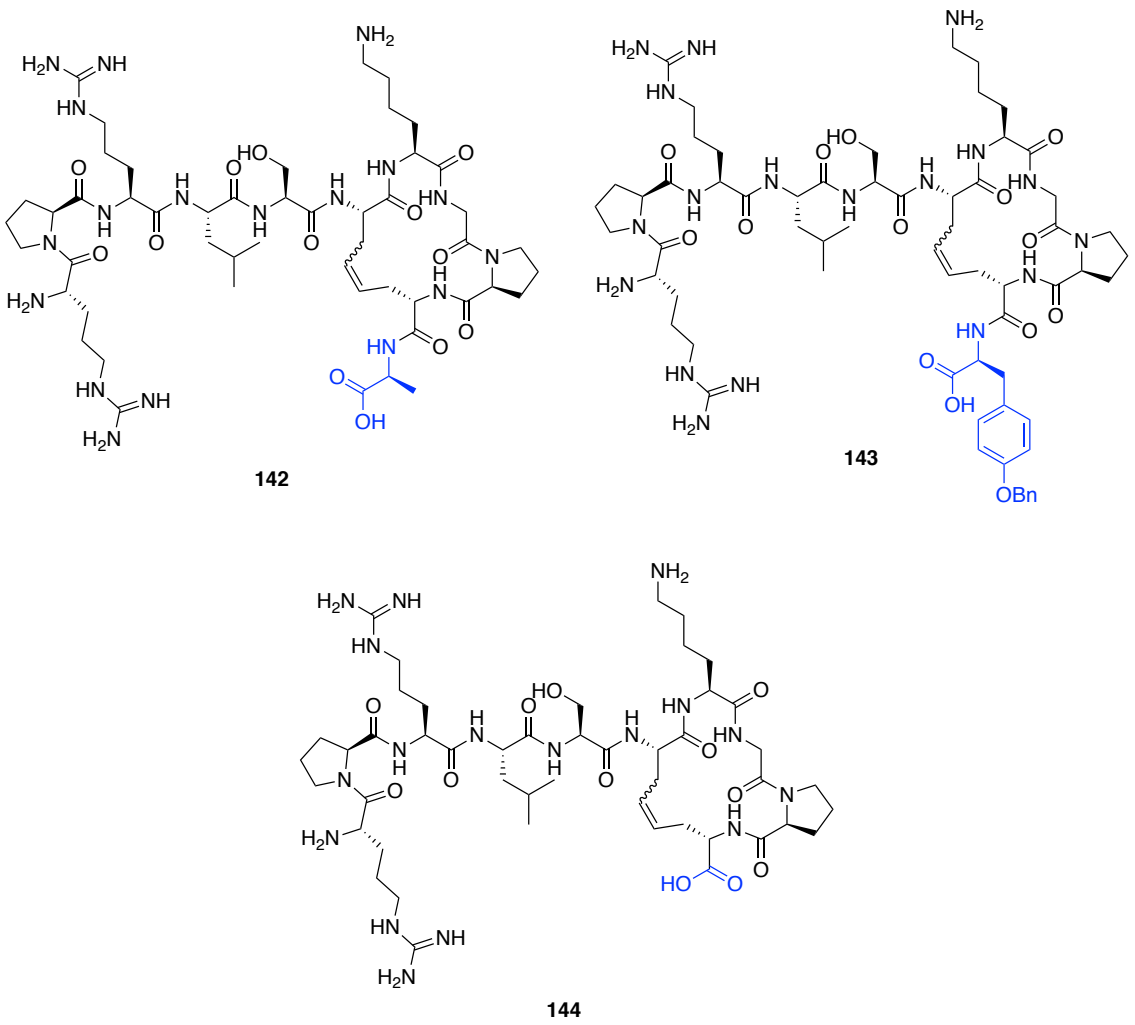

*Figure 4-6: Active cyclic apelin-13 derivatives **142-144** with C-terminal phenylalanine modifications.*

4.4 Results and Discussion of Cyclic Apelin Analogues

4.4.1 Synthesis of Cyclic Apelin Analogues

Using the method described in Chapter 2, a variety of orthogonally protected diamino diacids were synthesized for the purpose synthesizing cyclic apelin analogues. Without knowing which ring size would be most effective, DADAs **44**, **45**, **47** and **48** were synthesized for the purpose of investigating varying chain lengths and ring size for the apelin analogues. Derivatives of both [pyr]^{1}-apelin-13 and apelin-17 peptides were sought after; therefore, ACE-2, NEP and KLKB1 resistance modifications would be incorporated where applicable (*Figure 4-7*).

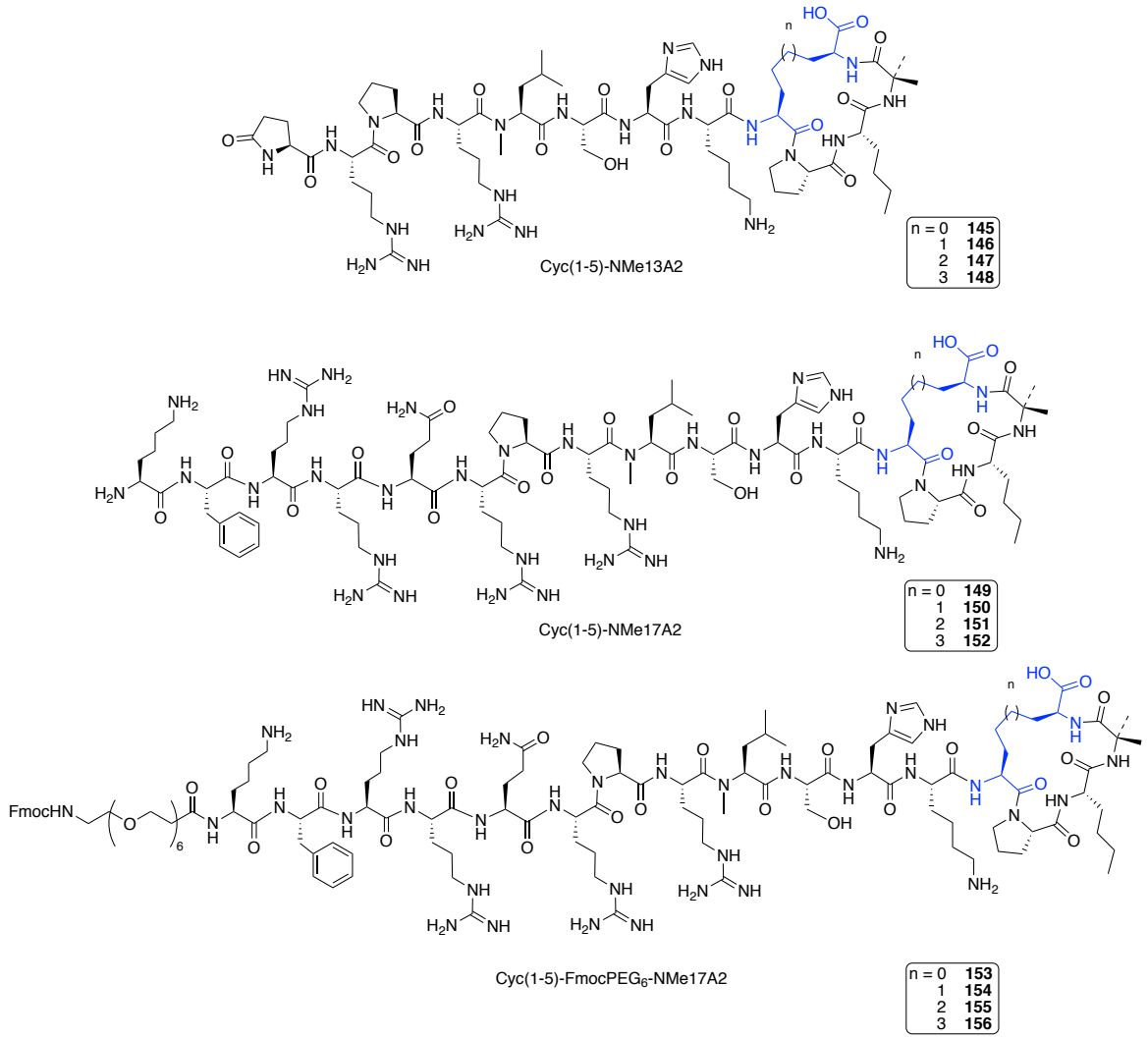

*Figure 4-7: Proposed cyclic apelin analogues incorporating various ring sizes into apelin-13A2 (**145-148**), apelin-17A2 (**149-152**) and PEG$_6$-apelin17A2 (**153-156**) peptides*

The general synthesis for the cyclic apelin analogues closely followed the synthesis for neopetrosiamide analogues **87**-**89**. Beginning with 2-chlorotrityl chloride resin with reduced loading (~0.1 mmol/g) to achieve high effective dilution of the desired orthogonally protected diamino diacid, the peptide chain could be extended to the tetrapeptide stage for all analogues, no matter the DADA used or length of peptide (*Scheme 4-9*). Once extended, allyl/alloc deprotection using Pd(PPh$_3$)$_4$, in the presence of the scavenger PhSiH$_3$, followed by intermolecular cyclization using PyAOP, HOBt and DIPEA afforded the cyclized residues 1-5. Further extension of the peptide by Fmoc-based SPPS was conducted up until Arg12. At this point, the resin was split with 1/3

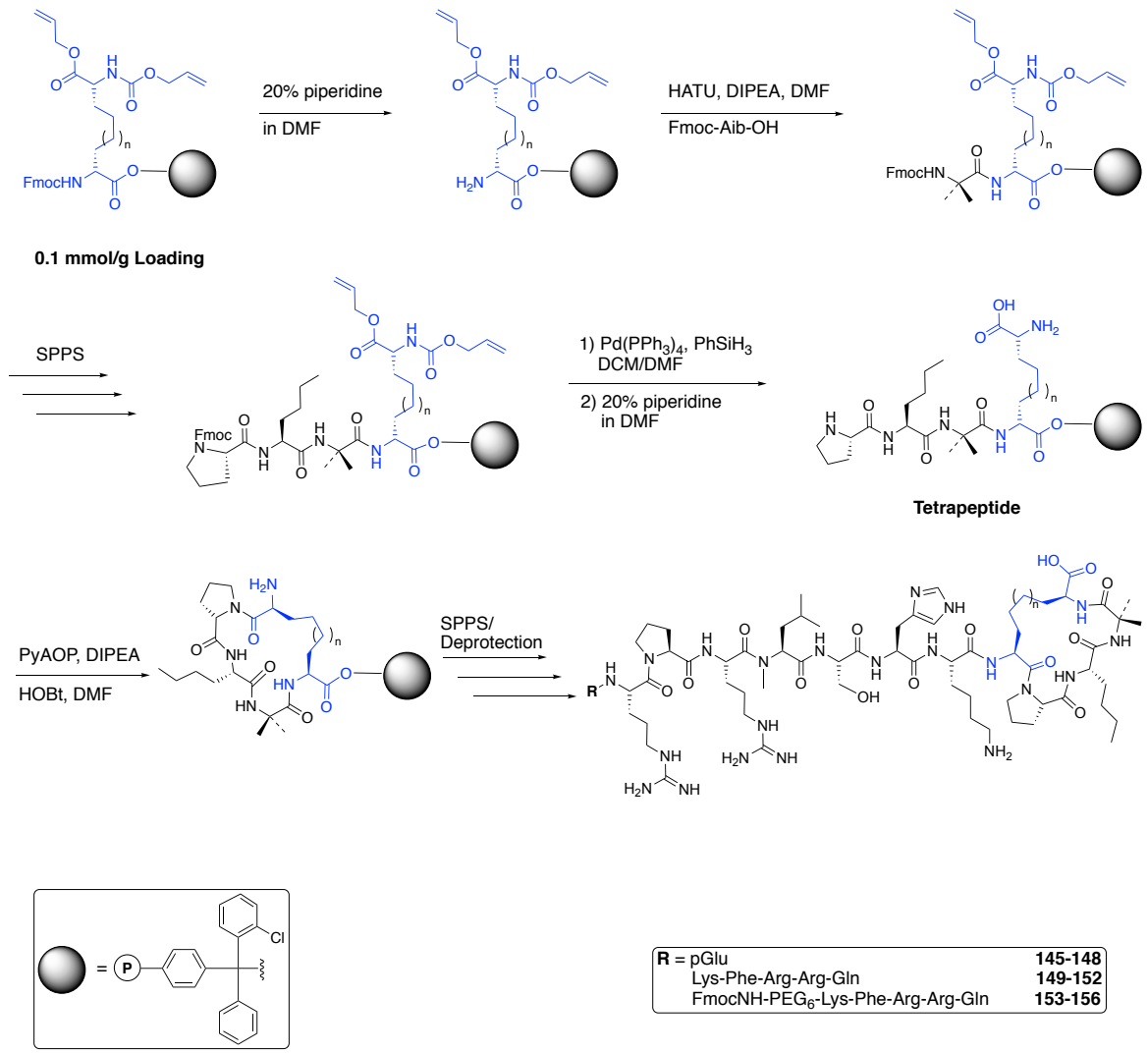

Scheme 4-9: General method for the synthesis and cyclization of apelin derivatives using orthogonally protected diamino diacids.

being coupled with pyroglutamic acid (pGlu) to yield Cyc(1-5)-NMe13A2 derivatives **145-148**, while the other 2/3 of the resin was extended until Lys17. Once the peptide was fully extended, it was *N*-terminally deprotected to give Cyc(1-5)-NMe17A2 analogues (**149-152**) and 1/2 of the remaining resin had an FmocPEG$_6$ chain coupled on to the *N*-terminus to yield Cyc(1-5)-FmocPEG$_6$-NMe17A2 derivatives **153-156**.

Initially, orthogonally protected diaminosuberic acid **44** was used to generate the first cyclic analogues **146**, **150** and **154** using the method depicted in *Scheme 4-9*. Purification of the peptides was achieved with a RP-HPLC on a C18 Column; however, the PEGylated analogue **154** would not elute from the C18 column. This was rectified by

switching to a biphenyl column. Following the synthesis of the first round of cyclic analogues using DAS, the synthesis of orthogonally protected diaminopimelic acid **45** and diaminoazelaic acid **47** cyclic derivatives were commenced concurrently while the analogues **146**, **150** and **154** were sent to collaborators for physiological testing.

4.4.2 Physiological Testing and Radioligand Displacement of Cyclic Apelin Analogues

Cyclic apelin analogues **146**, **150**, and **153** were tested by Dr. Oudit for their blood pressuring lowering capabilities (MABP, SBP, DBP) and their ability to raise heart rate in mice. Surprisingly, the novel analogues displayed virtually no activity (*Figure 4-8*). Administration of the analogues, indicated by the red arrows, did not lower MABP, DBP or SBP in any capacity, nor did they raise the heart rate. Acetylcholine (Ach) was administered, indicated by the grey arrows as a positive control to ensure the tests were working. Upon addition of Ach, the blood pressures of the mice were lowered, suggesting the novel cyclic analogues were simply not active.

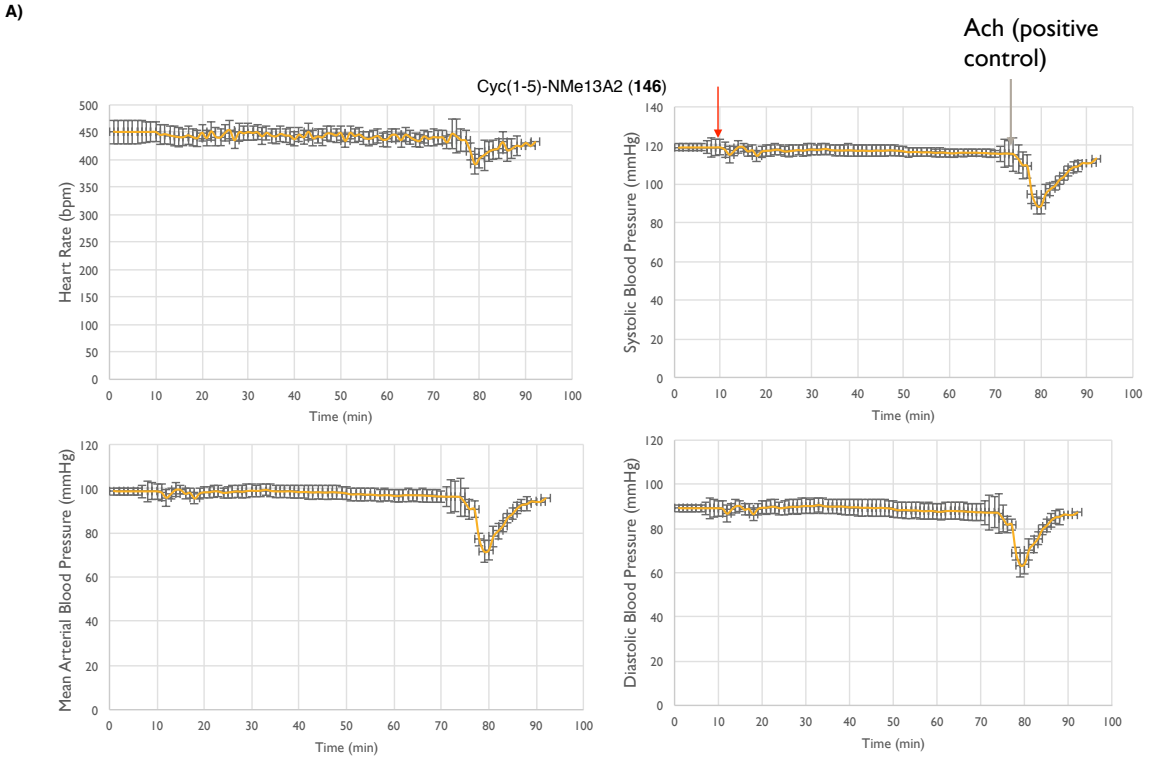

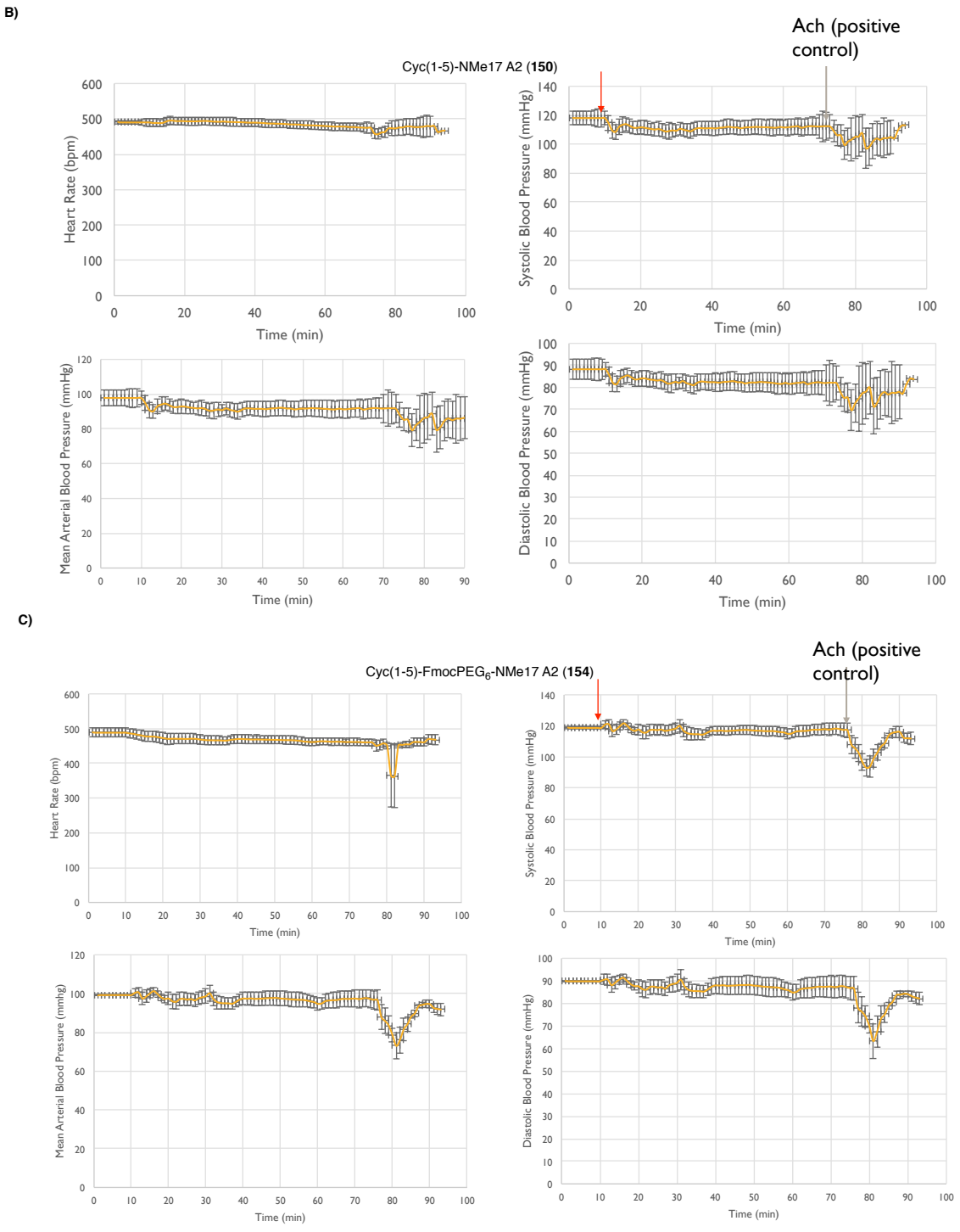

*Figure 4-8: Heart rate (HR), mean arterial blood pressure (MABP), systolic blood pressure (SBP) and diastolic blood pressure (DBP) of cyclic apelin analogues. Red arrows indicate analogue administration, grey arrows indicate Ach administration A) Cyc(1-5)-NMe13A2 analogue (**146**); B) Cyc(1-5)-NMe17A2 analogue (**150**); C) Cyc(1-5)-FmocPEG$_6$-NMe17A2 analogues (**154**)*

Nevertheless, the cyclic apelin derivatives **146**, **150**, and **154** were sent to Dr. Llorens-Cortes for radioligand displacement assays to confirm the results of the physiological tests. The results for the analogues from the displacement assay were exceedingly poor (*Table 4-2*). Each analogue displayed an abysmal ability to bind to the APJ receptor, with pIC_{50} values in the micromolar range, as opposed to the nanomolar concentrations required for more potent analogues to bind to the APJ receptor. Diaminoazelaic acid cyclic apelin analogues **147, 151** and **155** had already been synthesized and purified. Consequently, the synthesis of further analogues of this variation were promptly abandoned due to their inability to elicit an adequate physiological response at an appropriate concentration.

	Cyc(1-5)-NMe13A2 (146)	**Cyc(1-5)-NMe17A2 (150)**	**Cyc(1-5)-FmocPEG$_6$-NMe17A2 (154)**
***p*IC$_{50}$ (nM)**	12000 ± 300	3100 ± 3000	850 ± 40

*Table 4-2: pIC_{50} values from radioligand displacement assays for Cyc(1-5)-NMe13A2 (**146**), Cyc(1-5)-NMe17A2 (**150**), Cyc(1-5)-FmocPEG$_6$-NMe17A2 (**154**).*

4.5 Conclusions and Future Directions

Using orthogonally protected diamino diacids, cyclic apelin derivatives **146, 147**, **150, 151**, **154** and **155**, incorporating a ring between residues 1 though 5, were synthesized. The size of the macrocycle was to be varied using different lengths of diamino diacids to generate Cyc(1-5)-NMe13A2 **145-148**, Cyc(1-5)-NMe17A2 **149-152** and Cyc(1-5)-FmocPEG$_6$-NMe17A2 **153-156** analogues; however, due to the poor results displayed from the apelin analogues using diaminosuberic acid based macrocycles, synthesis of the rest of the analogues were not pursued any further.

There is literature precedent[207,208] for cyclic apelin analogues displaying activity towards the APJ receptor, eliciting a physiological response. There are variations between these active analogues and the newly synthesized ones described herein. Perhaps the *C*-terminal phenylalanine residue is required in some capacity to effectively bind to the APJ receptor. Pre-stapling of apelin analogues could be achieved in the same way but keeping

the critical phenylalanine residue intact and beginning the macrocycle form the second residue instead. By keeping the other ACE-2 and the NEP stabilization modifications, analogues akin to those synthesized by Dr. Marsault could be made and investigated. Additionally, the positioning of the macrocycle could be probed by varying the residues cyclized near the *C*-terminus, with addition or removal of amino acids to further vary the size of the ring.

5 Experimental Procedures

5.1 General Information

5.1.1 Reagents and Solvents

All commercially available reagents and protected amino acids were purchased from Aldrich Chemical Company Inc. (Madison, WI), Sigma Chemical Company (St. Louis, MO), Fisher Scientific Ltd. (Ottawa, ON) or Chem-Impex International (Wood Dale, IL) and used without further purification. All solvents used for reactions were used without further purification unless otherwise noted. Dry solvents refer to solvents freshly distilled over appropriate drying agents prior to use. Commercially available ACS grade solvents (> 99.0% purity) were used for column chromatography without any further purification. Heating of reactions was achieved using oil baths.

5.1.2 Silica Purifications

All reactions and column chromatography fractions were monitored by thin layer chromatography (TLC) using glass plates (5 × 2.5 cm), pre-coated (0.25 mm) with silica gel (SiO_2, Merck 60 F254). Visualization of TLC plates was performed by UV fluorescence at 254 nm, as well as staining with potassium permanganate ($KMnO_4$) or ninhydrin. Flash chromatography was performed using Merck type 60, 200-400 mesh silica gel at elevated pressures.

5.1.3 Characterization

Nuclear magnetic resonance (NMR) spectra were obtained using an Agilent VNMRS (700 MHz), Agilent/Varian VNMRS (600 MHz), Agilent/Varian VNMRS (500 MHz), Agilent/Varian Inova (500 MHz), or Agilent/Varian DD2 MR (400 MHz) spectrometer. For ^{1}H (700, 600, 500, 400 MHz) spectra, δ values were referenced to $CDCl_3$ (7.26 ppm) or D_2O (4.80 ppm); and for ^{13}C (175, 150, 125 MHz) spectra, δ values were referenced to $CDCl_3$ (77.06 ppm) as the solvents. Infrared spectra (IR) were recorded on a Nicolet Magna 750 spectrometer. Thin film refers to the evaporation of a solution of the compound on a NaCl plate. Mass spectra were recorded on a ZabSpec IsoMass VG (high resolution electrospray (ESI)) or Applied Biosystems Voyager Elite MALDI-TOF. All MALDI MS were acquired on an Applied Biosystems Voyager Elite MALDI-TOF with

delayed extraction in reflectron mode. A two-layer method was used for the matrix using 3,5-dimethoxy-4-hydroxycinnamic acid (sinapinic acid).

5.2 Methods for Peptide Synthesis

5.2.1 2-Chlorotrityl Chloride Resin Loading Procedure

The desired Fmoc protected amino acid (0.1 or 0.8 mmol/g) was loaded onto 2-chlorotrityl chloride resin using DIPEA (5 equiv) in CH_2Cl_2 (10 mL/g) and shaken at room temperature overnight. The resin was washed with CH_2Cl_2 (3 × 10 mL) and then the mixture was shaken with CH_2Cl_2:MeOH:DIPEA (v:v:v, 15 mL, 13:1.25:0.75) for 1 h to cap remaining sites. Resin was washed with CH_2Cl_2 (3 × 10 mL), then DMF (3 × 10 mL), and then CH_2Cl_2 (3 × 10 mL) again to give the loaded resin.

5.2.2 Wang Resin Loading Procedure

Desired Fmoc protected amino acid (0.1 mmol/g) was loaded onto Wang resin using DIC (6 equiv), HOBt (6 equiv) and DMAP (6 equiv) in CH_2Cl_2 (10 mL/g) and shaken at room temperature overnight. The resin was washed with CH_2Cl_2 (3 × 10 mL) and then shaken with Ac_2O:DIPEA (v:v, 10 mL, 1:1) for 1 h to cap remaining sites. Resin was washed with CH_2Cl_2 (3 × 10 mL), then DMF (3 × 10 mL), and then CH_2Cl_2 (3 × 10 mL) again to give the loaded resin.

5.2.3 Wang Resin Loading Procedure for Resin Bound Cross-Metathesis

Fmoc protected allylglycine **27** or **29** (0.1 mmol/g) was loaded onto Wang resin using DIC (6 equiv), HOBt (6 equiv) and DMAP (0.6 equiv) in CH_2Cl_2 (10 mL/g) and shaken at room temperature overnight. The resin was washed with CH_2Cl_2 (3 × 10 mL/g) and then had Boc-Ala-OH (0.5 mmol/g) or Boc-Val-OH (0.5 mmol/g), DIC (1 equiv), HOBt (1 equiv) and DMAP (0.1 equiv) added and shaken overnight or shaken with Ac_2O:DIPEA (v:v, 10 mL, 1:1) for 1 h to cap remaining sites. In the case of Boc-Ala-OH or Boc-Val-OH, resin was washed with CH_2Cl_2 (3 × 10 mL) and then shaken with Ac_2O:DIPEA (v:v, 10 mL, 1:1) for 1 h to cap remaining sites. Resin was washed with CH_2Cl_2 (3 x 10 mL), DMF (3 × 10 mL), and then CH_2Cl_2 (3 × 10 mL) again to give the loaded resin

5.2.4 General Procedure for Resin Bound Cross-Metathesis and Cleavage

Resins **30** or **33**, loaded according to the loading procedures, were dried under vacuum overnight to ensure dryness. The resin was suspended in degassed DCE (10 mL/g) in a vial under an atmosphere of argon. Either Grubbs second generation catalyst (5-15 mol%) or protected allylglycine **27** or **29** (5-10 equiv) were added to the vial, and heated to 70 ºC and stirred for 5 mins, followed by the addition of the other reagent. The reaction was stirred under argon at 70 ºC for 4 or 8 h with a constant stream of argon bubbling through it, then the resin was filtered, washed with DMF (1 × 10 mL), CH_2Cl_2 (1 × 10 mL) and then DCE (3 × 10 mL) and dried under vacuum once more. This was repeated 2-3 times before the resin was cleaved with 20% HFIP in CH_2Cl_2 and the resin was filtered off and the filtrate was concentrated *in vacuo* to be analyzed.

5.2.5 General SPPS Procedure

Unless otherwise noted, standard cycles for SPPS are as follows. A fritted reaction vessel was used with an Ar inlet for reagent/resin bubbling during couplings. Fmoc deprotection was performed by bubbling a solution of 20% piperidine in DMF using argon for 10 mins at 10 mL/g (3 × 10 mL) with a DMF (10 mL) between each repetition. After deprotection, resin was washed with DMF (3 × 10 mL). The appropriate amino acid to be coupled (5.05 equiv) was dissolved in DMF (10 mL) along with HATU (5.0 equiv) and DIPEA (10 equiv) and pre-activated for 10 mins. The coupling solution was then added to the resin and bubbled under argon for 2 h. Couplings were checked by a Kaiser test[20] and repeat coupling were done as needed. Peptide was cleaved from resin using a mixture of TFA:thioanisole:DTT:anisole (90:5:3:2 v:v:v:v, 10 mL/g of resin) for neopetrosiamide or TFA:H_2O:TIPS (95:2.5:2.5 v:v:v, 10 mL/g of resin) for apelin. Cleavage solution was shaken for 1 h and filtered through a pipette with a cotton plug and rinsed with CH_2Cl_2 and concentrated *in vacuo*. Cold ether addition caused the peptide to precipitate and the solid peptide was centrifuged and the mother liquor was decanted. Side chain protection of natural amino acids are as follows: Fmoc-Cys(Trt)-OH, Fmoc-Cys(*t*Bu)-OH Fmoc-Cys(Acm)-OH, Fmoc-Asp(*t*Bu)-OH, Fmoc-Ser(*t*Bu)-OH, Fmoc-Thr(*t*Bu)-OH, Fmoc-Arg(Pbf)-OH, Fmoc-Asn(Trt)-OH, Fmoc-Lys(Boc)-OH, Fmoc-His(Trt)-OH, Fmoc-Gln(Trt)-OH, Fmoc-Glu(O^{t}Bu)-OH.

5.2.6 General End-Capping Protocol

Growing peptide chains were *N*-capped by adding a solution of DIPEA:Ac_2O:DMF (v:v:v, 1:1:8, 10 mL/g) to the resin and bubbling under argon for 10 mins to cap any unreacted amines. The resin was then rinsed with DMF (3 × 10 mL) before carrying forward.

5.2.7 Allyl/Alloc Deprotection and General Cyclization Procedure

Allyl and alloc groups were removed from the resin bound peptide using $Pd(PPh_3)_4$ (2.0 equiv) and $PhSiH_3$ (10 equiv) in DMF (10 mL/g of resin). The reaction vessel was covered in aluminum foil and shaken at room temperature for 2 h. The resin was washed with CH_2Cl_2 (5 × 10 mL), then DMF (5 × 10 mL), then 0.5% sodium diethyldithiocarbamate in DMF (3 × 10 mL), and then again with CH_2Cl_2 (3 × 10 mL) and DMF (3 × 10 mL). The *N*-terminus was then deprotected with 20% piperidine as previously described. The peptide was cyclized by adding a solution of PyAOP (5.0 equiv), HOBt (5.0 equiv) and DIPEA (10.0 equiv) in DMF (10 mL/g of resin) and bubbling under argon for 3 h. The resin was washed with DMF (3 × 10 mL), and cyclization was checked by MALDI. Deprotection and cyclization repeated as necessary until completion.

5.2.8 General *N*-Terminal PEGylation Procedure

Fmoc-deprotected peptide (1 equiv) still attached to resin was combined with an *N*-terminally protected PEG chain (5 equiv), HOBt (5 equiv), and DIC (5 equiv) in dry DMF (5mL) and shaken for 24 h at room temperature. The solution was filtered to collect the resin beads, and then, the peptide was cleaved from the resin and checked by MALDI.

5.2.9 Bis-Disulfide Formation (Two-Step Method)

Linear peptide (free from resin), with Cys residues still protected (Trt and *t*Bu), was dissolved in glacial acetic acid (0.5 mg/mL) and had iodine (10 equiv) dissolved in methanol (< 5 mL) added. This mixture was stirred at room temperature for 2 h and quenched with 0.1 M ascorbic acid until the solution was colourless. Following concentration *in vacuo*, the peptide was redissolved in minimal 10% MeCN in H_2O. This was loaded onto a Strata C18-E column to desalt the peptide. Salts were eluted using H_2O

and peptide was eluted using increasing concentrations of in H_2O (10-90%), followed by MeOH. Fractions were checked by MALDI and those containing the desired peptide were pooled and concentrated *in vacuo*. The mono-disulfide peptide with two remaining *t*Bu protected Cys residues was dissolved in TFA (0.1 mg/mL) in the presence of DMSO (100 equiv) and anisole (4 equiv) and stirred at room temperature 6 h. Reaction was diluted with H_2O until colourless and concentrated *in vacuo*. Crude peptide was purified by RP-HPLC and fractions containing the peptide, as checked by MALDI, were pooled and lyophilized.

5.2.10 Bis-Disulfide Formation (One-Step Method)

Linear peptide (free from resin), with Cys residues still protected (Trt and *t*Bu), was dissolved in TFA (0.1 mg/mL) in the presence of DMSO (100 equiv) and anisole (4 equiv) and stirred at room temperature for 6 h. Reaction was diluted with H_2O until colourless and concentrated *in vacuo*. Crude peptide was purified by RP-HPLC and fractions containing the peptide, as checked by MALDI, were pooled and lyophilized.

5.3 Peptide Purification

5.3.1 Neopetrosiamide and Analogues HPLC Purification Procedure

5.3.1.1 General Method for Purification of Complete Peptides by HPLCs

The peptide analogues were purified on a C8 column (Vydac 208TP1010) with a flow rate of 3 or 5 mL/min and peptide detection was done at 220 and 280 nm. The gradient began with 10% MeCN/90% H_2O (0.1% TFA) for the first 5 mins. The gradient was ramped up to 30% MeCN over 5 mins and then ramped up to 55% MeCN over 20 mins. A final ramp up to 90% MeCN over 5 mins was conducted and held at 90% for 7 mins. The gradient was ramped down to 10% MeCN over 3 mins and held at 10% for 10 mins.

5.3.1.2 HPLC Purification of Completed Peptides Before and After Disulfide Formation

The peptide analogues were purified on a C8 column (Vydac 208TP1010) with a flow rate of 5 or 10 mL/min and peptide detection was done at 220 and 280 nm. The gradient began with 10% MeCN/90% H_2O (0.1% TFA) for the first 5 mins. The gradient was ramped up to 50% MeCN over 5 mins and then ramped up to 65% MeCN over 24 mins. A final ramp

up to 90% MeCN over 3 mins was conducted and held at 90% for 7 mins. The gradient was ramped down to 10% MeCN over 3 mins and held at 10% for 10 mins.

5.3.1.3 HPLC Purification of Intermediate Peptides After Carbon Macrocycle Formation

The peptide analogues were purified on a C8 column (Vydac 208TP1010) with a flow rate of 5 or 10 mL/min and peptide detection was done at 220 and 280 nm. The gradient began with 10% MeCN/90% H_2O (0.1% TFA) for the first 5 mins. The gradient was ramped up to 40% MeCN over 5 mins and then ramped up to 65% MeCN over 24 mins. A final ramp up to 90% MeCN over 3 mins was conducted and held at 90% for 7 mins. The gradient was ramped down to 10% MeCN over 3 mins and held at 10% for 10 mins

5.3.2 Apelin Analogues HPLC Purification Procedure

Crude peptides were purified by RP-HPLC using either a C_{18} column (Phenomenex Luna 5u) column or a biphenyl column with a flow rate of 5 mL/min. Detection was done at 220 and 280 nm. Purification was conducted with aqueous 0.1% TFA (solvent A) and 0.1% TFA in acetonitrile (solvent B) as eluents. Gradient began with 10%MeCN/90% H_2O (0.1% TFA) for the first 3 mins. Gradient ramped up to 45% MeCN over 15 mins, then final ramp up to 100% MeCN over the next 7 mins and held for 1 min. Gradient rapidly ramped down to 10% over 1 min and held at 10% for 9 mins.

5.4 Neopetrosiamide Cloning and Invasion Assay

5.4.1 Cloning and Expression of Neopetrosiamide A

The following was performed by Dr. van Belkum. DNA encoding neopetrosiamide A (NeoA) was obtained from Genscript and codon-optimized for expression in *Escherichia coli*. The *neoA* gene was amplified through PCR using forward primer MVB311 (5'-TTCTTTTGCCCGTTTGGCTG-3') and reverse primer MVB312 (5'-TTAGCAATCACAGCTCATAAA-3') and cloned into the pET SUMO (small ubiquitin-like modifier) expression plasmid according to the manufacturer's instructions (Invitrogen). The recombinant plasmid was sequenced to confirm that NeoA was fused in frame with the His-tagged SUMO protein and the vector was subsequently transformed into *E. coli* BL21(DE3). The resulting transformant was induced with 0.5 mM isopropyl

β-d-1-thiogalactopyranoside in Luria Broth Base, Miller (Difco) for 3-4 h at 37 °C to express the fusion protein. Cells were harvested by centrifugation (4000 × *g* for 10 min at 4 °C) and resuspended in lysis buffer (20 mM Tris-HCl pH 7.8, 150 mM NaCl, 5 mM imidazole). Cells were lysed by sonication and cellular debris was removed by centrifugation (27000 × *g* for 30 min at 4 °C). The supernatant was loaded onto Ni-NTA resin column (Qiagen) and the resin was washed with 5 column volumes of lysis buffer containing 20 mM imidazole. The fusion protein was eluted with 40-500 mM imidazole in lysis buffer and eluted fractions were analyzed by sodium dodecyl sulphate-polyacrylamide gel electrophoresis (SDS-PAGE). Fractions containing the fusion protein were pooled and dialyzed against 20 mM Tris-HCl buffer (pH 7.8) containing 150 mM NaCl and 1 mM DTT. The SUMO tag was cleaved from the fusion protein after digestion with His-tagged SUMO protease (McLab, South San Francisco, CA) for 2 h at 4 °C as suggested by the manufacturer. The SUMO tag and SUMO protease were removed by loading the cleavage mixture onto Ni-NTA resin column and isolating NeoA from the flow through. Linear NeoA was then purified following the general method for purification of peptides by HPLC to be oxidized later.

5.4.2 Cell Culture Protocols

MDA-MB-231 cells were cultured in Alpha-Minimal Essential Medium (MEM) (GIBCO) supplemented with a 10% fetal bovine serum solution (FBS) (Millipore Sigma) and a 1% penicillin-streptomycin (GIBCO) mixture. Cells were incubated under 5% CO_2 atmosphere at 37 °C until 60% confluence was obtained. Cells were collected and harvested using 0.5% trypsin-EDTA mixture in HBSS (GIBCO).

5.4.3 Procedure for Invasion Assay of Neopetrosiamide Analogues

An aliquot of 100 mL freshly trypsinized MDA-MB-231 cells in MEM were added to wells of a 96-well plate. Each well contained ~25,000 cells. Stock solutions of the analogues (2 mg/mL) were made in 30% acetonitrile in water. MICs were determined using a two-fold dilution technique. Analogues were added to wells such that the final volume per well was 110 mL. Cells were left to incubate at 37 °C and checked after 2.5 h and 24 h. Visualization of each well was achieved using an inverted phase contrast microscope with 20× objective magnification (Axiovert 25, Zeiss).

5.5 General Method for Peptide NMRs

The peptide analogues were dissolved in 300 mL 4:1 d_3-MeCN:H_2O and placed in a MeOH Shigemi tube to afford a concentration of 1 mM. Spectra were taken on a 700 MHz NMR spectrometer.

5.6 Experimental Procedures

5.6.1 2-(Trimethylsilyl)ethyl-(*S*)-2-((((9*H*-fluoren-yl)methoxy)carbonyl)amino)pent-4-enoate (26)

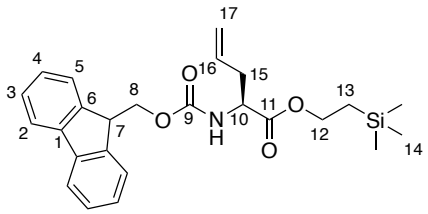

26

Fmoc-L-allylglycine (1.50 g, 4.45 mmol), DCC (1.01 g, 4.85 mmol) and DMAP (0.0543 g, 0.445 mmol) were dissolved in dry CH_2Cl_2 (25 mL) and the solution was stirred for 10 mins at 0 °C. 2-(Trimethylsilyl)ethanol (0.701 mL, 4.85 mmol) was added and the reaction mixture was allowed to warm up slowly to room temperature overnight. The reaction was filtered to remove urea by-product and the filtrate was concentrated *in vacuo*. The crude oil was purified using flash column chromatography (silica gel, 5% EtOAc in hexanes) to yield **26** (1.94 g, 77%) as a clear, yellow oil. (R_f = 0.5 on SiO_2, 20% EtOAc in hexanes); $[\alpha]_D^{26}$: -0.45 (*c* = 1.63, CH_2Cl_2); IR (CH_2Cl_2 cast) 3338, 3067, 2953, 2898, 1715, 1642, 1522, 1450, 1414, 1342, 1250, 1218, 1195, 1049, 859, 838, 835, 740 cm^{-1}; ^{1}H-NMR ($CDCl_3$, 600 MHz): δ 7.77 (2H, d, *J* = 7.8 Hz, Ar-H), 7.60 (2H, app t, *J* = 7.2 Hz, Ar-H), 7.40 (2H, t, *J* = 7.2 Hz, Ar-H), 7.32 (2H, t, *J* = 7.8 Hz, Ar-H), 5.75 – 5.68 (1H, m, H16), 5.33 (1H, d, *J* = 7.8 Hz, NH), 5.18 – 5.12 (2H, m, H17), 4.46 – 4.36 (3H, m, H8, H10), 4.29 – 4.21 (3H, m, H7, H12), 2.64 – 2.59 (2H, m, H15), 1.03 (2H, app t, *J* = 8.4 Hz, H13), 0.03 (9H, s, $Si(CH_3)_3$); ^{13}C-NMR δ ($CDCl_3$ 125 MHz): 171.8 (C11), 155.7 (C9), 144.0 (Ar-C), 143.8 (Ar-C), 141.3 (Ar-C), 132.2 (C16), 127.8 (Ar-C), 127.1, 125.1 (Ar-C), 120.0 (C17), 119.4 (Ar-C), 67.1 (C8), 64.0 (C12), 53.4 (C10), 47.2 (C7), 36.8 (C15), 17.5 (C13), -1.29 (C14); HRMS (ESI-TOF) Calc'd for $C_{25}H_{31}NO_4SiNa$ $[M+Na]^+$ 437.2022, found 437.2022.

5.6.2 2-(Trimethylsilyl)ethyl-(*S*)-2-(((2-(trimethylsilyl)ethoxy)carbonyl)amino)pent-4-enoate (27)

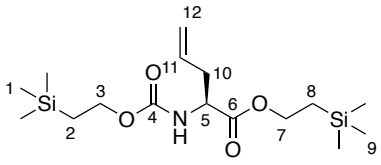

27

Compound **27** was prepared by first dissolving **26** (1.35 g, 3.08 mmol) in DEA/CH_2Cl_2 (1:1, 20 mL) and stirring at room temperature for 2 h. The reaction mixture was concentrated *in vacuo* and co-evaporated with CH_2Cl_2 (3 × 20 mL) to remove excess DEA. The oil was re-dissolved in CH_2Cl_2 (20 mL), then Teoc-OSu (0.880 g, 3.39 mmol) and Et_3N (0.472 mL, 3.39 mL) were added and mixture was stirred at room temperature overnight. The solution was quenched with H_2O (30 mL) and organic layer was separated, and subsequently washed with 10% aqueous K_2CO_3 (30 mL), H_2O (30 mL), and brine (30 mL). The organic layer was then dried over Na_2SO_4, filtered and concentrated *in vacuo*. The crude oil was purified by flash column chromatography (silica gel, 5% EtOAc in hexanes) to yield **27** (1.23 g, 95%) as a yellow oil. (R_f = 0.6 on SiO_2, 20% EtOAc in hexanes); $[\alpha]_D^{26}$: +0.30 (*c* = 1.21, CH_2Cl_2); IR (CH_2Cl_2 cast) 3435, 3348, 3080, 2954, 2899, 1724, 1508, 1439, 1342, 1250, 1217, 1178, 861, 838, 767 cm^{-1}; ^{1}H-NMR ($CDCl_3$, 500 MHz): δ 5.69 (1H, ddt, *J* = 15.5, 9.5, 7.0 Hz, H11), 5.20 – 5.15 (3H, m, H12, NH), 4.43 (1H, app q, *J* = 6.4 Hz, H5), 4.31 – 4.24 (2H, m, H7), 4.22 – 4.17 (2H, m, H3), 2.65 – 2.48 (2H, m, H10), 1.06 – 1.00 (4H, m, H2, H8), 0.08 (9H, s, H9), 0.06 (9H, s, H1); ^{13}C-NMR ($CDCl_3$ 125 MHz): δ 172.0 (C6), 156.1 (C4), 132.3 (C11), 119.2 (C12), 63.9 (C7) 63.4 (C3), 53.2 (C5), 36.9 (C10), 17.7 (C8), 17.5 (C2), -1.47 (C9), -1.51 (C1); HRMS (ESI-TOF) Calc'd for $C_{16}H_{33}NO_4Si_2Na$ $[M+Na]^+$ 359.1948, found 359.1945.

5.6.3 4-Nitrobenzyl-(*S*)-2-((((9*H*-fluoren-9-yl)methoxy)carbonyl)amino)pent-4-enoate (28)

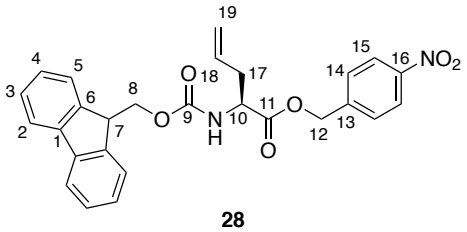

28

Fmoc-L-allylglycine (1.50 g, 4.45 mmol), DIPEA (0.852 mL, 4.85 mmol) and 4-nitrobenzyl bromide (1.05 g, 0.489 mmol) were dissolved in dry DMF (25 mL) and the reaction mixture was allowed to stir at room temperature overnight. The reaction mixture was quenched with H_2O (25 mL) and separated. The aqueous layer was extracted with EtOAc (3 × 100 mL) and pool organic layers were washed with brine (100 mL), dried over Na_2SO_4, filtered and concentrated *in vacuo* to yield a crude oil. The crude oil was purified using flash column chromatography (silica gel, 20% EtOAc in hexanes) to yield **28** (2.03 g, 97%) as a powdery, white solid. (R_f = 0.5 on SiO_2, 30% EtOAc in hexanes); $[\alpha]_D^{26}$: -6.6 (*c* = 0.59, CH_2Cl_2); IR (CH_2Cl_2 cast) 3413, 3337, 3067, 2949, 1748, 1723, 1607, 1522, 1449, 1346, 1251, 1190, 1049, 760, 739 cm^{-1}; ^{1}H-NMR ($CDCl_3$, 500 MHz): δ 8.21 (2H, d, *J* = 8.4 Hz, Ar-H), 7.77 (2H, d, *J* = 7.2 Hz, Ar-H), 7.58 (2H, d, *J* = 7.2 Hz, Ar-H), 7.51 (2H, d, *J* = 8.4 Hz, Ar-H), 7.40 (2H, t, *J* = 7.8 Hz, Ar-H), 7.30 (2H, d, *J* = 7.8 Hz, Ar-H), 5.71 – 5.64 (1H, m, H18), 5.30 – 5.25 (3H, m, H12, NH), 5.17 – 5.13 (2H, m, H19), 4.52 (1H, app q, *J* = 7.0, H10), 4.41 (2H, d, *J* = 7.5 Hz, H8), 4.22 (1H, t, *J* = 7.5 Hz, H7), 2.65– 2.53 (2H, m, H17); ^{13}C ($CDCl_3$ 125 MHz): δ 171.5 (C11), 155.8 (C9), 147.9 (Ar-C), 143.7 (Ar-C), 142.4 (Ar-C), 141.3 (Ar-C), 131.7 (C18), 128.6 (Ar-C), 127.8 (Ar-C), 127.1 (Ar-C), 125.0 (Ar-C), 123.9 (Ar-C), 120.1 (Ar-C), 119.8 (C19), 67.2 (C8), 65.7 (C12), 53.3 (C10), 47.1 (C7), 36.6 (C17); HRMS (ESI-TOF) Calc'd for $C_{27}H_{24}N_2O_6Na$ $[M+Na]^+$ 472.1634, found 472.1635

5.6.4 4-Nitrobenzyl-(*S*)-2-((((4-nitrobenzyl)oxy)carbonyl)amino)pent-4-enoate (29)

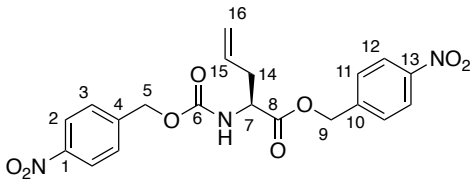

29

Compound **29** was prepared by first dissolving **27** (1.96 g, 4.14 mmol) in DEA/CH_2Cl_2 (1:1, 20 mL) and stirring at room temperature for 2 h. The reaction mixture was concentrated *in vacuo* and co-evaporated with CH_2Cl_2 (3 x 20mL) to remove excess DEA. The oil was re-dissolved in CH_2Cl_2 (20 mL), then *p*-nitrobenzylchloroformate (0.981 g, 4.55 mmol) and Et_3N (0.634 mL, 4.55 mL) were added and mixture was stirred at room temperature overnight. The solution was quenched with 10% aqueous citric acid (50 mL) and organic layer was separated, and subsequently washed with H_2O (50 mL) and brine (50 mL). The pooled aqueous layer was then extracted with CH_2Cl_2 (3 × 50 mL). The organic layer was then dried over Na_2SO_4, filtered and concentrated *in vacuo*. The crude oil was purified by flash column chromatography (silica gel, 25% EtOAc in hexanes) to yield **28** (1.25 g, 70%) as a chunky, white solid. (R_f = 0.2 on SiO_2, 30% EtOAc in hexanes); $[\alpha]_D^{26}$: -1.3 (*c* = 0.67, CH_2Cl_2); IR (CH_2Cl_2 cast) 3399, 3113, 3081, 2983, 2947, 2857, 1725, 1607, 1519, 1440, 1382, 1263, 1214, 1190, 1109, 1060, 1014, 855, 738 cm^{-1}; ^{1}H-NMR ($CDCl_3$, 500 MHz): δ 8.28 – 8.23 (4H, m, Ar-H), 7.59 – 7.52 (4H, m, Ar-H), 5.70 (1H, ddt, *J* = 14.5, 10.0, 7.0 Hz , H15), 5.38 (1H, d, *J* = 8.0 Hz, NH), 5.31 (2H, br s, H9), 5.21 (2H, br s, H5), 5.20 – 5.16 (2H, m, H16), 4.56 (1H, app q, *J* = 8.0 Hz, H7), 4.22 (1H, t, *J* = 7.2 Hz, Fmoc-CH), 2.70 – 2.56 (2H, m, H14); ^{13}C-NMR ($CDCl_3$ 125 MHz): δ 171.3 (C8), 155.3 (C6), 147.9 (Ar-C), 147.7 (Ar-C), 143.5 (Ar-C), 142.3 (Ar-C), 131.5 (C15), 128.6 (Ar-C), 128.1 (Ar-C), 123.9 (Ar-C), 123.8 (Ar-C), 120.0 (C16), 65.7 (C9), 65.6 (C5), 53.3 (7), 36.5 (C14); HRMS (ESI-TOF) Calcd for $C_{20}H_{19}N_3O_8Na$ $[M+Na]^+$ 429.1172, found 429.1170.

5.6.5 (2*S*, 7*S*, *Z/E*)-2,7-bis((((9*H*-fluoren-9-yl)methoxy)carbonyl)amino)oct-4-enedioic acid (32)

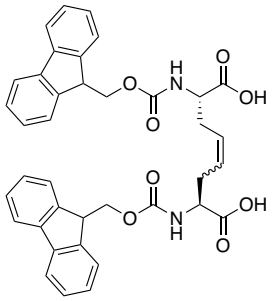

32

The following side product was detected by LCMS during the attempted synthesis of **31** and **34**. The product was not isolated but was characterized by mass spectrometry. LCMS (ESI-TOF) Calc'd for $C_{38}H_{34}N_2O_8$ $[M-H]^-$ 645.2309, found 645.2304.

5.6.6 2-(Hydroxymethyl)benzyl-(*S*)-2-((*tert*-butoxycarbonyl)amino)pent-4-enoate (38)

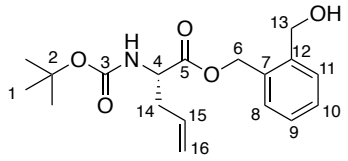

38

The following was prepared according to literature procedure.[165] (S)-2-((tert-Butoxycarbonyl)amino)pent-4-enoic acid (2.71 g, 12.6 mmol), DMAP (0.155 g, 1.26 mmol) and 1,2-benzenedimethanol (6.87 g, 50.4 mmol) were dissolved in CH_2Cl_2 (125 mL) and cooled down to 0 °C. Once cooled, EDCI (3.14 g, 16.4 mmol) was added and the reaction mixture was allowed to warm up to room temperature over 3 h and stirred overnight at room temperature. The reaction mixture was then concentrated *in vacuo* and purified via flash column chromatography (silica gel, 40% EtOAc in hexanes) to yield compound **38** (3.45 g, 82%) as a colourless oil and 1,2-benzenedimethanol (5.27 g) was also recovered. (R_f = 0.58 on SiO_2, 1:1 hexanes:EtOAc); $[\alpha]_D^{26}$ -4.4 (*c* = 0.63, CH_2Cl_2); IR (CH_2Cl_2 cast) 3375, 3077, 3004, 2978, 2931, 1743, 1714, 1697, 1507, 1455, 1367,

1285, 1252, 1162, 1052, 1022 cm^{-1}; ^{1}H-NMR ($CDCl_3$, 500 MHz) δ 7.43 (1H, dd, *J* = 7.5, 1.5 Hz, Ar-H), 7.37 (1H, d, *J* = 6.5 Hz, Ar-H), 7.36 (1H, dd, *J* = 7.5, 1.5 Hz, Ar-H), 7.31 (1H, dd, *J* = 7.5, 1.5 Hz, Ar-H), 5.64 (1H, ddt, *J* = 16.0, 10.5, 7.5 Hz, H15), 5.31 (1H, d, *J* = 12.5 Hz, H6), 5.28 (1H, d, *J* = 12.5 Hz, H6), 5.11 – 5.07 (2H, m, H16), 5.00 (1H, d, *J* = 6.5 Hz, NH), 4.76 (1H, d, *J* = 12.5 Hz, H13), 4.72 (1H, d, *J* = 12.5 Hz, H13), 4.37 (1H, app q, *J* = 5.5 Hz, H4), 2.57 – 2.44 (2H, m, H14), 2.21 (1H, br s, OH), 1.41 (9H, s, H1); ^{13}C-NMR ($CDCl_3$, 125 MHz) δ 172.0 (C5), 155.4 (C3), 139.5 (Ar-C), 133.3 (Ar-C), 132.2 (C15), 130.1 (Ar-C), 129.1 (Ar-C), 129.0 (Ar-C), 128.1 (Ar-C), 119.4 (C16), 80.2 (C2), 64.9 (C6), 62.9 (C13), 53.0 (C4), 36.5 (C14), 28.3 (C1); HRMS (ESI-TOF) Calc'd for $C_{18}H_{25}NO_5Na$ $[M+Na]^+$ 358.1625, found 358.1624.

5.6.7 2-((((4-Nitrophenoxy)carbonyl)oxy)methyl)benzyl-(*S*)-2-((*tert*-butoxycarbonyl)amino)pent-4-enoate (39)

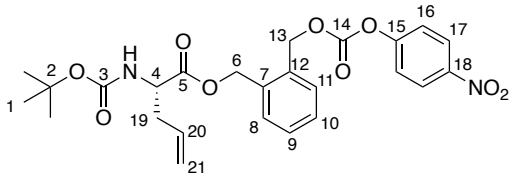

39

The following was prepared according to an adapted literature procedure.[165] Compound **38** (3.28 g, 9.79 mmol) was dissolved in CH_2Cl_2 (100 mL) and had bis(4-nitrophenyl) carbonate (4.47 g, 14.7 mmol) and DIPEA (3.75 mL, 21.5 mmol) added to it. The resulting reaction mixture was stirred overnight. It was then diluted with EtOAc (200 mL), quenched with 10% aqueous citric acid (200 mL) and the layers were separated. The organic layer was then washed with saturated aqueous Na_2CO_3 until the aqueous layer was no longer yellow and then washed with brine (2 × 200 mL), dried over Na_2SO_4, filtered and concentrated *in vacuo*. The crude product was then purified via flash column chromatography (silica gel, 0-2% acetone in CH_2Cl_2) to give **39** (4.63 g, 95%) as a yellow oil. (R_f = 0.44 on SiO_2, 30% EtOAc in hexanes); $[\alpha]_D^{26}$ -0.39 (*c* = 0.52, CH_2Cl_2); IR (CH_2Cl_2 cast) 3426, 3084, 2979, 2936, 1769, 1713, 1617, 1594, 1526, 1492, 1394, 1217,

1189, 1161 cm^{-1}; ^{1}H-NMR ($CDCl_3$, 500 MHz) δ 8.27 (2H, app d, *J* = 10.0 Hz, H17), 7.51 – 7.40 (4H, m, Ar-H), 7.39 (2H, app d, *J* = 10.0 Hz, H16), 5.64 (1H, ddt, *J* = 16.5, 10.0, 7.5 Hz, H20), 5.41 (2H, s, H6), 5.34 (1H, d, *J* = 13.0 Hz, H13), 5.31 (1H, d, *J* = 13.0 Hz, H13), 5.09 – 5.05 (2H, m, H21), 5.01 (1H, d, *J* = 7.0 Hz, NH), 4.42 (1H, app q, *J* = 7.0 Hz, H4), 2.58 – 2.45 (2H, m, H19), 1.42 (9H, s, H1); ^{13}C-NMR ($CDCl_3$, 125 MHz) δ 171.9 (C5), 155.5 (C3), 152.3 (C14), 145.5 (C18), 134.4 (Ar-C), 133.0 (Ar-C), 132.1 (C20), 130.4 (Ar-C), 130.3 (Ar-C), 129.6 (Ar-C), 129.2 (Ar-C), 125.3 (C17), 121.8 (C16) 119.3 (C21), 80.0 (C2), 68.4 (C6), 64.4 (C13), 53.0 (C4), 36.7 (C19), 28.3 (C1); HRMS (ESI-TOF) Calcd for $C_{25}H_{28}N_2O_9Na$ $[M+Na]^+$ 523.1687, found 523.1686.

5.6.8 (*2S, 7S*)-2-((((9*H*-Fluoren-9-yl)methoxy)carbonyl)amino)-8-(allyloxy)-7-(((allyloxy)carbonyl)amino)-8-oxooctanoic acid (44)

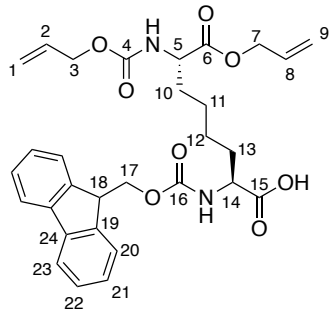

44

Fully protected diamino diacid **52** (2.00 g, 3.21 mmol) was dissolved in TFA:CH_2Cl_2 (1:1, 6 mL) and stirred at room temperature for 6 h. The reaction mixture was then concentrated *in vacuo* and co-evaporated with CH_2Cl_2. The resultant crude oil was dissolved in THF:H_2O (2.5:1, 35 mL) and had $NaHCO_3$ (0.595 g, 7.09 mmol) and allyl chloroformate (0.752 mL, 7.09 mmol) added to it and stirred overnight. Reaction was quenched with 1 M aqueous HCl (35 mL) and then extracted with EtOAc (3 × 50 mL). Pooled aqueous extracts were washed with brine (50 mL), dried over Na_2SO_4, filtered and concentrated *in vacuo*. The crude oil was then purified via flash column chromatography (silica gel, 1:1 EtOAc:hexanes, 0.1% AcOH) to yield the final diamino diacid **44** (1.77 g, 90% over 2 steps) as a white solid. (R_f = 0.38 on SiO_2, 100% EtOAc, 0.1% AcOH). $[\alpha]_D^{26}$ +5.7 (*c* = 0.63, CH_2Cl_2); IR (CH_2Cl_2 cast) 3328, 3067, 2949, 1712, 1529, 1450, 1273, 1245, 1218, 1049 cm^{-1}; ^{1}H-NMR ($CDCl_3$, 500 MHz) δ 9.38 (1H, br s, COOH), 7.75 (2H,

d, J = 7.5 Hz, Ar-H), 7.59 (2H, m, Ar-H), 7.38 (2H, t, J = 7.5 Hz, Ar-H), 7.30 (2H, t, J = 7.5 Hz, Ar-H), 5.94 – 5.84 (2H, m, H2, H8), 5.46 (1H, d, J = 7.5 Hz, NH), 5.39 (1H, d, J = 7.0 Hz, NH), 5.33 – 5.19 (4H, m, H1, H9), 4.63 (2H, app d, J = 5.0 Hz, H7), 4.59 – 4.54 (2H, m, H3), 4.54 – 4.49 (1H, m, H14) 4.46 – 4.33 (3H, m, H5, H17), 4.21 (1H, t, J = 6.5 Hz, H18), 1.94 – 1.79 (2H, m, H10, H13), 1.76 – 1.62 (2H, m, H10, H13), 1.48 – 1.28 (4H, m, H11, H12); ^{13}C-NMR ($CDCl_3$, 125 MHz) δ 176.2 (C15), 172.2 (C6), 156.1 (C4), 156.0 (C16), 143.9 (Ar-C), 143.7 (Ar-C), 141.3 (Ar-C), 132.5 (C8), 131.5 (C2), 127.7 (Ar-C), 127.1 (Ar-C), 125.1 (Ar-C), 120.0 (Ar-C), 119.1 (C9), 118.0 (C1), 67.1 (C17), 66.1 (C7), 66.0 (C3), 53.7 (C5), 53.6 (C14), 47.2 (C18), 32.4 (C10), 32.1 (C13), 24.7 (C11, C12); HRMS (ESI-TOF) Calc'd for $C_{30}H_{33}N_2O_8$ $[M-H]^-$ 549.2242, found 549.2244.

5.6.9 (*2S, 6S*)-2-((((9*H*-Fluoren-9-yl)methoxy)carbonyl)amino)-7-(allyloxy)-6-(((allyloxy)carbonyl)amino)-7-oxoheptanoic acid (45)

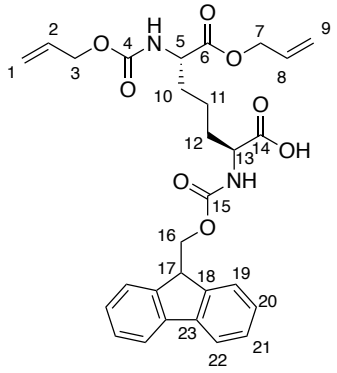

45

Fully protected diamino diacid **55** (0.243 g, 0.400 mmol) was dissolved in TFA:CH_2Cl_2 (1:1, 4 mL) and stirred at room temperature for 6 h. The reaction mixture was then concentrated *in vacuo* and co-evaporated with CH_2Cl_2. The resultant crude oil was dissolved in THF:H_2O (2.5:1, 3.5 mL) and had $NaHCO_3$ (0.0840 g, 0.997 mmol) and allyl chloroformate (0.106 mL, 0.997 mmol) added to it and stirred overnight. Reaction was quenched with 1 M aqueous HCl (5 mL) and then extracted with EtOAc (3 × 5 mL). Pooled aqueous extracts were washed with brine (10 mL), dried over Na_2SO_4, filtered and concentrated *in vacuo*. The crude oil was then purified via flash column chromatography (silica gel, 40% EtOAc in hexanes, 0.1% AcOH) to yield the final diamino diacid **45** (0.191 g, 90% over 2 steps) as a white solid. (R_f = 0.47 on SiO_2, 100% EtOAc, 0.1%

AcOH). $[\alpha]_D^{26}$ +2.87 (*c* = 1.08, CH_2Cl_2); IR (CH_2Cl_2 cast) 3333, 3066, 3022, 2951, 1721, 1530, 1450, 1338, 1251, 1212 cm^{-1}; ^{1}H-NMR ($CDCl_3$, 500 MHz) δ 7.75 (2H, d, *J* = 7.5 Hz, Ar-H), 7.62 – 7.55 (2H, m, Ar-H), 7.39 (2H, t, *J* = 7.5 Hz, Ar-H), 7.33 – 7.28 (2H, m, Ar-H), 5.93 – 5.80 (2H, m, H3, H8), 5.68 (1H, d, *J* = 7.5 Hz, NH), 5.50 (1H, d, *J* = 7.5 Hz, NH), 5.34 – 5.13 (4H, m, H1, H9), 4.73 (2H, app s, H7), 4.64 – 4.59 (2H, m, H3), 4.58 – 4.49 (2H, m, H16), 4.40 – 4.33 (2H, m, H5, H13), 4.21 (1H, t, *J* = 6.5 Hz, H17), 1.95 – 1.82 (2H, m, H10, H12), 1.82 – 1.68 (2H, m, H10, H12), 1.53 – 1.39 (2H, m, H11); ^{13}C-NMR ($CDCl_3$, 125 MHz) δ 175.5 (C14), 172.2 (C6), 156.5 (C15), 156.3 (C4), 144.0 (Ar-C), 143.7 (Ar-C), 141.3 (Ar-C), 139.3 (Ar-C), 132.4 (C8), 131.5 (C2), 129.8 (Ar-C), 128.7 (Ar-C), 127.8 (Ar-C), 127.1 (Ar-C), 125.1 (Ar-C), 120.0 (Ar-C), 119.1 (C9), 118.0 (C1), 67.2 (C16), 66.1 (C3), 64.3 (C7), 53.4 (C13), 53.3 (C5), 47.2 (C17), 32.1 (C12), 31.2 (C10), 21.1 (C11); HRMS (ESI-TOF) Calc'd for $C_{29}H_{31}N_2O_8$ $[M-H]^-$ 535.2086, found 535.2080.

5.6.10 (*2S, 8S*)-2-((((9*H*-Fluoren-9-yl)methoxy)carbonyl)amino)-9-(allyloxy)-8-(((allyloxy)carbonyl)amino)-9-oxononanoic acid (46)

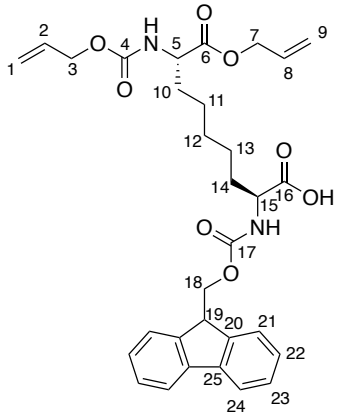

46

Fully protected diamino diacid **66** (0.121 g, 0.191 mmol) was dissolved in TFA:CH_2Cl_2 (1:1, 4 mL) and stirred at room temperature for 6 h. The reaction mixture was then concentrated *in vacuo* and co-evaporated with CH_2Cl_2. The resultant crude oil was dissolved in THF:H_2O (2.5:1, 3.5 mL) and had $NaHCO_3$ (0.0350 g, 0.419 mmol) and allyl chloroformate (0.0450 mL, 0.419 mmol) added to it and stirred overnight. The reaction

was quenched with 1 M aqueous HCl (5 mL) and then extracted with EtOAc (3 × 5 mL). Pooled aqueous extracts were washed with brine (10 mL), dried over Na_2SO_4, filtered and concentrated *in vacuo*. The crude oil was then purified via flash column chromatography (silica gel, 2:1 EtOAc:hexanes, 0.1% AcOH) to yield the final diamino diacid **46** (0.099 g, 92% over 2 steps) as a white solid. (R_f = 0.51 on SiO_2, 100% EtOAc, 0.1% AcOH). $[\alpha]_D^{26}$ +3.6 (*c* = 0.94, CH_2Cl_2); IR (CH_2Cl_2 cast) 3328, 3066, 3045, 3023, 2929, 1722, 1529, 1450, 1338, 1258 cm^{-1}; ^{1}H-NMR ($CDCl_3$, 500 MHz) δ 7.76 (2H, *J* = 8.5 Hz, Ar-H), 7.61 – 7.54 (2H, m, Ar-H), 7.39 (2H, t, *J* = 6.5 Hz, Ar-H), 7.33 – 7.28 (2H, m, Ar-H), 5.96 – 5.85 (2H, m, H2, H8), 5.34 – 5.20 (5H, m, H1, H9, NH), 4.63 (2H, app d, *J* = 5.5 Hz, H7), 4.57 (2H, app d, *J* = 4.0 Hz, H3), 4.45 – 4.33 (4H, m, H5, H15, H18), 4.22 (1H, app t, *J* = 6.5 Hz, H19), 4.05 (1H, d, *J* = 6.0 Hz, NH), 1.93 – 1.78 (2H, m, H10, H14), 1.75 – 1.61 (2H, m, H10, H14), 1.44 – 1.27 (6H, m, H11, H12, H13); ^{13}C-NMR ($CDCl_3$, 125 MHz) δ 176.2 (C16), 172.2 (C6), 156.1 (C17), 156.0 (C4), 144.3 (Ar-C), 143.9 (Ar-C), 143.0 (Ar-C), 141.6 (Ar-C), 141.3 (Ar-C), 132.5 (C8), 131.5 (C2), 127.8 (Ar-C), 127.7 (Ar-C), 127.1 (Ar-C), 125.1 (Ar-C), 124.7 (Ar-C), 120.1 (Ar-C), 120.0 (Ar-C), 119.1 (C9), 118.0 (C1), 67.1 (C18), 66.1 (C7), 66.0 (C3), 53.8 (C5), 53.7 (C15), 47.2 (C19), 32.4 (C14), 32.1 (C10), 28.6 (C13), 28.5 (C11), 24.7 (C12); HRMS (ESI-TOF) Calc'd for $C_{31}H_{35}N_2O_8$ $[M-H]^-$ 563.2399, found 563.2400.

5.6.11 (*2S, 9S*)-2-((((9*H*-Fluoren-9-yl)methoxy)carbonyl)amino)-10-(allyloxy)-9-(((allyloxy)carbonyl)amino)-10-oxodecanoic acid (47)

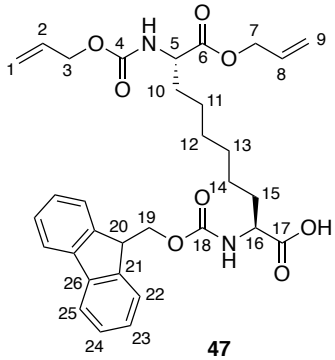

47

Fully protected diamino diacid **69** (0.136 g, 0.210 mmol) was dissolved in TFA:CH_2Cl_2 (1:1, 10 mL) and stirred at room temperature for 6 h. The reaction mixture was then

concentrated *in vacuo* and co-evaporated with CH_2Cl_2. The resultant crude oil was dissolved in THF:H_2O (2.5:1, 7 mL) and had $NaHCO_3$ (0.044 g, 0.524 mmol) and allyl chloroformate (0.056 mL, 0.524 mmol) added to it and stirred overnight. Reaction was quenched with 1 M aqueous HCl (10 mL) and then extracted with EtOAc (3 × 10 mL). Pooled aqueous extracts were washed with brine (10 mL), dried over Na_2SO_4, filtered and concentrated *in vacuo*. The crude oil was then purified via flash column chromatography (silica gel, 1:1 EtOAc:hexanes, 0.1% AcOH) to yield the final diamino diacid **47** (0.121 g, 89% over 2 steps) as a colourless oil. (R_f = 0.59 on SiO_2, 100% EtOAc, 0.1% AcOH). $[\alpha]_D^{26}$ -0.30 (*c* = 0.58, CH_2Cl_2); IR (CH_2Cl_2 cast) 3326, 3068, 3020, 2929, 1722, 15230, 1450, 1407, 1337, 1248, 1105, 1049 cm^{-1}; ^{1}H-NMR ($CDCl_3$, 500 MHz) δ 7.75 (2H, d, *J* = 7.5 Hz, Ar-H), 7.62 (2H, d, *J* = 7.0 Hz, Ar-H), 7.40 (2H, t, *J* = 7.5 Hz, Ar-H), 7.30 (2H, t, *J* = 7.0 Hz, Ar-H), 5.94 – 5.86 (2H, m, H2, H8), 5.39 – 5.20 (6H, m, H1, H9, 2 x NH), 4.92 (1H, dd, *J* = 9.5, 5.5 Hz, H16), 4.71 (2H, app d, *J* = 7.0 Hz, H19), 4.65 – 4.62 (2H, m, H7), 4.60 – 4.56 (2H, m, H3), 4.37 (1H, app q, *J* = 5.5 Hz, H5) 4.27 (1H, t, *J* = 6.0 Hz, H20), 1.99 – 1.91 (1H, m, H15), 1.86 – 1.77 (1H, m, H10), 1.76 – 1.69 (1H, m, H15), 1.68 – 1.60 (1H, m, H10), 1.39 – 1.20 (8H, m, H11, H12, H13, H14); ^{13}C-NMR ($CDCl_3$, 125 MHz) δ 174.7 (C17), 172.4 (C6), 155.8 (C18), 153.4 (C4), 153.1 (Ar-C), 143.4 (Ar-C), 143.3 (Ar-C), 141.4 (Ar-C), 132.7 (C8), 131.6 (C2), 131.2 (Ar-C), 128.0 (Ar-C), 127.9 (Ar-C), 127.2 (Ar-C), 125.0 (Ar-C), 120.1 (Ar-C), 120.0 (Ar-C), 119.3 (Ar-C), 118.9 (C9), 117.9 (C1), 69.1 (C19), 68.2 (C7), 66.0 (C3), 58.6 (C16), 53.9 (C5), 46.8 (C20), 32.7 (C15), 29.2 (C10), 29.0 (C13), 28.9 (C12), 26.2 (C14), 25.1 (C11); HRMS (ESI-TOF) Calc'd for $C_{32}H_{38}N_2O_8$ $[M-H]^-$ 577.2555, found 577.2564.

5.6.12 *tert*-Butyl-(*S*)-2-aminopent-4-enoate (50)

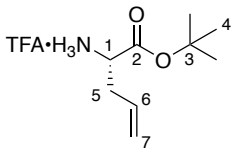

50

Commercially available (2*S*)-2-(9*H*-fluoren-9-ylmethoxycarbonylamino)pent-4-enoic acid (1.55 g, 4.60 mmol) was dissolved in CH_2Cl_2 (50 mL), followed by *tert*-butyl 2,2,2-

trichloroacetimidate (1.65 mL, 9.23 mmol) and stirred at room temperature for 72 h. The reaction mixture was filtered and the filtrate was concentrated *in vacuo* and redissolved in CH_2Cl_2:diethylamine (1:1, 10 mL) and stirred at room temperature for 2 h. The resultant mixture was then concentrated *in vacuo* and co-evaporated with CH_2Cl_2. The crude material was then purified via flash column chromatography (silica gel, 1:1 EtOAc:hexanes, 0.1% DIPEA) to yield amine **50** (0.614 g, 78% over 2 steps) as a yellow oil. (R_f = 0.07 on SiO_2, 30% EtOAc in hexanes, 0.1% DIPEA); $[\alpha]_D^{26}$ -6.4 (*c* = 0.81, CH_2Cl_2); IR (CH_2Cl_2 cast) 3380, 3350, 3078, 3008, 2979, 2934, 1750, 1458, 1368, 1155 cm^{-1}; ^{1}H-NMR ($CDCl_3$, 600 MHz) δ 5.75 (1H, ddt, *J* = 16.8, 10.2, 7.2, Hz, H6), 5.16 – 5.12 (2H, m, H7), 3.41 (1H, dd, *J* = 5.4, 5.4 Hz, H1), 2.48 – 2.44 (1H, m, H5), 2.38 –2.34 (1H, m, H5), 1.46 (9H, s, H3); ^{13}C-NMR ($CDCl_3$, 175 MHz) δ 174.6 (C2), 133.7 (C6), 118.5 (C7), 81.2 (C1), 54.4 (C3), 39.4 (C5), 28.1 (C4); HRMS (ESI-TOF) Calc'd for $C_9H_{18}NO_2$ $[M+H]^+$ 172.1332, found 172.1331 $(M+H)^+$

5.6.13 2-(((((*S*)-1-(*tert*-Butoxy)-1-oxopent-4-en-2-yl)carbamoyl)oxy)methyl)benzyl-(*S*)-2-((*tert*-butoxycarbonyl)amino)pent-4-enoate (51)

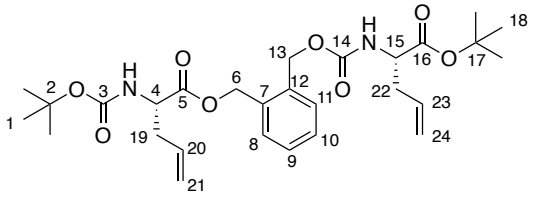

51

The following was adapted according to an adapted literature procedure.[165] Compound **39** (1.33 g, 2.66 mmol) and amine **50** (0.680 g, 3.97 mmol) were dissolved in DMF (25 mL). DIPEA (1.16 mL, 6.66 mmol) was then added to the mixture and this was left to stir at room temperature overnight. The reaction was diluted with EtOAc (150 mL) and quenched with 10% aqueous citric acid (150 mL). The layers were then separated and the organic layer was washed with saturated aqueous Na_2CO_3 until the aqueous layer was no longer yellow. Organic layer was then washed with brine (2 × 150 mL), dried over Na_2SO_4, filtered and concentrated *in vacuo*. The crude material was purified via flash column chromatography (silica gel, 15% EtOAc in hexanes) to give **51** (1.34 g, 95%) as a

yellow oil. (R_f = 0.44 on SiO_2, 30% EtOAc in hexanes); $[\alpha]_D^{26}$ +7.7 (*c* = 0.48, CH_2Cl_2); IR (CH_2Cl_2 cast) 3353, 3079, 2979, 2931, 1720, 1510, 1465, 1367, 1252, 1224, 1158, 1055 cm^{-1}; ^{1}H-NMR ($CDCl_3$, 500 MHz) δ 7.42 – 7.30 (4H, m, Ar-H), 5.73 – 5.60 (2H, m, H20, H23), 5.40 (1H, s, NH), 5.28 (1H, d, *J* = 12.5 Hz, H6), 5.25 (1H, d, *J* = 12.5 Hz, H6), 5.19 (2H, s, H13), 5.12 – 5.05 (5H, m, H21, H24, NH) 4.42 (1H, app q, *J* = 6.0 Hz, H4), 4.31 (1H, app q, *J* = 7.0 Hz, H15) 2.60 – 2.45 (4H, m, H19, H22), 1.45 (9H, s, H18), 1.42 (9H, s, H1); ^{13}C-NMR ($CDCl_3$, 125 MHz) δ 171.8 (C5), 170.7 (C16), 155.5 (C3), 155.2 (C14), 135.1 (Ar-C), 133.9 (Ar-C), 132.6 (C20, C23), 129.9 (Ar-C), 129.8 (Ar-C), 128.9 (Ar-C), 128.7 (Ar-C), 119.3 (C21), 119.1 (C24), 82.2 (C17), 79.9 (C2), 64.5 (C6), 64.3 (C13), 53.5 (C15), 53.0 (C4), 36.9 (C22), 36.0 (C19), 28.3 (C18), 28.0 (C1); HRMS (ESI-TOF) Calc'd for $C_{28}H_{40}N_2O_8Na$ $[M+Na]^+$ 555.2677, found 555.2671.

5.6.14 8-Allyl-1-(*tert*-butyl)-(*2S, 7S*)-2-((((9*H*-fluoren-9-yl)methoxy)carbonyl)amino)-7-((*tert*-butoxycarbonyl)amino)octanedioate (52)

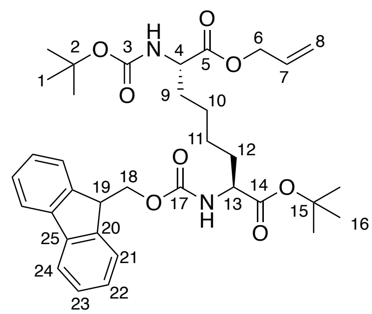

52

Compound **51** (2.43 g, 4.81 mmol) was dissolved in a large excess of degassed 1,2-dichloroethane (900 mL) and had Grubbs 2nd generation catalyst (0.190 g, 0.224 mmol) added to it. The reaction was heated at reflux for 72 h to afford the cross-metathesis intermediate. The reaction was concentrated down to a brown oil and passed through a silica plug (25% EtOAC in hexanes) to remove the catalyst. The macrocycle (2.11 g, 4.18 mmol) was dissolved in THF:MeOH (1:1, 40 mL) and had Pd/C (10%) (200 mg) added to it. This was stirred at room temperature under 1 atm of H_2 for 8 h. The reaction mixture was then filtered through Celite® and concentrated *in vacuo* to produce a white solid. This was then redissolved in THF:H_2O (2.5:1, 40 mL), followed by the addition of

$NaHCO_3$ (0.879 g, 10.6 mmol) and Fmoc-Cl (1.08 g, 4.18 mmol) and stirred overnight. Reaction mixture was quenched with 1 M aqueous HCl (50 mL) and the solution was extracted with EtOAc (3 × 50 mL). Combined organic extracts were then washed with brine (150 mL), dried over Na_2SO_4, filtered and concentrated down to a white solid. The intermediate was redissolved in DMF (40 mL) and then had $NaHCO_3$ (0.879 g, 10.5 mmol) and allyl bromide (0.904 mL, 10.5 mmol) added to it and stirred at room temperature overnight. The reaction was quenched with 1 M aqueous HCl (50 mL), and the aqueous layer was extracted with EtOAc (3 × 50 mL). Combined organic extracts were then washed with H_2O (150 mL), then brine (150 mL), dried over Na_2SO_4, filtered and concentrated *in vacuo*. The crude product was then purified via flash column chromatography (silica gel, 20% EtOAc in hexanes) to give **52** (2.18 g, 84% over 4 steps) as a white solid. (R_f = 0.41 on SiO_2, 30% EtOAc in hexanes). $[\alpha]_D^{26}$ +3.7 (*c* = 0.91, CH_2Cl_2); IR (CH_2Cl_2 cast) 3345, 3066, 2978, 2935, 1715, 1517, 1478, 1451, 1367, 1248, 1160, 1048 cm^{-1}; ^{1}H-NMR ($CDCl_3$, 500 MHz) δ 7.77 (2H, d, *J* = 7.5 Hz, Ar-H), 7.60 (2H, d, *J* = 7.5 Hz, Ar-H), 7.40 (2H, t, *J* = 7.5 Hz, Ar-H), 7.31 (2H, t, *J* = 7.5 Hz, Ar-H), 5.91 (1H, ddt, *J* = 16.0, 10.5, 6.0 Hz, H7), 5.35 – 5.25 (3H, m, H8, NH), 5.00 (1H, d, *J* = 6.5 Hz, NH), 4.63 (2H, app t, *J* = 6.0 Hz, H6), 4.39 (2H, d, *J* = 7.0 Hz, H18), 4.31 (1H, app q, *J* = 5.0 Hz, H4), 4.26 – 4.21 (2H, m, H13, H19), 1.86 – 1.76 (2H, m, H9, H12), 1.68 – 1.58 (2H, m, H9, H12), 1.47 (9H, s, H16), 1.44 (9H, s, H1), 1.38 – 1.24 (4H, m, H10, H11); ^{13}C-NMR ($CDCl_3$, 175 MHz) δ 172.5 (C5), 171.6 (14), 155.9 (C3), 155.4 (C17), 144.0 (Ar-C), 143.9 (Ar-C), 141.3 (Ar-C), 131.7 (C7), 127.7 (Ar-C), 127.2 (Ar-C), 125.1 (Ar-C), 120.0 (Ar-C), 120.0 (Ar-C), 118.9 (C8), 82.2 (C15), 79.9 (C2), 67.0 (C18), 65.9 (C6), 54.5 (C13), 54.2 (C4), 47.2 (C19), 32.7 (C9), 32.6 (C12), 28.4 (C16), 28.1 (C1), 25.0 (C10), 24.7 (C11); HRMS (ESI-TOF) Calc'd for $C_{35}H_{46}N_2O_8Na$ $[M+Na]^+$ 645.3146, found 645.3143.

5.6.15 (*S*)-5-(*tert*-Butoxy)-4-((((2-((((*S*)-2-((*tert*-butoxycarbonyl)amino)pent-4-enoyl)oxy)methyl)benzyl)oxy)carbonyl)amino-5-oxopentanoic acid (54)

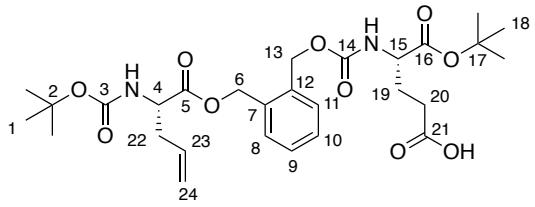

54

The following was adapted according to a literature procedure.[165] Compound **39** (5.06 g, 10.1 mmol) and H-L-Glu-O^{t}Bu (4.52 g, 22.2 mmol) were dissolved in DMF (100 mL). DIPEA (43.9 mL, 22.2 mmol) was then added to the mixture and this was left to stir at room temperature overnight. The reaction was quenched with 1 M aqueous HCl (100 mL) and the reaction was extracted with EtOAc (3 × 100 mL). Combined organic extracts were washed with brine (100 mL), dried over Na_2SO_4, filtered and concentrated *in vacuo*. The crude material was purified via flash column chromatography (silica gel, 40% EtOAc in hexanes, 0.1% AcOH) to give **54** (5.64 g, 99%) as a colourless oil. (R_f = 0.30 on SiO_2, 1:1 EtOAc:hexanes, 0.1% AcOH). $[\alpha]_D^{26}$ -3.3 (*c* = 0.89, CH_2Cl_2); IR (CH_2Cl_2 cast) 3338, 3077, 2979, 2935, 1716, 1519, 1455, 1386, 1251, 1224, 1158, 1055 cm^{-1}; ^{1}H-NMR ($CDCl_3$, 500 MHz) δ 7.43 – 7.31 (4H, m, Ar-H), 5.72 – 5.60 (2H, m, H23, NH), 5.28 (1H, d, *J* = 13.0 Hz, H6), 5.24 (1H, d, *J* = 13.0 Hz, H6), 5.17 (2H, s, H13), 5.13 (1H, d, *J* = 7.5 Hz, NH), 5.10 – 5.04 (2H, m, H24), 4.47 (1H, app q, *J* = 5.0 Hz, H15), 4.26 (1H, app q, *J* = 5.0 Hz, H4), 2.59 – 2.36 (4H, m, H20, H22), 2.26 – 2.14 (1H, m, H19), 2.02 – 1.92 (1H, m, H19), 1.45 (9H, s, H18), 1.41 (9H, s, H1); ^{13}C-NMR ($CDCl_3$, 125 MHz) δ 176.8 (C21), 172.0 (C5), 170.9 (C16), 155.9 (C3), 155.5 (C14), 134.9 (Ar-C), 134.2 (Ar-C), 132.2 (C23), 130.2 (Ar-C), 130.1 (Ar-C), 128.9 (Ar-C), 128.8 (Ar-C), 119.3 (C24), 82.4 (C17), 80.2 (C2), 64.5 (C6), 64.6 (C13), 54.1 (C15), 53.0 (C4), 36.7 (C22), 30.0 (C20), 28.3 (C19), 28.0 (C18), 27.3 (C1); HRMS (ESI-TOF) Calc'd for $C_{28}H_{40}N_2O_{10}Na$ $[M+Na]^+$ 587.2575, found 587.2573.

5.6.16 2-(((((*S*)-1-(*tert*-Butoxy)-1-oxobut-3-en-2-yl)carbamoyl)oxy)methyl)benzyl-(*S*)-2-((*tert*-butoxycarbonyl)amino)pent-4-enoate (55)

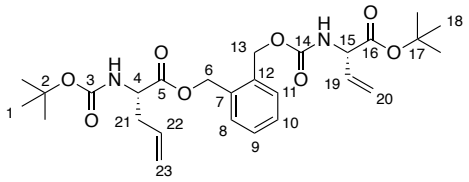

55

The following was adapted according to a literature procedure.[169] Compound **54** (1.36 g, 2.41 mmol) and cupric acetate (0.121 g, 0.604 mmol) were dissolved in dry benzene (40 mL) in a flame dried round bottom flask. This mixture was heated at reflux under argon for 1 h. Lead tetraacetate (2.22 g, 5.01 mmol) was then added and reflux was continued under argon overnight. The reaction was filtered through Celite® and diluted with EtOAc (50 mL). The organic layer was washed with 1 M aqueous HCl (2 × 50 mL), followed by brine (50 mL), dried over Na_2SO_4, filtered and concentrated *in vacuo*. The crude material was purified via flash column chromatography (silica gel, 20% EtOAc in hexanes, then 50% EtOAc in hexanes, 0.1% AcOH to elute the remaining starting material) to give the vinyl glycine product **55** (0.52 g, 42%) as a yellow oil. The starting material **54** (0.37 g, 30%) was recovered as a yellow oil. (R_f = 0.45 on SiO_2, 30% EtOAc in hexanes). $[\alpha]_D^{26}$ -3.5 (*c* = 0.68, CH_2Cl_2); IR (CH_2Cl_2 cast) 3349, 3081, 3002, 2979, 2934, 1720, 1634, 1514, 1456, 1368, 1339, 1251, 1228, 1158, 1049 cm^{-1}; ^{1}H-NMR ($CDCl_3$, 500 MHz) δ 7.46 – 7.31 (4H, m, Ar-H), 5.89 (1H, ddd, *J* = 17.0, 10.5, 5.5 Hz, H19), 5.69 – 5.57 (2H, m, H22, NH) 5.33 (1H, d, *J* = 17.0 Hz, H20), 5.27 – 5.18 (5H, m, H6, H13, H20), 5.11 – 5.02 (3H, m, H23, NH), 4.78 (1H, t, *J* = 5.5 Hz, H15), 4.41 (1H, app q, *J* = 6.0 Hz, H4), 2.59 – 2.43 (2H, m, H21), 1.45 (9H, s, H18), 1.42 (9H, s, H1); ^{13}C-NMR ($CDCl_3$, 125 MHz) δ 171.9 (C3), 169.4 (C14), 155.4 (C5), 155.3 (C16), 135.0 (Ar-C), 134.0 (Ar-C), 133.0 (C19), 132.2 (C22), 129.9 (Ar-C), 128.9 (Ar-C), 128.7 (Ar-C), 119.3 (C20), 117.1 (C23), 82.6 (C17), 80.0 (C2), 64.6 (C6), 64.4 (C13), 56.8 (C15), 53.0 (C4), 36.7 (C21), 28.3 (C18), 28.0 (C1); HRMS (ESI-TOF) Calc'd for $C_{27}H_{38}N_2O_8Na$ $[M+Na]^+$ 541.2520, found 541.2521.

5.6.17 7-Allyl-1-(*tert*-butyl)-(*2S,6S*)-2-((((9*H*-fluoren-9-yl)methoxy)carbonyl)amino)-6-((*tert*-butoxycarbonyl)amino)heptanedioate (56)

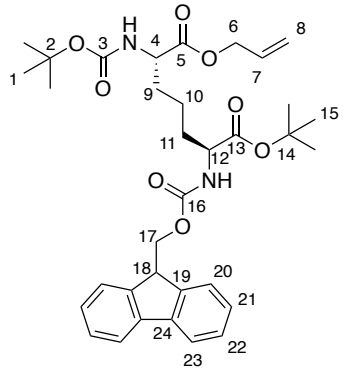

56

Compound **55** (0.431 g, 0.833 mmol) was dissolved in a large excess of degassed 1,2-dichloroethane (500 mL) and had Grubbs 2nd generation catalyst (0.070 g, 0.084 mmol) added to it. The reaction was heated at reflux for 72 h to afford the cross-metathesis intermediate. The reaction was concentrated down to a brown oil and passed through a silica plug (20% EtOAc in hexanes) to remove the catalyst. The macrocycle (0.332 g, 0.677 mmol) was dissolved in THF:MeOH (1:1 15 mL) and had Pd/C (10%) (40 mg) added to it. This was stirred at room temperature under 1 atm of H_2 for 8 h. The reaction mixture was then filtered through Celite® and concentrated *in vacuo* to produce a white solid. This was then redissolved in THF:H_2O (2.5:1, 15 mL), followed by the addition of $NaHCO_3$ (0.142 g, 1.69 mmol) and Fmoc-Cl (0.197 g, 0.763 mmol) and stirred overnight. Reaction mixture was quenched with 1 M aqueous HCl (15 mL) and the solution was extracted with EtOAc (3 × 15 mL). Combined organic extracts were then washed with brine (15 mL), dried over Na_2SO_4, filtered and concentrated down to a white solid. The intermediate was redissolved in DMF (15 mL) and then had $NaHCO_3$ (0.142 g, 1.69 mmol) and allyl bromide (0.146 mL, 1.69 mmol) added to it and stirred at room temperature overnight. The reaction was quenched with 1 M aqueous HCl (15 mL), and the aqueous layer was extracted with EtOAc (3 × 15 mL). Combined organic extracts were then washed with H_2O (15 mL), then brine (15 mL), dried over Na_2SO_4, filtered and concentrated *in vacuo*. The crude product was then purified via flash column

chromatography (silica gel, 20% EtOAc in hexanes) to give **56** (0.354 g, 70% over 4 steps) as a white solid. (R_f = 0.45 on SiO_2, 30% EtOAc in hexanes). $[\alpha]_D^{26}$ +3.2 (*c* = 0.59, CH_2Cl_2) IR (CH_2Cl_2 cast) 3345, 3072, 2978, 2940, 1717, 1517, 1451, 1367, 1250, 1228, 1160, 1059 cm^{-1}; ^{1}H-NMR ($CDCl_3$, 500 MHz) δ 7.76 (2H, d, *J* = 7.5 Hz, Ar-H), 7.61 (2H, d, *J* = 7.5 Hz, Ar-H), 7.40 (2H, t, *J* = 7.5 Hz, Ar-H), 7.32 (2H, tt, *J* = 7.5, 1.5 Hz, Ar-H), 5.90 (1H, ddt, *J* = 17.0, 10.5, 6.0 Hz, H7), 5.38 (1H, d, *J* = 7.5 Hz, NH), 5.32 (1H, d, *J* = 17.0 Hz, H8), 5.24 (1H, d, *J* = 10.5 Hz, H8) 5.10 (1H, d, *J* = 7.5 Hz, NH), 4.64 – 4.60 (2H, m, H6), 4.46 – 4.40 (1H, m, H17), 4.37 – 4.32 (1H, m, H17), 4.31 – 4.27 (1H, m, H4), 4.25 – 4.20 (2H, m, H12, H18), 1.89 – 1.79 (2H, m, H9, H11), 1.75 – 1.66 (2H, m, H9, H11), 1.47 (9H, s, H15), 1.44 – 1.43 (2H, m, H10), 1.44 (9H, s, H1); ^{13}C-NMR ($CDCl_3$, 125 MHz) δ 172.5 (C5), 171.5 (C13), 156.1 (C16), 155.6 (C3), 144.0 (Ar-C), 143.8 (Ar-C), 141.4 (Ar-C), 131.7 (C7), 127.8 (Ar-C), 127.1 (Ar-C), 125.2 (Ar-C), 120.0 (Ar-C), 118.9 (C8), 82.3 (C14), 80.0 (C2), 67.1 (C17), 65.9 (C6), 54.0 (C4) 53.3 (C12), 47.2 (C18), 32.3 (C9), 32.2 (C11), 28.4 (C15), 28.1 (C1), 21.1 (C10); HRMS (ESI-TOF) Calc'd for $C_{34}H_{44}N_2O_8Na$ $[M+Na]^+$ 631.2990, found 631.2290.

5.6.18 1-(*tert*-Butyl)-5-methyl-(*tert*-butoxycarbonyl)-*L*-glutamate (58)

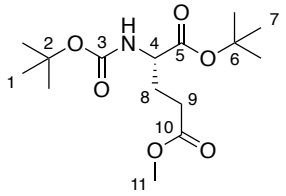

58

The following was prepared according to an adapted literature procedure.[171] Boc-L-glutamic acid 1-*tert*-butyl ester (15.0 g, 49.5 mmol) was dissolved in dry CH_2Cl_2 (500 mL), followed by the addition of Et_3N (10.4 mL, 74.3 mmol) and cooled to 0 °C. Once cooled down, DMAP (0.608 g, 4.98 mmol) and methyl chloroformate (5.74 mL, 74.3 mmol) were added and the reaction was allowed to warm up to room temperature and stirred for 0.5 h. The reaction was diluted with CH_2Cl_2 (100 mL) and quenched with 1 M aqueous $NaHCO_3$ (500 mL). The layers were separated and the aqueous layer was then extracted with CH_2Cl_2 (3 x 200 mL). Pooled organic layers were dried over Na_2SO_2,

filtered and concentrated *in vacuo*. The crude oil was purified via flash column chromatography (silica gel, 2:1 hexanes:EtOAc) to yield the methyl ester product **58** (14.4 g, 92%) as a white solid. (R_f = 0.64 on SiO_2, 1:1 hexanes:EtOAc). $[\alpha]_D^{26}$ +5.7 (*c* = 0.63, CH_2Cl_2); IR (CH_2Cl_2 cast) 3380, 2979, 1740, 1717, 1512, 1453, 1368, 1252, 1156 cm^{-1}; ^{1}H-NMR ($CDCl_3$, 600 MHz) δ 5.07 (1H, d, *J* = 6.6 Hz, NH), 4.20 (1H, app q, *J* = 5.4 Hz, H4), 3.68 (3H, s, H11), 2.43 (1H, ddd, *J* = 16.0, 9.2, 6.6 Hz, H9), 2.36 (1H, dd, *J* = 16.0, 9.2, 6.0 Hz, H9), 2.19 – 2.12 (1H, m, H8), 1.95 – 1.89 (1H, m, H8), 1.47 (9H, s, H7), 1.44 (9H, s, H1); ^{13}C-NMR ($CDCl_3$, 175 MHz) δ 173.4 (C5), 171.4 (C10), 155.4 (C3), 82.3 (C6), 79.8 (C2), 53.5 (C4), 51.8 (C11), 30.2 (C9), 28.4 (C8), 28.2 (C7), 28.1 (C1); HRMS (ESI-TOF) Calc'd for $C_{15}H_{27}NO_6Na$ $[M+Na]^+$ 340.1731, found 340.1730.

5.6.19 1-(*tert*-Butyl)-5-methyl-*N,N*-bis(*tert*-butoxycarbonyl)-*L*-glutamate (59)

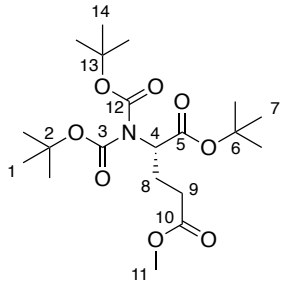

59

The following was prepared according to an adapted literature procedure.[171] Compound **58** (14.4 g, 45.4 mmol) and DMAP (1.11 g, 9.09 mmol) were dissolved in MeCN (150 mL). A solution of Boc anhydride (39.7 g, 182 mmol) in MeCN (40 mL) was then added to the reaction and left to stir overnight at room temperature. The reaction was concentrated *in vacuo* and purified via flash column chromatography (silica gel, 8:1 hexanes:EtOAc) to yield **59** (18.9 g, quant.) as clear oil. (R_f = 0.46 on SiO_2, 4:1 hexanes:EtOAc). $[\alpha]_D^{26}$ -22.7 (*c* = 0.78, CH_2Cl_2); IR (CH_2Cl_2 cast) 2979, 2935, 1740, 1701, 1367, 1275, 1141 cm^{-1}; ^{1}H-NMR ($CDCl_3$, 600 MHz) δ 4.78 (1H, dd, *J* = 10.2, 4.8 Hz, H4), 3.67 (3H, s, H11), 2.45 – 2.34 (3H, m, H8, H9), 2.19 – 2.13 (1H, m, H8), 1.50 (18H, s, H1, H14), 1.45 (9H, s, H7); ^{13}C-NMR ($CDCl_3$, 175 MHz) δ 173.2 (C10), 169.3 (C5), 152.3 (C3, C12), 82.9 (C2, C13), 81.4 (C6), 58.1 (C4), 51.6 (C11), 30.8 (C9), 28.0

(C1, C14), 27.9 (C7), 24.7 (C8); HRMS (ESI-TOF) Calc'd for $C_{20}H_{35}NO_8Na$ $[M+Na]^+$ 440.2255, found 440.2253.

5.6.20 *tert*-Butyl-(*S*)-2-(bis(*tert*-butoxycarbonyl)amino)-5-oxopentanoate (60)

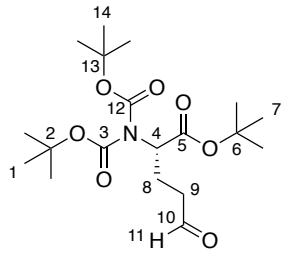

60

The following was prepared according to an adapted literature procedure.[171] Compound **59** (18.9 g, 45.4 mmol) was dissolved in dry Et_2O (220 mL) under an argon atmosphere and cooled down to -78 °C. DIBAL-H (63.5 mL, 63.5 mmol) was added via syringe over 20 mins. The reaction stirred at -78 °C for 5 mins before being quenched with water (8.20 mL) and warmed up to room temperature. A saturated aqueous solution of Rochelle salt (150 mL) was added and stirred vigorously for 1 h. The reaction was then extracted with EtOAc (3 × 300 mL) and the pooled organic layers were dried over Na_2SO_4, filtered and concentrated *in vacuo*. The crude product was purified via flash column chromatography (silica gel, 9:1 hexanes:EtOAc) to yield aldehyde **60** (13.0 g, 74%) as a colourless oil. (Rf = 0.41 on SiO_2, 4:1 hexanes:EtOAc). $[\alpha]_D^{26}$ -20.5 (*c* = 0.77, CH_2Cl_2); IR (CH_2Cl_2 cast) 2980, 2933, 2825, 2721, 1791, 1739, 1701, 1368, 1255, 1148, 1123 cm^{-1}; ^{1}H-NMR ($CDCl_3$, 500 MHz) δ 9.76 (1H, s, H11), 4.73 (1H, dd, *J* = 9.5, 5.5 Hz, H4), 2.61 – 2.39 (3H, m, H8, H9), 2.19 – 2.10 (1H, m, H8), 1.50 (18H, s, H1, H14), 1.45 (9H, s, H7); ^{13}C-NMR ($CDCl_3$, 125 MHz) δ 201.2 (C10), 169.2 (C5), 152.4 (C3, C12), 83.1 (C2, C13), 81.5 (C6), 58.2 (C4), 40.7 (C9), 28.0 (C1, C14), 28.0 (C7), 22.0 (C9); HRMS (ESI-TOF) Calc'd for $C_{19}H_{33}NO_7Na$ $[M+Na]^+$ 410.2149, found 410.2146.

5.6.21 *tert*-Butyl-(*S*)-2-(bis(*tert*-butoxycarbonyl)amino)-hex-5-enoate (61)

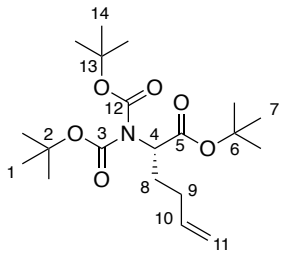

61

The following was prepared according to an adapted literature procedure.[171] To a flame dried flask cooled to -78 °C was added methyltriphenylphosphonium iodide (14.5 g, 35.7 mmol) and potassium *tert*-butoxide (4.01 g, 35.7 mmol) and dissolved in dry THF (350 mL). This solution was then allowed to warm up to 0 °C over 1.5 h. Compound **60** (6.20 g, 16.0 mmol) was dissolved in dry THF (160 mL) in a flame dried flask and cooled down to 0 °C. This solution was cannulated into the ylide solution and stirred at 0 °C for 30 mins. The reaction mixture was quenched with saturated aqueous NH_4Cl (65 mL) and vigorously stirred for 5 mins. Reaction was then diluted with H_2O (300 mL) and extracted with EtOAc (3 × 300 mL). Pooled organic extracts were dried over Na_2SO_4, filtered and concentrated *in vacuo*. The crude product was purified via flash column chromatography (silica gel, 9:1 hexanes:EtOAc) to give olefin **61** (5.81 g, 95%) as a colourless oil. (Rf = 0.55 on SiO_2, 6:1 hexanes:EtOAc). $[\alpha]_D^{26}$ -8.08 (*c* = 1.00, CH_2Cl_2); IR (CH_2Cl_2 cast) 3078, 2980, 2935, 1740, 1703, 1642, 1367, 1255, 1232, 1156, 1129 cm^{-1}; ^{1}H-NMR ($CDCl_3$, 400 MHz) δ 5.81 (1H, ddt, *J* = 17.4, 10.4, 6.8 Hz, H10), 5.04 (1H, app dq, *J* = 17.4, 1.2 Hz, H11), 4.98 (1H, app dq, *J* = 10.4, 1.2 Hz, H11), 4.73 (1H, dd, *J* = 9.6, 4.8 Hz, H4), 2.21 – 2.07 (3H, m, H8, H9), 1.99 – 1.90 (1H, m, H8), 1.50 (18H, s, H1, H14), 1.44 (9H, s, H7); ^{13}C-NMR ($CDCl_3$, 175 MHz) δ 169.8 (C5), 152.4 (C3, C12), 137.6 (C10), 115.3 (C11), 82.7 (C2, C13), 81.1 (C6), 58.3 (C4), 30.5 (C9), 28.7 (C8), 28.0 (C1, C14), 27.9 (C7); HRMS (ESI-TOF) Calc'd for $C_{20}H_{35}NO_6Na$ $[M+Na]^+$ 408.2357, found 408.2357.

5.6.22 *(S)*-2-((*tert*-Butoxycarbonyl)amino)-hex-5-enoic acid (62)

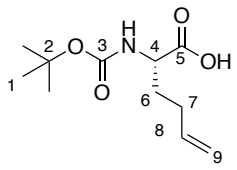

62

Fully protected olefin **61** (1.73 g, 4.49 mmol) was dissolved in TFA/CH_2Cl_2 (1:1, 15 mL) and stirred at room temperature and the reaction was complete after 6 h. The crude mixture was concentrated down and co-evaporated with CH_2Cl_2 to a yellow oil/white solid. This was redissolved in THF/H_2O (2.5:1, 45 mL) and had $NaHCO_3$ (0.770 g, 9.25 mmol) and Boc_2O (2.02, 9.25 mmol) added to it and was stirred at room temperature overnight. The reaction was quenched via 1 M aqueous HCl (25 mL) and then extracted with EtOAc (3 × 50 mL). Combined organic extracts were then washed with brine (50 mL), dried over Na_2SO_4, filtered and concentrated *in vacuo* to a yellow oil. The crude oil was purified by flash column chromatography (silica gel, 1:1 hexanes:EtOAC, 0.1% AcOH) to give the free acid **62** (0.76 g, 74%) as a colourless oil. (Rf = 0.26 on SiO_2, 1:1 hexanes:EtOAc, 0.1% AcOH). $[\alpha]_D^{26}$ +0.470 (*c* = 1.10, CH_2Cl_2); IR (CH_2Cl_2 cast) 3407, 3317, 3068, 3023, 2980, 2952, 1720, 1519, 1450, 1420, 1341, 1228, 1052 cm^{-1}; ^{1}H-NMR ($CDCl_3$, 500 MHz) δ 8.65 (1H, br s, COOH), 5.84 – 5.77 (1H, m, H8), 5.11 – 5.03 (3H, m, H9, NH), 4.36 (1H, app s, H4), 2.19 (2H, app q, *J* = 7.0 Hz, H7), 2.05 – 1.94 (1H, m, H6), 1.79 (1H, app sext., *J* = 7.0 Hz, H6), 1.48 (9H, s, H1); ^{13}C-NMR ($CDCl_3$, 125 MHz) δ 177.3 (C5), 155.6 (C3), 136.7 (C8), 115.9 (C9), 80.4 (C2), 52.9 (C4), 31.6 (C7), 29.5 (C6), 28.3 (C1); HRMS (ESI-TOF) Calc'd for $C_{11}H_{18}NO_4$ 228.1241 $[M-H]^-$, found 228.1241.

5.6.23 2-(Hydroxymethyl)benzyl-(*S*)-2-((*tert*-butoxycarbonyl)amino)hex-5-enoate (63)

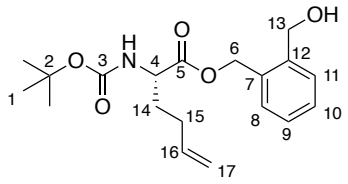

63

The following was adapted from a literature procedure.[165] Compound **62** (0.680 g, 2.30 mmol), DMAP (0.0431 g, 0.353 mmol) and 1,2-benzenedimethanol (2.38 g, 17.2 mmol) were dissolved in CH_2Cl_2 (125 mL) and cooled down to 0 °C. Once cooled, EDCI (0.788 g, 4.11 mmol) was added and the reaction mixture was allowed to warm up to room temperature over 3 h and stirred overnight at room temperature. The reaction mixture was then concentrated *in vacuo* and purified via flash column chromatography (silica gel, 30% EtOAc in hexanes) to yield **63** (0.848 g, 82%) as a colourless oil. (R_f = 0.59 on SiO_2, 1:1 hexanes:EtOAc). $[\alpha]_D^{26}$ +0.180 (*c* = 1.24, CH_2Cl_2); IR (CH_2Cl_2 cast) 3363, 3075, 3034, 2978, 2932, 1739, 1714, 1697, 1516, 1454, 1367, 1252, 1212, 1163, 1051, 1022 cm^{-1}; ^{1}H-NMR ($CDCl_3$, 500 MHz) δ 7.43 (1H, d, *J* = 7.0 Hz, Ar-H), 7.38 – 7.30 (3H, m, Ar-H), 5.75 (1H, ddt, *J* = 17.0, 10.5, 6.5 Hz, H16), 5.31 (1H, d, *J* = 12.5 Hz, H6), 5.28 (1H, d, *J* = 12.5 Hz, H6), 5.02 – 4.97 (3H, m, H17, NH), 4.78 (1H, d, *J* = 12.5 Hz, H13), 4.73 (1H, d, *J* = 12.5 Hz, H13), 4.32 (1H, app q, *J* = 5.5 Hz, H4), 2.13 – 2.02 (3H, m, H15, OH), 1.94 – 1.87 (1H, m, H14), 1.75 – 1.67 (1H, m, H14), 1.41 (9H, s, H1); ^{13}C-NMR ($CDCl_3$, 125 MHz) δ 172.7 (C5), 155.4 (C3), 139.4 (Ar-C), 136.8 (C16), 133.3 (Ar-C), 130.0 (Ar-C), 129.1 (Ar-C), 129.0 (Ar-C), 128.1 (Ar-C), 115.8 (C17), 80.1 (C2), 64.8 (C6), 62.9 (C13), 53.2 (C4), 31.7 (C15), 29.5 (C14), 28.3 (C1); HRMS (ESI-TOF) Calc'd for $C_{19}H_{27}NO_5Na$ $[M+Na]^+$ 372.1781, found 372.1778.

5.6.24 2-((((4-Nitrophenoxy)carbonyl)oxy)methyl)benzyl-(*S*)-2-((*tert*-butoxycarbonyl)amino)hex-5-enoate (64)

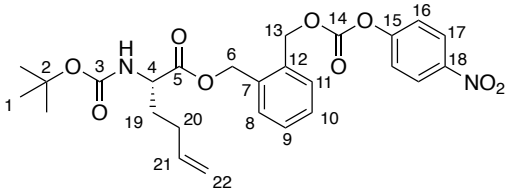

64

The following was prepared according to an adapted literature procedure.[165] Compound **63** (0.719 g, 2.06 mmol) was dissolved in CH_2Cl_2 (25 mL) and had bis(4-nitrophenyl) carbonate (1.16 g, 3.81 mmol) and DIPEA (0.538 mL, 3.09 mmol) added to it. The resulting reaction mixture was stirred overnight. It was then diluted with EtOAc (150 mL), quenched with 10% aqueous citric acid (150 mL) and the layers were separated. The organic layer was then washed with saturated aqueous Na_2CO_3 until the aqueous layer was no longer yellow and then washed with brine (2 × 300 mL), dried over Na_2SO_4, filtered and concentrated *in vacuo*. The crude product was then purified via flash column chromatography (silica gel, 0-2% acetone in CH_2Cl_2) to give **64** (1.06 g, 98%) as a white solid. (R_f = 0.76 on SiO_2, 1:1 EtOAc:hexanes). $[\alpha]_D^{26}$ +1.4 (*c* = 0.70, CH_2Cl_2); IR (CH_2Cl_2 cast) 3382, 3080, 2978, 2931, 1768, 1715, 1616, 1594, 1526, 1454, 1367, 1348, 1289, 1216, 1163 cm^{-1}; ^{1}H-NMR ($CDCl_3$, 500 MHz) δ 8.27 (2H, app d, *J* = 10.0 Hz, H17), 7.50 – 7.33 (6H, m, H16, Ar-H), 5.73 (1H, ddt, *J* = 17.0, 10.0, 6.5 Hz, H21), 5.41 (2H, s, H6), 5.34 (1H, d, *J* = 12.5 Hz, H13), 5.31 (1H, d, *J* = 12.5 Hz, H13), 5.03 – 4.93 (3H, m, H22, NH), 4.36 (1H, app q, *J* = 5.5 Hz, H4), 2.12 – 2.03 (2H, m, H20), 1.96 – 1.87 (1H, m, H19), 1.77 – 1.67 (1H, m, H19), 1.42 (9H, s, H1); ^{13}C-NMR ($CDCl_3$, 125 MHz) δ 172.6 (C5), 155.5 (C14), 152.4 (C3), 136.8 (C21), 134.4 (Ar-C), 133.0 (Ar-C), 130.4 (Ar-C), 130.3 (Ar-C), 129.7 (Ar-C), 129.1 (Ar-C), 126.2 (Ar-C), 125.4 (Ar-C), 121.8 (Ar-C), 115.9 (C22), 115.7 (Ar-C), 80.1 (C2), 68.4 (C6), 64.4 (C13), 53.1 (C4), 31.9 (C20), 29.5 (C19), 28.4 (C1); HRMS (ESI-TOF) Calc'd for $C_{26}H_{30}N_2O_9Na$ $[M+Na]^+$ 537.1844, found 537.1839.

5.6.25 2-(((((*S*)-1-(*tert*-Butoxy)-1-oxopent-4-en-2-yl)carbamoyl)oxy)methyl)benzyl-(*S*)-2-((*tert*-butoxycarbonyl)amino)hex-5-enoate (65)

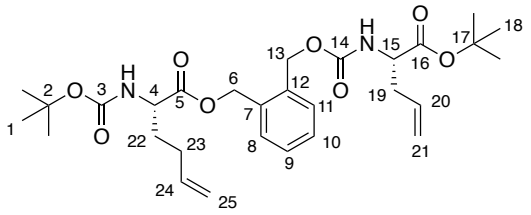

65

The following was adapted according to a literature procedure.[165] Compound **64** (0.502 g, 2.93 mmol) and amine **50** (0.972 g, 1.89 mmol) were dissolved in DMF (25 mL). DIPEA (0.823 mL, 4.59 mmol) was then added to the mixture and this was left to stir at room temperature overnight. The reaction was diluted with EtOAc (50 mL) and quenched with 10% aqueous citric acid (50 mL). The layers were then separated and the organic layer was washed with saturated aqueous Na_2CO_3 until the aqueous layer was no longer yellow. Organic layer was then washed with brine (2 × 50 mL), dried over Na_2SO_4, filtered and concentrated *in vacuo*. The crude material was purified via flash column chromatography (silica gel, 20% EtOAc in hexanes) to give **65** (0.858 g, 83%) as a colourless oil. (R_f = 0.44 on SiO_2, 30% EtOAc in hexanes). $[\alpha]_D^{26}$ +9.6 (*c* = 0.64, CH_2Cl_2); IR (CH_2Cl_2 cast) 3360, 3079, 2979, 2930, 1722, 1528, 1455, 1367, 1251, 1217, 1159, 1051 cm^{-1}; ^{1}H-NMR ($CDCl_3$, 500 MHz) δ 7.50 – 7.33 (4H, m, Ar-H), 5.80 – 5.65 (2H, m, H20, H24), 5.41 (1H, app s, H6), 5.32 (1H, app s, H6), 5.27 – 5.24 (1H, m, H13), 5.21 – 5.17 (1H, m, H13), 5.14 – 4.94 (5H, m, H21, H25, NH) 4.45 – 4.28 (2H, m, H4, H15), 2.60 – 2.48 (2H, m, H19), 2.15 – 2.04 (2H, m, H23), 2.00 – 1.90 (1H, m, H22), 1.79 – 1.69 (1H, m, H22), 1.48 (9H, s, H18), 1.45 (9H, s, H1); ^{13}C-NMR ($CDCl_3$, 125 MHz) δ 171.6 (C5), 156.2 (C16), 155.5 (C14), 155.4 (C3), 137.0 (C24), 132.7 (C24), 130.4 (Ar-C), 130.3 (Ar-C), 129.7 (Ar-C), 128.7 (Ar-C), 125.4 (Ar-C), 121.8 (Ar-C), 118.8 (C21), 115.7 (C25), 82.3 (C17), 82.0 (C2), 68.4 (C6), 64.5 (C13), 53.5 (C15), 52.9 (C4), 37.3 (C19), 31.9 (C23), 29.5 (C22) 28.3 (C1), 28.1 (C18); HRMS (ESI-TOF) Calc'd for $C_{29}H_{42}N_2O_8Na$ $[M+Na]^+$ 569.2833, found 569.2835.

5.6.26 9-Allyl-1-(*tert*-butyl)-(*2S, 8S*)-2-((((9*H*-fluoren-9-yl)methoxy)carbonyl)amino)-8-((*tert*-butoxycarbonyl)amino)nonanedioate (66)

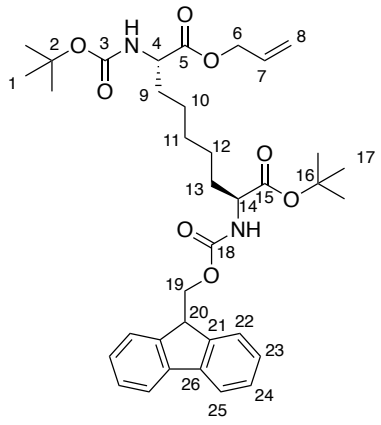

66

Compound **65** (0.263 g, 0.481 mmol) was dissolved in a large excess of degassed 1,2-dichloroethane (500 mL) and had Grubbs 2nd generation catalyst (0.0200 g, 0.0240 mmol) added to it. The reaction was heated at reflux for 72 h to afford the cross-metathesis intermediate. The reaction was concentrated down to a brown oil and passed through a silica plug (25% EtOAc in hexanes) to remove the catalyst. The macrocycle (0.187 g, 0.361 mmol) was dissolved in THF:MeOH (1:1 10 mL) and had Pd/C (10%) (20 mg) added to it. This was stirred at room temperature under 1 atm of H_2 for 8 h. The reaction mixture was then filtered through Celite® and concentrated *in vacuo* to produce a white solid. This was then redissolved in THF:H_2O (2.5:1, 10 mL), followed by the addition of $NaHCO_3$ (0.0760 g, 0.903 mmol) and Fmoc-Cl (0.0930 g, 0.361 mmol) and stirred overnight. Reaction mixture was quenched with 1 M aqueous HCl (10 mL) and the solution was extracted with EtOAc (3 × 10 mL). Combined organic extracts were then washed with brine (10 mL), dried over Na_2SO_4, filtered and concentrated down to a white solid. The intermediate was redissolved in DMF (10 mL) and then had $NaHCO_3$ (0.0760 g, 0.903 mmol) and allyl bromide (0.0780 mL, 0.903 mmol) added to it and stirred at room temperature overnight. The reaction was quenched with 1 M aqueous HCl (10 mL), and the aqueous layer was extracted with EtOAc (3 × 10 mL). Combined organic extracts were then washed with H_2O (10 mL), then brine (10 mL), dried over Na_2SO_4, filtered and concentrated *in vacuo*. The crude product was then purified via flash column

chromatography (silica gel, 15% EtOAc in hexanes) to give **66** (0.184 g, 60% over 4 steps) as a pale gum. (R_f = 0.40 on SiO_2, 30% EtOAc in hexanes). $[\alpha]_D^{26}$ +2.3 (*c* = 0.36, CH_2Cl_2); IR (CH_2Cl_2 cast) 3345, 3068, 2976, 2933, 1716, 1518, 1478, 1451, 1367, 1250, 1160, 1050 cm^{-1}; ^{1}H-NMR ($CDCl_3$, 500 MHz) δ 7.76 (2H, d, *J* = 7.5 Hz, Ar-H), 7.60 (2H, d, *J* = 7.5 Hz, Ar-H), 7.40 (2H, t, *J* = 7.5 Hz, Ar-H), 7.31 (2H, t, *J* = 7.5 Hz, Ar-H), 5.90 (1H, ddt, *J* = 16.5, 11.0, 6.0 Hz, H7), 5.34 – 5.23 (3H, m, H8, NH), 4.99 (1H, d, *J* = 7.5 Hz, NH), 4.62 (2H, app t, *J* = 6.0 Hz, H6), 4.38 (2H, d, *J* = 7.0 Hz, H19), 4.34 – 4.28 (1H, m, H4), 4.27 – 4.20 (2H, m, H14, H20), 1.85 – 1.76 (2H, m, H9, H13), 1.67 – 1.59 (2H, m, H9, H13), 1.47 (9H, s, H17), 1.44 (9H, s, H1), 1.40 – 1.28 (6H, m, H10, H11, H12); ^{13}C-NMR ($CDCl_3$, 125 MHz) δ 172.6 (C5), 171.7 (C15), 155.9 (C3), 155.4 (C18), 144.0 (Ar-C), 143.9 (Ar-C), 141.6 (Ar-C), 141.4 (Ar-C), 131.7 (C7), 127.7 (Ar-C) 127.6 (Ar-C), 127.1 (Ar-C), 127.1 (Ar-C), 125.2 (Ar-C), 124.7 (Ar-C), 120.1 (Ar-C), 120.0 (Ar-C), 118.8 (C8), 82.1 (C16), 79.9 (C2), 67.0 (C6), 65.8 (C19), 54.3 (C4), 53.5 (C14), 47.3 (C20), 32.8 (C9, C13), 28.9 (C11), 28.4 (C1), 28.1 (C17), 25.2 (C10), 24.9 (C12); HRMS (ESI-TOF) Calc'd for $C_{36}H_{48}N_2O_8Na$ $[M+Na]^+$ 659.3303, found 659.3302.

5.6.27 2-(((((*S*)-1-(*tert*-butoxy)-1-oxohex-5-en-2-yl)carbamoyl)oxy)methyl)benzyl-(*S*)-2-((*tert*-butoxycarbonyl)amino)hex-5-enoate (68)

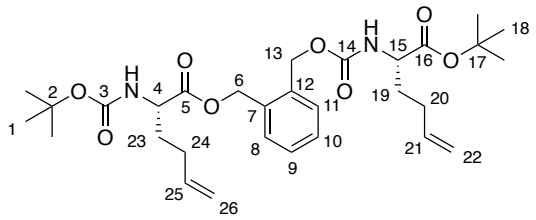

68

The following was adapted according to a literature procedure.[165] Olefin **61** (0.440 g, 1.14 mmol) was dissolved in TFA:CH_2Cl_2 (1:4, 15 mL) and stirred for 30 mins. Reaction was concentrated *in vacuo* and coevaporated with CH_2Cl_2. The oil was dissolved in saturated $NaHCO_3$ until pH was 9, and extracted with EtOAc (3 × 20 mL). Combined extracts were dried over Na_2SO_4, filtered and concentrated to a crude oil. The crude oil and **64** (0.392 g, 0.763 mmol) were dissolved in DMF (15 mL). DIPEA (0.439 mL, 2.52 mmol) was then added to the mixture and this was left to stir at room temperature overnight. The reaction

was diluted with EtOAc (50 mL) and quenched with 10% aqueous citric acid (50 mL). The layers were then separated and the organic layer was washed with saturated aqueous Na_2CO_3 until the aqueous layer was no longer yellow. The organic layer was then washed with brine (2 x 50 mL), dried over Na_2SO_4, filtered and concentrated *in vacuo*. The crude material was purified via flash column chromatography (silica gel, 0–2% acetone in CH_2Cl_2) to give **68** (0.763 g, 75%) as a colourless oil. (R_f = 0.76 on SiO_2, 5% acetone in CH_2Cl_2). $[\alpha]_D^{26}$ +0.17 (*c* = 1.16, CH_2Cl_2); IR (CH_2Cl_2 cast) 3340, 3076, 2978, 2932, 1719, 1522, 1453, 1367, 1250, 1222, 1159, 1050 $cm^{-1;}$ ^{1}H-NMR ($CDCl_3$, 500 MHz) δ 7.44 – 7.31 (4H, m, Ar-H), 5.84 – 5.71 (2H, m, H21, H25), 5.43 (1H, s, NH), 5.30 – 5.24 (2H, m, H6), 5.23 – 5.15 (2H, m, H13), 5.08 – 4.94 (5H, m, H22, H26, NH) 4.40 – 4.30 (1H, m, H4), 4.25 (1H, app q, *J* = 5.0 Hz, H15), 2.16 – 2.03 (3H, m, H20, H24), 1.96 – 1.84 (2H, m, H20, H23), 1.79 – 1.68 (2H, m, H19, H23), 1.64 – 1.56 (1H, m, H19), 1.46 (9H, s, H18), 1.42 (9H, s, H1); ^{13}C-NMR ($CDCl_3$, 125 MHz) δ 172.5 (C5, C16), 155.8 (C3), 155.4 (C14), 137.2 (C25), 137.0 (C21), 135.1 (Ar-C), 134.1 (Ar-C), 130.0 (Ar-C), 129.9 (Ar-C), 128.9 (Ar-C), 128.7 (Ar-C), 115.7 (C26), 115.6 (C22), 82.1 (C17), 79.9 (C2), 64.5 (C6), 64.3 (C13), 54.0 (C4), 53.2 (C15), 32.1 (C24), 31.9 (C20), 29.5 (C23), 29.4 (C19), 28.3 (C18), 28.0 (C1); HRMS (ESI-TOF) Calc'd for $C_{30}H_{44}N_2O_8Na$ $[M+Na]^+$ 583.2990, found 583.2990.

5.6.28 10-Allyl-1-(*tert*-butyl)-(*2S, 9S*)-2-((((9*H*-fluoren-9-yl)methoxy)carbonyl)amino)-9-((*tert*-butoxycarbonyl)amino)decanedioate (69)

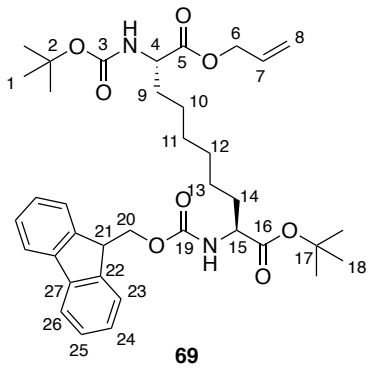

69

Compound **68** (0.310 g, 0.554 mmol) was dissolved in a large excess of degassed 1,2-dichloroethane (500 mL) and had Grubbs 2nd generation catalyst (0.0560 g, 0.0660 mmol) added to it. The reaction was heated at reflux for 72 h to afford the cross-metathesis intermediate. The reaction was concentrated down to a brown oil and passed through a silica plug (25% EtOAc in hexanes) to remove the catalyst. The macrocycle (0.251 g, 0.471 mmol) was dissolved in THF:MeOH (1:1 15 mL) and had Pd/C (10%) (30 mg) added to it. This was stirred at room temperature under 1 atm of H_2 for 8 h. The reaction mixture was then filtered through Celite® and concentrated *in vacuo* to produce a white solid. This was then redissolved in THF:H_2O (2.5:1, 15 mL), followed by the addition of $NaHCO_3$ (0.087 g, 1.04 mmol) and Fmoc-Cl (0.134 g, 0.518 mmol) and stirred overnight. Reaction mixture was quenched with 1 M aqueous HCl (15 mL) and the solution was extracted with EtOAc (3 × 15 mL). Combined organic extracts were then washed with brine (15 mL), dried over Na_2SO_4, filtered and concentrated down to a white solid. The intermediate was redissolved in DMF (15 mL) and then had $NaHCO_3$ (0.087 g, 1.04 mmol) and allyl bromide (0.090 mL, 1.04 mmol) added to it and stirred at room temperature overnight. The reaction was quenched with 1 M aqueous HCl (15 mL), and the aqueous layer was extracted with EtOAc (3 × 15 mL). Combined organic extracts were then washed with H_2O (15 mL), then brine (15 mL), dried over Na_2SO_4, filtered and concentrated *in vacuo*. The crude product was then purified via flash column chromatography (silica gel, 15% EtOAc in hexanes) to give **69** (0.297 g, 83% over 4 steps) as a white solid. (R_f = 0.37 on SiO_2, 30% EtOAc in hexanes). $[\alpha]_D^{26}$ -0.43 (*c* = 1.06, CH_2Cl_2); IR (CH_2Cl_2 cast) 3345, 3067, 2976, 2930, 1716, 1517, 1478, 1451, 1391, 1249, 1160, 1049 cm^{-1}; ^{1}H-NMR ($CDCl_3$, 500 MHz) δ 7.79 (2H, d, *J* = 7.5 Hz, Ar-H), 7.63 (2H, d, *J* = 7.5 Hz, Ar-H), 7.43 (2H, t, *J* = 7.5 Hz, Ar-H), 7.34 (2H, t, *J* = 7.5 Hz, Ar-H), 5.93 (1H, ddt, *J* = 17.0, 11.0, 5.5 Hz, H7), 5.35 (1H, d, *J* = 17.0 Hz, H8), 5.32 (1H, s, NH), 5.27 (1H, d, *J* = 11 Hz), 5.01 (1H, d, *J* = 7.5 Hz, NH), 4.65 (2H, app t, *J* = 6.0 Hz, H6), 4.38 (2H, d, *J* = 6.5 Hz, H20), 4.33 (1H, app q, *J* = 4.5 Hz, H4), 4.29 – 4.20 (2H, m, H15, H21), 1.88 – 1.78 (2H, m, H9, H14), 1.70 – 1.60 (2H, m, H9, H14), 1.50 (9H, s, H18), 1.47 (9H, s, H1), 1.43 – 1.30 (8H, m, H10, H11, H12, H13); ^{13}C-NMR ($CDCl_3$, 125 MHz) δ 172.7 (C5), 171.8 (C16), 155.9 (C3), 155.4 (C19), 144.0 (Ar-C), 143.9 (Ar-C), 141.4 (Ar-C), 131.7 (C7), 127.7 (Ar-C), 127.1 (Ar-C), 125.2 (Ar-C), 120.0 (Ar-C), 118.8

(C8), 82.1 (C17), 79.9 (C2), 67.0 (C6), 65.8 (C20), 54.3 (C4), 53.5 (C15), 47.3 (C21), 32.9 (C9), 32.8 (C13), 29.8 (C11), 29.1 (C12), 28.4 (C1), 28.1 (C17), 25.3 (C10), 25.0 (C13); HRMS (ESI-TOF) Calcd for $C_{37}H_{50}N_2O_8Na$ $[M+Na]^+$ 673.3000, found 673.3000.

5.6.29 5-Allyl 1-(2-(hydroxymethyl)benzyl) (*tert*-butoxycarbonyl)-*L*-glutamate (71)

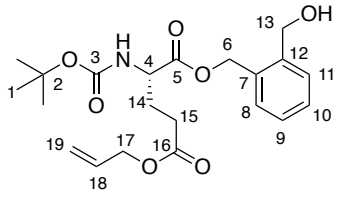

71

The following was adapted from a literature procedure.[165] (S)-5-(Allyloxy)-4-(tert-butoxycarbonylamino)-5-oxopentanoic acid (1.06 g, 3.69 mmol), DMAP (0.0451 g, 0.369 mmol) and 1,2-benzenedimethanol (2.33 g, 16.8 mmol) were dissolved in CH_2Cl_2 (100 mL) and cooled down to 0 °C. Once cooled, EDCI (0.778 g, 4.06 mmol) was added and the reaction mixture was allowed to warm up to room temperature over 3 h and stirred overnight at room temperature. The reaction mixture was then concentrated *in vacuo* and purified via flash column chromatography (silica gel, 30% EtOAc in hexanes) to yield the product **71** (0.813 g, 54%) as a cream oil. (R_f = 0.42 on SiO_2, 1:1 hexanes:EtOAc). $[\alpha]_D^{26}$ +0.53 (*c* = 0.87, CH_2Cl_2); IR (CH_2Cl_2 cast) 3370, 3070, 2978, 2933, 1737, 1717, 1649, 1517, 1445, 1367, 1253, 1167, 1052, 1027 cm^{-1}; ^{1}H-NMR ($CDCl_3$, 400 MHz) δ 7.45 – 7.29 (4H, m, Ar-H), 5.89 (1H, ddt, *J* = 17.2, 10.4, 5.6 Hz, H18), 5.30 (1H, dq, *J* = 17.2, 1.6 Hz, H19), 5.30 (3H, s, H6), 5.23 (1H, dq, *J* = 10.4, 1.6 Hz, H19), 5.11 (1H, d, *J* = 5.2, NH), 4.78 (1H, app d, *J* = 12.8 Hz, H13), 4.74 (1H, app d, *J* = 12.8 Hz, H13), 4.56 (2H, dt, *J* = 5.6, 1.6 Hz, H17), 4.34 (1H, app q, *J* = 5.2 Hz, H4), 2.48 – 2.31 (2H, m, H15), 2.27 (1H, br s, OH), 2.22 – 2.14 (1H, m, H14), 2.03 – 1.09 (1H, m, H14), 1.41 (9H, s, H1); ^{13}C-NMR ($CDCl_3$, 100 MHz) δ 172.1 (C5), 171.9 (C16), 155.2 (C3), 137.8 (Ar-C), 133.2 (Ar-C), 132.0 (C18), 130.1 (Ar-C), 129.2 (Ar-C), 129.0 (Ar-C), 128.1 (Ar-C), 118.5 (C19), 80.2 (C2), 65.4 (C17), 65.1 (C6), 62.9 (C13), 53.3 (C4), 30.1 (C15), 28.3 (C1), 27.4 (C14); HRMS (ESI-TOF) Calc'd for $C_{21}H_{29}NO_7Na$ $[M+Na]^+$ 430.1826, found 430.1828.

5.6.30 5-Allyl 1-(2-((((4-nitrophenoxy)carbonyl)oxy)methyl)benzyl) (*tert*-butoxycarbonyl)-*L*-glutamate (72)

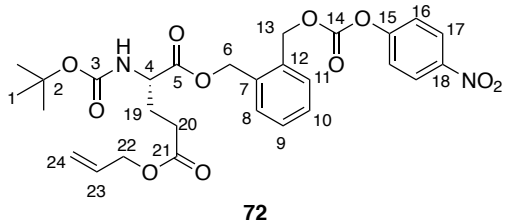

72

The following was adapted from a literature procedure.[165] Compound **71** (0.693 g, 1.72 mmol) was dissolved in dry CH_2Cl_2 (20 mL) and had bis(4-nitrophenyl)carbonate (0.965 g, 3.17 mmol)added to it, followed by DIPEA (0.448 mL, 2.57 mmol). The resulting reaction mixture was stirred overnight. It was then diluted with EtOAc (50 mL), quenched with 10% aqueous citric acid (50 mL) and the layers were separated. The organic layer was then washed with saturated aqueous Na_2CO_3 until the aqueous layer was no longer yellow and then washed with brine (2 × 50 mL), dried over Na_2SO_4, filtered and concentrated *in vacuo*. The crude product was then purified via flash column chromatography (silica gel, 0–2% acetone in CH_2Cl_2) to give **72** (0.982 g, quant.) as a yellow oil. (R_f = 0.33 on SiO_2, 30% EtOAc in hexanes). $[\alpha]_D^{26}$ -3.57 (*c* = 1.13, CH_2Cl_2); IR (CH_2Cl_2 cast) 3385, 3085, 2978, 2934, 1767, 1738, 1714, 1650, 1616, 1594, 1526, 1494, 1348, 1215, 1165 cm^{-1}; ^{1}H-NMR ($CDCl_3$, 600 MHz) δ 8.27 (2H, app d, *J* = 9.6 Hz, H17), 7.51 – 7.40 (4H, m, Ar-H), 7.39 (2H, app d, *J* = 9.6 Hz, H16), 5.88 (1H, ddt, *J* = 16.8, 10.8, 6.0 Hz, H23), 5.41 (2H, s, H6), 5.34 (1H, d, *J* = 13.2 Hz, H13), 5.31 (1H, d, *J* = 13.2 Hz, H13), 5.29 (1H, dq, *J* = 16.8, 1.2 Hz, H24), 5.21 (1H, dq, *J* = 10.8, 1.2 Hz, H24), 5.09 (1H, d, *J* = 7.2 Hz, NH), 4.55 (2H, app dt, *J* = 6.0, 1.2 Hz, H22), 4.39 (1H, app q, *J* = 7.2 Hz, H4), 2.26 – 2.34 (2H, m, H20), 2.25 – 2.17 (1H, m, H19), 2.01 – 1.93 (1H, m, H19), 1.41 (9H, s, H1); ^{13}C-NMR ($CDCl_3$, 125 MHz) δ 172.0 (C21), 171.6 (C5), 155.4 (C3), 152.1 (C14), 145.7 (C18), 133.9 (Ar-C), 132.5 (Ar-C), 132.3 (C23), 131.6 (Ar-C), 130.0 (Ar-C), 129.9 (Ar-C), 129.2 (Ar-C), 128.8 (C15), 124.9 (C17), 121.4 (C16) 118.0 (C24), 80.5 (C2), 67.9 (C6), 65.0 (C22), 64.2 (C13), 52.5 (C4), 29.8 (C20), 28.9 (C1), 27.2 (C19); HRMS (ESI-TOF) Calc'd for $C_{28}H_{32}N_2O_9Na$ $[M+Na]^+$ 595.1898, found 595.1091.

5.6.31 (*S*)-4-((((2-((((*S*)-5-(Allyloxy)-2-((*tert*-butoxycarbonyl)amino)-5-oxopentanoyl)oxy)methyl)benzyl)oxy)carbonyl)amino)-5-(*tert*-butoxy)-5-oxopentanoic acid (73)

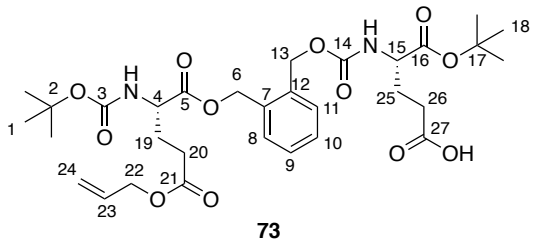

73

The following was adapted from a literature procedure.[165] Compound **72** (0.889 g, 1.55 mmol) was dissolved in 25 mL of dry DMF and then had H-L-Glu-O*t*Bu (0.472 g, 2.32 mmol) and DIPEA (0.674 mL, 3.87 mmol) added to it. This reaction was left to stir at room temperature overnight. Reaction was diluted with EtOAc (100 mL) and quenched with 10% aqueous citric acid (200 mL). The aqueous layer was then extracted with EtOAc (3 × 100 mL) and the combined organic layers were then washed with H_2O (200 mL), then brine (200 mL), dried over Na_2SO_4, filtered and concentrated *in vacuo*. The crude product was then purified via flash column chromatography (silica gel, 40% EtOAc in hexanes w/ 0.1% AcOH) to give **73** (0.551 g, 56%) as a clear oil. (R_f = 0.20 on SiO_2, 1:1 Hex:EtOAc w/ 0.1% AcOH). $[\alpha]_D^{26}$ -3.6 (*c* = 0.69, CH_2Cl_2); IR (CH_2Cl_2 cast) 3346, 2979, 2936, 1718, 1522, 1454, 1393, 1368, 1252, 1228, 1160, 1055 cm^{-1}; ^{1}H-NMR ($CDCl_3$, 600 MHz) δ 7.44 – 7.33 (4H, m, Ar-H), 5.94 – 5.85 (1H, m, H23), 5.78 (1H, d, *J* = 6.6 Hz, NH), 5.33 – 5.11 (6H, m, H6, H13, H24), 4.60 – 4.55 (2H, m, H22), 4.47 (1H, app q, *J* = 6.6 Hz, H4), 4.29 – 4.23 (1H, m, H15), 2.51 – 2.35 (4H, m, H20, H26), 2.25 – 2.16 (2H, m, H19, H25), 2.03 – 1.95 (2H, m, H19, H25), 1.45 (9H, s, H18), 1.42 (9H, s, H1); ^{13}C-NMR ($CDCl_3$, 125 MHz) δ 175.2 (C27), 172.9 (C21), 170.9 (C5), 169.8 (C16), 156.0 (C3), 154.6 (C14), 134.9 (Ar-C), 134.2 (Ar-C), 132.0 (C23), 130.7 (Ar-C), 130.3 (Ar-C), 129.0 (Ar-C), 128.9 (Ar-C), 118.4 (C24), 82.3 (C17), 80.5 (C2), 65.4 (C22), 64.9 (C6), 64.8 (C13), 54.4 (C4), 53.0 (C15), 30.1 (C20), 29.7 (C26), 28.3 (C18), 28.0 (C1), 27.5 (C19), 27.0 (C25); HRMS (ESI-TOF) Calc'd for $C_{31}H_{43}N_2O_{12}Na$ $[M-H]^-$ 635.2821, found 635.2816.

5.6.32 (*S*)-4-((((2-((((*S*)-5-(allyloxy)-2-((*tert*-butoxycarbonyl)amino)-5-oxopentanoyl)oxy)methyl)benzyl)oxy)carbonyl)amino)-5-(*tert*-butoxy)-5-oxopentanoic acid (74)

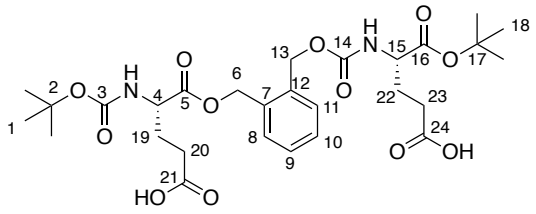

74

Compound **73** (0.471 g, 0.740 mmol) was dissolved in CH_2Cl_2 (10 mL) and had $Pd(PPh_3)_4$ (0.089 g, 0.077 mmol) and morpholine (0.647 mL, 7.40 mmol) added to it, wrapped in foil and stirred for 2 h at room temperature. Reaction was diluted with EtOAc (50 mL) and then had 1 M aqueous HCl (50 mL) added. The aqueous layer was then extracted with EtOAc (3 × 50 mL) and the combined organic layers were washed with brine (50 mL), dried over Na_2SO_4, filtered and concentrated *in vacuo*. The crude product was purified via flash column chromatography (silica gel, 1:1 Hex:EtOAc, w/ 0.1% AcOH) to give **74** (0.265 g, 60%) as a yellow oil. (R_f = 0.11 on SiO_2, 1:1 Hex:EtOAc w/ 0.1% AcOH). $[\alpha]_D^{26}$ +3.6 (*c* = 0.94, CH_2Cl_2); IR (CH_2Cl_2 cast) 3333, 2980, 2938, 1715, 1523, 1454, 1394, 1369, 1252, 1228, 1159, 1057 cm^{-1}; ^{1}H-NMR ($CDCl_3$, 600 MHz) δ 7.42 – 7.30 (4H, m, Ar-H), 5.76 (1H, d, *J* = 6.6 Hz, NH), 5.37 – 5.11 (5H, m, H6, H13, NH), 4.48 (1H, app q, *J* = 6.6 Hz, H4), 4.35 – 4.28 (1H, m, H15), 2.50 – 2.38 (4H, m, H20, H26), 2.26 – 2.13 (2H, m, H19, H25), 2.08 – 1.98 (2H, m, H19, H25), 1.46 (9H, s, H18), 1.43 (9H, s, H1); ^{13}C-NMR ($CDCl_3$, 125 MHz) δ 178.2 (C21), 177.8 (C21), 172.1 (C5), 171.2 (C16), 155.9 (C3), 155.4 (C14), 134.3 (Ar-C), 134.2 (Ar-C), 130.4 (Ar-C), 129.4 (Ar-C), 128.9 (Ar-C), 128.8 (Ar-C), 82.7 (C17), 80.4 (C2), 65.1 (C6), 64.6 (C13), 54.4 (C4), 52.7 (C15), 30.4 (C20), 29.7 (C23), 28.3 (C18), 28.0 (C1), 27.4 (C19), 27.0 (C22); HRMS (ESI-TOF) Calc'd for $C_{28}H_{39}N_2O_{12}$ $[M-H]^-$ 595.2508, found 595.2607.

5.6.33 2-(((((*S*)-1-(*tert*-Butoxy)-1-oxobut-3-en-2-yl)carbamoyl)oxy)methyl)benzyl (*S*)-2-((*tert*-butoxycarbonyl)amino)but-3-enoate (75)

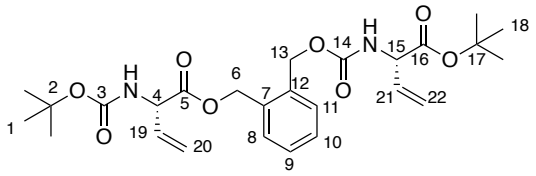

75

To a flame dried flask under an argon atmosphere was added cupric acetate monohydrate (0.0450 g, 0.224 mmol). A solution of **74** (0.265 g, 0.444 mmol) in dry benzene (20 mL) was cannulated into the flask and stirred at room temperature for 1 h. Lead tetraacetate (0.523 g, 1.18 mmol) was then added and the mixture was heated to reflux and stirred overnight. Reaction was then filtered though a pad of Celite® and diluted with EtOAc (200 mL). The organic layer was then washed with H_2O (3 × 200 mL), then brine (200 mL), dried over $MgSO_4$, filtered and concentrated *in vacuo*. The product was purified by flash column chromatography (silica gel, 20% EtOAc in hexanes) to yield **75** (0.0358, g 16%) as a white solid. (R_f = 0.42 on SiO_2, 30% EtOAc in hexanes). $[\alpha]_D^{26}$ -3.2 (*c* = 0.71, CH_2Cl_2); IR (CH_2Cl_2) 3350, 3033, 2980, 2938, 1719, 1631, 1520, 1452, 1390, 1369, 1251, 1226, 1159, 1055 cm^{-1}; ^{1}H-NMR ($CDCl_3$, 500 MHz) δ 7.44 – 7.31 (4H, m, Ar-H), 5.95 – 5.84 (2H, m, H19, H21), 5.57 (1H, br s, NH), 5.38 – 5.14 (9H, m, H6, H13, H20, H22, NH), 4.95 – 4.87 (1H, m, H4), 4.80 – 4.75 (1H, m, H15), 1.45 (9H, s, H18), 1.43 (9H, s, H1); ^{13}C-NMR ($CDCl_3$, 125 MHz) δ 170.5 (C5), 169.4 (C16), 155.4 (C3), 155.0 (C14), 135.0 (Ar-C), 133.9 (Ar-C), 133.0 (Ar-C), 132.6 (C19), 132.5 (C21), 129.9 (Ar-C), 128.9 (Ar-C), 128.7 (Ar-C), 117.7 (C20), 117.1 (C22), 82.6 (C17), 80.1 (C2), 64.9 (C6), 64.4 (C13), 56.7 (C4), 55.9 (C15), 28.3 (C18), 27.9 (C1); HRMS (ESI-TOF) Calc'd for $C_{26}H_{36}N_2O_8Na$ $[M+Na]^+$ 527.2364, found 527.2361.

5.6.34 Neopetrosiamide Analogue A1 (87)

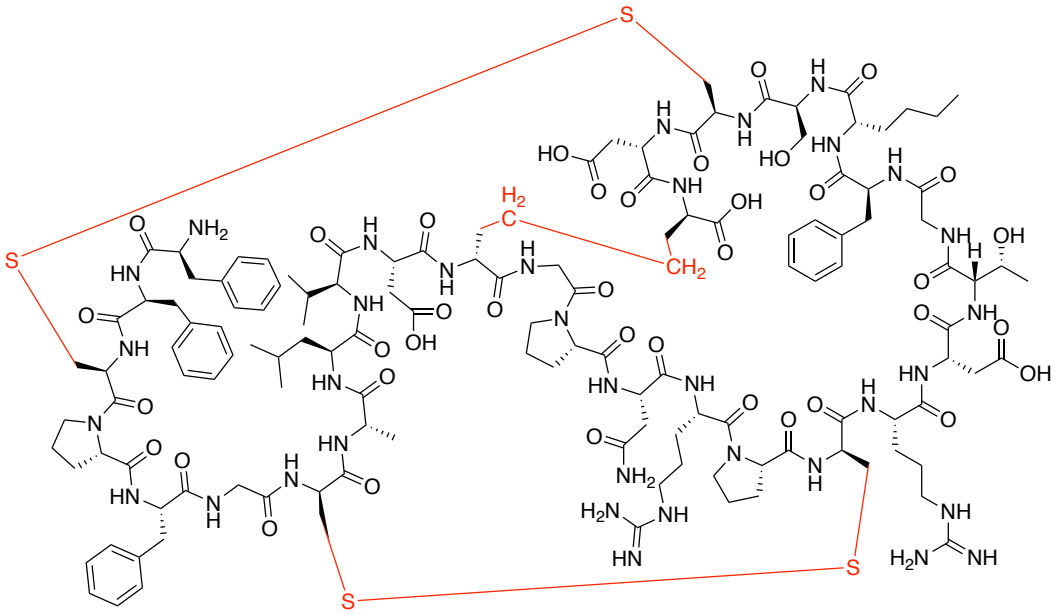

87

Neopetrosiamide analogue **87** was synthesized according to the general SPPS protocol, incorporating orthogonally protected diamino diacid **44** into position 28, followed by cyclizing onto position 12 using the allyl/alloc deprotection protocol and the cyclization protocol. Oxidation of cysteines was done using the bis-disulfide formation (2-step method) and purified by semi-preparative RP-HPLC following the general protocol (t_R = 27.1 min) to give peptide **87** (1.8 mg, 3% yield, relative to 60 mg of crude peptide, over 60 steps) as a fluffy white solid. LCMS (ESI-TOF) Calc'd for $C_{132}H_{191}N_{35}O_{38}S_4$ $[M+2H]^{2+}$ 3002.2811, found 3002.2816.

5.6.35 Neopetrosiamide Analogue A2 (88)

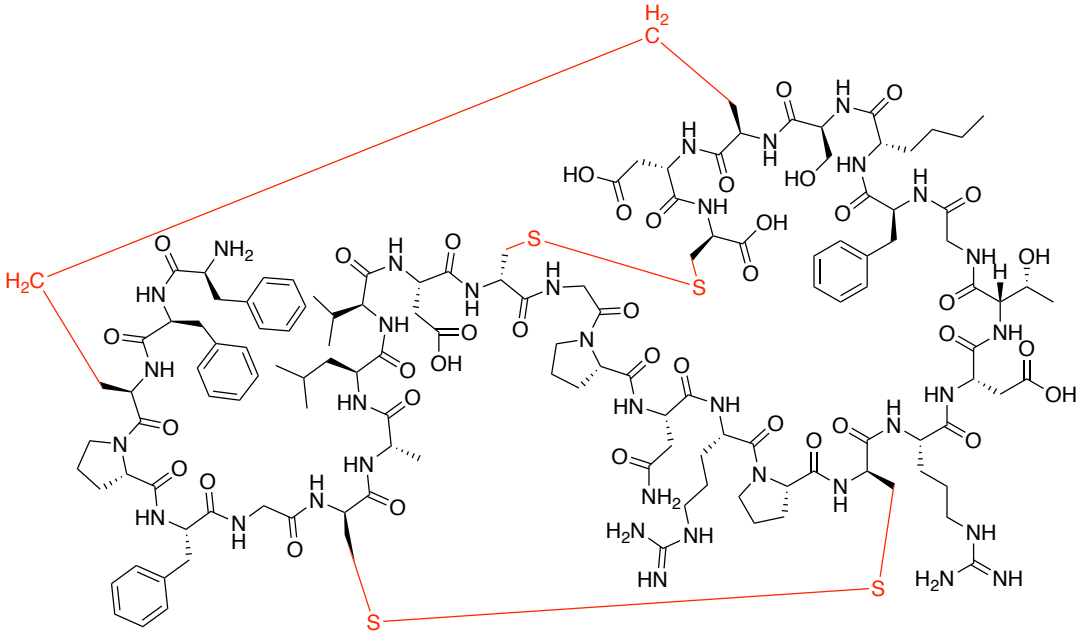

88

Neopetrosiamide analogue **88** was synthesized according to the general SPPS protocol, incorporating orthogonally protected diamino diacid **44** into position 26, followed by cyclizing onto position 3 using the allyl/alloc deprotection protocol and the cyclization protocol. Oxidation of cysteines was done using the bis-disulfide formation (2-step method) and purified by semi-preparative RP-HPLC following the general protocol (t_R = 31.8 min) to give peptide **88** (1.2 mg, 2% yield, relative to 60 mg of crude, over 60 steps) as a fluffy white solid. LCMS (ESI-TOF) Calc'd for $C_{132}H_{191}N_{35}O_{38}S_4$ $[M+2H]^{2+}$ 3002.2812, found 3002.2816.

Signal (ppm) / Residue	NH	Hα	Hβ	Hδ	Hγ	Others
Phe[1]	–	–	–	–	–	–
Phe[2]	–	–	–	–	–	–
Das[3]	7.88	4.69	3.35, 3.12	2.87	1.75, 1.58	
Pro[4]	N/A	–	–	–	–	–
Phe[5]	–	–	–	–	–	
Gly[6]	7.21	4.09, 3.88				

Cys[7]	8.34	4.43	2.90, 2.70			
Ala[8]	8.11	4.05	1.45			
Leu[9]	7.34	3.96	1.93	1.69	1.19	
Val[10]	7.27	4.01	2.19	1.01, 0.92		
Asp[11]	7.96	4.97	3.02, 2.58			
Cys[12]	8.62	4.82	2.59			
Gly[13]	8.23	4.34, 3.40				
Pro[14]	N/A	4.01	1.01	2.23	3.73	
Asn[15]	8.43	4.33	2.90			
Arg[16]	8.01	4.69	1.39	1.80	3.37, 2.59	
Pro[17]	N/A	4.34	2.15	1.90	3.38, 3.28	
Cys[18]	8.51	4.93	2.99, 2.78			
Arg[19]	9.06	4.12	1.95, 1.81	1.35, 1.21	3.10	
Asp[20]	8.75	4.95	3.23, 3.01			
Thr[21]	8.47	4.32	4.20	1.01		
Gly[22]	7.53	4.08, 3.81				
Phe[23]	8.13	4.58	2.96, 2.69			7.90
Nle[24]	8.28	3.58	1.51	1.09	0.69	
Ser[25]	7.23	5.15	3.31, 3.25			
Das[26]	7.95	4.21	3.48	1.90, 1.81	2.69	
Asp[27]	8.96	4.62	1.62, 1.52			
Cys[28]	8.03	4.85	2.91, 2.58			

*Table 5-1: Amino acid residue assignments based on TOCSY for neopetrosiamide analogue A2 (**88**)*

5.6.36 Neopetrosiamide Analogue A3 (89)

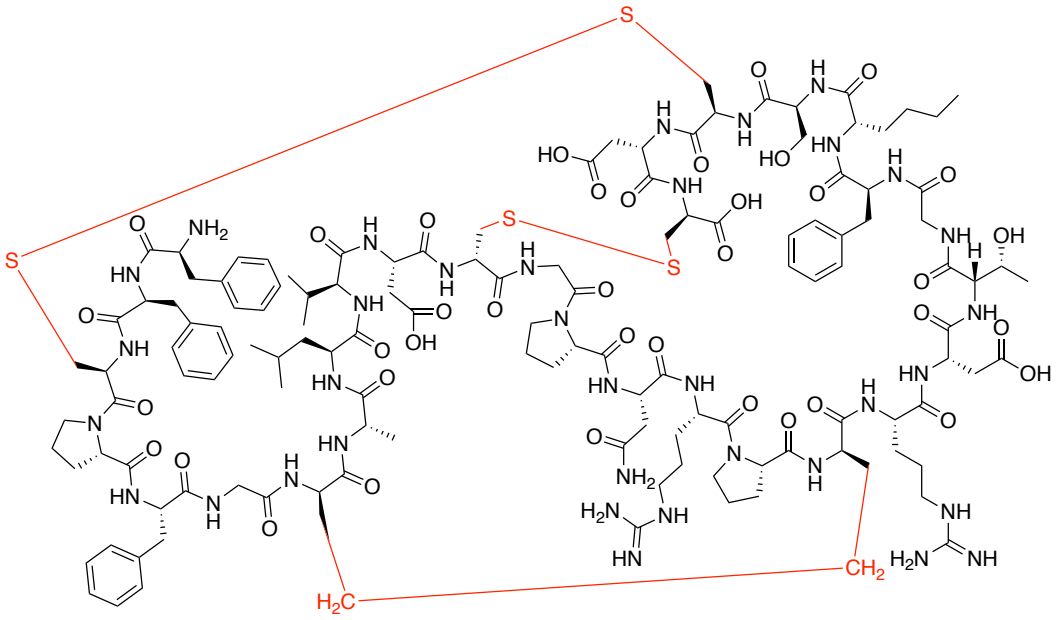

89

Neopetrosiamide analogue **89** was synthesized according to the general SPPS protocol, incorporating orthogonally protected diamino diacid **44** into position 18, followed by cyclizing onto position 7 using the allyl/alloc deprotection protocol and the cyclization protocol. Oxidation of cysteines was done using the bis-disulfide formation (2-step method) and purified by semi-preparative RP-HPLC following the general protocol (t_R = 33.1 min) to give peptide **89** (1.8 mg, 6% yield, relative to 30 mg of crude, over 60 steps) as a fluffy white solid. LCMS (ESI-TOF) Calc'd for $C_{132}H_{191}N_{35}O_{38}S_4$ $[M+2H]^{2+}$ 3002.2809, found 3002.2816.

Signal (ppm) / Residue	NH	Hα	Hβ	Hδ	Hγ	Others
Phe[1]	–	–	–	–	–	–
Phe[2]	–	–	–	–	–	–
Cys[3]	8.16	4.97	2.93, 2.63			
Pro[4]	N/A	–	–	–	–	–
Phe[5]	7.98	4.76	3.41, 2.66			7.51
Gly[6]	–	–	–	–	–	–
Das[7]	8.05	4.58	1.79, 1.61	1.31	1.52	

Ala[8]	7.70	4.31	1.4			
Leu[9]	6.89	4.74	2.34	1.76, 1.52	1.22	
Val[10]	7.25	3.89	2.15	0.89		
Asp[11]	8.28	5.04	2.84, 2.34			
Cys[12]	–	–	–	–	–	–
Gly[13]	7.76	4.34, 3.80				
Pro[14]	N/A	4.20	1.71, 1.60	2.16, 1.92	3.57, 3.41	
Asn[15]	8.25	4.55	2.87, 2.72			
Arg[16]	7.05	4.76	1.54, 1.41	1.82	3.17	7.27
Pro[17]	N/A	4.38	2.76	1.32, 1.25	3.46	
Das[18]	8.07	4.01	1.82	1.49	1.31	
Arg[19]	8.70	4.53	1.55, 1.47	1.35	3.10	
Asp[20]	8.82	4.93	3.21, 3.06			
Thr[21]	8.36	4.33	4.23	0.93		
Gly[22]	7.61	4.13, 3.71				
Phe[23]	8.47	4.60	3.26, 2.94			7.30
Nle[24]	8.29	3.53	1.61, 1.52	1.13	0.72	0.51
Ser[25]	7.29	5.06	3.32			
Cys[26]	8.38	5.49	2.44, 1.87			
Asp[27]	8.67	4.77	2.69, 2.62			
Cys[28]	8.10	4.94	3.26, 2.93			

*Table 5-2: Amino acid residue assignments based on TOCSY for neopetrosiamide analogue 3 (**89**)*

5.6.37 Apelin Analogue NMeArg14-NMe17A2 (109)

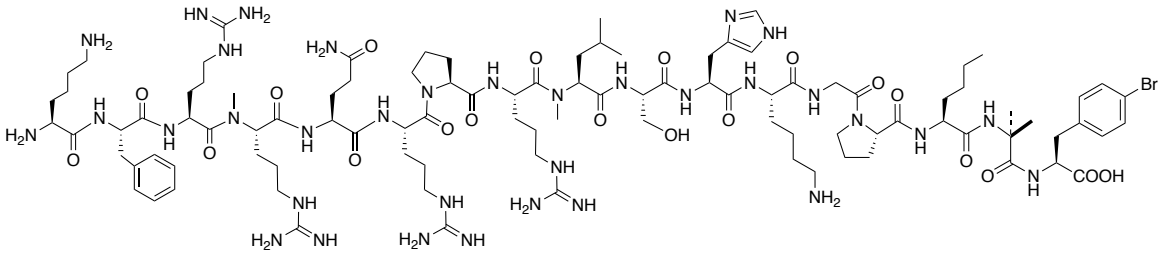

109

Fmoc-Phe(4-Br)-OH was loaded onto 2-chlorotrityl chloride resin using the general resin loading procedure at 1.5 mmol/g loading scale. Resin bound Fmoc-Phe(4-Br)-OH was then subject to manual SPPS (general method), introducing L-amino acids in the following order: Fmoc-Aib-OH, Fmoc-Nle-OH, Fmoc-Pro-OH, Fmoc-Gly-OH, Fmoc-Lys(Boc)-OH, Fmoc-His(Trt)-OH, and Fmoc-Ser(O^{t}Bu)-OH, with end-capping after each step. The NMeLeu subunit was added as a Fmoc-Arg(Boc)-NMeLeu-OH dipeptide (**117**) The dipeptide was coupled according to the general method, but allowed to couple for an extended time of 4 h, followed by end-capping. The manual SPPS was then continued with the L-amino acids in the following order: Fmoc-Pro-OH, Fmoc-Arg(Pmc)-OH, Fmoc-Gln(Trt)-OH with end-capping after each step. The NMeArg amino acid was added as Fmoc-NMeArg(Mtr) OH, following the general method, but for an extended time of 4 h, followed by end-capping. The next amino acid Fmoc-Arg(Pmc)-OH was coupled using the general method, but allowed to couple for an extended time of 4 h. Fmoc-Arg(Pmc)-OH was then coupled again before Fmoc deprotection, using half the equivalents used in the general method and allowed to couple for another 4 h, followed by end-capping. The final two amino acids Fmoc-Phe-OH, and Fmoc-Lys(Boc)-OH were coupled according to the general method, then end-capped and *N*-terminally deprotected. The peptide was then cleaved from resin and purified using the HPLC general method and a Phenomenex Luna C_{18} RP-HPLC column (100 Å, 5µm, 250 mm × 10.00 mm). The desired peptide was isolated as a white solid after lyophilization (0.075 mmol, 12 mg, 8%). LCMS (ESI-TOF) Calc'd for $C_{98}H_{162}BrN_{34}O_{20}$ $[M+H]^+$ 2214.1825, found 2214.1810.

5.6.38 Apelin Analogue αMeArg14-NMe17A2 (110)

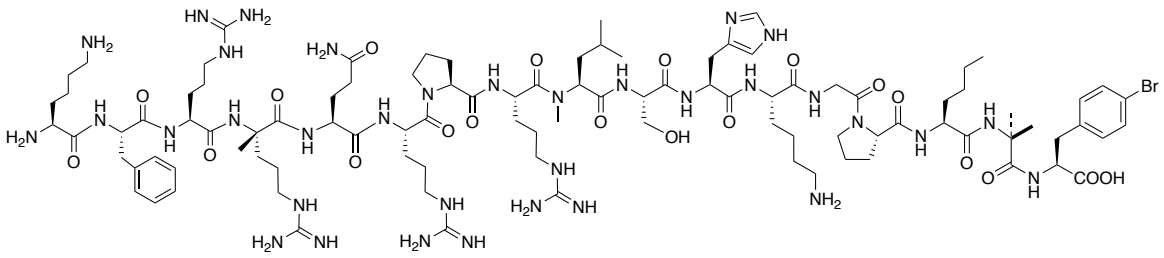

110

Fmoc-Phe(4-Br)-OH was loaded onto 2-chlorotrityl chloride resin using the general resin loading procedure at 0.8 mmol/g loading scale. Resin bound Fmoc-Phe(4-Br)-OH was then subject to manual SPPS (general method), introducing L-amino acids in the following order: Fmoc-Aib-OH, Fmoc-Nle-OH, Fmoc-Pro-OH, Fmoc-Gly-OH, Fmoc-Lys(Boc)-OH, Fmoc-His(Trt)-OH, and Fmoc-Ser(O′Bu)-OH, with end-capping after each step. The NMeLeu subunit was added as a Fmoc-Arg(Boc)-NMeLeu-OH dipeptide (**117**) The dipeptide was coupled according to the general method, but allowed to couple for an extended time of 4 h, followed by end-capping. The manual SPPS was then continued with the L-amino acids in the following order: Fmoc-Pro-OH, Fmoc-Arg(Pmc)-OH, Fmoc-Gln(Trt)-OH with end-capping after each step. The αMeArg subunit was added as Fmoc-αMeArg(Boc)-OH (**130**). The αMeArg was coupled following the general method, but for an extended time of 4 h, followed by end-capping. The final three amino acids Fmoc-Arg(Pmc)-OH, Fmoc-Phe-OH, and Fmoc-Lys(Boc)-OH were coupled according to the general method, then end-capped and *N*-terminally deprotected. The peptide was then cleaved from resin and purified using the HPLC general method and a Phenomenex Luna C_{18} RP-HPLC column (100 Å, 5μm, 250 mm × 10.00 mm). The desired peptide was isolated as a white solid after lyophilization (0.075 mmol, 10 mg, 6%). LCMS (ESI-TOF) Calc'd for $C_{98}H_{121}BrN_{34}O_{20}$ $[M+H]^+$ 2214.1833, found 2214.1810.

5.6.39 Benzyl *N*-((*S*)-2-((((9*H*-fluoren-9-yl)methoxy)carbonyl)amino)-5-((*tert*-butoxycarbonyl)amino)pentanoyl)-*N*-methyl-*L*-leucinate (114)

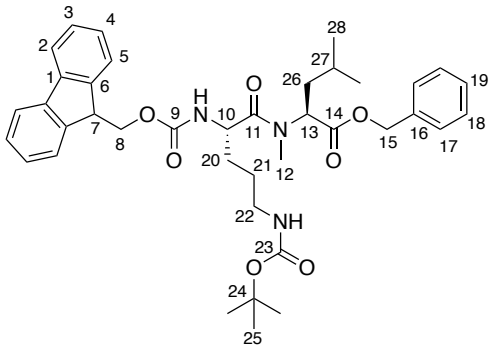

114

Fmoc-L-Orn(Boc)-OH **112** (3.64 g, 8.00 mmol), PyBOP (4.16 g, 8.00 mmol), HATU (1.08 g, 8.00 mmol) and DIPEA (3.80 mL, 21.8 mmol) were dissolved in 30 mL dry DMF and stirred for 10 mins. A solution of NMe-Leu-OBn *p*-toluenesulfonate salt **113** (2.96 g, 7.26 mmol) and DIPEA (1.30 mL, 7.46 mmol) in 30 mL of dry CH_2Cl_2 were added to the reaction and stirred at room temperature overnight. The reaction was washed 10% aqueous $NaHCO_3$ (30 mL), then 10% aqueous citric acid (30 mL) and then brine (30 mL). The organic layer was then dried with Na_2SO_4, filtered and concentrated *in vacuo*. The product was purified via flash column chromatography (silica gel, 25% EtOAc in hexanes) to give **114** (3.51 g, 72%) as a white solid. (R_f = 0.81 on SiO_2, 1:3 hexanes:EtOAc); $[\alpha]_D^{26}$ -17.2 (*c* = 0.77, CH_2Cl_2); IR (CH_2Cl_2 cast) 3317, 3060, 2980, 2977, 1718, 1642, 1523, 1452, 1399, 1369, 1251, 1220, 1179, 1055 cm^{-1};^{1}H-NMR ($CDCl_3$, 500 MHz): δ 7.74 (2H, d, *J* = 7.5 Hz, Ar-H), 7.55 (2H, d, *J* = 7.5 Hz, Ar-H), 7.49 – 7.30 (9H, m, Ar-H), 5.68 (1H, d, *J* = 8.5 Hz, NH), 5.31 (1H, dd, *J* = 10.5, 5.0 Hz, H13), 5.17 – 5.06 (2H, m, H15), 4.77 (1H, dt, *J* = 8.0, 5.0 Hz, H10), 4.33 (1H, s, NH), 4.33 (2H, app dq, *J* = 10.5, 7.0 Hz, H8), 4.16 (1H, t, *J* = 7.1 Hz, H7), 3.15 – 3.01 (2H, m, H22), 2.93 (3H, s, H12), 1.80 – 1.65 (3H, m, H20, H26), 1.57 – 1.43 (4H, m, H20, H21, H27), 1.46 (9H, s, H25), 1.03 – 0.84 (6H, m, H28); ^{13}C-NMR ($CDCl_3$, 125 MHz): δ 172.3 (C14), 171.0 (C11), 156.1 (C9), 155.9 (C23), 144.0 (Ar-C), 143.7 (Ar-C), 141.3 (Ar-C), 141.2 (Ar-C), 135.2 (Ar-C), 128.6 (Ar-C), 128.2 (Ar-C), 128.1 (Ar-C), 127.7 (Ar-C), 127.4 (Ar-C), 125.2 (Ar-C), 199.8 (Ar-C), 79.7 (C24), 66.8 (C15), 66.7 (C8), 55.6 (C13), 49.9 (C10), 47.1 (C7), 40.1 (C12), 37.0 (C22), 31.2 (C20), 28.8 (C26), 25.4 (C27), 25.0

(C21), 23.2 (C25), 21.2 (C28); HRMS (ESI-TOF) Calc'd for $C_{39}H_{50}N_3O_7$ 672.3648 $[M+H]^+$, found 672.3645.

5.6.40 Benzyl (11*S*,14*S*)-11-((((9*H*-fluoren-9-yl)methoxy)carbonyl)amino)-6-((*tert*-butoxycarbonyl)amino)-14-isobutyl-2,2,13-trimethyl-4,12-dioxo-3-oxa-5,7,13-triazapentadec-5-en-15-oate (116)

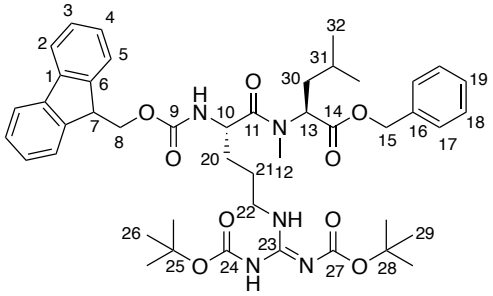

116

The following was adapted from a literature procedure.[209] Dipeptide **114** (3.06 g, 4.56 mmol) was dissolved in dry CH_2Cl_2 (15 mL) and had TFA (10 mL) added to it and stirred at room temperature for 1 h. The reaction was then concentrated *in vacuo* and co-evaporated with diethyl ether to remove residual TFA. The crude oil was then redissolved in dry CH_2Cl_2 (50 mL) and had 1,3-di-Boc-2-(trifluoromethylsulfonyl)guanidine **115** (2.00 g, 5.10 mmol) and Et_3N (1.40 mL, 10.0 mmol) added to it and stirred at room temperature for 90 mins. The reaction was quenched with 2 N aqueous sodium bisulfate (50 mL), then 10% aqueous $NaHCO_3$ (50 ml), then washed with brine (50 mL), dried over Na_2SO_4, filtered and concentrated *in vacuo*. The product was purified via flash column chromatography (silica gel, 20% EtOAc in hexanes) to yield **116** (3.49 g, 94% over 2 steps) as a white solid. (R_f = 0.32 on SiO_2, 30% EtOAc in hexanes). $[\alpha]_D^{26}$ -12.2 (*c* = 0.69, CH_2Cl_2); IR (CH_2Cl_2 cast) 3330, 3061, 2989, 2971, 1715, 1640, 1451, 1401, 1378, 1249, 1220, 1178, 1051 cm^{-1}; ^{1}H-NMR ($CDCl_3$, 500 MHz): δ 8.27 (1H, t, *J* = 5.0 Hz, NH), 7.77 (2H, d, *J* = 7.5 Hz, Ar-H), 7.62 (2H, d, *J* = 7.5 Hz, Ar-H), 7.40 – 7.25 (9H, m, Ar-H), 5.65 (1H, d, *J* = 8.5 Hz, NH), 5.30 – 5.21 (1H, m, H13), 5.19 – 5.07 (2H, m, H15), 4.64 (1H, dt, *J* = 8.0, 4.5 Hz, H10), 4.40 – 4.29 (2H, m, H8), 4.17 (1H, t, *J* = 7.0 Hz, H7), 3.33 (2H, ddd, *J* = 7.5, 5.0, 3.0 Hz, H22), 2.99 (3H, s, H12), 1.77 – 1.70 (1H, m, H30),

1.68 – 1.61 (2H, m, H30, H20), 1.60 – 1.54 (3H, m, H20, H21) 1.52 (10H, m, H29, H31), 1.49 (9H, s, H26), 1.02 – 0.94 (6H, m, H32); ^{13}C-NMR ($CDCl_3$, 125 MHz): δ 172.3 (C14), 171.0 (C11), 163.6 (C23), 156.2 (C27), 156.0 (C9), 153.3 (C24), 144.1 (Ar-C), 143.7 (Ar-C), 141.2 (Ar-C), 141.1 (Ar-C), 135.7 (Ar-C), 129.0 (Ar-C), 128.7 (Ar-C), 128.4 (Ar-C), 127.9 (Ar-C), 127.0 (Ar-C), 126.9 (Ar-C), 125.3 (Ar-C), 125.1(Ar-C), 120.0 (Ar-C), 83.3 (C28), 79.1 (C25), 67.4 (C15), 67.1 (C8), 55.1 (C13), 50.7 (C10), 47.2 (C7), 40.1 (C12), 36.1 (C22), 30.9 (C20), 29.9 (C30), 28.3 (C31), 28.1 (C21), 24.9 (C29), 23.2 (C26), 21.4 (C32); HRMS (ESI-TOF) Calc'd for $C_{45}H_{60}N_5O_9$ 814.4382 $[M+H]^+$, found 814.4380.

5.6.41 (11*S*,14*S*)-11-((((9*H*-Fluoren-9-yl)methoxy)carbonyl)amino)-6-((*tert*-butoxycarbonyl)amino)-14-isobutyl-2,2,13-trimethyl-4,12-dioxo-3-oxa-5,7,13-triazapentadec-5-en-15-oic acid (117)

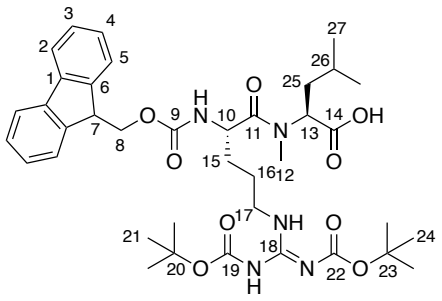

117

Dipeptide **116** (3.43 g, 4.22 mmol) was dissolved in THF:MeOH (1:1, 50 mL) and had 10% Pd/C (200 mg) added to it. This suspension was stirred under 1 atm of H_2 for 22 h, filtered through a pad of Celite® and concentrated *in vacuo*. The crude product (2.75 g, 90%) was carried forward without further purification as a white solid. (R_f = 0.22 on SiO_2, 1% AcOH in EtOAc); $[\alpha]_D^{26}$ -1.40 (*c* = 1.13, CH_2Cl_2); IR (CH_2Cl_2 cast) 3390, 3059, 2991, 2950, 1716, 1643, 1617, 1451, 1411, 1250, 1140, 1050 cm^{-1}; ^{1}H-NMR ($CDCl_3$, 500 MHz): δ 8.50 (1H, s, NH), 7.77 (2H, d, *J* = 7.5 Hz, Ar-H), 7.60 (2H, d, *J* = 7.5 Hz, Ar-H), 7.51 (2H, t, *J* = 7.5 Hz, Ar-H), 7.29 (2H, ddt, *J* = 7.5, 3.0, 1.5 Hz, Ar-H), 6.07 (1H, d, *J* = 7.5 Hz, NH), 5.41 (1H, dd, *J* = 10.5, 5.0 Hz, H13), 4.77 (1H, app q, *J* = 5.5 Hz, H10), 4.42 (2H, d, *J* = 10.5, H8), 4.18 (1H, t, *J* = 7.5 Hz, H7), 3.50 – 3.39 (1H, m, H17), 3.21 – 3.11

(1H, m, H17), 3.01 (3H, s, H12), 1.97 – 1.71 (6H, m, H15, H16, H25), 1.49 (9H, s, H24), 1.46 (10H, m, H21, H26), 0.96 (6H, m, H27); ^{13}C-NMR ($CDCl_3$, 125 MHz): δ 172.1 (C11), 172.0 (C14), 162.5 (C18), 156.8 (C22), 156.0 (C19), 153.1 (C9), 144.7 (Ar-C), 143.5 (Ar-C), 141.4 (Ar-C), 141.1 (Ar-C), 127.8 (Ar-C), 127.7 (Ar-C), 127.1 (Ar-C), 127.0 (Ar-C), 125.1 (Ar-C), 125.0 (Ar-C), 119.9 (Ar-C), 119.8 (Ar-C), 83.0 (C23), 80.7 (C20), 67.1 (C8), 54.5 (C13), 51.0 (C10), 47.1 (C7), 40.2 (C12), 36.1(C22), 30.5 (C15), 29.1 (C25), 28.3 (C26), 28.1 (C16), 24.8 (C21), 23.2 (C24), 21.4 (C27); HRMS (ESI-TOF) Calc'd for $C_{38}H_{54}N_5O_9$ 724.3919 $[M+H]^+$, found 724.3921.

5.6.42 Apelin Analogue Ac-NMeArg14-NMe17A2 (124)

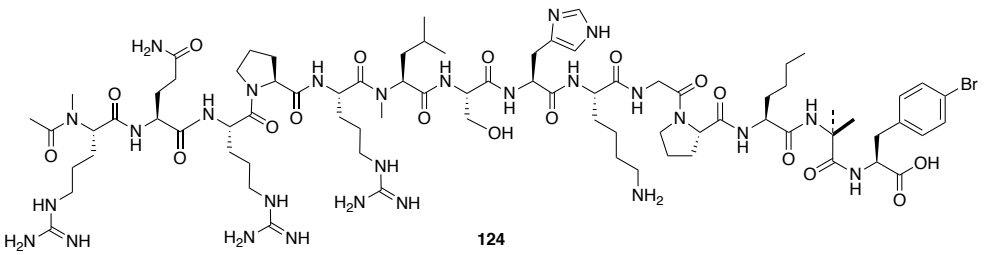

124

Fmoc-Phe(4-Br)-OH was loaded onto 2-chlorotrityl chloride resin using the general resin loading procedure at 1.5 mmol/g loading scale. Resin bound Fmoc-Phe(4-Br)-OH was then subject to manual SPPS (general method), introducing L-amino acids in the following order. Fmoc-Aib-OH, Fmoc-Nle-OH,Fmoc-Pro-OH, Fmoc-Gly-OH, Fmoc-Lys(Boc)-OH, Fmoc-His(Trt)-OH, and Fmoc-Ser(O^{t}Bu)-OH, with end-capping after each step. The NMeLeu subunit was added as a Fmoc-Arg(Boc)-NMeLeu-OH dipeptide (**117**) The dipeptide was coupled according to the general method, but allowed to couple for an extended time of 4 h, followed by end-capping. The manual SPPS was then continued with the L-amino acids in the following order: Fmoc-Pro-OH, Fmoc-Arg(Pmc)-OH, Fmoc-Gln(Trt)-OH with end-capping after each step. The NMeArg amino acid was added as Fmoc-NMeArg(Mtr) OH, following the general method, but for an extended time of 4 h, followed by end-capping. The peptide was then cleaved from resin and purified using the HPLC general method and a Phenomenex Luna C 18 RP-HPLC column (100 Å, 5µm, 250 mm × 10.00 mm). The desired peptide was isolated as a white solid after

lyophilization (0.104 mmol, 19 mg, 12%). LCMS (ESI-TOF) Calcd for $C_{79}H_{131}BrN_{27}O_{18}$ $[M+H]^+$ 1824.9362, found 1824.9331.

5.6.43 (*S*)-2-Amino-5-azido-2-methylpentanoic acid (128)

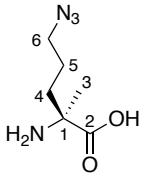

128

Amino acid **128** was prepared with an adapted literature procedure.[210] Nickel complex **127** (1.49 g, 2.51 mmol), prepared by Dr. Fischer, was dissolved in MeOH:CH_2Cl_2 (2:1, 15 mL) and added dropwise to 3 N HCl:MeOH (1:1, 20 mL) over 5 mins. The reaction mixture was stirred for 30 mins at 60 °C, turning the reaction mixture from bright red to green. The reaction mixture was cooled to room temperature and concentrated *in vacuo* to produce a green/brown solid. The solid was resuspended in CH_2Cl_2:H_2O (1:1, 50 mL), filtered and the aqueous layer was washed with CH_2Cl_2 (3 × 25 mL). The aqueous layer was then concentrated *in vacuo* and the product was purified by ion exchange column (Dowex 50WX2 50-100 mesh) and the amino acid was eluted using H_2O:NH_4OH (10-80% gradient), yielding **128** (0.360 g, 84%) as a fluffy white solid. $[\alpha]_D^{26}$ +1.8 (*c* = 0.56 H_2O); IR (H_2O cast) 3117, 2973, 2940, 2099, 1607, 1522, 1460, 1407, 1269 cm^{-1} ; ^{1}H-NMR (D_2O, 400 MHz): δ 3.40 (2H, app t, *J* = 6.8 Hz, H6), 2.01 – 1.93 (1H, m, H4), 1.89 – 1.81 (1H, m, H4), 1.77 – 1.66 (1H, m, H5), 1.62 – 1.54 (1H, m, H5), 1.52 (3H, s, H3); ^{13}C-NMR (D_2O, 175 MHz): δ 177.3 (C2), 62.1 (C6), 51.5 (C1), 35.2 (C4), 23.9 (C3), 23.2 (C5); HRMS (ESI-TOF) Cal'd for $C_6H_{11}N_4O_2$ $[M-H]^-$ 171.0960, found 171.0960.

5.6.44 (*S*)-2-((((9*H*-Fluoren-9-yl)methoxy)carbonyl)amino)-5-azido-2-methylpentanoic acid (129)

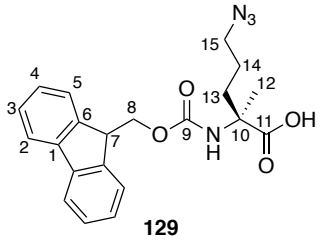

129

This reaction was adapted from a literature procedure.[210] Amino acid **128** (0.223 g, 1.30 mmol) was suspended in dry CH_2Cl_2 (20 mL) and had TMSCl (0.495 mL, 3.90 mmol) added to it and heated at reflux for 3 h. The reaction mixture was cooled down to room temperature, then to 0 °C. Fmoc-Cl (0.369 g, 1.43 mmol) was dissolved in dry CH_2Cl_2 (5 mL) and added dropwise to the reaction mixture over 5 mins. Finally, DIPEA (0.680 mL, 3.90 mmol) was added and the mixture was allowed to warm up to room temperature and stir for 3 h. The reaction was quenched with 1 N aqueous HCl (20 mL) and the aqueous layer was extracted with EtOAc (2 × 20 mL). The organic layer was dried over Na_2SO_4, filtered and concentrated *in vacuo*. The product was purified by flash chromatography (silica gel, 40% EtOAc in hexanes 0.1% AcOH), yielding **129** (0.446 g, 87%) as a white solid. (R_f = 0.53 on SiO_2, 9:1 EtOAc:MeOH 0.1% AcOH); $[\alpha]_D^{26}$ +2.3 (*c* = 0.36 CH_2Cl_2); IR (CH_2Cl_2 cast) 3398, 3334, 3066, 3050, 3019, 2941, 2878, 2098, 1715, 1510, 1478, 1451, 1262, 1088 cm^{-1}; ^{1}H-NMR ($CDCl_3$, 600 MHz): δ 7.77 (2H, d, *J* = 7.8 Hz, Ar-H), 7.59 (2H, d, *J* = 6.6 Hz, Ar-H), 7.41 (2H, dt, *J* = 7.2, 3.0 Hz, Ar-H), 7.32 (2H, dt, *J* = 7.8, 1.2 Hz, Ar-H), 5.54 (1H, br s, NH), 4.42 (2H, d, *J* = 7.2 Hz, H8), 4.21 (1H, t, *J* = 7.2 Hz, H7), 3.34 – 3.20 (2H, m, H15), 2.28 – 2.18 (1H, m, H13), 2.02 – 1.92 (1H, m, H13), 1.61 (3H, s, H12), 1.50 – 1.40 (1H, m, H14), 1.38 – 1.26 (1H, m, H14); ^{13}C-NMR ($CDCl_3$, 175 MHz): δ 177.1 (C11), 155.4 (C9), 144.0 (Ar-C), 143.9 (Ar-C), 127.9 (Ar-C), 127.2 (Ar-C), 125.1 (Ar-C), 120.2 (Ar-C), 66.6 (C8), 59.6 (C10), 51.2 (C7), 47.4 (C15), 33.6 (C13), 23.8 (C12), 23.7 (C14); HRMS (ESI-TOF) Calc'd for $C_{21}H_{21}N_4O_4$ $[M-H]^-$ 393.1568, found 393.1558.

5.6.45 (*S*)-2-((((9*H*-Fluoren-9-yl)methoxy)carbonyl)amino)-5-(2,3-bis(*tert*-butoxycarbonyl)guanidino)-2-methylpentanoic acid (130)

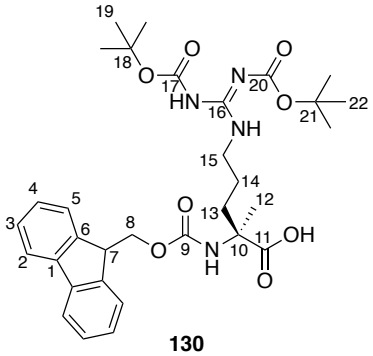

130

This reaction was adapted from a literature procedure.[210] Amino acid **129** (0.305 g, 0.772 mmol) was dissolved in dry CH_2Cl_2 (15 mL) and had 10% Pd/C (0.026 g) added. The suspension was stirred under 1 atm of H_2 gas for 18 h, filtered through a pad of Celite® and concentrated *in vacuo*. The crude mixture was dissolved in dry CH_2Cl_2 (20 mL), had TMSCl (0.293 mL, 2.31 mmol) added and was heated at reflux for 3 h. The reaction mixture was cooled down to room temperature, then to 0 °C and then had Et_3N (0.322 mL, 2.31 mmol) and 1,3-di-Boc-2-(trifluoromethylsulfonyl)guanidine (0.333 g, 0.851 mmol) added. The reaction was left to warm up to room temperature and stir overnight. Mixture was diluted with CH_2Cl_2 (20 mL) and then washed with 1 N aqueous HCl (3 × 20 mL). The organic layer was dried over Na_2SO_4, filtered, concentrated *in vacuo* and purified using flash chromatography (silica gel, 10–50% acetone in CH_2Cl_2 gradient), yielding **130** (0.260 g, 55%) as a white solid. (R_f = 0.41 on SiO_2, 1:1 CH_2Cl_2:acetone); $[\alpha]_D^{26}$ +10.2 (*c* = 0.44 CH_2Cl_2); IR (CH_2Cl_2 cast) 3408, 3325, 3161, 3067, 3050, 3008, 2981, 2937, 1721, 1641, 1617, 1503, 1478, 1451, 1368, 1331, 1138 cm^{-1}; ^{1}H-NMR ($CDCl_3$, 600 MHz): δ 8.41 (1H, br s, NH), 7.76 (2H, d, *J* = 7.2 Hz, Ar-H), 7.60 (2H, d, *J* = 7.2 Hz, Ar-H), 7.39 (2H, t, *J* = 7.2 Hz, Ar-H), 7.31 (2H, dt, *J* = 7.2, 1.2 Hz, Ar-H), 5.87 (1H, br s, NH), 4.48 – 4.32 (2H, m, H8), 4.23 (1H, t, *J* = 6.6 Hz, H7), 3.42 – 3.26 (2H, m, H15), 2.48 – 2.28 (1H, m, H13), 1.92 – 1.80 (1H, m, H13), 1.62 (3H, s, H12), 1.58 – 1.44 (20H, m, H14, H19, H22); ^{13}C-NMR ($CDCl_3$, 175 MHz): 177.5 (C11), 166.2 (C16), 156.1 (C17), 155.9 (C20), 153.3 (C9), 144.1 (Ar-C), 144.0 (Ar-C), 141.5 (Ar-C), 127.8 (Ar-C), 127.2 (Ar-C), 120.1 (Ar-C), 83.6 (C21), 79.3 (C18), 66.5 (C8), 53.9 (C10), 47.4 (C15),

40.9 (C7), 29.4 (C13), 28.4 (C22), 28.2 (C19), 24.2 (C12), 23.7 (C14); HRMS (ESI-TOF) Calc'd for $C_{32}H_{41}N_4O_8$ $[M-H]^-$ 609.3003, found 609.3004.

5.6.46 *tert*-Butyl N^2-(2-(diphenylmethylene)hydrazine-1-carbonyl)-N^5-trityl-*L*-glutaminate (135)

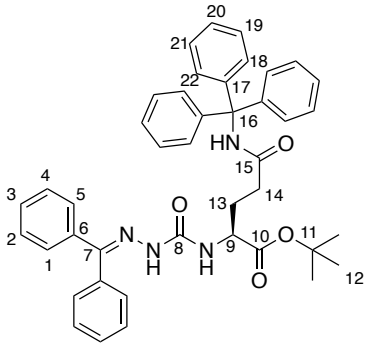

135

Semicarbazone **135** was prepared following an adapted literature procedure.[211] Disuccinimidyl carbonate **133** (0.895 g, 3.49 mmol) was dissolved in CH_2Cl_2/DMF (4:1, 25 mL), cooled down to 0 °C and had a 0 °C solution of benzophenone hydrazone **132** (0.623 g, 3.17 mmol) in dry CH_2Cl_2 (20 mL) cannulated into it. The reaction was allowed to warm to room temperature over 45 mins, then cooled down to 0 °C. To this reaction mixture was cannulated a 0 °C solution of H-L-Gln(Trt)-O^{t}Bu **134** (1.41 g, 3.17 mmol) and DIPEA (1.10 mL, 6.31 mmol) in dry CH_2Cl_2 (20 mL). The resulting solution was warmed slowly to room temperature over 24 h. The reaction was concentrated *in vacuo* and purified by flash column chromatography (silica gel, 10% EtOAc in hexanes) to yield **135** (0.599 g, 33%) as a fluffy white solid. (R_f = 0.46 on SiO_2, 1:1 EtOAc:hexanes); $[\alpha]_D^{26}$: +0.43 (*c* = 0.52 CH_2Cl_2); IR (CH_2Cl_2 cast) 3400, 3349, 3060, 3023, 3000, 2978, 2928 1730, 1678, 1519, 1492, 1446, 1393 1143 cm^{-1}; ^{1}H-NMR ($CDCl_3$, 400 MHz): δ 7.62 (1H, s, NH), 7.58 – 7.52 (5H, m, Ar-H), 7.39 – 7.34 (3H, m, Ar-H), 7.30 – 7.26 (5H, m, Ar-H), 7.24 – 7.20 (12H, m, Ar-H), 7.07 (1H, d, *J* = 8.4 Hz, NH), 4.51 (1H, ddd, *J* = 10.2, 8.2, 4.0 Hz, H9), 2.56 – 2.39 (2H, m, H14), 2.36 – 2.28 (1H, m, H13), 2.04 – 1.94 (1H, m, H13), 1.52 (9H, s, H12); ^{13}C-NMR ($CDCl_3$, 175 MHz): δ 171.5 (C10), 155.5 (C8), 148.7 (C7), 144.9 (C15), 137.0 (Ar-C), 132.0 (Ar-C), 129.9 (Ar-C), 129.8 (Ar-C), 129.6 (Ar-C), 128.9 (Ar-C), 128.6 (Ar-C), 128.5 (Ar-C), 128.0 (Ar-C), 127.7 (Ar-C), 127.4 (Ar-C),

127.0 (Ar-C), 82.5 (C11), 70.7 (C16), 53.1 (C9), 34.1 (C14), 30.4 (C13), 28.2 (C12); HRMS (ESI-TOF) Calc'd for $C_{42}H_{43}N_4O_4$ $[M+H]^+$ 667.3206, found 667.3213.

5.6.47 *tert*-Butyl N^2-(1-(3-azidopropyl)-2-(diphenylmethylene)hydrazine-1-carbonyl)-N^5-trityl-*L*-glutaminate (137)

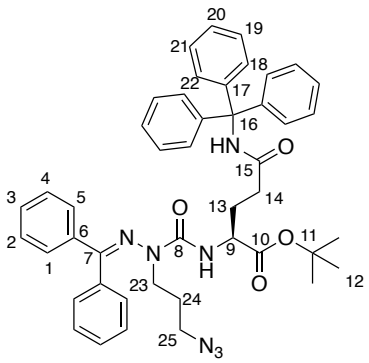

137

The alkylation procedure was adapted from a literature procedure.[31] Semicarbazone **135** (0.121 g, 0.181 mmol) was dissolved in dry THF (3 mL) and the solution cooled to 0 °C. Potassium *tert*-butoxide (0.0456 g, 0.406 mmol) was then added and the mixture stirred for 30 mins, after which 1-azido-3-iodopropane **136** (0.0844 g, 0.406 mmol) was added dropwise. The reaction was left to slowly warm up to room temperature overnight. Reaction mixture was quenched with the addition of 10% aqueous citric acid (10 mL), followed by brine (10 mL). Organic components were then extracted with EtOAc (3 × 25 mL). Pooled organic layer was dried over Na_2SO_4, filtered and concentrated *in vacuo*. The crude oil was purified by flash column chromatography (silica gel, 20% EtOAc in hexanes) to yield **137** (0.0994 g, 73%) as an off-white solid. (R_f = 0.6 on SiO_2, 1:1 EtOAc:hexanes); $[\alpha]_D^{26}$: +13.2 (*c* = 0.47 CH_2Cl_2); IR (CH_2Cl_2 cast) 3318, 3057, 3029, 2976, 2932, 2868, 2097, 1730, 1675, 1495, 1446, 1367, 1265, 1154, 1035 cm^{-1}; ^{1}H-NMR ($CDCl_3$, 600 MHz): δ 7.51 (2H, dd, *J* = 8.4, 1.2 Hz, Ar-H), 7.47 (2H, d, *J* = 7.2 Hz, Ar-H), 7.43 – 7.42 (2H, m, Ar-H), 7.53 (2H, app t, *J* = 7.8 Hz, Ar-H), 7.31 (2H, dd, *J* = 7.2, 1.8 Hz, Ar-H), 7.29 – 7.26 (3H, m, Ar-H), 7.25 – 7.20 (12H, m, Ar-H), 6.99 (1H, d, *J* = 8.4 Hz, NH), 4.48 (1H, ddd, *J* = 10.2, 8.2, 4.0 Hz, H9), 3.41 (1H, dt, *J* = 15.0, 7.2 Hz, H23), 3.24 (1H, dt, *J* = 15.0, 7.2 Hz, H23), 3.01 (2H, t, *J* = 7.2 Hz, H25), 2.50 – 2.45 (1H, m,

H14), 2.40 – 2.35 (1H, m, H14) 2.29 – 2.22 (1H, m, H13), 1.91 – 1.85 (1H, m, H13) 1.51 (2H, app quint., J = 7.2 Hz, H24), 1.47 (9H, s, H12); ^{13}C-NMR ($CDCl_3$, 175 MHz): δ 171.4 (C10), 158.8 (C8), 148.9 (C7), 145.0 (C15), 138.4 (Ar-C), 135.9 (Ar-C), 130.4 (Ar-C), 129.9 (Ar-C), 129.3 (Ar-C), 129.0 (Ar-C), 128.9 (Ar-C), 128.9 (Ar-C), 128.7 (Ar-C), 128.4 (Ar-C), 128.0 (Ar-C), 127.0 (Ar-C), 82.1 (C11), 70.5 (C16), 53.6 (C9), 48.9 (C25), 43.8 (C23), 34.3 (C14), 30.7 (C13), 28.2 (C12), 26.3 (C24); HRMS (ESI-TOF) Calc'd for $C_{45}H_{49}N_7O_4$ $[M+H]^+$ 750.3690, found 750.3693.

5.6.48 *tert*-Butyl N^2-(1-(3-azidopropyl)hydrazine-1-carbonyl)-N^5-trityl-*L*-glutaminate (138)

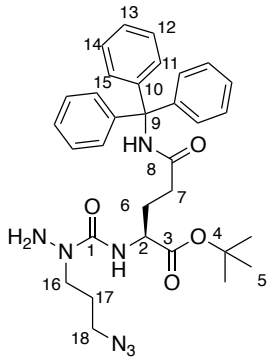

138

The following was adapted from a literature procedure.[211,212] Alkylated semicarbazone **137** (0.127 g, 0.170 mmol) was dissolved in a solution of hydroxylamine hydrochloride (0.0492 g, 0.708 mmol) in pyridine (5 mL) and heated to 60 °C for 24 h. The reaction mixture was allowed to cool to room temperature, and then concentrated *in vacuo*, using toluene, EtOAc, and diethyl ether coevaporations to remove residual pyridine. The crude oil was purified using flash column chromatography (silica gel, 40% EtOAc in hexanes, 0.1% DIPEA) yielding **138** (0.0573 g, 58%) as a white solid. (R_f = 0.1 on SiO_2, 1:1 EtOAc:hexanes); $[\alpha]_D^{26}$: +2.7 (c = 0.70 CH_2Cl_2); IR (CH_2Cl_2 cast) 3387, 3334, 3057, 3025, 3005, 2979, 2931, 2860, 2097, 1730, 1648, 1511, 1447, 1368, 1257, 1153 cm^{-1}; ^{1}H-NMR ($CDCl_3$, 400 MHz): δ 8.58 (2H, s, NH_2), 7.25 – 7.15 (15H, m, Ar-H), 7.10 (1H, d, J = 8.4 Hz, NH), 4.15 – 4.09 (1H, m, H2), 3.50 (2H, dt, J = 7.2, 2.4 Hz, H16), 3.29 – 3.26 (2H, m, H18), 2.42 – 2.33 (2H, m, H7), 2.03 – 1.97 (1H, m, H6), 1.84 – 1.76 (3H, m, H6,

H17), 1.42 (9H, s, H5); ^{13}C-NMR ($CDCl_3$, 175 MHz): δ 171.5 (C3), 159.2 (C1), 145.0 (C8), 129.0 (Ar-C), 128.0 (Ar-C), 127.0 (Ar-C), 125.6 (Ar-C), 82.1 (C4), 71.6 (C9), 53.5 (C2), 49.4 (C18), 48.2 (C16), 34.2 (C7), 30.4 (C6), 28.2 (C5), 26.4 (C17); HRMS (ESI-TOF) Calc'd for $C_{32}H_{40}N_7O_4$ $[M+H]^+$ 586.3064, found 586.3069.

5.6.49 Cyclic Apelin Analogue Cyc(1-5)-NMe13A2 (DAS) (146)

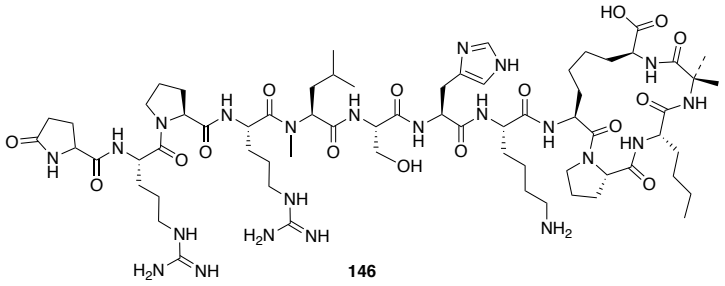

146

Orthogonally protected diamino diacid **44** was loaded onto 2-chlorotrityl chloride resin using the general resin loading procedure at 0.1 mmol/g loading scale. Resin bound **44** was then subject to manual SPPS (general method), introducing L-amino acids in the following order: Fmoc-Aib-OH, Fmoc-Nle-OH, Fmoc-Pro-OH, followed by cyclizing onto position 5 using the allyl/alloc deprotection protocol and the cyclization protocol, with end-capping after each step. Then, Fmoc-Lys(Boc)-OH, Fmoc-His(Trt)-OH, and Fmoc-Ser(O^{t}Bu)-OH were added with end-capping after each step. The NMeLeu subunit was added as a Fmoc-Arg(Boc)-NMeLeu-OH dipeptide (**117**) The dipeptide was coupled according to the general method, but allowed to couple for an extended time of 4 h, followed by end-capping. The manual SPPS was then continued with the L-amino acids in the following order: Fmoc-Pro-OH, Fmoc-Arg(Pmc)-OH, Fmoc-pGlu-OH with end-capping after each step and then *N*-terminally deprotected. The peptide was then cleaved from resin and purified using the HPLC general method and a Phenomenex Luna C_{18} RP-HPLC column (100 Å, 5µm, 250 mm × 10.00 mm). The desired peptide was isolated as a white solid after lyophilization (0.0040 mmol, 6.0 mg, 20%). LCMS (ESI-TOF) Calc'd for $C_{67}H_{113}N_{22}O_{16}$ $[M+H]^+$ 1481.8654, found 1481.8627.

5.6.50 Cyclic Apelin Analogue Cyc(1-5)-NMe13A2 (DAA) (147)

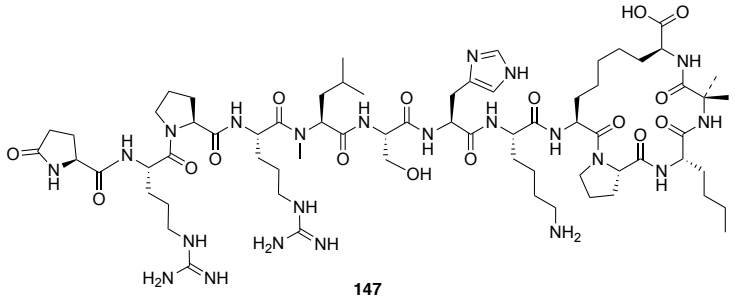

147

Orthogonally protected diamino diacid **46** was loaded onto 2-chlorotrityl chloride resin using the general resin loading procedure at 0.1 mmol/g loading scale. Resin bound **46** was then subject to manual SPPS (general method), introducing L-amino acids in the following order: Fmoc-Aib-OH, Fmoc-Nle-OH, Fmoc-Pro-OH, followed by cyclizing onto position 5 using the allyl/alloc deprotection protocol and the cyclization protocol, with end-capping after each step. Then, Fmoc-Lys(Boc)-OH, Fmoc-His(Trt)-OH, and Fmoc-Ser(O^{t}Bu)-OH were added with end-capping after each step. The NMeLeu subunit was added as a Fmoc-Arg(Boc)-NMeLeu-OH dipeptide (**117**) The dipeptide was coupled according to the general method, but allowed to couple for an extended time of 4 h, followed by end-capping. The manual SPPS was then continued with the L-amino acids in the following order: Fmoc-Pro-OH, Fmoc-Arg(Pmc)-OH, Fmoc-pGlu-OH with end-capping after each step and then *N*-terminally deprotected. The peptide was then cleaved from resin and purified using the HPLC general method and a Phenomenex Luna C_{18} RP-HPLC column (100 Å, 5µm, 250 mm × 10.00 mm). The desired peptide was isolated as a white solid after lyophilization (0.0030 mmol, 5.1 mg, 20%). LCMS (ESI-TOF) Calcd for $C_{68}H_{115}N_{22}O_{16}$ $[M+H]^+$ 1495.8760, found 1495.8783.

5.6.51 Cyclic Apelin Analogue Cyc(1-5)-NMe17A2 (DAS) (150)

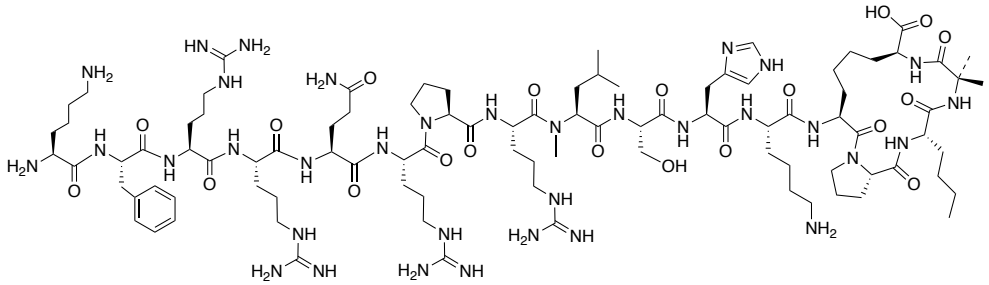

150

Orthogonally protected diamino diacid **44** was loaded onto 2-chlorotrityl chloride resin using the general resin loading procedure at 0.1 mmol/g loading scale. Resin bound **44** was then subject to manual SPPS (general method), introducing L-amino acids in the following order: Fmoc-Aib-OH, Fmoc-Nle-OH, Fmoc-Pro-OH, followed by cyclizing onto position 5 using the allyl/alloc deprotection protocol and the cyclization protocol, with end-capping after each step. Then, Fmoc-Lys(Boc)-OH, Fmoc-His(Trt)-OH, and Fmoc-Ser(O^{t}Bu)-OH were added with end-capping after each step. The NMeLeu subunit was added as a Fmoc-Arg(Boc)-NMeLeu-OH dipeptide (**117**) The dipeptide was coupled according to the general method, but allowed to couple for an extended time of 4 h, followed by end-capping. The manual SPPS was then continued with the L-amino acids in the following order: Fmoc-Pro-OH, Fmoc-Arg(Pmc)-OH, Fmoc-Gln(Trt)-OH, Fmoc-Arg(Pmc)-OH, Fmoc-Arg(Pmc)-OH, Fmoc-Phe-OH and Fmoc-Lys(Boc)-OH with end-capping after each step and then *N*-terminally deprotected. The peptide was then cleaved from resin and purified using the HPLC general method and a Phenomenex Luna C_{18} RP-HPLC column (100 Å, 5µm, 250 mm × 10.00 mm). The desired peptide was isolated as a white solid after lyophilization (0.0028 mmol, 5.8 mg, 14%). LCMS (ESI-TOF) Calc'd for $C_{94}H_{161}N_{34}O_{20}$ $[M+H]^+$ 2086.2529, found 2086.2548.

5.6.52 Cyclic Apelin Analogue Cyc(1-5)-NMe17A2 (DAA) (151)

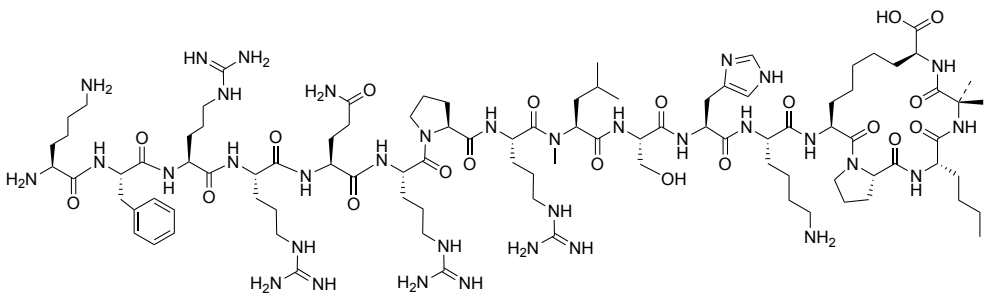

151

Orthogonally protected diamino diacid **46** was loaded onto 2-chlorotrityl chloride resin using the general resin loading procedure at 0.1 mmol/g loading scale. Resin bound **46** was then subject to manual SPPS (general method), introducing L-amino acids in the following order: Fmoc-Aib-OH, Fmoc-Nle-OH, Fmoc-Pro-OH, followed by cyclizing onto position 5 using the allyl/alloc deprotection protocol and the cyclization protocol, with end-capping after each step. Then, Fmoc-Lys(Boc)-OH, Fmoc-His(Trt)-OH, and Fmoc-Ser(O^{t}Bu)-OH were added with end-capping after each step. The NMeLeu subunit was added as a Fmoc-Arg(Boc)-NMeLeu-OH dipeptide (**117**) The dipeptide was coupled according to the general method, but allowed to couple for an extended time of 4 h, followed by end-capping. The manual SPPS was then continued with the L-amino acids in the following order: Fmoc-Pro-OH, Fmoc-Arg(Pmc)-OH, Fmoc-Gln(Trt)-OH, Fmoc-Arg(Pmc)-OH, Fmoc-Arg(Pmc)-OH, Fmoc-Phe-OH and Fmoc-Lys(Boc)-OH with end-capping after each step and then *N*-terminally deprotected. The peptide was then cleaved from resin and purified using the HPLC general method and a Phenomenex Luna C_{18} RP-HPLC column (100 Å, 5µm, 250 mm × 10.00 mm). The desired peptide was isolated as a white solid after lyophilization (0.0024 mmol, 5.0 mg, 14%). LCMS (ESI-TOF) Calc'd for $C_{95}H_{163}N_{34}O_{20}$ $[M+H]^+$ 2100.2732, found 2100.2705.

5.6.53 Cyclic Apelin Analogue Cyc(1-5)-FmocPEG$_6$-NMe17A2 (DAS) (154)

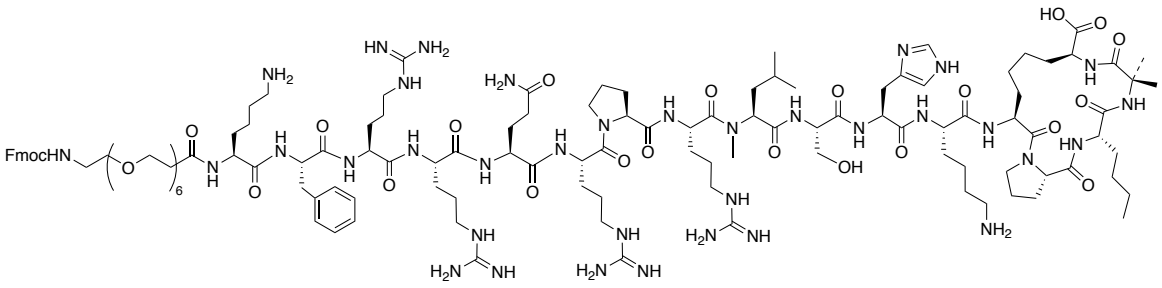

154

Orthogonally protected diamino diacid **44** was loaded onto 2-chlorotrityl chloride resin using the general resin loading procedure at 0.1 mmol/g loading scale. Resin bound **44** was then subject to manual SPPS (general method), introducing L-amino acids in the following order: Fmoc-Aib-OH, Fmoc-Nle-OH, Fmoc-Pro-OH, followed by cyclizing onto position 5 using the allyl/alloc deprotection protocol and the cyclization protocol, with end-capping after each step. Then, Fmoc-Lys(Boc)-OH, Fmoc-His(Trt)-OH, and Fmoc-Ser(O^{t}Bu)-OH were added with end-capping after each step. The NMeLeu subunit was added as a Fmoc-Arg(Boc)-NMeLeu-OH dipeptide (**117**) The dipeptide was coupled according to the general method, but allowed to couple for an extended time of 4 h, followed by end-capping. The manual SPPS was then continued with the L-amino acids in the following order: Fmoc-Pro-OH, Fmoc-Arg(Pmc)-OH, Fmoc-Gln(Trt)-OH, Fmoc-Arg(Pmc)-OH, Fmoc-Arg(Pmc)-OH, Fmoc-Phe-OH and Fmoc-Lys(Boc)-OH with end-capping after each step. The peptide then had a PEG$_6$ chain attached following the general *N*-terminal PEGylation protocol. The peptide was then cleaved from resin and purified using the HPLC general method and a Phenomenex Luna C$_{18}$ RP-HPLC column (100 Å, 5μm, 250 mm × 10.00 mm). The desired peptide was isolated as a white solid after lyophilization (0.0018 mmol, 4.8 mg, 9%). LCMS (ESI-TOF) Calc'd for $C_{124}H_{200}N_{35}O_{29}$ $[M+H]^+$ 2643.5198, found 2643.5173.

5.6.54 Cyclic Apelin Analogue Cyc(1-5)-FmocPEG$_6$-NMe17A2 (DAA) (155)

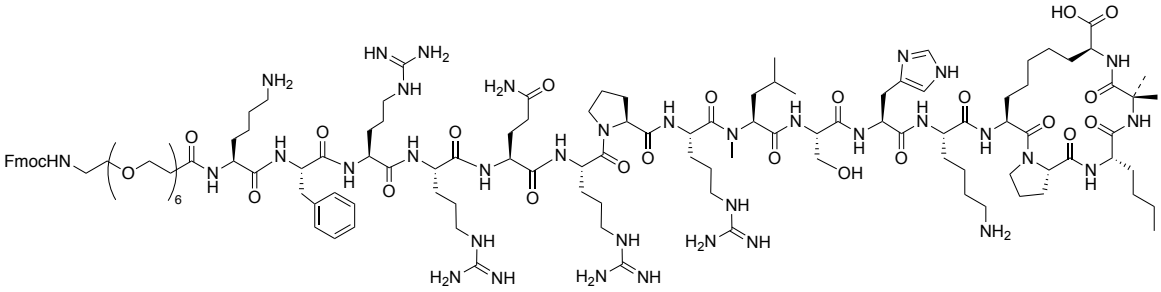

155

Orthogonally protected diamino diacid **46** was loaded onto 2-chlorotrityl chloride resin using the general resin loading procedure at 0.1 mmol/g loading scale. Resin bound **46** was then subject to manual SPPS (general method), introducing L-amino acids in the following order: Fmoc-Aib-OH, Fmoc-Nle-OH, Fmoc-Pro-OH, followed by cyclizing onto position 5 using the allyl/alloc deprotection protocol and the cyclization protocol, with end-capping after each step. Then, Fmoc-Lys(Boc)-OH, Fmoc-His(Trt)-OH, and Fmoc-Ser(O^{t}Bu)-OH were added with end-capping after each step. The NMeLeu subunit was added as a Fmoc-Arg(Boc)-NMeLeu-OH dipeptide (**117**) The dipeptide was coupled according to the general method, but allowed to couple for an extended time of 4 h, followed by end-capping. The manual SPPS was then continued with the L-amino acids in the following order: Fmoc-Pro-OH, Fmoc-Arg(Pmc)-OH, Fmoc-Gln(Trt)-OH, Fmoc-Arg(Pmc)-OH, Fmoc-Arg(Pmc)-OH, Fmoc-Phe-OH and Fmoc-Lys(Boc)-OH with end-capping after each step. The peptide then had a PEG$_6$ chain attached following the general *N*-terminal PEGylation protocol. The peptide was then cleaved from resin and purified using the HPLC general method and a Phenomenex Luna C$_{18}$ RP-HPLC column (100 Å, 5μm, 250 mm × 10.00 mm). The desired peptide was isolated as a white solid after lyophilization (0.0016 mmol, 4.2 mg, 8%). LCMS (ESI-TOF) Calc'd for $C_{125}H_{202}N_{35}O_{29}$ $[M+H]^+$ 2657.5337, found 2657.5329.

References

(1) Arias, E.; Xu, J. United States Life Tables, 2019. *Natl. Vital Stat. Rep.* **2022**, *70*, 59.

(2) Hansen, V.; Oren, E.; Dennis, L. K.; Brown, H. E. Infectious Disease Mortality Trends in the United States, 1980-2014. *JAMA* **2016**, *316*, 2149–2151.

(3) Brown, G. C. Living Too Long. *EMBO Rep.* **2015**, *16*, 137–141.

(4) Banting, F. G.; Best, C. H.; Collip, J. B.; Campbell, W. R.; Fletcher, A. A. Pancreatic Extracts in the Treatment of Diabetes Mellitus. *Can. Med. Assoc. J.* **1922**, *12*, 141–146.

(5) Lau, J. L.; Dunn, M. K. Therapeutic Peptides: Historical Perspectives, Current Development Trends, and Future Directions. *Bioorg. Med. Chem.* **2018**, *26*, 2700–2707.

(6) Diao, L.; Meibohm, B. Pharmacokinetics and Pharmacokinetic–Pharmacodynamic Correlations of Therapeutic Peptides. *Clin. Pharmacokinet.* **2013**, *52*, 855–868.

(7) Fosgerau, K.; Hoffmann, T. Peptide Therapeutics: Current Status and Future Directions. *Drug Discov. Today* **2015**, *20*, 122–128.

(8) Pan, X.; Xu, J.; Jia, X. Research Progress Evaluating the Function and Mechanism of Anti-Tumor Peptides. *Cancer Manag. Res.* **2020**, *12*, 397–409.

(9) Henninot, A.; Collins, J. C.; Nuss, J. M. The Current State of Peptide Drug Discovery: Back to the Future? *J. Med. Chem.* **2018**, *61*, 1382–1414.

(10) Lee, A. C.-L.; Harris, J. L.; Khanna, K. K.; Hong, J.-H. A Comprehensive Review on Current Advances in Peptide Drug Development and Design. *Int. J. Mol. Sci.* **2019**, *20*, 2383.

(11) Fischer, E.; Fourneau, E. Über einige Derivate des Glykocolls. In *Untersuchungen über Aminosäuren, Polypeptide und Proteïne (1899–1906)*; Fischer, E., Ed.; Springer: Berlin, Heidelberg, **1906,** 279–289.

(12) Bergmann, M.; Zervas, L. Über Ein Allgemeines Verfahren Der Peptid-Synthese. *Berichte Dtsch. Chem. Ges. B Ser.* **1932**, *65*, 1192–1201.

(13) Vigneaud, V. du; Ressler, C.; Swan, C. J. M.; Roberts, C. W.; Katsoyannis, P. G.; Gordon, S. The Synthesis of an Octapeptide Amide with the Hormonal Activity of Oxytocin. *J. Am. Chem. Soc.* **1953**, *75*, 4879–4880.

(14) Stawikowski, M.; Fields, G. B. Introduction to Peptide Synthesis. *Curr. Protoc. Protein Sci. Editor. Board John E Coligan Al* **2002**, *CHAPTER*, Unit-18.1.

(15) Merrifield, R. B. Solid Phase Peptide Synthesis. I. The Synthesis of a Tetrapeptide. *J. Am. Chem. Soc.* **1963**, *85*, 2149–2154.

(16) Carpino, L. A.; Han, G. Y. 9-Fluorenylmethoxycarbonyl Function, a New Base-Sensitive Amino-Protecting Group. *J. Am. Chem. Soc.* **1970**, *92*, 5748–5749.

(17) Atherton, E.; Sheppard, R. C. Solid Phase Peptide Synthesis Using N,-Fluorenylmethoxycarbonylamino Acid Pentafluorophenyl Esters. *J. Chem. Soc. Chem. Commun.* **1985**, *3*, 165–166

(18) Valeur, E.; Bradley, M. Amide Bond Formation: Beyond the Myth of Coupling Reagents. *Chem Soc Rev* **2009**, *38*, 606–631.

(19) El-Faham, A.; Albericio, F. Peptide Coupling Reagents, More than a Letter Soup. *Chem. Rev.* **2011**, *111*, 6557–6602.

(20) Kaiser, E.; Colescott, R. L.; Bossinger, C. D.; Cook, P. I. Color Test for Detection of Free Terminal Amino Groups in the Solid-Phase Synthesis of Peptides. *Anal. Biochem.* **1970**, *34*, 595–598.

(21) Dawson, P. E.; Muir, T. W.; Clark-Lewis, I.; Kent, S. B. H. Synthesis of Proteins by Native Chemical Ligation. *Science* **1994**, *266*, 776–779.

(22) Hartrampf, N.; Saebi, A.; Poskus, M.; Gates, Z. P.; Callahan, A. J.; Cowfer, A. E.; Hanna, S.; Antilla, S.; Schissel, C. K.; Quartararo, A. J.; Ye, X.; Mijalis, A. J.; Simon, M. D.; Loas, A.; Liu, S.; Jessen, C.; Nielsen, T. E.; Pentelute, B. L. Synthesis of Proteins by Automated Flow Chemistry. *Science* **2020**, *368*, 980–987.

(23) Kent, S. B. H. Total Chemical Synthesis of Proteins. *Chem. Soc. Rev.* **2009**, *38*, 338–351.

(24) Wang, L.; Wang, N.; Zhang, W.; Cheng, X.; Yan, Z.; Shao, G.; Wang, X.; Wang, R.; Fu, C. Therapeutic Peptides: Current Applications and Future Directions. *Signal Transduct. Target. Ther.* **2022**, *7*, 1–27.

(25) Rodriguez, J.; Gupta, N.; Smith, R. D.; Pevzner, P. A. Does Trypsin Cut Before Proline? *J. Proteome Res.* **2008**, *7*, 300–305.

(26) López-Otín, C.; Bond, J. S. Proteases: Multifunctional Enzymes in Life and Disease. *J. Biol. Chem.* **2008**, *283*, 30433–30437.

(27) Werner, H. M.; Cabalteja, C. C.; Horne, W. S. Peptide Backbone Composition and Protease Susceptibility: Impact of Modification Type, Position, and Tandem Substitution. *ChemBioChem* **2016**, *17*, 712–718.

(28) Chatterjee, J.; Rechenmacher, F.; Kessler, H. N-Methylation of Peptides and Proteins: An Important Element for Modulating Biological Functions. *Angew. Chem. Int. Ed.* **2013**, *52*, 254–269.

(29) Cheloha, R. W.; Watanabe, T.; Dean, T.; Gellman, S. H.; Gardella, T. J. Backbone Modification of a Parathyroid Hormone Receptor-1 Antagonist/Inverse Agonist. *ACS Chem. Biol.* **2016**, *11*, 2752–2762.

(30) Chingle, R.; Proulx, C.; Lubell, W. D. Azapeptide Synthesis Methods for Expanding Side-Chain Diversity for Biomedical Applications. *Acc. Chem. Res.* **2017**, *50*, 1541–1556.

(31) Traoré, M.; Doan, N.-D.; Lubell, W. D. Diversity-Oriented Synthesis of Azapeptides with Basic Amino Acid Residues: Aza-Lysine, Aza-Ornithine, and Aza-Arginine. *Org. Lett.* **2014**, *16*, 3588–3591.

(32) Pelay-Gimeno, M.; Glas, A.; Koch, O.; Grossmann, T. N. Structure-Based Design of Inhibitors of Protein–Protein Interactions: Mimicking Peptide Binding Epitopes. *Angew. Chem. Int. Ed Engl.* **2015**, *54*, 8896–8927.

(33) Koch, O.; Cole, J.; Block, P.; Klebe, G. Secbase: Database Module To Retrieve Secondary Structure Elements with Ligand Binding Motifs. *J. Chem. Inf. Model.* **2009**, *49*, 2388–2402.

(34) Jochim, A. L.; Arora, P. S. Systematic Analysis of Helical Protein Interfaces Reveals Targets for Synthetic Inhibitors. *ACS Chem. Biol.* **2010**, *5*, 919–923.

(35) Athanassiou, Z.; Dias, R. L. A.; Moehle, K.; Dobson, N.; Varani, G.; Robinson, J. A. Structural Mimicry of Retroviral Tat Proteins by Constrained β-Hairpin Peptidomimetics: Ligands with High Affinity and Selectivity for Viral TAR RNA Regulatory Elements. *J. Am. Chem. Soc.* **2004**, *126*, 6906–6913.

(36) White, C. J.; Yudin, A. K. Contemporary Strategies for Peptide Macrocyclization. *Nat. Chem.* **2011**, *3*, 509–524.

(37) Yang, P.-Y.; Zou, H.; Lee, C.; Muppidi, A.; Chao, E.; Fu, Q.; Luo, X.; Wang, D.; Schultz, P. G.; Shen, W. Stapled, Long-Acting Glucagon-like Peptide 2 Analog with Efficacy in Dextran Sodium Sulfate Induced Mouse Colitis Models. *J. Med. Chem.* **2018**, *61*, 3218–3223.

(38) Dougherty, P. G.; Wen, J.; Pan, X.; Koley, A.; Ren, J.-G.; Sahni, A.; Basu, R.; Salim, H.; Appiah Kubi, G.; Qian, Z.; Pei, D. Enhancing the Cell Permeability of Stapled Peptides with a Cyclic Cell-Penetrating Peptide. *J. Med. Chem.* **2019**, *62*, 10098–10107.

(39) Li, C. Y.; Yap, K.; Swedberg, J. E.; Craik, D. J.; de Veer, S. J. Binding Loop Substitutions in the Cyclic Peptide SFTI-1 Generate Potent and Selective Chymase Inhibitors. *J. Med. Chem.* **2020**, *63*, 816–826.

(40) Bray, F.; Ferlay, J.; Soerjomataram, I.; Siegel, R. L.; Torre, L. A.; Jemal, A. Global Cancer Statistics 2018: GLOBOCAN Estimates of Incidence and Mortality Worldwide for 36 Cancers in 185 Countries. *CA. Cancer J. Clin.* **2018**, *68*, 394–424.

(41) Xu, J.; Murphy, S. L.; Kochanek, K. D.; Arias, E. Deaths: Final Data 2019. *Natl. Vital Stat. Rep.* **2021**, *70*, 1–87.

(42) Um, P. Cancer, Definition. *Encyclopedia of Metagenomics: Environmental Metagenomics*. **2015**, 65–65.

(43) Hanahan, D.; Weinberg, R. A. The Hallmarks of Cancer. *Cell*. **2000**, *100*, 57–70.

(44) Hanahan, D.; Weinberg, R. A. Hallmarks of Cancer: The Next Generation. *Cell* **2011**, *144* (5), 646–674.

(45) Dunn, G. P.; Old, L. J.; Schreiber, R. D. The Three Es of Cancer Immunoediting. *Annu. Rev. Immunol.* **2004**, *22*, 329–360.

(46) Drake, C. G.; Jaffee, E.; Pardoll, D. M. Mechanisms of Immune Evasion by Tumors. *Advances in Immunology*. **2006**, *90*, 51–81.

(47) Boohaker, R. J.; Lee, M. W.; Vishnubhotla, P.; Perez, J. L. M.; Khaled, A. R. The Use of Therapeutic Peptides to Target and to Kill Cancer Cells. *Curr. Med. Chem. 19* , 3794–3804.

(48) Xie, M.; Liu, D.; Yang, Y. Anti-Cancer Peptides: Classification, Mechanism of Action, Reconstruction and Modification. *Open Biol.* **2020**, *10*, 1–10.

(49) Aljabery, F.; Shabo, I.; Gimm, O.; Jahnson, S.; Olsson, H. The Expression Profile of P14, P53 and P21 in Tumour Cells Is Associated with Disease-Specific Survival and the Outcome of Postoperative Chemotherapy Treatment in Muscle-Invasive Bladder Cancer. *Urol. Oncol. Semin. Orig. Investig.* **2018**, *36*, 530.e7-530.e18.

(50) Yu, W.-D.; Sun, G.; Li, J.; Xu, J.; Wang, X. Mechanisms and Therapeutic Potentials of Cancer Immunotherapy in Combination with Radiotherapy and/or Chemotherapy. *Cancer Lett.* **2019**, *452*, 66–70.

(51) Cai, Z.; Yin, Y.; Shen, C.; Wang, J.; Yin, X.; Chen, Z.; Zhou, Y.; Zhang, B. Comparative Effectiveness of Preoperative, Postoperative and Perioperative Treatments for Resectable Gastric Cancer: A Network Meta-Analysis of the Literature from the Past 20 Years. *Surg. Oncol.* **2018**, *27*, 563–574.

(52) GuanNan, L.; XueJuan, X.; YaoHang, L.; JiaoRong, L.; JingJie, W.; Yong, Z. Research progresses and applications of antimicrobial peptides. *Chin. J. Anim. Nutr.* **2014**, *26*, 17–25.

(53) Hilchie, A. L.; Hoskin, D. W.; Power Coombs, M. R. Anticancer Activities of Natural and Synthetic Peptides. *Antimicrobial Peptides: Basics for Clinical Application*. **2019**, 131–147.

(54) Schweizer, F. Cationic Amphiphilic Peptides with Cancer-Selective Toxicity. *Eur. J. Pharmacol.* **2009**, *625*, 190–194.

(55) Tyagi, A.; Tuknait, A.; Anand, P.; Gupta, S.; Sharma, M.; Mathur, D.; Joshi, A.; Singh, S.; Gautam, A.; Raghava, G. P. S. CancerPPD: A Database of Anticancer Peptides and Proteins. *Nucleic Acids Res.* **2015**, *43*, D837–D843.

(56) Thundimadathil, J. Cancer Treatment Using Peptides: Current Therapies and Future Prospects. *J. Amino Acids* **2012**, *2012*, 1–13

. (57) Vlieghe, P.; Lisowski, V.; Martinez, J.; Khrestchatisky, M. Synthetic Therapeutic Peptides: Science and Market. *Drug Discov. Today* **2010**, *15*, 40–56.

(58) Otvos, L. Peptide-Based Drug Design: Here and Now. *Peptide-Based Drug Design*. **2008**, *494*, 1–8

(59) Chiangjong, W.; Chutipongtanate, S.; Hongeng, S. Anticancer Peptide: Physicochemical Property, Functional Aspect and Trend in Clinical Application (Review). *Int. J. Oncol.* **2020**, *57*, 678–696.

(60) Zhang, W.; Li, J.; Liu, L.-W.; Wang, K.-R.; Song, J.-J.; Yan, J.-X.; Li, Z.-Y.; Zhang, B.-Z.; Wang, R. A Novel Analog of Antimicrobial Peptide Polybia-MPI, with Thioamide Bond Substitution, Exhibits Increased Therapeutic Efficacy against Cancer and Diminished Toxicity in Mice. *Peptides* **2010**, *31*, 1832–1838.

(61) Bae, S.; Oh, K.; Kim, H.; Kim, Y.; Kim, H.-R.; Hwang, Y.-I.; Lee, D.-S.; Kang, J. S.; Lee, W. J. The Effect of Alloferon on the Enhancement of NK Cell Cytotoxicity against Cancer via the Up-Regulation of Perforin/Granzyme B Secretion. *Immunobiology* **2013**, *218* (8), 1026–1033.

(62) Kitagaki, J.; Shi, G.; Miyauchi, S.; Murakami, S.; Yang, Y. Cyclic Depsipeptides as Potential Cancer Therapeutics. *Anticancer. Drugs* **2015**, *26* , 259–271.

(63) Gaspar, D.; Veiga, A. S.; Sinthuvanich, C.; Schneider, J. P.; Castanho, M. A. R. B. Anticancer Peptide SVS-1: Efficacy Precedes Membrane Neutralization. *Biochemistry* **2012**, *51*, 6263–6265.

(64) Sinthuvanich, C.; Veiga, A. S.; Gupta, K.; Gaspar, D.; Blumenthal, R.; Schneider, J. P. Anticancer β-Hairpin Peptides: Membrane-Induced Folding Triggers Activity. *J. Am. Chem. Soc.* **2012**, *134*, 6210–6217.

(65) Williams, D. E.; Diaz-Marrero, A. R.; Andersen, R. J.; Austin, P.; Roberge, M.; Roskelley, C. D.; Van Soest, R.; Matainaho, T. Neopetrosiamides, Peptides from the Marine Sponge *Neopetrosia* Sp. That Inhibit Amoeboid Invasion by Human Tumor Cells. *Org. Lett.* **2005**, *7*, 4173–4176.

(66) Austin, P.; Heller, M.; Williams, D. E.; McIntosh, L. P.; Vogl, A. W.; Foster, L. J.; Andersen, R. J.; Roberge, M.; Roskelley, C. D. Release of Membrane-Bound Vesicles and Inhibition of Tumor Cell Adhesion by the Peptide Neopetrosiamide A. *PLoS ONE* **2010**, *5*, 1–14.

(67) Liu, H.; Boudreau, M. A.; Zheng, J.; Whittal, R. M.; Austin, P.; Roskelley, C. D.; Roberge, M.; Andersen, R. J.; Vederas, J. C. Chemical Synthesis and Biological Activity of the Neopetrosiamides and Their Analogues: Revision of Disulfide Bond Connectivity. *J. Am. Chem. Soc.* **2010**, *132*, 1486–1487.

(68) Towle, K. M.; Chaytor, J. L.; Liu, H.; Austin, P.; Roberge, M.; Roskelley, C. D.; Vederas, J. C. Synthesis and Biological Studies of Neopetrosiamides as Inhibitors of Cancer Cell Invasion. *Org. Biomol. Chem.* **2013**, *11*, 1476–1481.

(69) Paňková, K.; Rösel, D.; Novotný, M.; Brábek, J. The Molecular Mechanisms of Transition between Mesenchymal and Amoeboid Invasiveness in Tumor Cells. *Cell. Mol. Life Sci.* **2010**, *67*, 63–71.

(70) Talkenberger, K.; Cavalcanti-Adam, E. A.; Voss-Böhme, A.; Deutsch, A. Amoeboid-Mesenchymal Migration Plasticity Promotes Invasion Only in Complex Heterogeneous Microenvironments. *Sci. Rep.* **2017**, *7*, 1–12

(71) Brooks, P. C.; Strömblad, S.; Sanders, L. C.; von Schalscha, T. L.; Aimes, R. T.; Stetler-Stevenson, W. G.; Quigley, J. P.; Cheresh, D. A. Localization of Matrix Metalloproteinase MMP-2 to the Surface of Invasive Cells by Interaction with Integrin Avβ3. *Cell* **1996**, *85*, 683–693.

(72) Ruoslahti, E.; Pierschbacher, M. D. Arg-Gly-Asp: A Versatile Cell Recognition Signal. *Cell* **1986**, *44*, 517–518.

(73) Dunehoo, A. L.; Anderson, M.; Majumdar, S.; Kobayashi, N.; Berkland, C.; Siahaan, T. J. Cell Adhesion Molecules for Targeted Drug Delivery. *J. Pharm. Sci.* **2006**, *95*, 1856–1872.

(74) Roth, G. A.. *et. al.* Global Burden of Cardiovascular Diseases and Risk Factors, 1990–2019: Update From the GBD 2019 Study. *J. Am. Coll. Cardiol.* **2020**, *76*, 2982–3021.

(75) Mendis, S.; Puska, P.; Norrving, B. *Global Atlas on Cardiovascular Disease Prevention and Control*, 1st ed.; WHO, 2011.

(76) Hausenloy, D. J.; Yellon, D. M. Myocardial Ischemia-Reperfusion Injury: A Neglected Therapeutic Target. *J. Clin. Invest.* **2013**, *123*, 92–100.

(77) Laubach, V. E.; French, B. A.; Okusa, M. D. Targeting of Adenosine Receptors in Ischemia-Reperfusion Injury. *Expert Opin. Ther. Targets* **2011**, *15*, 103–118.

(78) Wang, X.; Ouyang, Y.; Liu, J.; Zhu, M.; Zhao, G.; Bao, W.; Hu, F. B. Fruit and Vegetable Consumption and Mortality from All Causes, Cardiovascular Disease, and Cancer: Systematic Review and Dose-Response Meta-Analysis of Prospective Cohort Studies. *The BMJ*. **2014**, *349*, 1–14.

(79) Ettehad, D.; Emdin, C. A.; Kiran, A.; Anderson, S. G.; Callender, T.; Emberson, J.; Chalmers, J.; Rodgers, A.; Rahimi, K. Blood Pressure Lowering for Prevention of Cardiovascular Disease and Death: A Systematic Review and Meta-Analysis. *The Lancet* **2016**, *387*, 957–967.

(80) Dibben, G.; Faulkner, J.; Oldridge, N.; Rees, K.; Thompson, D. R.; Zwisler, A.-D.; Taylor, R. S. Exercise-based Cardiac Rehabilitation for Coronary Heart Disease. *Cochrane Database Syst. Rev.* **2021**, No. 11.

(81) Kathiresan, S.; Srivastava, D. Genetics of Human Cardiovascular Disease. *Cell* **2012**, *148*, 1242–1257.

(82) Gutierrez, J.; Ramirez, G.; Rundek, T.; Sacco, R. L. Statin Therapy in the Prevention of Recurrent Cardiovascular Events: A Sex-Based Meta-Analysis. *Arch. Intern. Med.* **2012**, *172*, 909–919.

(83) Berger, J. S.; Lala, A.; Krantz, M. J.; Baker, G. S.; Hiatt, W. R. Aspirin for the Prevention of Cardiovascular Events in Patients without Clinical Cardiovascular Disease: A Meta-Analysis of Randomized Trials. *Am. Heart J.* **2011**, *162*, 115-124.e2.

(84) Recio, C.; Maione, F.; Iqbal, A. J.; Mascolo, N.; De Feo, V. The Potential Therapeutic Application of Peptides and Peptidomimetics in Cardiovascular Disease. *Front. Pharmacol.* **2017**, *7*, 1–11.

(85) González-Montero, J.; Brito, R.; Gajardo, A. I.; Rodrigo, R. Myocardial Reperfusion Injury and Oxidative Stress: Therapeutic Opportunities. *World J. Cardiol.* **2018**, *10*, 74–86.

(86) Chhabra, L.; Zain, M. A.; Siddiqui, W. J. *Angioplasty*; StatPearls Publishing, 2021.

(87) Grieco, P.; Gomez-Monterrey, I. Natural and Synthetic Peptides in the Cardiovascular Diseases: An Update on Diagnostic and Therapeutic Potentials. *Arch. Biochem. Biophys.* **2019**, *662*, 15–32.

(88) Burley, D. S.; Hamid, S. A.; Baxter, G. F. Cardioprotective Actions of Peptide Hormones in Myocardial Ischemia. *Heart Fail. Rev.* **2007**, *12*, 279–291.

(89) Gøtzsche, P. C.; Hróbjartsson, A. Somatostatin Analogues for Acute Bleeding Oesophageal Varices. *Cochrane Database Syst. Rev.* **2008**, No. 3.

(90) Anthony, L.; Freda, P. U. From Somatostatin to Octreotide LAR: Evolution of a Somatostatin Analogue. *Curr. Med. Res. Opin.* **2009**, *25*, 2989–2999.

(91) Gariani, K.; Meyer, P.; Philippe, J. Implications of Somatostatin Analogues in the Treatment of Acromegaly. *Eur. Endocrinol.* **2013**, *9*, 132–135.

(92) Gomaa, R. S.; Mahmoud, N. M.; Mohammed, N. A. Octreotide (Somatostatin Analog) Attenuates Cardiac Ischemia/Reperfusion Injury via Activating Nuclear Factor (Erythroid-Derived 2)-like 2 (Nrf2) Signaling Pathway in Rat Model of Hyperthyroidism. *Future J. Pharm. Sci.* **2020**, *6*, 1–10.

(93) Woeste, G.; Wullstein, C.; Meyer, S.; Usadel, K. H.; Hopt, U. T.; Bechstein, W. O.; von Dobschuetz, E. Octreotide Attenuates Impaired Microcirculation in Postischemic Pancreatitis When Administered Before Induction of Ischemia. *Transplantation* **2008**, *86*, 961–967.

(94) Yildirim, N.; Yigitturk, G.; Sahingoz Yildirim, A. G.; Akdemir, A.; İlgen, O.; Yeniel, O.; Ergenoglu, M.; Erbas, O. Octreotide Protects Ovary against Ischemia–Reperfusion Injury in Rats: Evaluation of Histological and Biochemical Parameters. *J. Obstet. Gynaecol. Res.* **2015**, *41*, 1591–1597.

(95) Takano, T.; Yonemitsu, Y.; Saito, S.; Itoh, H.; Onohara, T.; Fukuda, A.; Takai, M.; Maehara, Y. A Somatostatin Analogue, Octreotide, Ameliorates Intestinal Ischemia-Reperfusion Injury Through the Early Induction of Heme Oxygenase-1. *J. Surg. Res.* **2012**, *175*, 350–358.

(96) Wang, T.-L.; Huang, Y.-H.; Chang, H. Somatostatin Analogue Mimics Acute Ischemic Preconditioning in a Rat Model of Myocardial Infarction. *J. Cardiovasc. Pharmacol.* **2005**, *45*, 327–332.

(97) de Lecea, L.; Criado J. R.; Prospero-Garcia, O.; Gautvik, K. M.; Schweitzer, P, Danielson, P. E.; Dunlop, C. L.; Siggins, G. R.; Henriksen, S. J.; Sutcliffe, J. G. A cortical neuropeptide with neuronal depressant and sleep-modulating properties. *Nature*. **1996**, *381*, 242–245.

(98) de Lecea, L. Cortistatin—Functions in the Central Nervous System. *Mol. Cell. Endocrinol.* **2008**, *286*, 88–95.

(99) Méndez-Díaz, M.; Guevara-Martínez, M.; Alquicira, C. R.; Guzmán Vásquez, K.; Prospéro-García, O. Cortistatin, a Modulatory Peptide of Sleep and Memory, Induces Analgesia in Rats. *Neurosci. Lett.* **2004**, *354*, 242–244.

(100) Jiang, J.; Peng, Y.; Liang, X.; Li, S.; Chang, X.; Li, L.; Chang, M. Centrally Administered Cortistation-14 Induces Antidepressant-Like Effects in Mice via Mediating Ghrelin and GABAA Receptor Signaling Pathway. *Front. Pharmacol.* **2018**, *9*, 1–12.

(101) Yan, S.; Li, M.; Chai, H.; Yang, H.; Lin, P. H.; Yao, Q.; Chen, C. TNF-Alpha Decreases Expression of Somatostatin, Somatostatin Receptors, and Cortistatin in Human Coronary Endothelial Cells. *J. Surg. Res.* **2005**, *123*, 294–301.

(102) Shi, Z.-Y.; Liu, Y.; Dong, L.; Zhang, B.; Zhao, M.; Liu, W.-X.; Zhang, X.; Yin, X.-H. Cortistatin Improves Cardiac Function After Acute Myocardial Infarction in Rats by Suppressing Myocardial Apoptosis and Endoplasmic Reticulum Stress. *J. Cardiovasc. Pharmacol. Ther.* **2017**, *22*, 83–93.

(103) Liang, J.; Bai, Y.; Chen, W.; Fu, Y.; Liu, Y.; Yin, X. Cortistatin, a Novel Cardiovascular Protective Peptide. *Cardiovasc. Diagn. Ther.* **2019**, *9*, 394–399.

(104) La, M.; D'Amico, M.; Bandiera, S.; Filippo, C. D.; Oliani, S. M.; Gavins, F. N. E.; Flower, R. J.; Perretti, M. Annexin 1 Peptides Protect against Experimental Myocardial Ischemia-Reperfusion: Analysis of Their Mechanism of Action. *FASEB J.* **2001**, *15*, 2247–2256.

(105) Hecht, I.; Rong, J.; Sampaio, A. L. F.; Hermesh, C.; Rutledge, C.; Shemesh, R.; Toporik, A.; Beiman, M.; Dassa, L.; Niv, H.; Cojocaru, G.; Zauberman, A.; Rotman, G.; Perretti, M.; Vinten-Johansen, J.; Cohen, Y. A Novel Peptide Agonist of Formyl-Peptide Receptor-Like 1 (ALX) Displays Anti-Inflammatory and Cardioprotective Effects. *J. Pharmacol. Exp. Ther.* **2009**, *328*, 426–434.

(106) Tatemoto, K.; Hosoya, M.; Habata, Y.; Fujii, R.; Kakegawa, T.; Zou, M. X.; Kawamata, Y.; Fukusumi, S.; Hinuma, S.; Kitada, C.; Kurokawa, T.; Onda, H.; Fujino, M. Isolation and Characterization of a Novel Endogenous Peptide Ligand for the Human APJ Receptor. *Biochem. Biophys. Res. Commun.* **1998**, *251*, 471–476.

(107) Zhong, J.-C.; Zhang, Z.-Z.; Wang, W.; McKinnie, S. M. K.; Vederas, J. C.; Oudit, G. Y. Targeting the Apelin Pathway as a Novel Therapeutic Approach for Cardiovascular Diseases. *Biochim. Biophys. Acta BBA - Mol. Basis Dis.* **2017**, *1863*, 1942–1950.

(108) Pitkin, S. L.; Maguire, J. J.; Bonner, T. I.; Davenport, A. P. International Union of Basic and Clinical Pharmacology. LXXIV. Apelin Receptor Nomenclature, Distribution, Pharmacology, and Function. *Pharmacol. Rev.* **2010**, *62*, 331–342.

(109) Narayanan, S.; Harris, D. L.; Maitra, R.; Runyon, S. P. Regulation of the Apelinergic System and Its Potential in Cardiovascular Disease: Peptides and Small Molecules as Tools for Discovery. *J. Med. Chem.* **2015**, *58*, 7913–7927.

(110) Wang, W.; McKinnie, S. M. K.; Patel, V. B.; Haddad, G.; Wang, Z.; Zhabyeyev, P.; Das, S. K.; Basu, R.; McLean, B.; Kandalam, V.; Penninger, J. M.; Kassiri, Z.; Vederas, J. C.; Murray, A. G.; Oudit, G. Y. Loss of Apelin Exacerbates Myocardial Infarction Adverse Remodeling and Ischemia-reperfusion Injury: Therapeutic Potential of Synthetic Apelin Analogues. *J. Am. Heart Assoc.* **2013**, *2*, e000249.

(111) Maguire, J. J.; Kleinz, M. J.; Pitkin, S. L.; Davenport, A. P. [Pyr1]Apelin-13 Identified as the Predominant Apelin Isoform in the Human Heart. *Hypertension* **2009**, *54*, 598–604.

(112) Ma, Y.; Yue, Y.; Ma, Y.; Zhang, Q.; Zhou, Q.; Song, Y.; Shen, Y.; Li, X.; Ma, X.; Li, C.; Hanson, M. A.; Han, G. W.; Sickmier, E. A.; Swaminath, G.; Zhao, S.; Stevens, R. C.; Hu, L. A.; Zhong, W.; Zhang, M.; Xu, F. Structural Basis for Apelin Control of the Human Apelin Receptor. *Structure* **2017**, *25*, 858-866.

(113) Japp, A. G.; Cruden, N. L.; Amer, D. A. B.; Li, V. K. Y.; Goudie, E. B.; Johnston, N. R.; Sharma, S.; Neilson, I.; Webb, D. J.; Megson, I. L.; Flapan, A. D.; Newby, D. E. Vascular Effects of Apelin In Vivo in Man. *J. Am. Coll. Cardiol.* **2008**, *52*, 908–913.

(114) Wang, W.; McKinnie, S. M. K.; Farhan, M.; Paul, M.; McDonald, T.; McLean, B.; Llorens-Cortes, C.; Hazra, S.; Murray, A. G.; Vederas, J. C.; Oudit, G. Y. Angiotensin-Converting Enzyme 2 Metabolizes and Partially Inactivates Pyr-Apelin-13 and Apelin-17. *Hypertension* **2016**, *68*, 365–377.

(115) McKinnie, S. M. K.; Wang, W.; Fischer, C.; McDonald, T.; Kalin, K. R.; Iturrioz, X.; Llorens-Cortes, C.; Oudit, G. Y.; Vederas, J. C. Synthetic Modification within the "RPRL" Region of Apelin Peptides: Impact on Cardiovascular Activity and Stability to Neprilysin and Plasma Degradation. *J. Med. Chem.* **2017**, *60*, 6408–6427.

(116) McKinnie, S. M. K.; Fischer, C.; Tran, K. M. H.; Wang, W.; Mosquera, F.; Oudit, G. Y.; Vederas, J. C. The Metalloprotease Neprilysin Degrades and Inactivates Apelin Peptides. *Chem. Bio. Chem* **2016**, *17*, 1495–1498.

(117) Fischer, C.; Lamer, T.; Wang, W.; McKinnie, S. M. K.; Iturrioz, X.; Llorens-Cortes, C.; Oudit, G. Y.; Vederas, J. C. Plasma Kallikrein Cleaves and Inactivates

Apelin-17: Palmitoyl- and PEG-Extended Apelin-17 Analogs as Metabolically Stable Blood Pressure-Lowering Agents. *Eur. J. Med. Chem.* **2019**, *166*, 119–124.

(118) Murza, A.; Parent, A.; Besserer-Offroy, É.; Beaudet, N.; Sarret, P.; Marsault, E. Elucidation of the Structure-Activity Relationships of Apelin: Influence of Unnatural Amino Acids on Binding, Signaling and Plasma Stability. *Chem. Med. Chem*. **2012**, *7*, 318–325

(119) Fernandez, K. X.; Fischer, C.; Vu, J.; Gheblawi, M.; Wang, W.; Gottschalk, S.; Iturrioz, X.; Llorens-Cortés, C.; Oudit, G. Y.; Vederas, J. C. Metabolically Stable Apelin-Analogues, Incorporating Cyclohexylalanine and Homoarginine, as Potent Apelin Receptor Activators. *RSC Med. Chem.* **2021**, *12*, 1402–1413.

(120) Fischer, C.; Lamer, T.; Fernandez, K.; Gheblawi, M.; Wang, W.; Pascoe, C.; Lambkin, G.; Iturrioz, X.; Llorens-Cortes, C.; Oudit, G. Y.; Vederas, J. C. Optimizing PEG-Extended Apelin Analogues as Cardioprotective Drug Leads: Importance of the KFRR Motif and Aromatic Head Group for Improved Physiological Activity. *J. Med. Chem.* **2020**, *63*, 12073–12082.

(121) O'Dowd, B. F.; Heiber, M.; Chan, A.; Heng, H. H. Q.; Tsui, L.-C.; Kennedy, J. L.; Shi, X.; Petronis, A.; George, S. R.; Nguyen, T. A Human Gene That Shows Identity with the Gene Encoding the Angiotensin Receptor Is Located on Chromosome 11. *Gene* **1993**, *136*, 355–360.

(122) Digby, G. J.; Lober, R. M.; Sethi, P. R.; Lambert, N. A. Some G Protein Heterotrimers Physically Dissociate in Living Cells. *Proc. Natl. Acad. Sci. U. S. A.* **2006**, *103* , 17789–17794.

(123) Masri, B.; Morin, N.; Pedebernade, L.; Knibiehler, B.; Audigier, Y. The Apelin Receptor Is Coupled to Gi1 or Gi2 Protein and Is Differentially Desensitized by Apelin Fragments. *J. Biol. Chem.* **2006**, *281*, 18317–18326.

(124) Szokodi, I.; Tavi, P.; Földes, G.; Voutilainen-Myllylä, S.; Ilves, M.; Tokola, H.; Pikkarainen, S.; Piuhola, J.; Rysä, J.; Tóth, M.; Ruskoaho, H. Apelin, the Novel Endogenous Ligand of the Orphan Receptor APJ, Regulates Cardiac Contractility. *Circ. Res.* **2002**, *91*, 434–440.

(125) Stryer, U. L.; Stryer, L.; Tasker, R.; Rhodes, C. *Biochemistry*; W.H. Freeman, 1995.

(126) Fleming, I.; Busse, R. Molecular Mechanisms Involved in the Regulation of the Endothelial Nitric Oxide Synthase. *Am. J. Physiol.-Regul. Integr. Comp. Physiol.* **2003**, *284*, R1–R12.

(127) Kalea, A. Z.; Batlle, D. Apelin and ACE2 in Cardiovascular Disease. *Curr. Opin. Investig. Drugs Lond. Engl. 2000* **2010**, *11*, 273–282.

(128) Chapman, N. A.; Dupré, D. J.; Rainey, J. K. The Apelin Receptor: Physiology, Pathology, Cell Signalling, and Ligand Modulation of a Peptide-Activated Class A GPCR. *Biochem. Cell Biol.* **2014**, *92*, 431–440.

(129) Chambard, J.-C.; Lefloch, R.; Pouysségur, J.; Lenormand, P. ERK Implication in Cell Cycle Regulation. *Biochim. Biophys. Acta BBA - Mol. Cell Res.* **2007**, *1773*, 1299–1310.

(130) Lee, D. K.; Ferguson, S. S. G.; George, S. R.; O'Dowd, B. F. The Fate of the Internalized Apelin Receptor Is Determined by Different Isoforms of Apelin Mediating Differential Interaction with β-Arrestin. *Biochem. Biophys. Res. Commun.* **2010**, *395*, 185–189.

(131) Rabenstein, D. L.; Weaver, K. H. Kinetics and Equilibria of the Thiol/Disulfide Exchange Reactions of Somatostatin with Glutathione. *J. Org. Chem.* **1996**, *61*, 7391–7397.

(132) Palomo, C.; Oiarbide, M. β-Lactam Ring Opening: A Useful Entry to Amino Acids and Relevant Nitrogen-Containing Compounds. *Heterocyclic Scaffolds I: ß-Lactams*. **2010**, 211–259.

(133) Gómez-Bombarelli, R.; Calle, E.; Casado, J. Mechanisms of Lactone Hydrolysis in Neutral and Alkaline Conditions. *J. Org. Chem.* **2013**, *78*, 6868–6879.

(134) Brik, A. Metathesis in Peptides and Peptidomimetics. *Adv. Synth. Catal.* **2008**, *350*, 1661–1675.

(135) Mangold, S. L.; O'Leary, D. J.; Grubbs, R. H. Z-Selective Olefin Metathesis on Peptides: Investigation of Side-Chain Influence, Preorganization, and Guidelines in Substrate Selection. *J. Am. Chem. Soc.* **2014**, *136*, 12469–12478

(136) Jacobsen, Ø.; Klaveness, J.; Rongved, P. Structural and Pharmacological Effects of Ring-Closing Metathesis in Peptides. *Molecules* **2010**, *15*, 6638–6677.

(137) Derksen, D. J.; Stymiest, J. L.; Vederas, J. C. Antimicrobial Leucocin Analogues with a Disulfide Bridge Replaced by a Carbocycle or by Noncovalent Interactions of Allyl Glycine Residues. *J. Am. Chem. Soc.* **2006**, *128*, 14252–14253.

(138) Liu, W.; Chan, A. s. h.; Liu, H.; Cochrane, S. a.; Vederas, J. c. Solid Supported Chemical Syntheses of Both Components of the Lantibiotic Lacticin 3147. *J. Am. Chem. Soc.* **2011**, *133*, 14216–14219.

(139) Cui, H.-K.; Guo, Y.; He, Y.; Wang, F.-L.; Chang, H.-N.; Wang, Y.-J.; Wu, F.-M.; Tian, C.-L.; Liu, L. Diaminodiacid-Based Solid-Phase Synthesis of Peptide Disulfide Bond Mimics. *Angew. Chem.* **2013**, *125*, 9737–9741.

(140) Qi, Y.-K.; Qu, Q.; Bierer, D.; Liu, L. A Diaminodiacid (DADA) Strategy for the Development of Disulfide Surrogate Peptides. *Chem.: Asian J.* **2020**, *15*, 2793–2802.

(141) Ross, A. C.; McKinnie, S. M. K.; Vederas, J. C. The Synthesis of Active and Stable Diaminopimelate Analogues of the Lantibiotic Peptide Lactocin S. *J. Am. Chem. Soc.* **2012**, *134*, 2008–2011.

(142) Qu, Q.; Gao, S.; Wu, F.; Zhang, M.-G.; Li, Y.; Zhang, L.-H.; Bierer, D.; Tian, C.-L.; Zheng, J.-S.; Liu, L. Synthesis of Disulfide Surrogate Peptides Incorporating Large-Span Surrogate Bridges Through a Native-Chemical-Ligation-Assisted Diaminodiacid Strategy. *Angew. Chem.* **2020**, *132*, 6093–6101.

(143) Gilbert, H. F. Thiol/Disulfide Exchange Equilibria and Disulfidebond Stability. *Methods Enzymol.* **1995**, *251*, 8–28.

(144) Lohans, C. T.; Vederas, J. C. Structural Characterization of Thioether-Bridged Bacteriocins. *J. Antibiot. (Tokyo)* **2014**, *67*, 23–30.

(145) Seltmann, G.; Holst, O. The Outer Membrane of the Gram-Negative Bacteria and Their Components. *The Bacterial Cell Wall*. **2002**, 9–102.

(146) Ongey, E. L.; Neubauer, P. Lanthipeptides: Chemical Synthesis versus in Vivo Biosynthesis as Tools for Pharmaceutical Production. *Microb. Cell Factories* **2016**, *15*, 97.

(147) Van Lierop, B .J.; Belgi, A.; Robinson, A. J.; Robinson, S. D.; Macraild, C. A.; Norton, R. S.; Kompella, S. N.; McArthur, J. R.; Hung, A.; Adams, D. J.; Dicarba α-Conotoxin Vc1.1 Analogues with Differential Selectivity for Nicotinic Acetylcholine and GABAB Receptors. *ACS Chem. Biol.* **2013**, *8*, 1815–1821.

(148) Keller, O.; Rudinger, J. Synthesis of [1, 6-α, A′-Diaminosuberic Acid]Oxytocin ('Dicarba-Oxytocin'). *Helv. Chim. Acta* **1974**, *57*, 1253–1259.

(149) Stymiest, J. L.; Mitchell, B. F.; Wong, S.; Vederas, J. C. Synthesis of Oxytocin Analogues with Replacement of Sulfur by Carbon Gives Potent Antagonists with Increased Stability. *J. Org. Chem.* **2005**, *70*, 7799–7809.

(150) Allen, F. H.; Kennard, O.; Watson, D. G.; Brammer, L.; Orpen, A. G.; Taylor, R. Tables of Bond Lengths Determined by X-Ray and Neutron Diffraction. Part I . Bond Lengths in Organic Compounds. *J Chem Soc Perkin Trans.* **1987**, *19*.

(151) Lebar, M. D.; Lupoli, T. J.; Tsukamoto, H.; May, J. M.; Walker, S.; Kahne, D. Forming Cross-Linked Peptidoglycan from Synthetic Gram-Negative Lipid II. *J. Am. Chem. Soc.* **2013**, *135*, 4632–4635.

(152) Spantulescu, M. D.; Jain, R. P.; Derksen, D. J.; Vederas, J. C. Photolysis of Diacyl Peroxides: A Radical-Based Approach for the Synthesis of Functionalized Amino Acids. *Org. Lett.* **2003**, *5* , 2963–2965.

(153) Qin, T.; Malins, L. R.; Edwards, J. T.; Merchant, R. R.; Novak, A. J. E.; Zhong, J. Z.; Mills, R. B.; Yan, M.; Yuan, C.; Eastgate, M. D.; Baran, P. S. Nickel-Catalyzed Barton Decarboxylation and Giese Reactions: A Practical Take on Classic Transforms. *Angew. Chem. Int. Ed.* **2017**, *56*, 260–265.

(154) Hsiao, Y.-T.; Beadle, J.; Pascoe, C.; Annadate, R.; Vederas, J. C. Decarboxylative Radical Addition to Methylideneoxazolidinones for Stereocontrolled Synthesis of Selectively Protected Diamino Diacids. *Org. Lett.* **2021**, *23*, 7270–7273.

(155) Yang, J.; Sun, W.; He, Z.; Yu, C.; Bao, G.; Li, Y.; Liu, Y.; Hong, L.; Wang, R. Access to α,γ-Diamino Diacid Derivatives via Organocatalytic Asymmetric 1,4-Addition of Azlactones and Dehydroalanines. *Org. Lett.* **2018**, *20*, 7080–7084.

(156) Testero, S. A.; Mata, E. G. Synthesis of 3-(Aryl)Alkenyl-β-Lactams by an Efficient Application of Olefin Cross-Metathesis on Solid Support. *Org. Lett.* **2006**, *8*, 4783–4786.

(157) Poeylaut-Palena, A. A.; Mata, E. G. Solid-Phase Cross Metathesis: The Effect of the Non-Immobilized Olefin and the Precatalyst on the Intrasite Interference. *Arkivoc* **2009**, *2010*, 216–227.

(158) Khan, S. N.; Kim, A.; Grubbs, R. H.; Kwon, Y.-U. Cross Metathesis Assisted Solid-Phase Synthesis of Glycopeptoids. *Org. Lett.* **2012**, *14*, 2952–2955.

(159) Sieber, P. Der 2-Trimethylsilyläthyl-Rest Als Selektiv Abspaltbare Carboxy-Schutzgruppe. *Helv. Chim. Acta* **1977**, *60*, 2711–2716.

(160) Shute, R. E.; Rich, D. H. Synthesis and Evaluation of Novel Activated Mixed Carbonate Reagents for the Introduction of the 2-(Trimethylsilyl)Ethoxycarbonyl(Teoc)-Protecting Group. *Synthesis* **1987**, *1987*, 346–349.

(161) Royo, M.; Farrera-Sinfreu, J.; Solé, L.; Albericio, F. Four-Dimensional Orthogonal Solid-Phase Synthesis of New Scaffolds Based on Cyclic Tetra-β-Peptides. *Tetrahedron Lett.* **2002**, *43* , 2029–2032.

(162) Gracia, C.; Isidro-Llobet, A.; Cruz, L. J.; Acosta, G. A.; Álvarez, M.; Cuevas, C.; Giralt, E.; Albericio, F. Convergent Approaches for the Synthesis of the Antitumoral Peptide, Kahalalide F. Study of Orthogonal Protecting Groups. *J. Org. Chem.* **2006**, *71*, 7196–7204.

(163) Yuen, T. Y.; Brown, C. J.; Xue, Y.; Tan, Y. S.; Gago, F. J. F.; Lee, X. E.; Neo, J. Y.; Thean, D.; Kaan, H. Y. K.; Partridge, A. W.; Verma, C. S.; Lane, D. P.; Johannes, C. W. Stereoisomerism of Stapled Peptide Inhibitors of the P53-Mdm2 Interaction: An Assessment of Synthetic Strategies and Activity Profiles. *Chem. Sci.* **2019**, *10*, 6457–6466.

(164) Pasto, D. J.; Taylor, R. T. Reduction with Diimide. *Organic Reactions*. **2004**, 40, 91–155.

(165) Williams, R. M.; Liu, J. Asymmetric Synthesis of Differentially Protected 2,7-Diaminosuberic Acid, a Ring-Closure Metathesis Approach. *J. Org. Chem.* **1998**, *63* , 2130–2132.

(166) Williams, R. M.; Im, M. N. Asymmetric Synthesis of Monosubstituted and .Alpha.,.Alpha.-Disubstituted .Alpha.-Amino Acids via Diastereoselective Glycine Enolate Alkylations. *J. Am. Chem. Soc.* **1991**, *113*, 9276–9286.

(167) Schneider, W.; Diller, W. Phosgene. *Ullmann's Encyclopedia of Industrial Chemistry*. **2000**, *26*, 623–632.

(168) Paul, M.; Donk, W. A. van der. Chemical and Enzymatic Synthesis of Lanthionines. *Mini-Rev. Org. Chem. 2*, 23–37.

(169) Hanessian, S.; Sahoo, S. P. A Novel and Efficient Synthesis of L–vinylglycine. *Tetrahedron Lett.* **1984**, *25*, 1425–1428.

(170) Sheldon, R. A.; Kochi, J. K. Oxidative Decarboxylation of Acids by Lead Tetraacetate. *Organic Reactions*. **2011**, 279–421.

(171) Usuki, T.; Sugimura, T.; Komatsu, A.; Koseki, Y. Biomimetic Chichibabin Pyridine Synthesis of the COPD Biomarkers and Elastin Cross-Linkers Isodesmosine and Desmosine. *Org. Lett.* **2014**, *16*, 1672–1675.

(172) Zakharkin, L. I.; Khorlina, I. M. Reduction of Esters of Carboxylic Acids into Aldehydes with Diisobutylaluminium Hydride. *Tetrahedron Lett.* **1962**, *3*, 619–620.

(173) Pascoe, C. A.; Engelhardt, D. B.; Rosana, A. R. R.; van Belkum, M. J.; Vederas, J. C. Methylene Analogues of Neopetrosiamide as Potential Antimetastatic Agents: Solid-Supported Syntheses Using Diamino Diacids for Pre-Stapling of Peptides with Multiple Disulfides. *Org. Lett.* **2021**, *23*, 9216–9220.

(174) Sytniczuk, A.; Kajetanowicz, A.; Grela, K. Fishing for the Right Catalyst for the Cross-Metathesis Reaction of Methyl Oleate with 2-Methyl-2-Butene. *Catal. Sci. Technol.* **2017**, *7*, 1284–1296.

(175) Blackwell, H. E.; O'Leary, D. J.; Chatterjee, A. K.; Washenfelder, R. A.; Bussmann, D. A.; Grubbs, R. H. New Approaches to Olefin Cross-Metathesis. *J. Am. Chem. Soc.* **2000**, *122*, 58–71.

(176) Ephritikhine, M. A New Look at the McMurry Reaction. *Chem. Commun.* **1998**, *23*, 2549–2554.

(177) Richards, I. C. Titanium(IV) Chloride–Zinc. In *Encyclopedia of Reagents for Organic Synthesis*; John Wiley & Sons, Ltd, 2001.

(178) Tanaka, M. Design and Synthesis of Chiral α,α-Disubstituted Amino Acids and Conformational Study of Their Oligopeptides. *Chem. Pharm. Bull.* **2007**, *55*, 359–358.

(179) Schafmeister, C. E.; Po, J.; Verdine, G. L. An All-Hydrocarbon Cross-Linking System for Enhancing the Helicity and Metabolic Stability of Peptides. *J. Am. Chem. Soc.* **2000**, *122*, 5891–5892.

(180) Wang, F.-L.; Guo, Y.; Li, S.-J.; Guo, Q.-X.; Shi, J.; Li, Y.-M. Diaminodiacid-Based Solid-Phase Synthesis of All-Hydrocarbon Stapled α-Helical Peptides. *Org. Biomol. Chem.* **2015**, *13*, 6286–6290.

(181) Vogt, H.; Bräse, S. Recent Approaches towards the Asymmetric Synthesis of α,α-Disubstituted α-Amino Acids. *Org. Biomol. Chem.* **2007**, *5*, 406–430.

(182) Chen, B.; Gu, Y.-C.; Voogd, N. J. de; Wang, C.-Y.; Guo, Y.-W. Xidaosterols A and B, Two New Steroids with Unusual α-Keto-Enol Functionality from the South China Sea Sponge Neopetrosia Chaliniformis. *Nat. Prod. Res.* **2022**, *36*, 1941–1947.

(183) Krumpe, L. R. H.; Wilson, B. A. P.; Marchand, C.; Sunassee, S. N.; Bermingham, A.; Wang, W.; Price, E.; Guszczynski, T.; Kelley, J. A.; Gustafson, K. R.; Pommier, Y.; Rosengren, K. J.; Schroeder, C. I.; O'Keefe, B. R. Recifin A, Initial Example of the Tyr-Lock Peptide Structural Family, Is a Selective Allosteric Inhibitor of Tyrosyl-DNA Phosphodiesterase I. *J. Am. Chem. Soc.* **2020**, *142*, 21178–21188.

(184) Carstens, B. B.; Rosengren, K. J.; Gunasekera, S.; Schempp, S.; Bohlin, L.; Dahlström, M.; Clark, R. J.; Göransson, U. Isolation, Characterization, and Synthesis of the Barrettides: Disulfide-Containing Peptides from the Marine Sponge Geodia Barretti. *J. Nat. Prod.* **2015**, *78*, 1886–1893.

(185) Carroll, A. R.; Copp, B. R.; Davis, R. A.; Keyzers, R. A.; Prinsep, M. R. Marine Natural Products. *Nat. Prod. Rep.* **2021**, *38*, 362–413.

(186) Aguiar, A. C. C.; Parisi, J. R.; Granito, R. N.; de Sousa, L. R. F.; Renno, A. C. M.; Gazarini, M. L. Metabolites from Marine Sponges and Their Potential to Treat Malarial Protozoan Parasites Infection: A Systematic Review. *Mar. Drugs* **2021**, *19*, 134.

(187) Williams, D. E.; Andersen, R. J. Biologically Active Marine Natural Products and Their Molecular Targets Discovered Using a Chemical Genetics Approach. *Nat. Prod. Rep.* **2020**, *37*, 617–633.

(188) Gomes, N. G. M.; Dasari, R.; Chandra, S.; Kiss, R.; Kornienko, A. Marine Invertebrate Metabolites with Anticancer Activities: Solutions to the "Supply Problem." *Mar. Drugs* **2016**, *14*, 98.

(189) Arnison, P. G.; Bibb, M. J.; Bierbaum, G.; Bowers, A. A.; Bugni, T. S.; Bulaj, G.; Camarero, J. A.; Campopiano, D. J.; Challis, G. L.; Clardy, J.; Cotter, P. D.; Craik, D. J.; Dawson, M.; Dittmann, E.; Donadio, S.; Dorrestein, P. C.; Entian, K.-D.; Fischbach, M. A.; Garavelli, J. S.; Göransson, U.; Gruber, C. W.; Haft, D. H.; Hemscheidt, T. K.; Hertweck, C.; Hill, C.; Horswill, A. R.; Jaspars, M.; Kelly, W. L.; Klinman, J. P.; Kuipers, O. P.; Link, A. J.; Liu, W.; Marahiel, M. A.; Mitchell, D. A.; Moll, G. N.; Moore, B. S.; Müller, R.; Nair, S. K.; Nes, I. F.; Norris, G. E.; Olivera, B. M.; Onaka, H.; Patchett, M. L.; Piel, J.; Reaney, M. J. T.; Rebuffat, S.; Ross, R. P.; Sahl, H.-G.; Schmidt, E. W.; Selsted, M. E.; Severinov, K.; Shen, B.; Sivonen, K.; Smith, L.; Stein, T.; Süssmuth, R. D.; Tagg, J. R.; Tang, G.-L.; Truman, A. W.; Vederas, J. C.; Walsh, C. T.; Walton, J. D.; Wenzel, S. C.; Willey, J. M.; Donk, W. A. van der. Ribosomally Synthesized and Post-Translationally Modified Peptide Natural Products: Overview and Recommendations for a Universal Nomenclature. *Nat. Prod. Rep.* **2012**, *30*, 108–160.

(190) Acedo, J. Z.; Chiorean, S.; Vederas, J. C.; van Belkum, M. J. The Expanding Structural Variety among Bacteriocins from Gram-Positive Bacteria. *FEMS Microbiol. Rev.* **2018**, *42*, 805–828.

(191) Kaur, K.; Andrew, L. C.; Wishart, D. S.; Vederas, J. C. Dynamic Relationships among Type IIa Bacteriocins: Temperature Effects on Antimicrobial Activity and on Structure of the C-Terminal Amphipathic α Helix as a Receptor-Binding Region. *Biochemistry* **2004**, *43*, 9009–9020.

(192) Sit, C. S.; Lohans, C. T.; van Belkum, M. J.; Campbell, C. D.; Miskolzie, M.; Vederas, J. C. Substitution of a Conserved Disulfide in the Type IIa Bacteriocin, Leucocin A, with L-Leucine and L-Serine Residues: Effects on Activity and Three-Dimensional Structure. *ChemBioChem* **2012**, *13*, 35–38.

(193) Ehrlich, A.; Heyne, H.-U.; Winter, R.; Beyermann, M.; Haber, H.; Carpino, L. A.; Bienert, M. Cyclization of All-l-Pentapeptides by Means of 1-Hydroxy-7-Azabenzotriazole-Derived Uronium and Phosphonium Reagents. *J. Org. Chem.* **1996**, *61*, 8831–8838.

(194) Fujii, N.; Otaka, A.; Funakoshi, S.; Bessho, K.; Watanabe, T.; Akaji, K.; Yajima, H. Studies on Peptides. CLI. Syntheses of Cystine-Peptides by Oxidation of s-Protected Cysteine-Peptides with Thallium(III) Trifluoroacetate. *Chem. Pharm. Bull. (Tokyo)* **1987**, *35*, 2339–2347.

(195) Redfield, C. Assignment of Protein NMR Spectra Using Heteronuclear NMR—A Tutorial. *Protein NMR*. **2015**, *32*, 1–42.

(196) Bochet, C. G. Photolabile Protecting Groups and Linkers. *J. Chem. Soc. Perkin 1* **2002**, *2*, 125–142.

(197) Hu, G.; Wang, Z.; Zhang, R.; Sun, W.; Chen, X. The Role of Apelin/Apelin Receptor in Energy Metabolism and Water Homeostasis: A Comprehensive Narrative Review. *Front. Physiol.* **2021**, *12*, 1–14

(198) Wysocka, M. B.; Pietraszek-Gremplewicz, K.; Nowak, D. The Role of Apelin in Cardiovascular Diseases, Obesity and Cancer. *Front. Physiol.* **2018**, *9*, 1–38.

(199) Chng, S. C.; Ho, L.; Tian, J.; Reversade, B. ELABELA: A Hormone Essential for Heart Development Signals via the Apelin Receptor. *Dev. Cell* **2013**, *27*, 672–680.

(200) Medhurst, A. D.; Jennings, C. A.; Robbins, M. J.; Davis, R. P.; Ellis, C.; Winborn, K. Y.; Lawrie, K. W. M.; Hervieu, G.; Riley, G.; Bolaky, J. E.; Herrity, N. C.; Murdock, P.; Darker, J. G. Pharmacological and Immunohistochemical Characterization of the APJ Receptor and Its Endogenous Ligand Apelin. *J. Neurochem.* **2003**, *84*, 1162–1172.

(201) Fan, X.; Zhou, N.; Zhang, X.; Mukhtar, M.; Lu, Z.; Fang, J.; DuBois, G. C.; Pomerantz, R. J. Structural and Functional Study of the Apelin-13 Peptide, an Endogenous Ligand of the HIV-1 Coreceptor, APJ. *Biochemistry* **2003**, *42*, 10163–10168.

(221) Ceraudo, E.; Galanth, C.; Carpentier, E.; Banegas-Font, I.; Schonegge, A.-M.; Alvear-Perez, R.; Iturrioz, X.; Bouvier, M.; Llorens-Cortes, C. Biased Signaling Favoring Gi over β-Arrestin Promoted by an Apelin Fragment Lacking the C-Terminal Phenylalanine. *J. Biol. Chem.* **2014**, *289*, 24599–24610.

(203) van Ameijde, J.; Poot, A. J.; van Wandelen, L. T. M.; Wammes, A. E. M.; Ruijtenbeek, R.; Rijkers, D. T. S.; Liskamp, R. M. J. Preparation of Novel Alkylated Arginine Derivatives Suitable for Click-Cycloaddition Chemistry and Their Incorporation into Pseudosubstrate- and Bisubstrate-Based Kinase Inhibitors. *Org. Biomol. Chem.* **2010**, *8*, 1629–1639.

(204) Freidinger, R. M.; Perlow, D. S.; Veber, D. F. Protected Lactam-Bridged Dipeptides for Use as Conformational Constraints in Peptides. *J. Org. Chem.* **1982**, *47*, 104–109.

(205) Belokon, Y. N.; Bakhmutov, V. I.; Chernoglazova, N. I.; Kochetkov, K. A.; Vitt, S. V.; Garbalinskaya, N. S.; Belikov, V. M. General Method for the Asymmetric Synthesis of α-Amino Acids via Alkylation of the Chiral Nickel(II) Schiff Base Complexes of Glycine and Alanine. *J. Chem. Soc. Perkin 1*. **1988**, *2*, 305–312.

(206) Brame, A. L.; Maguire, J. J.; Yang, P.; Dyson, A.; Torella, R.; Cheriyan, J.; Singer, M.; Glen, R. C.; Wilkinson, I. B.; Davenport, A. P. Design, Characterization, and First-in-Human Study of the Vascular Actions of a Novel Biased Apelin Receptor Agonist. *Hypertens. Dallas Tex 1979* **2015**, *65*, 834–840.

(207) Hamada, J.; Kimura, J.; Ishida, J.; Kohda, T.; Morishita, S.; Ichihara, S.; Fukamizu, A. Evaluation of Novel Cyclic Analogues of Apelin. *Int. J. Mol. Med.* **2008**, *22*, 547–552.

(208) Murza, A.; Sainsily, X.; Côté, J.; Bruneau-Cossette, L.; Besserer-Offroy, É.; Longpré, J.-M.; Leduc, R.; Dumaine, R.; Lesur, O.; Auger-Messier, M.; Sarret, P.; Marsault, É. Structure–Activity Relationship of Novel Macrocyclic Biased Apelin Receptor Agonists. *Org. Biomol. Chem.* **2017**, *15*, 449–458.

(209) Baker, T. J.; Tomioka, M.; Goodman, M. Preparation and Use of N,N′-Di-Boc-N″-Triflylguanidine. In *Organic Syntheses*; John Wiley & Sons, Ltd, **2003**; 91–91.

(210) Guerlavais, V.; Kawahata, N. *Peptidomimetic Macrocycles*. US8859723B2, October 14, **2014**.

(211) Garcia-Ramos, Y.; Lubell, W. D. Synthesis and Alkylation of Aza-Glycinyl Dipeptide Building Blocks. *J. Pept. Sci.* **2013**, *19*, 725–729.

(212) Bourguet, C. B.; Proulx, C.; Klocek, S.; Sabatino, D.; Lubell, W. D. Solution-Phase Submonomer Diversification of Aza-Dipeptide Building Blocks and Their Application in Aza-Peptide and Aza-DKP Synthesis. *J. Pept. Sci. Off. Publ. Eur. Pept. Soc.* **2010**, *16*, 284–296.